Molecular components and organelles involved in calcium-mediated signal-transduction in *Paramecium*

Zusammenwirken molekularer Komponenten und Organelle bei der Calcium-vermittelten Signaltranduktion in *Paramecium*

Dissertation

Zur Erlangung des akademischen Grades eines
„Doktors der Naturwissenschaften“
(Dr. rer. nat.)
des Fachbereiches für Biologie
an der Universität Konstanz

vorgelegt von

Ivonne Margarete Sehring

Tag der mündlichen Prüfung: 01.12.2006

1. Referent: Prof. Dr. H. Plattner
2. Referent: Prof. Dr. W. Hofer
3. Referentin: Prof. Dr. A. Noegel

Table of Contents

Chapter 1: Introduction

1.1.) Paramecium tetraurelia 5
1.1.2.) Movement 5
1.1.3.) Feeding 6
1.1.4.) Nuclear dimorphism 6
1.1.5.) Reproduction 7
1.1.6.) Osmoregulation 7
1.1.7.) Trichocysts 8
1.1.8.) Alveolar sacs 8
1.2.) Calcium 9
1.2.1.) Calcium sources, receptors, and their activation 10
1.2.2.) Ca^{2+} oscillations 12
1.2.3.) Activation of Ca^{2+} entry by store depletion 12
1.3.) Purinergic activation of *Paramecium* cells 13
1.4.) Actin 16
1.4.1.) Crystal structure of actin 17
1.4.2.) Actin isoforms 19
1.4.3.) Polymerization of actin monomers 19
1.4.4.) Structure of the actin filament 21
1.4.5.) Actin-binding proteins 22
1.4.6.) Functional role of F-actin 23
1.4.7.) Actin drugs 25
1.4.8.) Possible roles of actin in SOCE 26
1.4.9.) Actin in *Paramecium* 27

Chapter 2: Manuscript I

Ca^{2+} oscillations mediated by exogenous GTP in Paramecium cells: assessment of possible Ca^{2+} sources

2.1.) Summary 30
2.2.) Introduction 31
2.3.) Materials and methods 33
2.3.1.) Cell materials 33
2.3.2.) Stimulation conditions 33
2.3.3.) Ca^{2+} fluorochrome analysis 33
2.4.) Results 35
2.4.1.) Compatibility with previous electrophysiological and behavioral analyses 35
2.4.2.) Additional new aspects of GTP-mediated Ca^{2+} signaling 36
2.5.) Discussion 42
2.5.1.) Are there purinergic surface receptors in Paramecium and what may be their function? 42
2.5.2.) How would Ca^{2+} oscillations be produced? 43
2.5.3.) Effect on ciliary beat 44
2.5.4.) Why should a cell release GTP? 45
2.6.) Acknowledgements 46

Chapter 3: Manuscript II
Immunolocalization of actin in Paramecium cells
3.1.) Summary 47
3.2.) Introduction 48
3.3.) Materials and methods 50
3.3.1.) Stocks and cultures 50
3.3.2.) Expression of Paramecium Actin-specific Peptides in Escherichia coli 50
3.3.3.) Purification of Recombinant Actin1-1 Peptides 50
3.3.4.) Antibodies Used 50
3.3.5.) Cell Fractionation 51
3.3.6.) Electrophoretic Techniques and Western Blot Analysis 51
3.3.7.) Immunofluorescence Labeling 52
3.3.7.1.) Basic Procedure 52
3.3.7.2.) Deciliated Cells 52
3.3.7.3.) Light Microscopy 52
3.3.8.) Fixation and Embedding for Postembedding EM Analysis 53
3.3.9.) Immunogold Labeling and EM Analysis 53
3.3.9.1.) Postembedding Method 53
3.3.9.2.) Preembedding Labeling 53
3.3.9.3.) Specificity of Immunogold Labeling and Further Processing 54
3.3.9.4.) Further Processing and Quantitative Evaluation 54
3.4.) Results 55
3.4.1.) Actin-specific ABs, Cell Fractionation, and Western Blot Analysis 55
3.4.2.) Immunofluorescence Labeling 56
3.4.3.) Comparative Analysis of CLSM and Immunogold EM Labeling 57
3.4.4.) Specification of Results Obtained with Postembedding Labeling 60
3.5.) Discussion 65
3.5.1.) Background from Previous Work 65
3.5.2.) Additional Functional Aspects Derived from This Study 66
3.6.) Acknowledgement 69

Chapter 4: Manuscript III
The actin multigene family of Paramecium tetraurelia
4.1.) Summary 70
4.2.) Introduction 71
4.3.) Materials and methods 73
4.3.1.) Stocks and cultures 73
4.3.2.) PCR of genomic DNA and cDNAs 73
4.3.3.) Sequencing 73
4.3.4.) Preparation of non-radioactive and radioactive probes 73
4.3.5.) Hybridization cloning 74
4.3.6.) Annotation and characterization of further actin genes 74
4.4.) Results 75
4.4.1.) Actin1 subfamily 75
4.4.2.) Actin2 subfamily 76
4.4.3.) Other actin subfamilies 77
4.4.4.) Actin sequences 77
4.4.5.) Actin-related proteins (arps) 80
4.4.6.) Phylogenetic distribution 81
4.4.7.) Actin consensus pattern 83
4.4.8.) Amino acids influencing polymerization 84
4.4.9.) ATP binding 85

4.4.10.) Binding residues for myosin II 85
4.4.11.) Drug binding residues 86
4.5.) Discussion 88
4.5.1.) Identification of arps and alp 88
4.5.2.) Actin isoforms 89
4.5.3.) Phylogenetic distribution 90
4.5.4.) Actin consensus pattern 91
4.5.5.) Amino acids influencing polymerization 91
4.5.6.) ATP binding 92
4.5.7.) Binding residues for myosin II 92
4.5.8.) ATP binding 93
4.5.9.) Conclusion 93
4.6.) Acknowledgements 93

Chapter 5: Manuscript IV
A Broad Spectrum of Actin Paralogs in *Paramecium tetraurelia* Cells Displays Differential Localization and Function
5.1.) Summary 94
5.2.) Introduction 95
5.3.) Materials and methods 97
5.3.1.) Stocks and cultures 97
5.3.2.) Heterologous Expression and Purification of Paramecium Actin-Specific Peptides 97
5.3.3.) Antibodies 97
5.3.4.) Electrophoresis and Western Blots 97
5.3.5.) Immunofluorescence Labeling 98
5.3.6.) GFP Constructs 98
5.3.7.) Microinjection of GFP constructs 99
5.3.8.) Immuno-Electron Microscopy 99
5.3.9.) Gene Silencing Constructs 100
5.3.10.) Gene Silencing by Feeding 100
5.3.11.) Behavioral and Functional Assays 101
5.3.12.) Statistical Evaluation 102
5.4.) Results 103
5.4.1.) Actin Isoforms and their Localization 103
5.4.2.) RNA Interference by Feeding 109
5.4.3.) Salient Features of Results 113
5.5.) Discussion 114
5.5.1.) Comparison with Previous Localization Studies 114
5.5.2.) Aspects of Current Localization Studies and their Functional Implications 114
5.6.) Acknowledgements 115

Chapter 6: Discussion
6.1.) Calcium sources during GTP mediated Ca oscillations in *Paramecium* 118
6.2.) Actin in *Paramecium* 120

Chapter 7: List of references 122

Chapter 8: Supplementary material 160
8.1.) Oligonucleotides for the amplification and cloning of P. *tetraurelia* actin genes

Chapter 9: Summary

Summary 161
Zusammenfassung 162

Acknowledgements 164
Eigenabgrenzung 165

Chapter 1
Introduction

1.1.) *Paramecium tetraurelia*

Paramecium tetraurelia is a small unicellular organism that is often found in water containing bacteria and decaying organic matter. Paramecia belong to the phylum Ciliophora. Despite their great genetic diversity, the members of this phylum (ciliates) remain united by two characteristics: their external covering of continuously beating cilia, used for swimming or crawling and for phagocytotic food capture, and the presence of nuclear dimorphism. A *Paramecium* cell must perform all the same functions as a multicellular organism without the luxury of labor division amongst specialized cells, and it is their ability to fulfill these requirements along with their elaborate ultrastructure which places them among the functionally most complex cells.

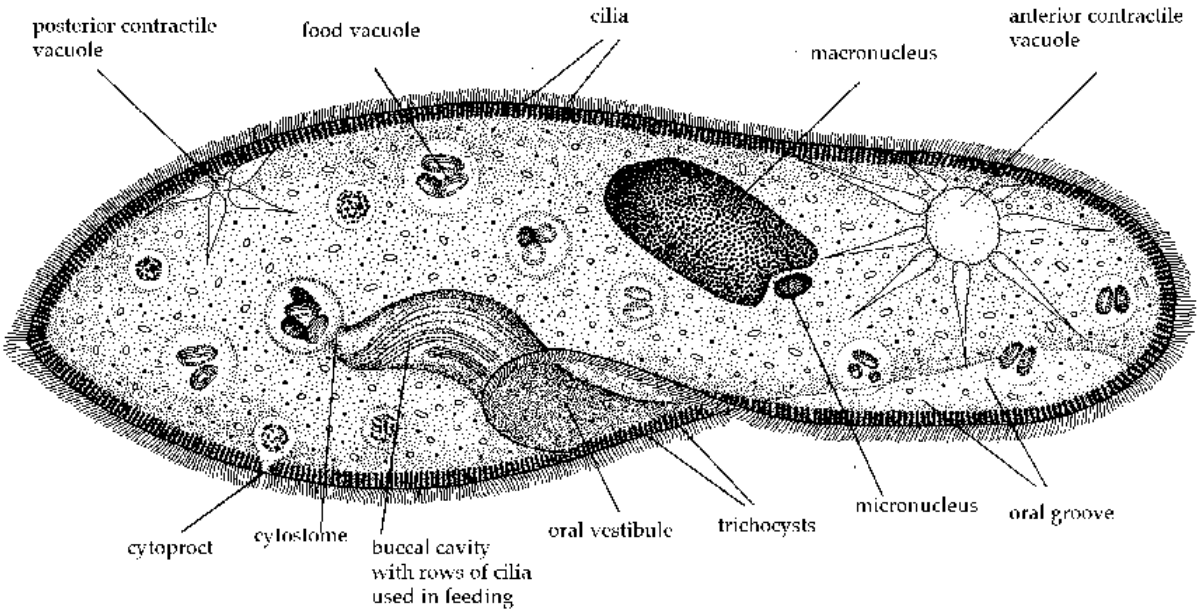

Fig 1. The structure of a *Paramecium*. The cell membrane is covered with rows of cilia. Along the oral groove, they beat rhythmically to wash food towards the oral vestibule and then to the buccal cavity. The buccal cavity terminates at the cytostome where the food is packaged in special food vacuoles for digestion. At the cytoproct, indigestible rests are released by exocytosis. In a precise pattern, trichocysts are attached to the plasma membrane. Osmoregulation is executed by two contractile vacuoles complexes. Like all ciliates, *Paramecium* has two types of nuclei. The polyploid macronucleus maintains cell growth and function by producing messenger RNA. The micronucleus is located close to the macronucleus, is involved in inheritance of genetic material during sexual reproduction and is only diploid. Note the difference in the shape of the two ends of the cell. The blunter end is anterior and the slightly pointed, broader end is posterior. *Paramecium* swims with the anterior end forward (from Vickerman and Cox, 1967).

1.1.2.) Movement

The outer surface of *Paramecium* is covered with cilia. The cilia occur in longitudinal rows (kineties), connected by an underlying infraciliature of basal bodies and fibers. This highly organized pattern allows that hundreds of separate cilia can be coordinated in locomotion.

Paramecium moves by the action of these thousands of beating cilia. The speed of motion is about four times its own length (~100µm) per second. Since the frequency of the oral groove cilia is steadier than that of the somatic cilia, a *Paramecium* does not swim in a perfectly straight line. As it moves through the water it rotates, due to the oblique beat of its cilia, around its axis and small particles of debris and food are collected and swept into the gullet. If *Paramecium* comes across an obstacle, it stops, reverses the beating of the cilia, swims backwards, turns through an angle and moves forward again on a slightly different course.

1.1.3.) Feeding

Paramecium has a permanent feeding mechanism, consisting of a funnel-shaped gullet into which food is drawn by the combined action of cilia which cover the body and other cilia lining the gullet. They feed on small organisms such as bacteria and even other smaller protozoa. When *Paramecium* comes in contact with bacteria, highly organized rows of beating cilia lining the oral region move the food down to the cytopharynx where it becomes engulfed in a food vacuole by the process of phagocytosis. Food vacuoles created in this way merge with the cell's lysosomes which dump in enzymes to digest the bacteria. The vacuoles move through the cell while the various events of digestion occur sequentially. The pH of the vacuole changes as it moves through the cell. A *Paramecium* has several food vacuoles with bacteria at different stages of ingestion. Undigested material is expelled out of the anal pore (cytoproct) at the posterior end of the cell.

1.1.4.) Nuclear dimorphism

Ciliates are exceptional among the eukaryotes since they possess one macronucleus and at least one micronucleus, whereas most eukaryotes have just one DNA containing nucleus. This nuclear dimorphism is a characteristic of ciliates. Each individual has two types of nuclei. A polyploid somatic nucleus (macronucleus) controls most of the metabolic functions of the organism. The macronucleus is the site for production of RNA; it participates in the day to day activities and assures transcriptional activity during vegetative cell growth and cell proliferation. At each sexual generation the macronucleus is destroyed and a new one is formed form the zygotic micronucleus by programmed rearrangements of the entire genome.

The diploid germline nucleus (micronucleus) remains relatively dormant until the cell undergoes some type of sexual process; it is used for sexual exchange of DNA. This nuclear dualism imparts a unique twist on the inheritance patterns of *Paramecium*.

Sequence analysis of genes of *Paramecium*, the related ciliate *Tetrahymena* and hypotrichs have revealed that the three codons TGA, TAG and TAA, which are universal stop

codons for nuclear genes in other eukaryotes, have evolved different codon meanings in ciliates (Harper and Jahn, 1989). In *Paramecium*, TAA and TAG code for glutamine (Caron and Meyer, 1985). That means that the only stop codon is TGA.

1.1.5.) Reproduction

Paramecium has two means of reproduction, simple division and conjugation.

A. Division. Under favorable conditions *Paramecium*, like other ciliates, usually reproduces by dividing in two by a process called binary fission. Fission results in two virtually identical individuals from one organism, each of which rapidly reforms any new structures required and increases in size. *Paramecium* divides transversely, splitting in two in the middle of the long axis of the organism. The macronucleus does not divide by mitosis; rather it elongates and then splits in two, roughly one half going to each of the new daughter cells. The whole process may take place two or three times a day if conditions are right. This type of reproduction involves no exchange of genetic material and is a type of asexual reproduction.

*B. Conjugation***.** Under certain conditions, such as overcrowding or environmental stress, *Paramecium* turns from strictly asexual reproduction to sexual reproduction. Sexual reproduction involves two cells coming together to exchange nuclear material. Through a process called conjugation, two *Paramecia* line up side by side and fuse together. All but one of the cell's micronuclei disintegrate. Involving meiosis, this diploid micronucleus divides into four haploid micronuclei. Three of these disintegrate, while one divides again to produce two swapping haploid micronuclei, one of which is exchanged during conjugation. The new micronucleus fuses with the old one. This new diploid micronucleus represents a combination of genetic material derived from the two genetically different individuals. The two cells then separate and continue to reproduce by simple division.

1.1.6.) Osmoregulation

Paramecium typically lives in a hypotonic environment, which means that *Paramecium* has a higher concentration of materials inside the cell than present in the outside environment. Thus, water is constantly diffusing from the outside into the cell through the process of osmosis. Many single celled organisms use a combination of techniques for maintaining osmotic balance. In *Paramecium,* two contractile vacuoles eliminate water entering the cell and help maintain osmotic equilibrium. Each vacuole is surrounded be 6 to 10 radiating ducts which collect water and pump it into the central vacuoles. In turn, the central vacuole contracts when it is full, forcing water to the outside of the cell. *Paramecium* must constantly

expell water as a means of balancing its salt concentration and to prevent the cell from becoming bloated with water and potentially bursting (Allen, 1988; Stock et al., 2002).

In addition, *Paramecium* and other Protista have a second technique for regulating osmotic balance which is the formation of crystals of salts. If the cytoplasm becomes excessively hypersonic, salts can be taken out of solution. Conversely if the cytoplasm becomes excessively dilute, *Paramecium* can release salts from these crystals to make the cytoplasm more hypersonic.

1.1.7.) Trichocysts

Embedded within the pellicle (a rigid outer covering that provides support for the cilia which project through it) are numerous (approximately 1000 per cell) thread-like structures (Fig. 2). These dense core secretory vesicles, the trichocysts, are synthesized through fusion and maturation of post-Golgi vesicles. After biogenesis as free granules within the cytoplasm, trichocysts have to be transported to their attachment site at the plasma membrane. Microfilaments of actin may play a role in the transport to the cell cortex and the recognition of the docking sites by trichocysts (Beisson and Rossignol, 1975; Plattner et al. 1982). The trichocysts can be fired out from the cell by exocytosis in a fraction of a second at the slightest mechanical or chemical stimulation. Discharged trichocysts elongate to long, sticky protein threads. The exact function of trichocysts is not known but it is thought they may be used for defense.

1.1.8.) Alveolar sacs

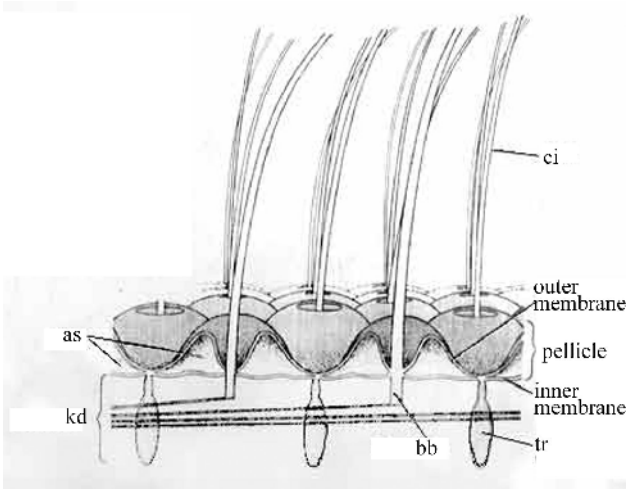

Fig. 2. The organization of the Paramecium cortex. The cilia (ci) are arranged in precise rows. Their basal bodies (bb) are associated with kinetodesmal fibers (kd) which extend anteriorly. The complex pellicle includes alveoli (as) and is provided with trichocysts (tr) which can be discharged from the surface for defense (from Vickerman and Cox, 1967).

Alveolar sacs are subplasmalemmal calcium storage compartments (Stelly et al. 1991). They are tightly attached at a distance of only 15 nm to the cell membrane. The identity of the connections between the alveolar sac membrane and the plasma membrane is still unknown (Plattner et al., 1991; Plattner and Klauke, 2001). They are ~ 100 nm wide and contain 43 mM Ca, which is almost identical to that in the sarcoplasmatic reticulum. Upon stimulation of exocytosis of trichocysts,

~40% of the stored calcium is released within 80 ms. Several data support a store operated current-type mechanism (see below) for this rapid Ca^{2+} release in *Paramecium* (Hardt et al., 1999; Plattner et al., 1997a; Mohamed et al., 2002). The alveolar sacs may be the protozoan equivalent of the sarcoplasmic reticulum of myocytes (Erxleben and Plattner, 1994). Together with the cilia and the trichocysts, they are part of the highly organized cortex of the *Paramecium* cell (Fig. 2).

1.2.) Calcium

Calcium is a ubiquitous intracellular second messenger. The concentration of cytosolic free calcium is critically important for the control of many essential cellular responses. The concentration of intracellular calcium $[Ca^{2+}]_i$ is determined by a balance between reactions through which Ca^{2+} is introduced into the cytoplasm and reactions that remove it by the combined action of buffers, pumps and exchangers. Changes in the concentration of cytosolic free calcium play a central role in the regulation of specialized functions like excitability, muscle contraction or neurotransmitter release, while also regulating universal cellular activities such as metabolism, gene expression, cell proliferation and many other processes. In order to accommodate so many control functions, the mechanisms responsible for generating calcium signals are very diverse. The versatility of Ca^{2+} signals in terms of speed, amplitude and spatio-temporal patterning emerges from the use of an extensive molecular repertoire of signaling components. Even more variations can be achieved through interactions of Ca^{2+} with other signaling pathways.

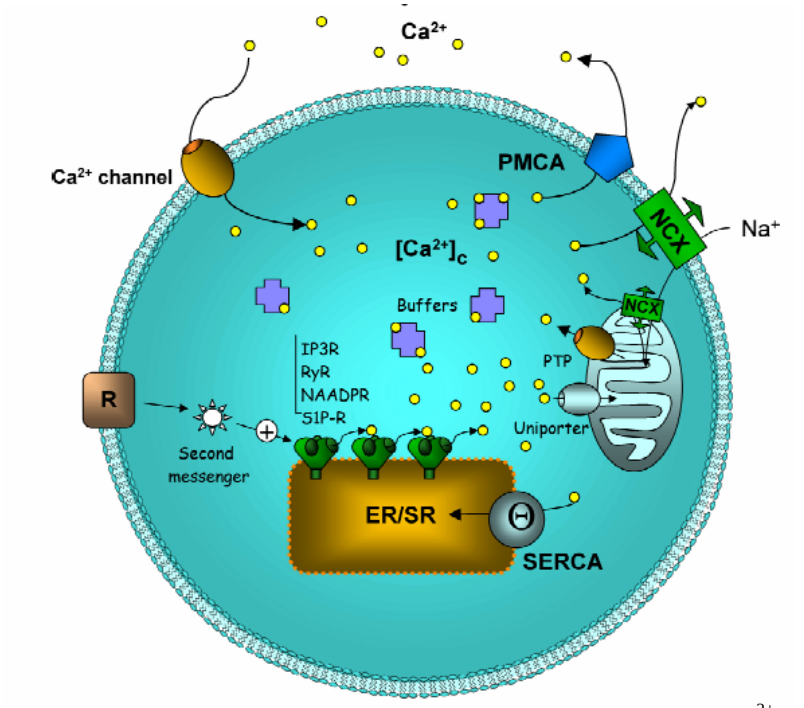

Fig. 3. Mechanisms of calcium signaling. Most of the cytosolic Ca^{2+} is inactive as it is bound to buffers. If a cell is stimulated by agonists upon specific receptor/ligand binding, the formation of second messengers is activated. Those induce the release of Ca^{2+} from internal stores (endoplasmic/sarcoplasmic reticulum ER/SR) through different receptors [IP_3 receptor (IP_3R), ryanodine receptor (RyR), NAADP receptor (NAADPR) or sphingosine 1-phosphate binding site (S1P-R)]. Extracellular agonists stimulate also the entry of extracellular Ca^{2+} through plasma membrane channels. To decrease the [Ca^{2+}] back to the resting level, Ca^{2+} is removed from the cytosol by various pumps and exchangers, both into internal stores and to the outside. The Na^+/Ca^{2+} exchanger (NCX) and the plasma membrane Ca^{2+} ATPase (PMCA) extrude Ca^{2+} from the cytosol, the sarcoendoplasmic reticulum Ca^{2+}-ATPase (SERCA) pumps Ca^{2+} back to the ER/SR. During the Ca^{2+} signal mitochondria sequester Ca^{2+} through a uniporter. It is released slowly into the cytoplasm through the NCX or the permeability transition pore (PTP; from Rosado et al., 2004).

1.2.1.) Calcium sources, receptors, and their activation

Elevations in $[Ca^{2+}]_i$ could arise from Ca^{2+} entry via Ca^{2+} channels in the surface membrane, Ca^{2+} release from internal stores, or both. This means there are two sources of signal calcium: external calcium and internal calcium stores (Berridge, 1996). The internal stores are held within the membrane systems of the endoplasmic reticulum (ER) or the equivalent organelle, the sarcoplasmatic reticulum (SR) of muscle cells. Calcium release from these stores is controlled by various channels, for example the inositol-1,4,5-trisphosphate receptor (IP_3R) and ryanodine receptor (RyR) families. The principal activator of these channels is Ca^{2+} itself, or an expanding group of messengers, such as inositol-1,4,5-trisphhosphat (IP_3), cyclic ADP ribose (cADPR) or nicotinic acid adenine dinucleotide phosphate (NAADP; Berridge et al., 2000). The Ca^{2+} sensitivity of the channels enables the calcium released from one receptor to excite its neighbors, thereby igniting a regenerative wave capable of sweeping through the

cytoplasm. This Ca^{2+} induced Ca^{2+} release (CICR) is a central element of Ca^{2+} signaling. For channels that control the entry of external Ca^{2+}, a classification on the basis of their regulatory mechanism leads to three main entry channels: voltage-operated channels VOCs, receptor-operated channels ROCs and store-operated channels SOCs (Berridge, 1996). VOCs and ROCs have different kinetic properties than SOCs as they usually provide brief bursts with high intensity whereas SOCs generate much smaller but sustained influx of calcium. This influx is called "capacitative Ca^{2+} entry" CCE. A synonym is store operated current SOC (Elliott, 2001). To avoid confusion because of the same abbreviation, some prefer the terms "store-operated calcium channels" SOCC and "store-operated calcium entry" SOCE, which will be used in this thesis. The mechanism of SOCE is illustrated in Fig. 4. As the term "store-operated current" indicates, SOCCs in the plasma membrane are activated through store depletion. The mechanism underlying this process is yet unknown. Once a Ca^{2+} signal is generated, various Ca^{2+} sensitive processes translate this into a cellular response. Involved are numerous Ca^{2+}-binding proteins, which can be divided into Ca^{2+} buffers and Ca^{2+} sensors, according to their main functions. The latter respond to an increase in Ca^{2+} by activating diverse processes.

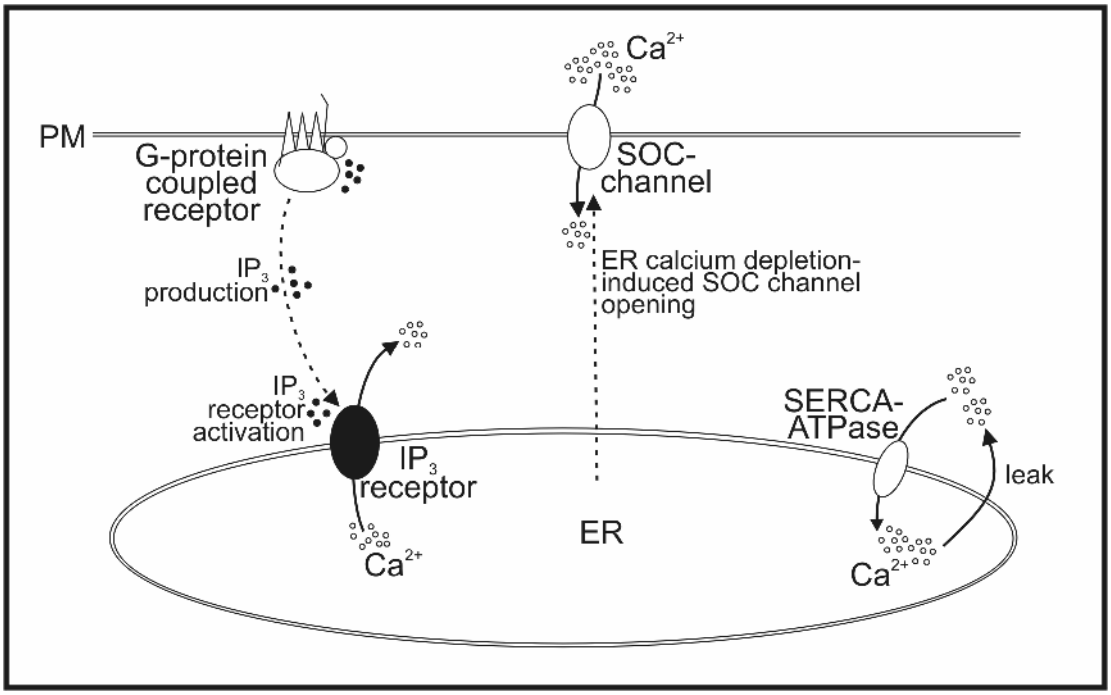

Fig. 4. Mechanism of SOCE. The activation of a plasma membrane receptor which is coupled to a G protein leads to the production of IP_3. IP_3 activates the IP_3 receptor in the ER, the calcium channel opens and stored Ca^{2+} is released. This store depletion activates SOC channels in the plasma membrane (PM) to open and causes Ca^{2+} influx form the extracellular space. Passive Ca^{2+} leak from the ER is counterbalanced by Ca^{2+} uptake by SERCA-type Ca^{2+}-ATPase.

Once Ca^{2+} has carried out its signaling functions, it is rapidly removed from the cytoplasm not only by binding to cytosolic Ca^{2+}-binding proteins, but also by various pumps

and exchangers. Ca^{2+} is as well extruded to the outside as it is pumped back into to the internal stores (Berridge et al., 2003).

1.2.2.) Ca^{2+} oscillations

Ca^{2+} signals are usually presented as brief spikes. When longer periods of signaling are necessary, spikes are repeated to give waves with different frequencies, ranging from 1-60 seconds to 24 hours. There is substantial evidence to show distinct roles of different spatial and temporal patterns of intracellular free Ca^{2+} concentration in the regulation of cellular processes (Thomas et al., 1996). Especially Ca^{2+} oscillations, which are observed not only in excitable cells but also in non-excitable cells, are suggested to participate in cellular differentiation or proliferation (Berridge et al., 2002). Intracellular Ca^{2+} oscillations which arise from periodic release from intracellular stores can be manifest either as transient oscillations from a base-line Ca^{2+} level or as sinusoidal oscillations upon a raised plateau level of Ca^{2+} (Thomas et al., 1996).

1.2.3.) Activation of Ca^{2+} entry by store depletion

A major unsolved problem concerns the nature of the mechanism that couples store emptying to channel opening. Two general types of theory have been evoked to explain the activation of Ca^{2+} entry by store depletion. One suggestion is that depletion of Ca^{2+} from the intracellular stores is associated with the production of an intracellular messenger called calcium influx factor (CIF) which then diffuses to the membrane to open the SOCCs (Fig. 5A).

An alternative theory, usually termed conformational coupling model, suggest intracellular stores located close to the membrane are physically coupled to the Ca^{2+} entry channels in the plasma membrane and that information is transferred more directly through the large cytoplasmic head of the IP_3 receptor (Fig. 5B). When the IP_3R channels open during intracellular Ca^{2+} release, the IP_3R undergoes a conformational change that is transmitted to the SOCCs in the plasma membrane to induce the influx of external calcium. For that model to work, there is a need for a close physical association between the plasma membrane and underlying ER or other calcium stores to permit the IP_3R to contact the SOCCs. A modification of this model - in recent publications called constitutive conformational coupling - is the *de novo* conformational coupling model (Fig. 5C). According to this model, membrane trafficking play a role in the activation of SOCC. Parts of the ER, which contain IP_3 receptors and are initially slightly distant from the plasma membrane, would be transported to the plasma membrane for *de novo* protein coupling. Therefore, Ca^{2+} store depletion would lead to a dynamic and reversible conformational coupling between IP_3 receptors and SOCCs (Rosado

et al., 2000). This coupling process is modulated by the actin cytoskeleton. It can impact the process in both facilitating and inhibitory ways. Cortical actin can act as a negative clamp that prevents coupling but also providing support for the coupling between IP_3 receptors and SOCCs (Patterson et al., 1999; Venkatachalam et al., 2002; Rosado et al., 2005).

Another, quite similar model where the actin cytoskeleton plays a key role is the secretion-like coupling model (Fig. 5D). This mechanism is suggested to involve a physical and reversible interaction between the endoplasmic reticulum and the plasma membrane, which is based on trafficking, likely to involve a GTP-dependent step (Rosado and Sage, 2000), of the ER towards the plasma membrane.

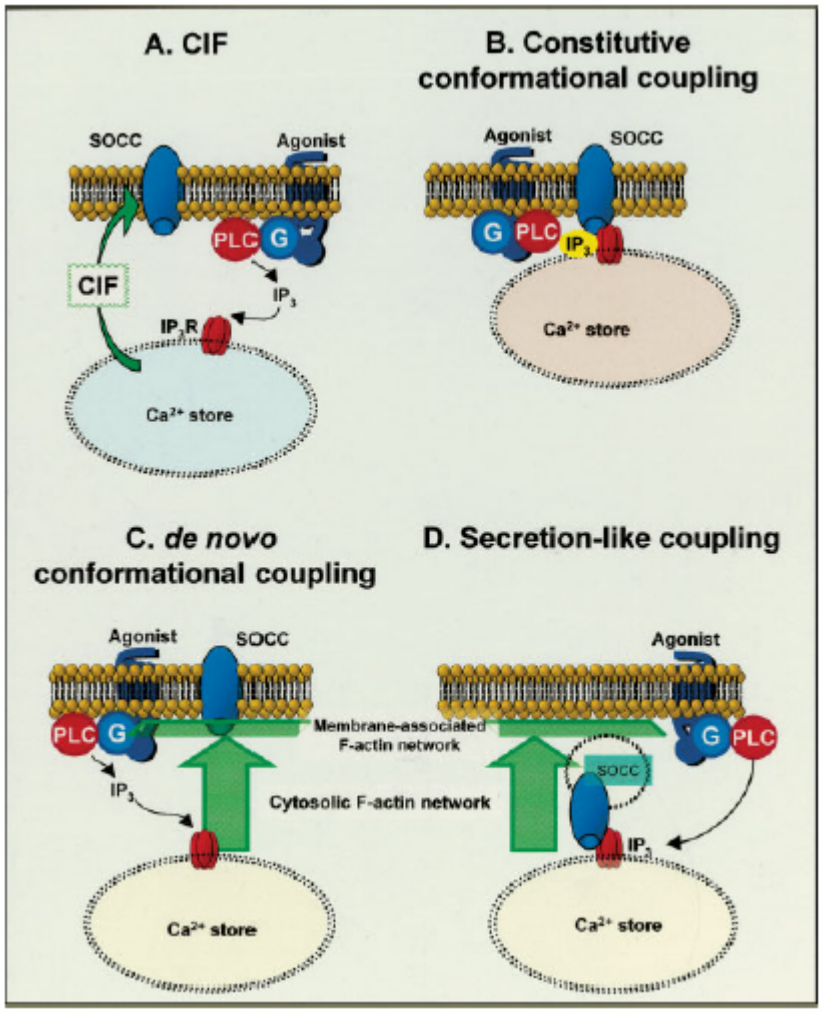

Fig. 5. Possible models for store-operated Ca^{2+} entry. (A) Agonist binding results, via the generation of IP_3, in the depletion of Ca^{2+} stores, which activate the release of CIF which opens the SOC channels in the plasma membrane. (B) A permanent and direct coupling between the IP_3 receptor and the SOC channel is affected by a conformational change of the IP_3 receptor upon store depletion. (C) An interaction between the IP_3 receptor and the SOC channel only takes place after depletion of the stores, when parts of the Ca^{2+} stores are translocated towards the plasma membrane. (D) Mobilization of the stores causes fusion of vesicles containing SOC channels with the plasma membrane. G, heterodimeric G-protein; PLC, phospholipase C (from Rosado et al., 2005).

1.3.) Purinergic activation of *Paramecium* cells

Single-cell, motile life forms are able to detect nutrients and ions in their extracellular environments which give them the chance to move to sites with optimal conditions. Likewise, unsuitable conditions can be avoided. *Paramecium* switch from predominantly forward swimming to an unusual pattern of repetitive bouts of backward and forward jerks with transition periods of whirling, which serve to re-orient the cells. This directs them away from the condition that elicited their response (Jennings, 1976). As it is a biased random walk instead of an oriented movement, this behavioral response is defined more as a chemokinetic response than a chemotaxis (VanHouten, 1978).

The purine nucleotide guanosine 5'-triphosphate (GTP), when added to the extracellular medium at micromolar concentrations, is actively avoided by *Paramecium* cells by producing avoiding reactions. *Paramecium* responds to GTP with periodic episodes of prolonged backward swimming, called continuous ciliary reversal (CCR, Clark et al., 1992). A CCR has a frequency of around 5/min, persisting for about 10 minutes. Pharmacologically, it is a unique response to GTP. While ATP is 1,000-fold less potent, other nucleotides such as CTP, XTP, UTP and ITP cause no backward swimming. The specificity of the response suggests that it is likely that a receptor in the cell membrane allows *Paramecium* to recognize the presence of this nucleotide and mediates the nucleotide signal transduction (Clark et al., 1993). When *Paramecia* are exposed to GTP while recording membrane potential, the repetitive bouts of CCR are consistent with oscillating membrane depolarizations and repolarisations (Clark et al., 1996).

The swimming behavior of *Paramecium* is tightly coupled to the electrophysiological state of the membrane. It has been shown that intraciliary Ca^{2+} is the link between membrane depolarizations and changes in swimming behavior (Eckert, 1972; Kung, 1971). Electrophysiologically, each avoiding reaction is accompanied by a Ca^{2+}-based action potential. Membrane depolarizations cause voltage-dependent Ca^{2+}-channels present in the ciliary membrane to open. This produces graded Ca^{2+}-based action potentials and consequent inward Ca^{2+} currents. The rise in intraciliary free Ca^{2+} causes the beat frequency to slow down. When the free Ca^{2+} exceeds 10^{-6} M the cilia reverse their power stroke (Machemer and Ogura, 1980). Therefore, if the generated somatic depolarization is strong enough, the cell whirls or swims backwards. Thus, binding of extracellular GTP to a putative surface receptor in *Paramecium* causes change in somatic membrane ion conductance to depolarize the cell to a threshold level, and thus generates action potentials and avoiding reactions (Hennessey, 2005).

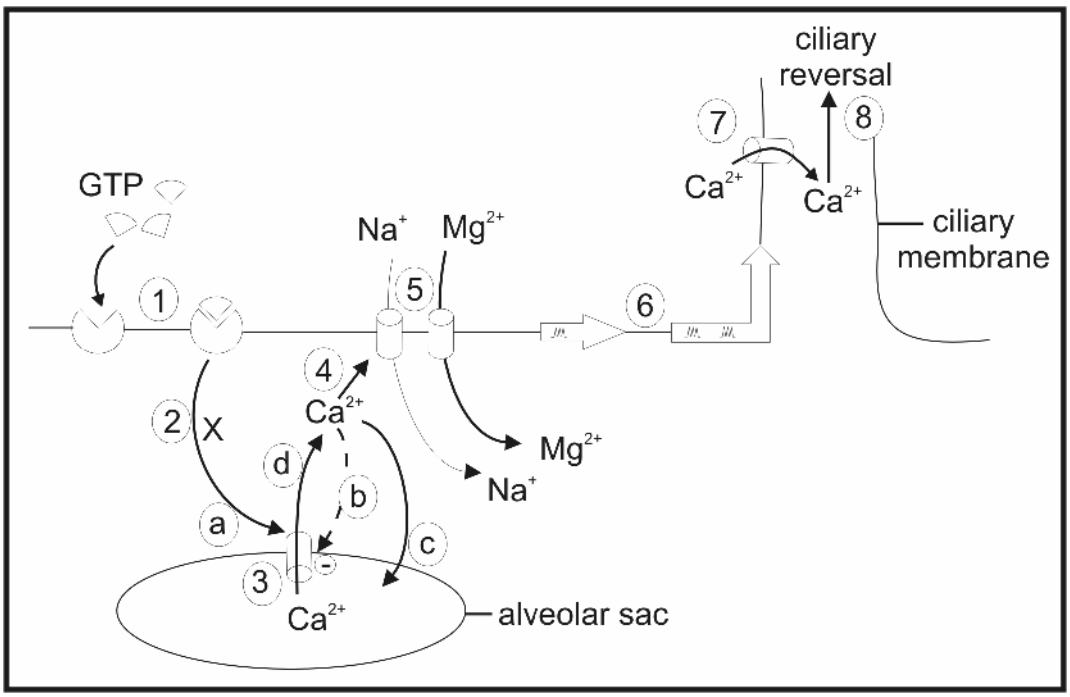

Fig. 6. A model for the possible signal transduction in *Paramecium* upon stimulation with GTP. (1) GTP binding to a cell-surface receptor stimulates (2) the production of a yet unidentified second messenger "x" which (3) triggers release of Ca^{2+} from alveolar sacs. The raising of [Ca^{2+}] activates Mg^{2+} and Na^{+} ion channels in the plasma membrane (4). The influx of one or both ions (5) depolarizes the plasma membrane (6) of the whole cell. Voltage-dependent Ca^{2+} channels in the ciliary membrane open upon membrane depolarization and Ca^{2+}streams into the cilia. The increase of ciliary Ca^{2+} (7) leads to a reversal of the ciliary beat and consequently to backward swimming (8). Following this model, calcium oscillations could be generated by repeated passes of Ca^{2+} increase upon "x" triggering Ca^{2+} release from alveolar sacs (a) until the [Ca^{2+}] inhibits the Ca^{2+} release channels (b), and a Ca^{2+} decrease due to the remove of Ca^{2+} from the cytosol by the SERCA pump (c). The abolishment of the inhibition induces another burst of Ca^{2+} from the alveoli (d). Model modified after Wassenberg et al., 1997.

The initial Ca^{2+} signal upon GTP may be amplified by release of Ca^{2+} from internal stores. However, it could also be possible that there is a receptor-mediated release of Ca^{2+} from internal stores without Ca^{2+} influx (Hennessey, 2005). Previous studies on metazoa have suggested that contributions to oscillations in intracellular Ca^{2+} can come from the extracellular space and/or from intracellular Ca^{2+} stores (Tsien & Tsien, 1990).

In *Paramecium*, the alveolar sacs accumulate Ca^{2+} in an ATP-dependent reaction (Stelly et al., 1991). Several inhibitors of sarcoplasmic/endoplasmic reticulum Ca^{2+}-dependent ATPase (BHQ, CPA and thapsigargin) have been shown to alter the response to extracellular GTP at the behavioral and electrophysiological level. These finding suggest that sequestration and/or release of Ca^{2+} from internal stores may be involved in the repetitive CCRs seen in response to GTP (Wassenberg et al., 1997).

The first goal of this thesis was to investigate the Ca^{2+}dynamics underlying the GTP response and to determine possible Ca^{2+} sources using fluorochrome analysis. The results are presented in the manuscript "Ca^{2+} oscillations mediated by exogenous GTP in *Paramecium* cells: assessment of possible Ca^{2+} sources".

1.4.) Actin

Until the mid-1970's actin was thought of as primarily a muscle protein. In muscle cells, actin is involved in myofibrillar construction: filamentous actin is the main component of the thin filaments in sarcomeres. In striated muscle cells, actin reaches a concentration of ~20% of the total protein amount (DosRemedios et al., 2003). By now it is known that actin is one of the most abundant proteins in all eukaryotic cells. Already in 1975 a study showed that the organization of actin in the cytoplasm was radically altered as cells became cancerous (Weber et al., 1975). In fact actin is the major component of the cytoskeletal system of nonmuscle cells, taking part in a multitude of biological functions. Actin is involved in different steps during mitosis (division-plane localization, chromosome segregation), secretion, endocytosis and organelle transport; it determines cell shape, it is important for cytoplasmic streaming, cell motility and cell elongation, and actin filaments form cross-linked bundles, which provide mechanical support for various cellular structures and extensions (Reisler, 1993). In yeast, actin is essential for polarized cell growth (Novick and Botstein, 1985). All these processes rely on the property of the actin cytoskeleton to respond to a variety of cellular signals and reorganize spatially and temporally independent into a number of specific structures (see 1.4.6).

The elucidation of the amino acid sequence of actin provided a solid basis for all further actin research (Elzinga et al., 1973). In most eukaryotes, except the most primitive ones such as yeast, actin is encoded by a multigene family (Cleveland et al., 1980). A possible reason for this phenomenon is the important role of actin in cellular life. Mutations in actin would probably fatally interfere with many cellular processes. With multiple actin genes this problem is circumvented by redundancy. At the amino acid sequence level, the different actin isoforms produced by the members of one actin gene family are typically highly conserved, obviously due to their critical functional roles in cells (Villalobo et al., 2001). The slightly different proteins could be expressed in different tissues of an organism or at different stages during development.

Primary structures of actins from different eukaryotic species exhibit unusual high sequence identities. The amino acid sequence for human cytoplasmic actins compared to actin in the simplest eukaryote, brewers yeast, showed only 39 amino acid differences (Genbank). Comparisons of actin from other low eukaryotes to humans revealed that actin has a remarkably conserved amino acid sequence, probably more than any other protein (Li and Graur, 1991, Reece et al., 1992). Such stringent conservation in such divergent life forms is inconvenient. One can conclude from this phenomenon that the cellular role of actin and its

conserved three-dimensional structure is of fundamental importance for the survival of the eukaryotic cell.

1.4.1.) Crystal structure of actin

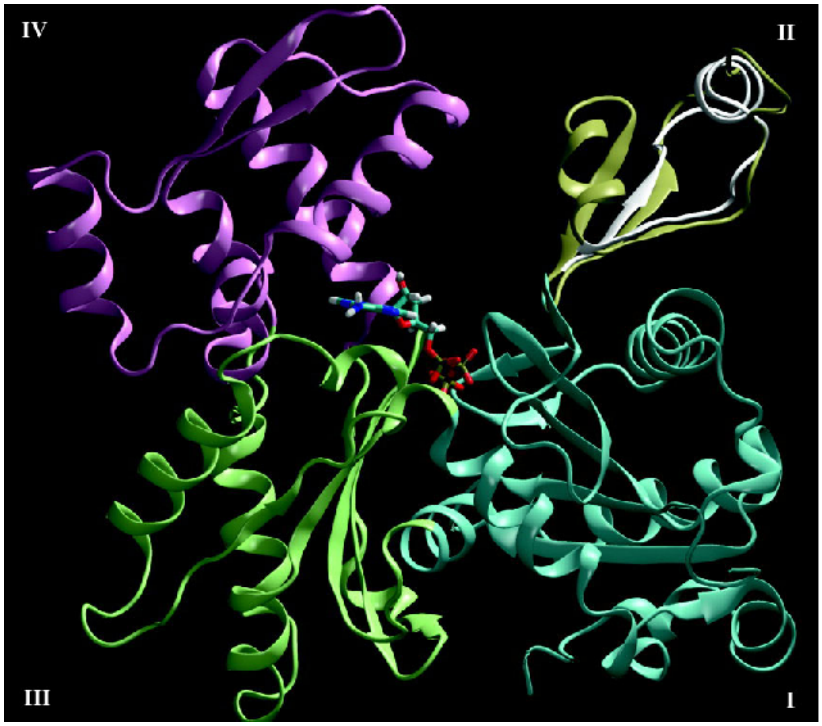

Fig. 7. A schematic representation of the x-ray structures of an ATP-bound actin monomer. Each subdomain of G-actin is colored differently, and the subdomain definition as introduced by Holmes *et al.* is used. Subdomain I, including the N- and C-terminus (residues 1–32, 70–144, and 338–375), is colored cyan; subdomain II (residues 33–69) is colored tan; subdomain III (residues 145–180 and 270–337) is colored lime; and subdomain IV (residues 181–269) is colored mauve. ATP is bound in the cleft between the subdomains. The x-ray structures of G-ADP are very similar to those of G-ATP except for the structure of the DNase I binding loop in subdomain II (see text). Residues 38–50 of subdomain II, including the DNase I binding loop of G-ADP, are overlaid with those of G-ATP and are shown in white (from Chu and Voth, 2005).

Actin consists of a single polypeptide chain of about 375 residues and an approximate molecular mass of nearly 43,000 Da. The amino acid sequence and biochemical properties of actin are highly conserved throughout evolution. First, crystallographic data indicated that the actin monomer is a globular protein consisting of two domains, called small and large domain, connected by a hinge region. Analysis with atomic resolutions (Kabsch et al., 1990) revealed that the two domains are not very different in size, with nearly equal numbers of

residues. Both, the amino- and carboxy-terminus of actin are located in the small domain which is made up of residues 1-144 and 338-375 (rabbit alpha-actin numbering). The large domain is built from residues 145-337. Each domain can be further subdivided into two subdomains. The small domain consists of subdomain 1 with the N- and C-terminus (residues 1-32, 70-144, and 338-375) and subdomain 2 (residues 33-69). The large domain comprises subdomain 3 (residues 145-180 and 270-337) and subdomain 4 (residues 181-269). The course of the polypeptide chain is very similar in subdomains 1 and 3, each having a repeating motif comprising a five-stranded beta-sheet consisting of a beta-meander and a right-handed beta-alpha-beta unit flanked by several alpha-helices (Kabsch & Vandekerckhove, 1992). About 40% of the structure is alpha-helical.

Subdomains 1 and 3 are thought to have evolved by duplication of an ancestral gene, and subdomains 2 and 4 may have been subsequently inserted into subdomains 1 and 3, respectively. The four subdomains are interconnected through a bound nucleotide and a metal ion residing in the cleft between the two domains (Kabsch et al., 1990). The tightly bound cation is directly associated with the phosphates of the nucleotide (Valentin-Rac et al., 1989). The nucleotide/cation complex is bound at the bottom of the cleft between subdomains 1 and 3, with the adenosine base resting in a hydrophobic pocket formed between subdomains 3 and 4. Theoretically, the four subdomains of actin can move independently or collectively, producing an opening and closing of the nucleotide cleft (Tirion et al., 1995). Allosteric interactions have been documented in the small domain between the DNase I loop (subdomain 2), the C terminus and the complex of the bound nucleotide and the tightly bound metal ion (Kim et al., 1995). This dynamic feature of actin structure would be important not only for the transformation of the globular actin monomer to the filamentous actin monomer during actin polymerization but also for actin filament dynamics. Monomeric actin binds 1 mol of ATP or ADP-P_i rather than ADP, which binds with lower affinity. In complex with the nucleotide, a divalent cation per mol of protein, either Mg^{2+} (K_d = 1.2nM) or Ca^{2+} (K_d = 0.12 nM), binds to the cleft. Actin is an Mg^{2+}-stimulated ATPase, with a single high affinity and several low affinity binding sites for divalent Mg^{2+}. At low salt concentrations, in which actin does not polymerize, the ATPase activity is low.

The property of monomeric actin to assemble under physiological salt concentrations to filamentous actin has so far prevented the crystallization of the uncomplexed monomer. The above shown structures have been derived from complexes of actin with deoxyribonuclease I (DNase I), gelsolin and profilin, all proteins that prevent polymerization.

1.4.2.) Actin isoforms

In vertebrates at least six actin isoforms are expressed in temporally and spatially regulated patterns. These highly conserved proteins have been classified by both their isoelectric point and primary tissue or cellular localization and comprise β and γ cytoplasmic, α skeletal, α cardiac and α and γ smooth muscle isoactins (Vandekerckhove & Weber, 1978).

These three main actin isotypes (alpha, beta and gamma) show >90% amino-acid (aa) homology between isotypes and >98% homology within members of a particular isotypic group. The isoforms differ little in sequence but have distinct expression patterns. The majority of the isotype heterogeneity is located in the amino-terminal 30 amino acids. The α-actins, mostly expressed in muscle cells where they are a major constituent of the contractile apparatus, differ in a few (mostly four to six) amino acids. β- and γ-actin, which are present in non-muscle cells, are different in just one amino acid and in 25 amino acids to α-actin genes (Doolittle, 1992). The β- and γ-actins co-exist in most cell types as components of the cytoskeleton and as mediators of internal cell motility. These cytoplasmic actins are evolutionary older than α-actins and also found in all cells of lower eukaryotes. In plants there are many isoforms which are probably involved in a variety of functions such as cytoplasmic streaming, cell shape determination, tip growth, graviperception, cell wall deposition, etc (Meagher and Williamson 1994; Meagher et al., 1999). The angiosperms contain complex and relatively highly divergent actin gene families comprising 8-40 genes (Bernatzky and Tanksley 1986a; Reece, McElroy, and Wu 1992; Moniz de Sa and Drouin 1996). More than 100 actin genes are present in the petunia genome, but most of them are thought to be pseudogenes (McLean et al. 1990).

The existence of multiple actin isoforms within tissues and even within a single cell suggests functional divergence among them. Actin isoforms exhibit different biophysical and biochemical properties under some experimental conditions in vitro (Allen et al., 1996; Just et al., 1994).

1.4.3.) Polymerization of actin monomers

Actin is a flexible molecule that exists in the cell as either a monomer, G-actin, or as a filamentous polymer, F-actin. In vitro, the former is obtained in low salt buffers while the latter is spontaneously formed upon addition of physiological concentrations of salt. G-actin provides the building blocks for filament assembly. The assembly of ATP-actin into filaments is initiated by a thermodynamically unfavorable nucleation step, in which two actin molecules must come together in a specific geometric conformation. As this dimer is more likely to rapidly dissociate to monomers than to assemble, several actin-binding proteins support that

nucleation step (see below). Addition of another monomer leads to a stable trimer, which is the nucleus for the elongation. Due to the arrangement of the asymmetric actin subunits in a specific orientation in the growing polymer, actin filaments have a polar structure. The ends of the filament are referred to as barbed and pointed according to the arrowhead-like appearance of myosin heads generated by decorating F-actin with heavy meromyosin or myosin subfragment 1 (S1). These ends correspond to exposed subdomains 1 and 3 and subdomains 2 and 4, respectively.

Incorporation of actin monomers into filaments stimulates the actin ATPase. When an actin molecule is incorporated into the filament, bound ATP is hydrolyzed to ADP. Nucleotide hydrolysis is not essential for polymerization of actin, but it is required for the normal function of F-actin. ATP-actin is added at a faster rate at the barbed end as compared to the binding to the pointed end of the filament. Because of this difference in the polymerization rate at the two ends, the critical concentration of G-actin differs, too: at the pointed end it is higher than at the barbed end. This behavior leads to the phenomenon known as treadmilling (Fig. 8; Selve and Wegner, 1986). In this steady state, at a given concentration of free actin, a net loss of actin molecules at the pointed end and a simultaneous net gain of monomers at the barbed end can be observed. As both actions level each other, the net length of the filament does not change. But importantly, this phenomenon creates a net flow of individual actin monomers through the filament, with monomers newly incorporated at the barbed end being translocated to the other end and released there. This allows for dynamic turnover of actin filaments.

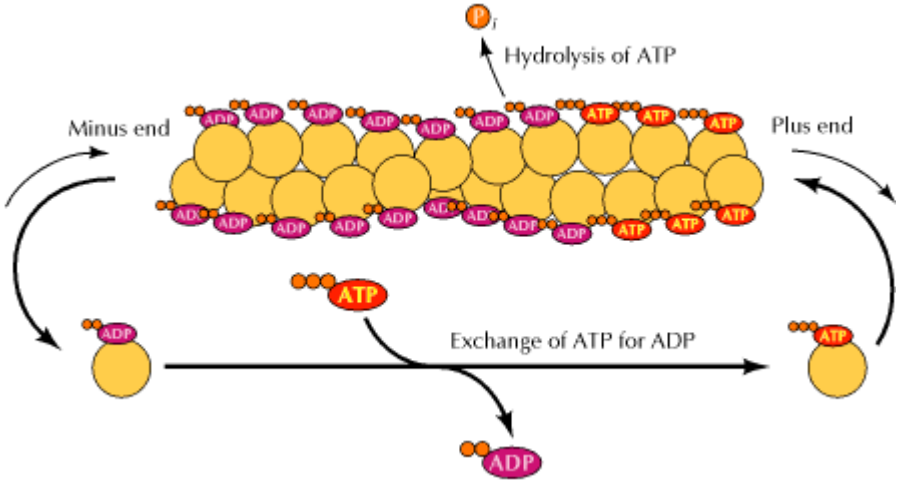

Fig. 8. Treadmilling of actin filament. After incorporation from ATP-actin into the filament, the ATP is hydrolyzed to ADP. Net addition of ATP-actin at the plus end and net loss of ADP-actin at the minus end allows dynamic turnover of the actin filament (from Cooper 2000, The Cell, 2nd Edition).

The release of phosphate after the hydrolysis of ATP to ADP of newly incorporated monomers proceeds more slowly than the formation of the filament. This leads to a cap of ATP-actin at the barbed end of the growing filament, carrying newly incorporated F-ATP subunits, while monomers containing ADP and phosphate transiently accumulate in the rest of the filament (Carlier et al., 1991). The hydrolysis during polymerization leads to a conformational change of the incorporated actin molecules and subsequent destabilization of the filament. These nucleotide-dependent allosteric changes might underlie the difference in the monomer-monomer affinity between ATP-monomers and ADP-monomers. Different studies have revealed that this conformational change is directly linked to subdomain 2, in particular the DNase- I-binding loop, and to the C-terminal area in subdomain 1 (Orlova and Egelman, 1992; Muhlrad et al., 1994). ADP-G-actin slowly but reversibly undergoes a conformational transition (Drewes & Faulstich 1991). Thus, the release of the inorganic phosphate is related to the destabilization of the filament and promotes its disassembly. ADP-actin filaments exhibit also a higher susceptibility to depolymerizing proteins (Pollard et al., 2000). The fact that these proteins can “distinguish” between ATP- and ADP-actin reinforces the assumption that these two states are structurally different. Dissociated ADP-actin subunits rapidly exchange their bound ADP for ATP.

As filaments are formed, the concentration of available monomers drops to the critical concentration of G-actin, the point at which the net rates of filament assembly and disassembly are equal. Below this critical concentration actin assembly cannot proceed and assembled filaments begin to depolymerize. The critical concentration in the cell is influenced by certain actin binding proteins and/or actin ligands. Judging from the polymerization properties of actin in vitro, most of the monomeric actin in cells must be sequestered by actin binding proteins and thereby reversibly hindered from assembling into filamentous actin.

1.4.4.) Structure of the actin filament

Till now, the structure of the actin filament is not yet resolved at atomic resolution. Electron microscopy and X-ray fiber diffraction have shown that F-actin consists of two parallel protofilaments interwoven with each other to form a tow-start long-pitch double helix which is right-handed (Pollard et al., 2000). They are related to each other by an axial rise per monomer of 27.5 A and a rotation angle of -166.2° around the filament axis (Holmes et al., 1990). The actin subunits in the two-start helix have an approximate 55 A spacing between center to center. The large domain of an actin monomer is located near the central axis of the filament, and the small domain is at a large radius from the filament axis. In the middle of the fiber, the density is low. The N-terminus of actin is well exposed at a large radius.

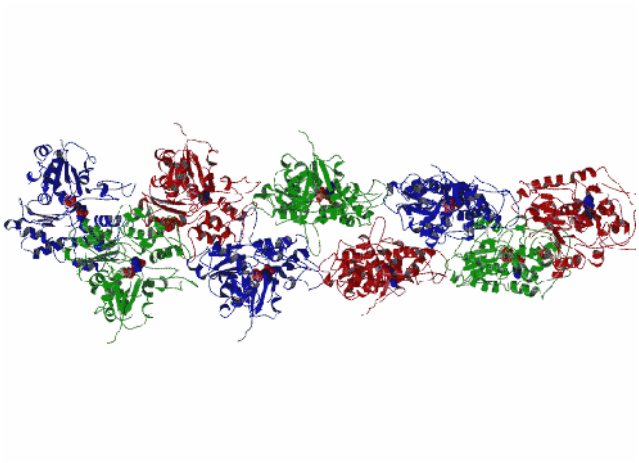

Fig. 9. Lorenz model of F-actin (Lorenz et al., 1997).

In the filament, each actin subunit is surrounded by four others. Extensive interactions occur between molecules along the long-pitch actin helix. About 45 residues are involved in actin-actin interactions. Subdomains 2 and 4 of one actin monomer have actin-actin interfaces interacting with subdomains 1 and 3 of the other actin monomer. A model by Egelman et al. (1982) suggested an unusual property for F-actin with incorporated actin monomers having the ability to rotate within the filaments, although the axial rise per subunit is quite fixed.

According to the observations collected so far about the structure of the actin filament, it is considered not to be a rigid structural element, but as a dynamic, responsive structure. Depending on the isoform of actin, the type of bound nucleotide and cation, and the presence of other proteins bound to actin, it can exist in multiple conformations (DosRemedios et al., 2003).

1.4.5.) Actin-binding proteins

Many processes important for the viability of eukaryotic cells depend upon the capacity of actin to be restructured in a controlled manner by polymerization, depolymerization, cross-linking and anchorage. All motility processes involving actin are controlled by the interaction in the G- or the F-form with a large number of actin-binding proteins (abps). Actin remodeling is influenced in different ways, resulting in a variety of actin filament structures. More than 160 abps that can control filament dynamics and participate in the assembly, disassembly, and rearrangement of the cytoskeleton have been identified (DosRemedios et al., 2003). These proteins are generally classified according to their effects on actin organization in vivo and in vitro. For instance, some abps connect the filaments with each other and form bundles or two- and three-dimensional web-like networks of F-actin (e.g. alpha-actinin). Other abps affect monomers by controlling sequestration or nucleotide exchange and thus maintain a pool of monomers in solution and hinder polymerization (e.g., profilin). There are abps that sever filaments and bind to the barbed ends, affecting F-actin turnover (e.g., gelsolin). Other abps control filament formation and stability by capping one of the ends of the filament (e.g., CapZ capping the barbed end, tropomodulin capping the pointed end of F-actin), thereby preventing the incorporation of G-actin. Moreover, abps can bind to F-actin

and accelerate filament disassembly (e.g., ADF/cofilin) or move along the filaments (e.g. myosins). Finally, small GTPases and cellular signaling molecules control actin remodeling by regulating the activities of abps and numerous direct and indirect effectors (Hartwig et al., 1991; Vandekerckhove, 1990; DosRemedios et al., 2003).

The geometry and internal dynamics of actin filaments might be functionally important in the interaction between F-actin and many actin-binding proteins. In addition, it was also possible to recognize smaller entities as actin-binding domains, linking the actin-binding activities with cellular signals. This efficient protein machinery can provide a fast response to extracellular stimuli. This is required for the rapid polymerization or depolymerization of actin filaments in the cell, for example under the leading membrane edge. The inventory of discovered actin-binding proteins is still growing steadily. Most families of abps have been widely conserved over phylogeny, in both amino acid sequence and biochemical properties, and they can be found in diverse organisms from humans to yeast (Pollard et al., 2001). However, the protist abps described so far seem to be somehow different (Villalobo et al., 2001; Morrissette and Sibley, 2002). The complexity of abps might well reflect the need of the cell to provide sufficient redundancy for maintaining crucial cellular functions. For instance, deletion of several actin regulatory proteins by mutagenesis often had no detectable effect on the cell, although those proteins were thought to be essential for actin organization and conserved throughout various species (Noegel and Schleicher, 1991).

1.4.6.) Functional role of F-actin

Although actin is a slow ATPase, the important function of it is not an enzymatic one. Even though it does inhibit DNase I and activate the myosin ATPase, actin has no relevant enzymatic activity. The momentous role of actin lies in its structural and dynamic role as a major component of the cytoskeleton in the cell. This property depends on its capacity to assemble and disassemble a variety of filamentous structures. Actin can form bundles or networks. In actin bundles, the filaments are parallel to each other by actin-bundling proteins. Other abps cross-link actin filaments to different types of networks. Actin networks are continuously reorganized in cells that rapidly change their shape. The dynamics of actin filaments is of primary importance for actin functions in the cell. Rapid filament assembly and disassembly is required for quick remodeling of the actin cytoskeleton in response to changing stimuli.

Actin filaments form an integral part of the structural framework that supports the plasma membrane of the cells while providing a platform for signaling and metabolic proteins. A variety of cellular organelles are held in place by the actin cytoskeleton, while on

the other hand the actin-driven process of cytoplasmic streaming is a well documented example of cytoskeleton-driven organelle movement (Fehrenbacher et al., 2003).

In addition to its structural role providing support for the cell, actin is also an important element in cellular motility. Movement of myosin along actin filaments produces force for muscle contraction, and amoeboid locomotion is brought about by the continuous assembly and disassembly of actin and myosin containing complexes in pseudopodia at the front end of a moving cell. Amoeboid cell motility plays a vital role in physiological and pathological processes ranging from embryonic development and immunological defense to tumor metastasis. In protozoan parasites related to *Paramecium*, like *Toxoplasma gondii*, filamentous actin is essential for gliding motility and cellular invasion of the host cell (Dobrowolski and Sibley, 1996). The bacteria *Listeria* hijack the biochemical cell machinery to move within cells. It forms tails made from the host cell's actin and these tails are used to propel the bacteria throughout the cell.

The view on the role of actin during endo- and exocytosis has changed in the recent years. As the actin network beneath the plasma membrane, the cortical actin, was long thought to build a barrier for endo- or exocytotic vesicle trafficking, cortical actin patches are now considered an integral part of the endocytotic machinery (Yarar, 2003). Actin may provide the force for the movement of endocytotic vesicles into the cytosol (Ayscough, 2005). In exocytotic systems, secretory granules were rapidly coated with F-actin during exocytosis, and it has been proposed that this actin coating facilitates the movement of granules across the actin network toward their fusion site (Valentijn *et al*., 2000, Nemoto et al., 2004). Intact actin filaments may be required for the transport of secretory graules to exocytotic sites (Oheim and Stuhmer, 2000; Lang et al., 2000). Actin also plays a role in the achievement of membrane homeostasis. The increased cell surface area, that results from stimulated exocytosis of large numbers of secretory vesicles, is compensated through endocytosis of membrane components. Actin filaments are important in secretory membrane recycling by providing the force for the membrane invagination or the pinching of the endocytic vesicles (Jeng and Welch, 2001, Schafer, 2004).

Actin is also found in the nucleus, where actin rods, bundles and tubules have been described by a number of investigators. Numerous reports link nuclear actin to the phenomenon of chromatin remodeling (Olave et al., 2002), whereas new studies implicate a role of actin in telomere clustering (Trelles-Sticken et al., 2005). Actin also plays a role in the mechanisms of nuclear positioning. Several proteins are discussed to play a role in the anchoring of nuclei, by directly or indirectly tethering the nuclear envelope to the actin cytoskeleton (Starr and Han, 2003; Padmakumar et al., 2005).

Various enzymes interact with actin. Together with the other components of the cytoskeleton, it may help to organize cellular processes in space as well as in time.

1.4.7.) Actin drugs

Actin binds about 30 ligands, including drugs and toxins. The most frequent approach to studies of actin participation in cell functions is manipulation of the cytoskeleton by actin-specific drugs. They can act both as filament stabilizing or filament destabilizing agents. The best-established ones are phalloidins and cytochalasins (Cooper, 1987).

Cytochalasins. The cytochalasins are a group of membrane permeable fungal metabolites. These fungal toxins are related by chemical structure. All are characterized by a highly substituted hydrogenated isoindole ring to which is fused a macrocyclic ring which varies between the different cytochalasins. Cytochalasin A and B are metabolites of the fungus *Drechslera* (previously *Helminthosporium*) *dematioideum*; cytochalasin C and D are isomeric metabolites of *Metarrhizium anisopliae*, cytochalasin E is a metabolite of *Rosellinia necatrix*, and cytochalasin H and J are metabolites of *Phomopsis paspali* found on *Paspalum scrobiculatum* Linn.. Cytochalasins bind to the barbed end of actin filaments where the rapid polymerization takes place (Cooper, 1987). This prevents both association and dissociation of subunits at that end. The stoichiometry of binding is about one cytochalasin per actin filament (Flanagan and Lin, 1980). They inhibit polymerization of actin in response to cell activation, but usually do not deplete cellular F-actin (Pendleton and Koffer, 2001). In addition to binding actin, cytochalasins A and B also inhibit monosaccharide and some other transport phenomena across the plasma membrane.

Phalloidin. Phalloidin is a bicyclic heptapeptide isolated from the poisonous mushroom *Amanita phalloides*. It binds to actin filaments in a 1:1 drug:actin protomer molar ratio (Steinmetz et al., 1998). But one phalloidin molecule interacts with more than one, most likely three, actin protomers in an actin filament (Oda et al., 2003). As a result, actin filaments became strongly stabilized. The equilibrium between filament and monomers shifts toward filaments, lowering the critical concentration for polymerization. Phalloidin is not permeant through the cell membrane. The phalloidin binding site was determined by Lorenz et al. in 1993. The usage of a fluorescent derivate of phalloidin is a common approach to visualize the actin cytoskeleton of a cell without the use of specific antibodies.

Jasplakinolide. Originally jasplakinolide was isolated from marine sponge *Jaspis johnstoni*. Chemically, it is a cyclo-depsipeptide containing a tripeptide moiety linked to a polypeptide chain. Jasplakinolide, hast a similar effect and binding site on F-actin as phalloidin, and is cell permeant (Bubb et al., 1994).

Latrunculin A. The marine toxin latrunculin A is isolated from the Red Sea sponge *Negombata magnifica*. It is a macrolide attached to a 2-thiazolidinone moiety. With monomeric actin, it forms 1:1 stoichiometric complexes which do not participate in the elongation of actin filaments (Yarmola et al., 2000). The observed effect is a depolymerization of actin filaments consequent to sequestration of monomeric actin by latrunculin (Spector et al., 1989). Over a period of time, latrunculin depletes cellular F-actin; the rate of this process depends on the rate of filament turnover (Maekawa et al., 1999). On a biochemical level, latrunculin A inhibits adenine nucleotide exchange on actin. It may limit the flexibility of the cleft between subdomain 2 and 4, trapping nucleotide and subsequently inhibiting the nucleotide exchange (Yarmola et al., 2000). Latrunculin A is membrane permeable.

1.4.8.) Possible roles of actin in SOCE

Secretion-like coupling between elements in the plasma membrane and Ca^{2+} stores has been proposed as the most likely mechanism to activate SOCE in several cell types. Membrane-associated actin network prevents constitutive Ca^{2+} entry. A possible role for the dense layer of submembrane cortical actin could be to put up a barrier preventing constitutive SOCE. This inhibitory effect of the cortical actin cytoskeleton on SOCE has been shown in platelets (Rosado et al., 2000), corneal endothelial cell (Xie et al., 2002) and pancreatic acinar cells (Redondo et al., 2003). A common approach to investigate the possible role of actin cytoskeleton on the SOCE pathway is the use of toxins which modify the actin cytoskeleton which is continually being turned over by polymerization and depolymerization. Such drugs can either stabilize actin filaments and thereby enhance actin polymerization (jasplakinolide), or inhibit actin polymerization and therefore leading to a progressive dismantling of the cytoskeleton (such as cytochalasin D or latrunculin A). A study on myocytes showed that CCE was enhanced when F-actin disrupting agents were present whereas it was reduced by treatment with F-actin stabilizing agent (Morales et al., 2005). These finding support a conformational coupling model with an active participation of actin reorganization in the implementation of CCE. In contrast, studies on human hepatocellular carcinoma cell line HepG2 (Rosado et al., 2001), glioma C6 cells (Sabala et al., 2002) and human pulmonary arterial endothelial cells (Mehta et al., 2003) revealed an inhibitory effect of actin disrupting drugs, while in human platelets (Rosado et al., 2000) and pancreatic acinar cell (Redondo et al., 2003) only a partial abolishment could be observed. Other studies on a basophilic cell line (Bakowski et al. 2001) and corneal endothelial cells (Xie et al. 2002) reported that

cytochalasin D did not affect SOCE at all. Cortical actin may also be involved in SOCC internalization (Itagaki et al., 2004), which results in the attenuation of SOCE.

Another role is suggested for the more diffuse cytosolic actin network. Such filaments could provide a support for intracellular trafficking. New actin polymerization may support membrane trafficking towards the plasma membrane (Rosado et al., 2004). Drugs like latrunculin A or cytochalasins, which inhibit actin polymerization, can disrupt this process.

Possible reasons for the variable effectiveness of the agents employed had been discussed. One point is that the architecture of the actin cytoskeleton varies between different cell types. In cell types with a strong dense layer of cortical actin, a dynamic reorganization might be required to facilitate coupling between proteins in the plasma membrane and in the Ca^{2+} store membranes. Such a reorganization of the subplasmalemmal actin network has been shown to be essential for the transport of exocytotic granules to the apical membrane in specialized secretory cells (Muallem et al., 1995, Malacombe et al., 2004, Gasman et al., 2004). In contrast, in cells with a more evenly distributed cytoskeleton, a reorganization of actin might not be necessary. In agreement with this, actin polymerization might not be necessary for the activation of SOCE in smooth muscle cells, which do not posses a dense cortical layer of actin (Patterson et al., 1999). Another point is that, although turnover of the actin cytoskeleton is seen in all cells, the rate of the process varies widely not only between different cell types, but also depending on other factors such as cell cycle status. Altogether, the variability could reflect cell-specific differences in the dynamics and architecture of the cytoskeleton. It is hardly possible to draw conclusions from the above mentioned studies to a potential role of the actin cytoskeleton on SOCE in a yet not investigated species, as it depends much on the specific cell structure and actin organization.

1.4.9.) Actin in *Paramecium*

Different approaches have been tried so far to localize actin in *Paramecium*. With DNase I and heavy meromyosin, labeling of cilia, ciliary basal bodies and a diffuse label of deeper layers could be observed (Tiggemann at al., 1981). Localization of actin in living cells was achieved by microinjecting fluorescent phalloidin (Kersken et al., 1986a). Again the ciliary basal bodies were labeled, together with the labeling of a thin cortical layer and ridges of the characteristic “kinetid” surface pattern. This occurrence of actin in the cortex of *Paramecium* was confirmed by Cohen and Beisson (1988). Additionally, structures around the oral cavity and the surface of food vacuoles were labeled (Kersken et al., 1986a, b). Labeling of these structures were already shown with HMM and S1 fragments (Cohen et al., 1984). Corresponding with these observations, cytochalasin B inhibited phagocytosis in *Paramecium*

(Cohen et al., 1984; Allen and Fok, 1985: Fok et al., 1985; Allen et al., 1995; Zackroff and Hufnagel, 2002). None of the efforts so far could proof the occurrence of actin in the cleavage furrow of a dividing cell, despite the fact that actin is unequivocally involved in cell division. It was neither stained by affinity labeling with phalloidin (Kersken et al., 1986a), nor was cytokinesis effected by cytochalasin B (Cohen et al., 1984).

In 1998, Diáz-Ramos et al. cloned an actin gene fragment of 1,138 bp, more than 96% of the coding sequence of a standard actin gene. As it was mostly homologous to α-actin of other organisms, it was called α-actin, although the position of its two small introns is unique in the intron catalogue of actins (with α-smooth human actin as guide sequence, Weber and Kabsch, 1994). With a pilot genome project, another actin coding gene fragment of ~600 bp could be identified in *Paramecium*, with homology to β-actin of other organism. In the diploma work of Wagner E. (2002), both sequences were completed and additionally two more α-actins and another β-actin were identified, at this moment called Ptα-actin 1, Ptα-actin 2, Ptα-actin 3, and Ptβ-actin 1 and Ptβ-actin 2. Against Ptα-actin 1, polyclonal antibodies were raised and investigated in Western Blot analysis and immuno-localization on LM an EM level. The obtained data is presented in the manuscript **"**Immunolocalization of Actin in *Paramecium* Cells".

Cortical actin could play, as previously discussed, a role in SOCE mechanism. Regarding this hypothesis in *Paramecium*, it would mean that cortical actin could be involved in the positioning of the alveolar sacs close to the plasma membrane. The identity of the short structures connecting the membrane of the alveoli with the plasma membrane is still unknown. The organization could be similar to the spectrin network in erythrocytes, where short actin filaments build up a complex with other proteins to anchor the spectrin network to the plasma membrane. This hypothesis was investigated in the diploma work of Sehring I. M. (2002). Consequences of incubation with cytochalasin B on the positioning of alveolar sacs were investigated on the EM-level, whereas effects on the function of alveolar sacs were investigated with calcium analysis during exocytosis. In both cases, no effect of the drug could be observed. As the sensitivity of *Paramecium* to drugs often varies from that of mammalian cells (Zackroff and Hufnagel, 1998), results obtained by different approaches with actin drugs may be crucial. With the ongoing genome project revealing more and more actin isoforms in *Paramecium*, it was also debatable whether all of them would be recognized by common actin drugs. The failure to label the cleavage furrow with fluorescent phalloidin points in that direction. Possibly also an assumed actin isoform involved in the positioning of alveolar sacs is not sensitive for cytochalasin. This could be the reason why no effect on

calcium signaling could be observed. Therefore, before any further analysis of calcium dynamics and a possible involvement of actin appeared feasible, it was necessary to identify and characterize all actin isoforms in *Paramecium*. The genetic characteristics of the actin family are described in the manuscript "The actin multigene family of *Paramecium tetraurelia*", while data obtained with localization studies using antibodies and GFP constructs, and functional studies using RNAi, are presented in the manuscript "A broad spectrum of actin paralogs in *Paramecium tetraurelia* cells displays differential localization and function".

Chapter 2: Manuscript I

Ca^{2+} oscillations mediated by exogenous GTP in *Paramecium* cells: assessment of possible Ca2+ sources

Ivonne M. Sehring and Helmut Plattner*

Universität Konstanz
Fachbereich Biologie
Universitätsstraße 10
D-78457 Konstanz, Germany
Tel.: 0049-7531883712
Fax.: 0049-7531882245

*) Author for correspondence: helmut.plattner@uni-konstanz.de
Published in: Cell Calcium 36, 409-420.

2.1.) Summary

We applied exogenous guanosine trisphosphate, GTP, to *Paramecium tetraurelia* cells injected with Fura Red for analyzing changes of free intracellular Ca^{2+} concentrations, $[Ca^{2+}]_i$, during periodic back-/forward swimming thus induced. Strain *ginA* (non-responsive to GTP) shows no Ca^{2+} signal upon GTP application. In strain *nd6* (normal Ca^{2+} signaling) an oscillating $[Ca^{2+}]_i$ response with a prominent first peak occurs upon GTP stimulation, but none after mock-stimulation or after 15 min adaptation to GTP. While this is in agreement with previous electrophysiological analyses, we now try to identify more clearly the source(s) of Ca^{2+}. Stimulation of *nd6* cells, after depletion of Ca^{2+} from their cortical stores (alveolar sacs), shows the same Ca^{2+} oscillation pattern but with reduced amplitudes, and a normal behavioral response is observed. Stimulation with GTP, supplemented with the Ca^{2+} chelator BAPTA, results in loss of the first prominent Ca^{2+} peak, in reduction of the following Ca^{2+} amplitudes, and in the absence of any behavioral response. Both these observations strongly suggest that for the initiation of GTP-mediated back-/forward swimming Ca^{2+} from the extracellular medium is needed. For the maintenance of the Ca^{2+} oscillations a considerable fraction must come from internal stores, probably other than alveolar sacs, rather likely from the endoplasmic reticulum.

2.2.) Introduction

Ca^{2+} regulates many cellular processes, like stimulated secretion by exocytosis, gene transcription, cell division (Verkhrastky and Toescu, 1998; Berridge et al., 1998; Berridge et al., 2000; Berridge et al., 2003), and ciliary activity (Eans and Sanderson, 1999; Lansley and Sanderson, 1999; Salathe and Bookman, 1999; Zhang and Sanderson, 2003). The origin of a Ca2+ signal can be manifold, e.g., influx from the outside medium and/or release from internal stores by widely different signaling mechanisms (Verkhrastky and Toescu, 1998; Berridge et al., 2000; Berridge et al., 2003; Barrit, 1999).

As in mammalian cells, these aspects also occur in ciliated protozoa including *Paramecium* (Plattner and Klauke, 2001). In these cells, the normal intracellular free Ca^{2+} concentration, $[Ca^{2+}]_i$, mediates normal ciliary beat during forward swimming, while increase of $[Ca^{2+}]_i$ in cilia causes beat reversal and backward swimming (Machemer, 1988; Machemer and Teunis, 1996; Preston, 1990). A reversal reaction is easily observed during depolarization-induced activation of voltage-dependent Ca^{2+} channels in the ciliary membrane (Naitoh and Eckert, 1969; Naitoh, 1995). But spill-over from cortical regions during exocytosis stimulation can also produce ciliary reversal (Plattner et al., 1985; Husser et al., 2004). In many cell types $[Ca^{2+}]_i$ can oscillate with widely different periodicity (from the sub-second range to hours), either spontaneously, or after different exogenous triggers, with the involvement of widely different signal transduction pathways (Petersen and Wakui, 1990; Tsien and Tsien, 1990).

In *Paramecium* the discovery has been made that exogenous guanosine trisphosphate, GTP, causes periodic back- and forward swimming, paralleled by oscillating Ca^{2+} currents (Clark et al., 1993). This observation has been extended to the related species, *Tetrahymena* (Kuruvilla et al., 1997). Evidence has been found that during GTP stimulation Ca^{2+} may in part come from the outside and in part from internal stores. Among them the cortical Ca^{2+} stores (alveolar sacs) have been envisaged (Wassenberg et al., 1997).

From this, the occurrence of surface receptors for GTP has been inferred in *Paramecium* (Kim et al., 1997; Mimikakis and Nelson, 1998; Wood and Hennessey, 2003) and *Tetrahymena* (Kuruvilla et al., 1997; Kim et al., 1999; Rosner et al., 2003). The typical receptor property, i.e., adaptation (VanHouten, 1994; Torre et al., 1995), has also been observed with GTP in *Paramecium* (Kim et al., 1997) and *Tetrahymena* (Kuruvilla et al., 1997). By definition, receptors would have to be of the purinergic type. For GTP this is remarkable, as up to now from other cells such receptors are known only for ATP, ADP, UTP, and UDP (Burnstock, 2003; Schwiebert, 2003). In contrast, in *Paramecium* GTP is ~1000 times more potent than ATP (Mimikakis and Nelson, 1998). Only the non-

hydrolysable β-y-methylene ATP analogue can produce a similar effect in *Paramecium* Kim et al., 1999).

If one considers a purinergic receptor for GTP in *Paramecium*, one would also have to consider the existence of different subtypes. This would include those represented (i) by multimers formed from units with two membrane-spanning domains, and those (ii) with seven membrane-spanning domains, as known from higher eukaryotes (Schwiebert, 2003; Braunstein and Schiwebert, 2003; Lazarowski, 2003). The first type is reported to form ion channels with low specificity (Boyce and Schwiebert, 2003). This may account for the well known permeabilising effect of exogenously added nucleoside trisphosphates (Boyce and Schwiebert, 2003). This can induce Ca^{2+}-dependent processes, such as exocytosis (Gomperts and Tatham, 1988), provided Ca^{2+} is in the medium. The second type is involved in signal transduction by coupling to trimeric G-proteins, followed by activation of either adenylate cyclase or phospholipase C (PL-C) and formation of the Ca^{2+}-mobilising agent, inositol 1,4,5-trisphosphate ($InsP_3$), (Lazarowski, 2003).

None of these molecules and pathways is established in *Paramecium* on a molecular level. Therefore, analysis of GTP-mediated effects on Ca^{2+}-based swimming behavior necessarily remains, though functionally stringent, on a merely descriptive level at this stage. However, by a more detailed analysis of the phenomena and by inclusion of Ca2+ imaging technology, we here try to set a new baseline, considering the rapidly expanding molecular biology work with *Paramecium*. Essentially we use fluorochrome imaging to localize Ca^{2+} signals under conditions of varying extracellular Ca^{2+} concentrations, $[Ca^{2+}]_o$, and we also deplete alveolar sacs of their Ca^{2+} before subsequent GTP stimulation. We aim at dissecting more clearly the different components of the GTP-mediated Ca^{2+} signals.

2.3.) Materials and methods

2.3.1.) Cell materials

Paramecium tetraurelia cells, mutant *nd6* (without trichocyst discharge (Lefort-Tran et al., 1981), were cultured in dried lettuce medium, monoxenically inoculated with *Enterobacter aerogenes* as feeding bacteria, at $[Ca^{2+}]_o$ = 50_M. In addition we used the mutant *pawnB* (Kung, 1971) and *ginA* (Mimikakis et al., 1998). All cell lines used additionally contained the *nd6* mutation. Both, non-discharge (*nd*) and *pawn* properties (lack of ciliary reversal reaction upon depolarization) were tested before use: (i) by adding the secretagogue aminoethyldextran, AED (40 kDa, 1-$NH3^+$/kDa [17]), and (ii) by chemical depolarization by adding 20mM KCl, respectively.

2.3.2.) Stimulation conditions

For $[Ca^{2+}]_i$ analysis, cells where washed in 1mM HEPES buffer adjusted to pH 7.2 with Tris. The solution was supplemented with 1mM KCl and 1mM Ca^{2+} (modified after Clark et al., 1997). Eventually lower values of $[Ca^{2+}]_o$ where achieved by adding the ultrafast Ca^{2+}-chelator, BAPTA (time constant = 0.5_s [42]), to the trigger solution to produce $[Ca^{2+}]_o$ of ~30 nM, i.e., slightly below $[Ca^{2+}]_i$ at rest (~65nM [Klauke and Plattner, 1997]). Aliquots were stimulated by AED to deplete cortical Ca^{2+} stores (Hardt and Plattner, 2000) before GTP was added within $\leq$3 min.

Cells were stimulated by adding, through a pipette, GTP (in 10mM Tris buffer, pH 7.2) to the medium at the anterior pole of individual cells. The actual concentration of GTP reaching the cell surface was estimated from the dilution after release from the microcapillary as 15 _M, according to the approach previously described (Klauke and Plattner, 1997). Although this is slightly above the 10 _M generally used in the *Paramecium* literature, in fact, slightly higher concentrations are required for maximal stimulation (Mimikakis et al., 1998).

Mock applications were performed with buffer, without GTP added to the trigger solution. $[Ca^{2+}]_o$ was eventually reduced to a calculated value of ~30nM by adding BAPTA to the stimulation medium - not before. Simultaneous application of stimulant and the Ca^{2+} chelator, BAPTA free acid, is an established method that avoids cell damage (Klauke et al., 2000).

2.3.3.) Ca^{2+} fluorochrome analysis

Cells loaded by microinjection with the Ca^{2+} fluorochrome Fura Red were stimulated and evaluated in a conventional light microscope by 2λ analysis, as previously described (Klauke and Plattner, 1997; Klauke et al., 2000). Fura Red was used at a concentration to yield an

intracellular concentration of ~50 µM. In the f/f_0 ratio analysis, any fluorescence readings during stimulation (f) are expressed as a ratio referred to the reading at rest, time t_0 (f_0), just before stimulation. The ratio method allows measurements of $[Ca^{2+}]_i$ independently from fluorochrome concentration in the cell. The maximum emission of Fura Red upon excitation is 650 nm. For excitation, wavelengths of 440 and 490 nm are used and the ratio of emission at both wavelengths is calculated. Thus, interference from auto-fluorescence and effects from shape change are eliminated [46], although the time required for filter changes (1.5 s per final data point) restricts time resolution. We recorded f/f_0 ratios over a time period of up to 1 min.

$[Ca^{2+}]_i$ analysis was performed at the cortical site (below cilia) where the stimulus had been applied. A frame of ~3× 10 µM was adjusted to such an area, just as in our previous work (Klauke and Plattner, 1997; Klauke et al., 2000).The f/f_0 ratios thus obtained were evaluated by the ANOVA test which allows statistical comparison of several data sets. Usually, per data set shown, the time course of five cells (unless indicated otherwise) has been analyzed by this point-per-point digital analysis.

2.4.) Results

2.4.1.) Compatibility with previous electrophysiological and behavioral analyses

Before analyzing new aspects by Ca^{2+}-fluorochrome imaging we tried to reproduce important aspects of GTP-mediated Ca^{2+} signaling in *Paramecium*, as reported from electrophysiological work. These analyses have been conducted in presence of extracellular Ca^{2+}, $[Ca^{2+}]_o$ = 1 mM. We measured f/f_0 ratios in a cortical region adjacent to the stimulation site, as specified in 2.3.3.

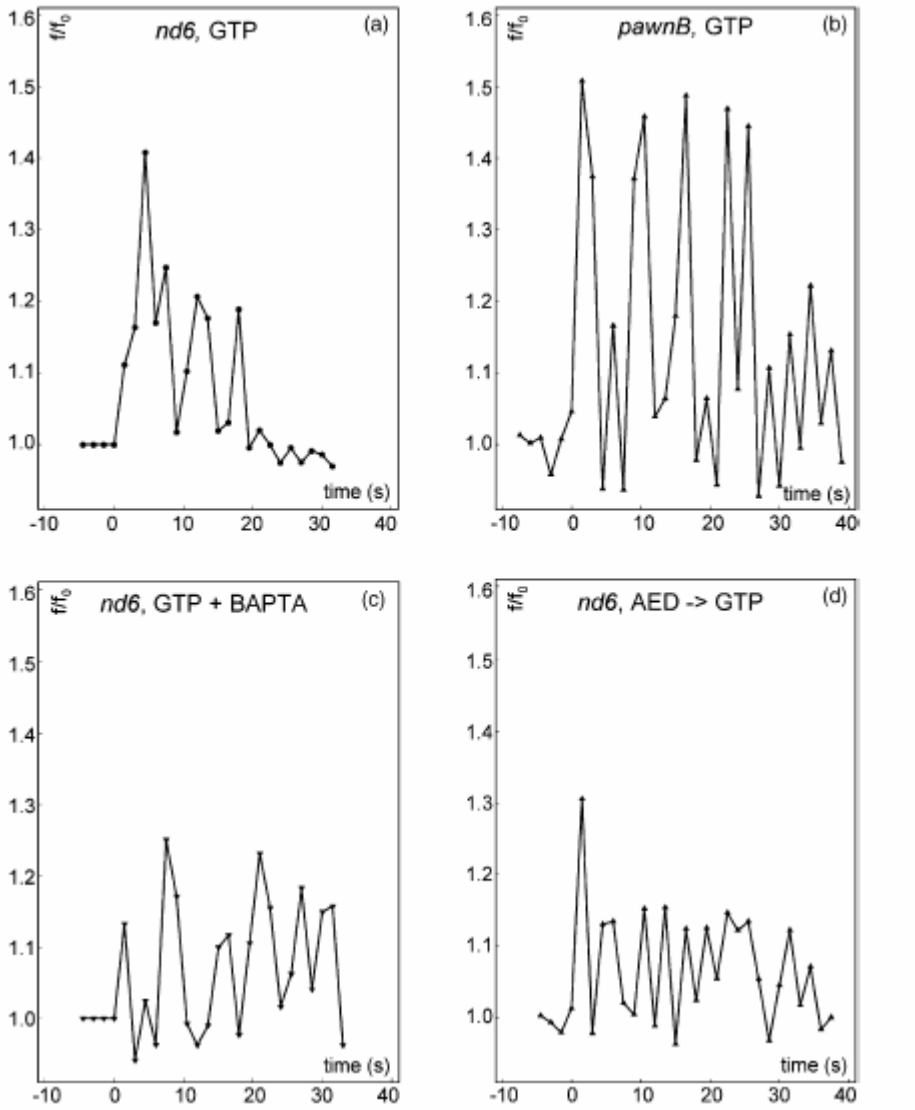

Fig. 1. Examples of Fura Red *f*/*f*0 recordings during GTP stimulation in *nd6* (a, c, d) and *pawnB* (b) cells under the conditions indicated. GTP was added to the cells at *t* = 0 s, usually in presence of Ca2+ (a, b, d), while in (c) BAPTA was added to the GTP stimulant, as specified in Section 2. In (d) AED was applied shortly before GTP stimulation (but after decay of the AED-mediated Fura Red *f*/*f*0 signal shown in Fig. 5d) to probe the response to GTP when alveolar sacs were depleted of most of their Ca2+. Note the eventual occurrence of a predominating first peak (a, d) which becomes more clear in the statistical evaluations shown in Fig. 3.

In all strains we analyzed (except *ginA*), GTP-induced $[Ca^{2+}]_i$ oscillations with a period of about 7 s (Figs. 1 and 2). This is within the frame of previous work, with periods of about 5–10 s (Wassenberg et al., 1997; Mimikakis and Nelson, 1998; Mimikakis et al., 1998; Clark et al., 1997), always depending on whether smaller peaks are also taken into consideration. Occurrence and absence of oscillating Ca^{2+} signals strictly correlates with the occurrence and absence of periodic ciliary reversal, respectively, interrupted by forward swimming (Table 1), also as reported in previous work on GTP stimulation. In *nd6* cells, for unknown reasons, adaptation to GTP reduces the oscillation frequency (an aspect not pursued here). Any further variation to this reaction pattern is specified in Table 1. Our findings include the occurrence of periodic $[Ca^{2+}]_i$ fluctuations in *nd6* cells as well as in both *pawn* strains analyzed, *pawnA* (not shown) and *pawnB*. The intensity (f/f_0) of GTP-induced $[Ca^{2+}]_i$ signals is evaluated in Fig. 3, either the first (abundant) peak only or the average of the following peaks, respectively. This appeared feasible to us since we frequently see that the first f/f_0 peak induced by GTP is larger than the subsequent ones (Fig. 3 columns a versus columns b). For unknown reasons *pawn* cells produce rather variable $[Ca^{2+}]_i$ amplitudes (see large S.E.M. for *pawnB* in Fig. 3) and their behavioral response also varies (Table 1). We can well reproduce reports on adaptation of *Paramecium* to GTP (Kim et al., 1997) showing that *nd6* cells become adapted to GTP over ~15 min (Figs. 4 and 5a). While the predominance of the first peak is a new aspect, all data are well compatible with the electrophysiological work cited above. This, together with the subsequent controls, made us confident about the imaging methodology we used for the first time on this subject.

Before extending our studies to new aspects we performed the following controls. Application of buffer to *nd6* cells does not evoke any Ca^{2+} signal (Fig. 3, 5th column pair, and Fig. 5b), thus excluding mechanical stimulation by the flush. This is important considering ongoing discussions on the interacting effects of mechanical stress and of nucleoside trisphosphates (Forrester, 2003). Similarly we see neither any $[Ca^{2+}]_i$, nor any behavioral response in the non-responder, strain *ginA*, when exposed to GTP (Fig. 3, 6th column pair, and Fig. 5c). All GTP-mediated $[Ca^{2+}]_i$ responses are clearly different from those obtained during AED-stimulated exocytosis (Fig. 5d), which are of the monophasic type reported in our previous work (Klauke and Plattner, 1997).

2.4.2.) Additional new aspects of GTP-mediated Ca^{2+} signaling

This includes the observation that, in all GTP-sensitive strains analyzed, the first f/f_0 peak generated by GTP frequently, although not always, exceeds any further peaks. These remain of fairly constant height, at least over several oscillations to follow (Figs. 1a, d, and 2). We analyzed GTP effects in *nd6* cells not only in presence of $[Ca^{2+}]_o$ = 1 mM, but also with GTP

with BAPTA added (Figs. 1c and 3). This is a very fast Ca^{2+} chelator, with a time constant of 0.5µs (Kao and Tsien, 1988). Such methodology - avoiding preincubation with the chelator - has been reliably applied to *Paramecium* in another context, without any deleterious side-effects (Klauke et al., 2000). Our findings with stimulation in presence of BAPTA are as follows (Fig. 3, 3rd column pair).

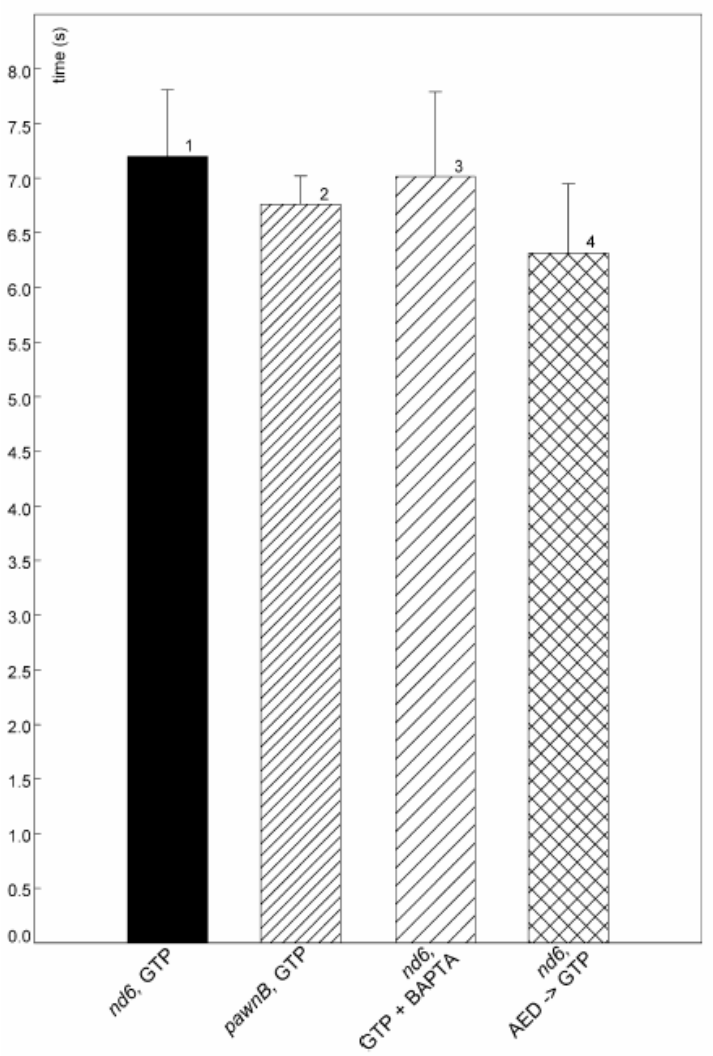

Fig. 2. Periodicity of Fura Red *f*/*f*0 signals recorded after GTP stimulation in *nd6* and *pawnB* cells under the conditions indicated. Note that in both strains the response shows similar periodicity of ~7 s, regardless whether Ca2+ is present in, or absent (+BAPTA) from the GTP stimulation solution, or whether alveolar sacs have been depleted of their Ca2+. Number of cells analyzed in columns 1–4, N = 5, 5, 5, 4. Error bars=S.E.M. According to the ANOVA test applied, the data contained in columns 1–4 are not significantly different from each other.

(i) The abundant first peak is reduced to the size of the following peaks. Concomitantly, in Fig. 3, column 3a is significantly smaller than column 1a ($P < 0.05$). (ii) All peaks are smaller with BAPTA present, when compared with stimulation by GTP in presence of $[Ca^{2+}]_o$. In Fig. 3, the difference between columns 1b and 3b is $P = 0.087$. This suggests two sources of Ca^{2+} during GTP-mediated signaling: (i) influx from the medium (GTP + $[Ca^{2+}]_o$), and (ii) mobilization from internal stores (GTP + BAPTA). It also implies (iii) that the latter component must be independent of the influx component, thus excluding a mechanism of the type Ca^{2+}-induced Ca^{2+}-release.

In sum, our data indicate that in *Paramecium*, during GTP stimulation, Ca^{2+} from influx and from store mobilization are independent processes which are superimposed to each other. There is no significant delay in the onset of the first Ca^{2+} oscillation peak (Fig. 1), regardless of whether $[Ca^{2+}]_o$ is high or low. Since a Ca^{2+}-induced Ca^{2+}-release mechanism seems to be excluded, one would have to expect some other intracellular signal, as discussed below.

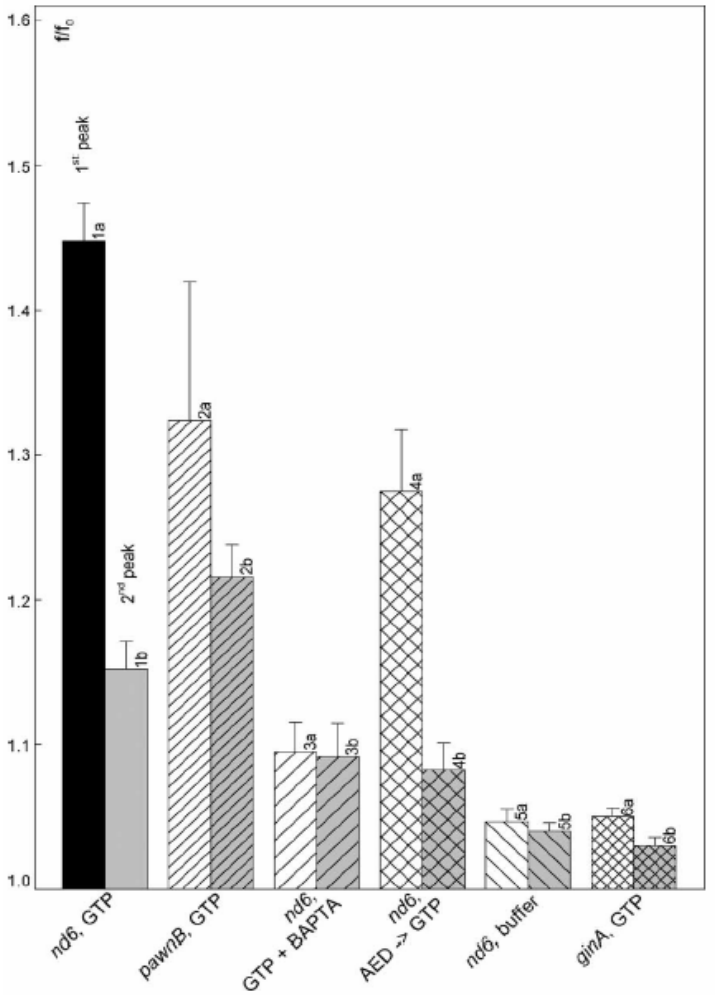

Fig. 3. Fura Red *f*/*f*0 signal increase upon GTP stimulation in different strains and under conditions indicated for the respective column pairs, 1–6. The 1st column ("a") of each pair shows the size of the first peak recorded immediately after stimulation, column "b" designates the average of all following peaks recorded. The first peak frequently predominates, e.g., in the columns 1a, 2a and 4a, but not in the column pair 3 (+BAPTA added), 5 (mock stimulation) and 6 (non-responding *ginA* cells). $N = 5$ (for each of the individual columns, 1a through 3b), 4 (columns 4a, 4b), 3 (columns 5a through 6b). $P < 0.05$ for comparison of columns 1a and 1b, 2a/2b, 4a/4b. No significant difference was found between columns 1a/3a, 1a/4a, 3a/3b, 3a/5a, 5a/5b, 6a/6b, 5a/6a, 3b/5b, and 5b/6b. For the column pair 1a/2a significance is only $P = 0.127$, for 1b/3b $P = 0.087$. Error bars=S.E.M. For abbreviations, see Fig. 2.

Similar signaling occurs with *nd6* cells and with strain *pawnB* (Figs. 1-3). This excludes ciliary voltage-dependent Ca^{2+}-channels as mediators of Ca^{2+}-influx. It suggests involvement of somatic channels or of ciliary channels of another type which is not known as yet. While this has been known from *pawn* cells already (Clark et al., 1993), the involvement of any Ca^{2+} channels has been questioned altogether (Clark et al., 1997). To us, involvement of some somatic Ca^{2+} channels appears appealing, not only because we see a Ca^{2+} influx component (Fig. 3 column 1a versus column 3a, and column 1b versus column 3b), but also because in another context we have found that spill-over of Ca^{2+} from somatic domains into cilia can easily take place, but not in the opposite direction (Husser et al., 2004). One has to recall that we record f/f_0 changes not directly in cilia, but in the nearby cell cortex, as frequently done in work with cilia (Evans and Sanderson, 1999; Zhang and Sanderson, 2003; Pernberg and Machemer, 1995). Our findings favor as a second component the involvement of intracellular Ca^{2+} stores in GTP-mediated Ca^{2+} signaling. However, for the following reasons we envisage other stores than previous work (Wassenberg et al., 1997).

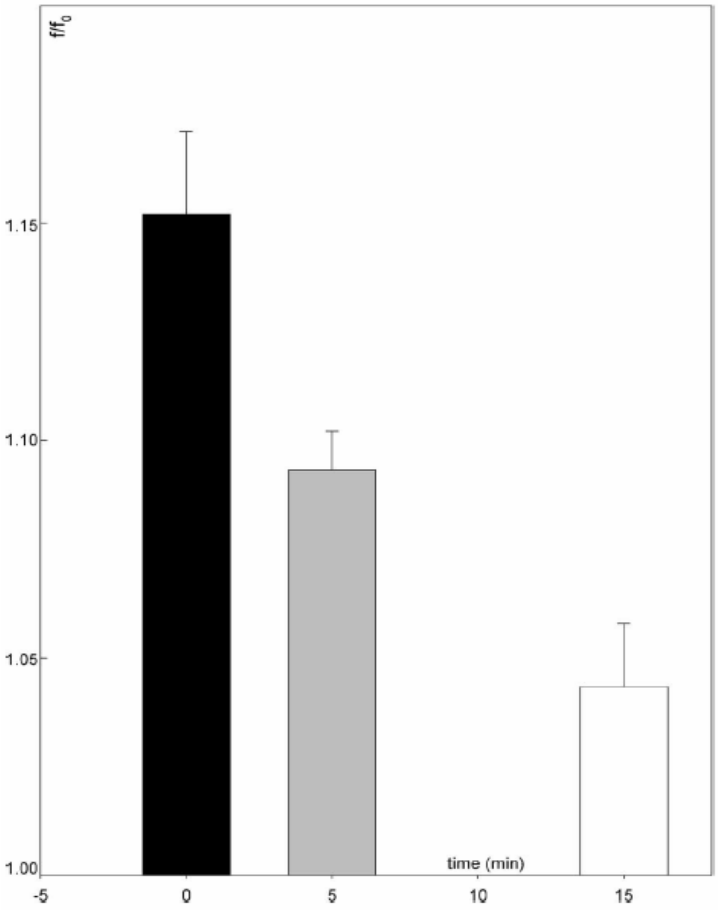

Fig. 4. Adaptation to GTP. The Fura Red *f*/*f*0 response, averaged from all peaks, has been determined immediately after GTP addition (column 1, black) and 5 (column 2, grey) or 15 min later (column 3, white). Column 3 is not significantly different from controls (*nd6* mock stimulation, *ginA*) shown in Fig. 3. *N* = 5, 3, 3 (columns 1–3). Error bars=S.E.M. Abbreviations as in Fig. 3.

We tried to figure out which intracellular calcium pool, i.e., particularly the cortical stores (alveolar sacs) or the endoplasmic reticulum (ER), may contribute to GTP-mediated Ca^{2+}-oscillations. The corollaries and the rationale of such analyses are as follows. From energy-dispersive X-ray microanalysis (EDX) we know that alveolar sacs (which line most part of the cell membrane) have a total calcium concentration, [Ca], of ~43mM (Hardt and Plattner, 1999, 2000), most of it presumably bound to high capacity/low affinity Ca-binding proteins (Plattner et al., 1997). During stimulation of synchronous exocytosis by AED, [Ca] in alveolar sacs is reduced to ~20% of its original value within 1 s (Hardt et al., 2000). We also know that refilling is unexpectedly slow, with a half-time of ~60 min (Mohamed et al., 2003). Although [Ca] may be less high in the ER, it deserves interest in the context of GTP-mediated Ca2+ signaling because it approaches ciliary bases where no alveolar sacs occur (Hauser et al., 2000). To differentiate between the two candidates for stores possibly involved in GTP-mediated signaling, i.e., the alveolar sacs and the ER, we proceeded as follows.

In a series of experiments with *nd6* cells we have depleted alveolar sacs of their Ca^{2+} by massive stimulation with AED. Following this, these cells have been stimulated with GTP. The time elapsed between the two stimuli was only ≤3 min, which is much too short to allow for any significant refilling (Mohamed et al., 2003). Under these conditions, during GTP stimulation, we observe oscillating *f*/*f*0 signals with a large first peak (Figs. 1d and 3, column 4a); subsequent peaks are quite similar to those occurring during stimulation by GTP + BAPTA, without previous depletion of Ca^{2+} from alveolar sacs (Fig. 1c versus d). Notably the first peak is very high, irrespective of AED pre-treatment (Fig. 3, column 4a). Taken together

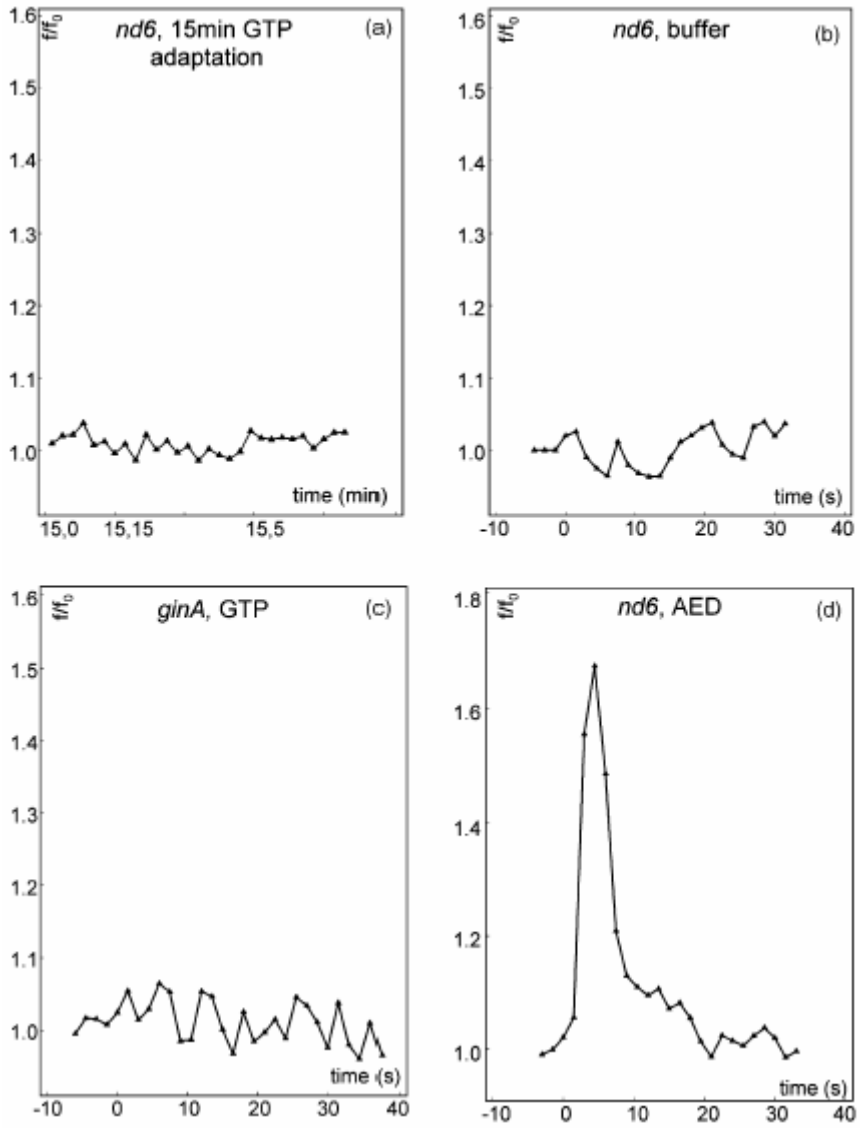

Fig. 5. Fura Red f/f_0 recordings representative of different controls. (a) Recording from a *nd6* cell 15 min after GTP stimulation (time shown: 15.0, 15.15, 15.5 min, etc.) shows adaptation when compared with Fig. 1a. (b) *nd6* cell, mock-stimulation, (c) *ginA* cell, GTP stimulation (no response). For comparison with GTP-mediated responses, we show in (d) the response of a *nd6* cell to AED (no GTP), as occurring during induction of synchronous exocytosis—in agreement with the literature cited in the text. This is to be compared with GTP stimulation *after* AED application (Fig. 1d).

this suggests the occurrence not only of a Ca^{2+} influx, but also the release from a store other than the alveolar sacs. The behavioral response under these conditions is variable, as summarized in Table 1, but periodic back- and forward swimming is observed.

Behavioral responses parallel rather strictly the periodic Ca^{2+} signals, notably the occurrence of a dominant first peak (Table 1). GTP + BAPTA causes no periodic back and forward swimming in *nd6* cells. A normal, though weaker response occurs after liberating Ca^{2+} from alveolar sacs by AED pre-treatment. The extent of the behavioral reaction to GTP is weaker in *pawnB* cells. The reason of this minor inconsistency between *nd6* and *pawnB* cells may be as follows. Absolute $[Ca^{2+}]_i$ levels (not determined by the method used here) at

rest or after stimulation may vary from strain to strain (Klauke and Plattner, 1997). This discrepancy can suffice to yield quantitatively different responses, as also shown in previous work (Mohamed et al., 2003), considering that we measure f/f_0 ratios irrespective of $[Ca^{2+}]_{rest\ i}$. Beyond this variability it is important to note that all strains, but *ginA*, produce Ca^{2+} oscillations under the conditions indicated. The requirement of a first strong peak for induction of a reversal reaction and the absence of both these phenomena in presence of BAPTA indicates the relevance of a Ca^{2+} influx signal, while ongoing $[Ca^{2+}]_i$ oscillations can be driven by internally released Ca^{2+}. The response after pre-treatment with AED indicates that the internal store contributing to f/f_0 oscillations during GTP stimulation is most likely the ER.

Table 1. $[Ca^{2+}]_i$ oscillations[a] and behavioral response

Strain	Stimulation	$[Ca^{2+}]_i$ Oscillations occurrence/1st peak	Behavioral response
nd6	GTP[b]	Oscillation/abundant	Periodic reversal
	GTP, 5 min	Oscillation/abundant	Periodic reversal
	GTP, 15 min	No oscillation/missing	None
	GTP+BAPTA[c]	No oscillation/missing	None
	Buffer	No oscillation/missing	None
	AED[d] → GTP	Weak oscillation/occurring (but weaker)	Less pronounced periodic response
pawnB	GTP	Weak oscillation/occurring (but weaker)	Less pronounced periodic response
ginA	GTP	No oscillation/missing	None

[a] Data are based on the respective figures. For number of cells analyzed, see figure legends.
[b] This indicates the immediate response to ~15µM GTP, unless indicated otherwise.
[c] BAPTA added to GTP, not before.
[d] AED: aminoethyldextran secretagogue used at ~2µM.

2.5.) Discussion

Using fluorochrome analysis, we first confirm that GTP-mediated periodic back- and forward swimming in *Paramecium* is paralleled by Ca^{2+} oscillations, as previously found by electrophysiology (see Sections 1 and 3). The new information we obtained includes the following aspects. (i) The occurrence of a dominant first peak (with higher amplitude than the following ones) is important for the induction of the behavioral response described. (ii) The occurrence of lower $[Ca^{2+}]_i$ amplitudes, though with unchanged period, at low $[Ca^{2+}]_o$, implies that these signals are driven from internal Ca^{2+} stores. (iii) The occurrence of identical oscillations after depleting alveolar sacs of their Ca^{2+} disqualifies these stores as relevant source of Ca^{2+} during GTP stimulation. From this we imply (i) the occurrence of GTP-activated Ca^{2+}-influx channels, most likely outside cilia, and (ii) the activation of Ca^{2+} release independent of Ca^{2+} influx. Our data allow us to re-interpret origin, mechanism and potential functional aspects of GTP-mediated Ca^{2+} signaling in *Paramecium*.

2.5.1.) Are there purinergic surface receptors in Paramecium and what may be their function?

To our knowledge there are no GTP receptors reported to occur on the cell surface of any other eukaryote (Schwiebert, 2003). Is it feasible to assume such an aberrant situation for *Paramecium*?

In fact, as far as the signal transduction machinery in *Paramecium* is concerned, we already know several striking deviations from the rule. An example relevant for a re-interpretation of previous data is as follows. For instance, the SERCA-type Ca^{2+}-pump is strictly insensitive (Länge et al., 1995) to the classical inhibitor, thapsigargin (Inesi and Sagara, 1994), probably because of an aberrant binding site (Hauser et al., 1998), while its activity is inhibited by caffeine (Kissmehl et al., 1998). No Ca^{2+} release from alveolar sacs is achieved, neither with ryanodine, nor with $InsP_3$ (Länge et al., 1995), but with the polyamine secretagogue AED (Hardt et al., 2000; Mohamed et al., 2002). These data, together with the unexpectedly slow refilling (Mohamed et al., 2003), shed some doubt on conclusions derived from experiments with SERCA inhibitors, assuming a role for alveolar sacs in Ca^{2+} release and uptake cycles during GTP stimulation (Wassenberg et al., 1997). Considering the endogenous Ca^{2+} signaling component which we assume for GTP activation, the ER is a more likely candidate than alveolar sacs (see below), unless one would concede to alveolar sacs an unexpected hybrid character. However, these aspects also require more detailed analysis, since one store may be susceptible to two different activators, at least in mammalian cells (Solovyova and Verkhratsky, 2003).

The fact that GTP causes the phenomena described, while ATP or UTP do not (Mimikakis and Nelson, 1998), remains undisputed, although non-hydrolysable ATP analogues work equally well at very low concentrations (Wood and Hennessey, 2003). Binding studies strongly suggest the occurrence of purinergic receptors in *Paramecium* (Wood and Hennessey, 2003) and *Tetrahymena* (Rosner et al, 2003). In the future, molecular cloning and modeling may specify such receptors in more detail. In metazoans, two subgroups of purinergic receptors exist (Schwiebert et al., 2003): (i) one family with Ca^{2+}-channel properties (Braunstein and Schwiebert, 2003; Boyce and Schwiebert, 2003), and (ii) another one involved in signaling by second messengers, e.g., $InsP_3$ (Lazarowski 2003). According to our findings with *Paramecium*, both receptor types would be required to account for the two components observed, one depending on $[Ca^{2+}]_o$ and another one operating by internal store mobilization, respectively. The first type is of unknown cation specificity and its relation to channels described in *Paramecium* electrophysiologically (Machemer, 1988; Machemer and Teunis, 1996; Preston, 1990; Preston et al., 1991) remains open. This is in contrast to previous studies with *Paramecium* which did not consider the involvement of Ca^{2+} influx (Clark et al., 1997). (On the other hand, our data are not appropriate to exclude the involvement of any other specific ion channel.) The second receptor type may use trimeric G-proteins with $G\alpha_{0/i}$ subunits of the type suggested to occur in *Paramecium* by DeOndarza et al. (DeOndarza et al., 2002) on the basis of Western blots with heterologous antibodies and of pertussis toxin-mediated ADP-ribosylation. Clearly, molecular identification is required also for these aspects. The large sequences of bona fide $InsP_3$ receptors meanwhile cloned in our lab (E.-M. Ladenburger, I. Korn, R. Kissmehl and H. Plattner, in preparation) may be another detail of the emerging puzzle. Channels with hybrid properties, sharing characteristics of $InsP_3$- and ryanodine-receptors, have been described on a pharmacological basis in *Toxoplasma gondii* (Lovett et al., 2002), a closely related member of the phylum Alveolata. Furthermore, a crosstalk between both types of stores in producing Ca^{2+} oscillations has been discussed in some mammalian systems (Tsien and Tsien, 1993).

2.5.2.) How would Ca^{2+} oscillations be produced?

A feedback between Ca^{2+} mobilization and Ca^{2+}-activated and Ca^{2+}-inhibited processes can cause $[Ca^{2+}]_i$ oscillations in widely different cells (Hajnóczky and Thomas, 1997; Grimaldi et al. 2003; Halet et al., 2003; Mccarron et al., 2003; Miyazaki et al., 1993; Parri and Crunelli, 2003; Pines et al., 2003). This could encompass, e.g., phospholipase C and Ca^{2+}-inhibited Ca^{2+} release via $InsP_3$ receptors. To explain oscillations at low $[Ca^{2+}]_o$ in *Paramecium*, this is just one theoretical option to be pursued. $InsP_3$ receptors may also occur in the cell membrane,

at least in mammals (Tanimura et al., 2000). If this turns out to be the case, it could be one among several possible explanations for our observation that, in *Paramecium*, oscillations are quite similar, though of different amplitudes, with and without Ca^{2+} in the medium. However, other activators of Ca^{2+} release channels can also produce $[Ca^{2+}]_i$ oscillations (Ng et al., 2001; Tomida et al., 2003). Examples are the interference of Ca^{2+} pumps and ion exchangers (Kawano et al., 2003) or other ion pumps with $InsP_3$ receptors (Miyakawa-Naito et al., 2003). Specifically, purinergic receptor activation in mammalian cells can produce Ca^{2+} mobilizing second messengers other than $InsP_3$ (Bruzzone et al., 2003). Finally, feed-back with, as well as adequate positioning of intracellular Ca^{2+} binding proteins has to be considered (Tomida et al., 2003; Falcke, 2003). In *Paramecium*, the periodic response may also be influenced by the ecto-ATPase which hydrolyses GTP equally well (Levin et al., 1989).

At this time, for *Paramecium* one can only speculate about the molecular machinery potentially involved in GTP-mediated $[Ca^{2+}]_i$ oscillations. Clearly more work is required to elucidate the chain of events leading to the ciliary response to be discussed below.

2.5.3.) Effect on ciliary beat

It is established that $[Ca^{2+}]_i$ in the ciliary basis is critical for beat regulation (Lansley and Sanderson, 1999; Tamm, 1994). Depending on the $[Ca^{2+}]_i$ actually "seen" by the basal portion of cilia, the actual Ca^{2+} level serves to drive either regular beating (forward swimming), or a beat reversal. The latter occurs in *Paramecium* after a $[Ca^{2+}]_i$ increase beyond a certain threshold (Husser et al., 2004).

Could the behavior observed be accounted for by store mobilization? We have seen in *Paramecium* cells by EDX analysis that, during stimulated exocytosis, Ca^{2+} spill-over occurs from the somatic cytosol into cilia, whereas Ca^{2+} fluxes in the opposite direction have never been observed [18]. Since depletion of Ca^{2+} from alveolar sacs still allows Ca^{2+} oscillations to occur in our experiments with GTP, we presume the ER as the relevant store, particularly since it reaches quite far out to the cell periphery (Hauser et al., 2000), where alveolar sacs spare the basis of cilia.

$[Ca^{2+}]_i$ oscillations could contain a code for back- and forward swimming. Such oscillations have been shown to activate in mammalian cells a Ca^{2+}/calmodulin-dependent protein kinase by superposition of waves (Koninck and Schulman, 1998). A related kinase with calmodulin motifs (Kim et al., 1998) has recently been discussed in the context of ciliary beat regulation in *Paramecium* (Kim et al., 2002). This is another track to be followed up.

2.5.4.) Why should a cell release GTP?

Release of ATP from the cytosol of undamaged cells is established with mammalian cells (Forrester, 2003) which may thus achieve an auto- and/or paracrine effect via purinergic surface receptors. Like in mammals, in *Paramecium* cells ATP and GTP occur in concentrations of 1 and 0.3 mM/l, respectively (Lumpert et al., 1990). Considering the small cell volume of 0.7 × 10.10 l (Erxleben et al., 1997), even a dense population (e.g., 103 cells/ml) could hardly account for the release of any sufficient GTP into the medium to deliver a concentration sufficiently high for a long range signaling effect ("blood in the water" effect after cell damage). Since purinergic receptors are activated by micromolar ligand concentrations (Schwiebert, 2003), an auto-/paracrine effect appears much more plausible, i.e., for near-range signaling by GTP in *Paramecium*. Along these lines, Iwamoto and Nakaoka (Iwamoto and Nakaoka, 2002) have shown that GTP at a concentration of 10 _M stimulates cell division in *Tetrahymena*. Moreover they found that shearing forces induced by slight centrifugation have the same effect. This is known from mammalian cells to cause nucleotide leakage (Forrester, 2003). In another study with *Paramecium*, Prajer et al. (Prajer et al., 1997) observed $[Ca^{2+}]_i$ oscillations accompanying cell division. More concise ideas on signaling into the nucleus by superposition of $[Ca^{2+}]_i$ oscillations are available from lymphocytes (Tomida et al., 2003). In a *P. caudatum* strain we had previously observed a spontaneous 8-s period (similar to our current observations) whose generation and functional effect has not been pursued (Plattner and Klauke, 2001). Taken together, all this would be compatible with an auto- and/or paracrine effect of GTP in viable cells via purinergic receptors. In fact, exogenous nucleoside trisphosphates are also known to stimulate ciliary beat activity, at least in higher eukaryotes (Zhang and Sanderson, 2003; Braunstein and Schwiebert, 2003) which, in contrast to lower eukaryotes, do not have the capacity to reverse their ciliary beat.

Could all this, in functional terms, imply that cells would be made susceptible by an auto-/paracrine pulse of GTP to ongoing divisions? Would such cells be at the same time liable to periodic back- and forward movement, thus to remain in a favorable environment? This is another distinct question raised by our observations. Altogether, the function we envisage is widely different from what has been discussed up to now for GTP-mediated [Ca2+]i oscillations.

2.6.) Acknowledgements

We thank Dr. R.R. Preston (Hahnemann University, Philadelphia, PA) for initiating this study, for providing the different *nd6*-based strains, and for his helpful suggestions, Dr. I.K. Mohamed for training I.M.S. in calcium recordings, both at the beginning of her thesis work in our lab. Supported by grants from the Deutsche Forschungsgemeinschaft to H.P.

Chapter 3: Manuscript II
Immunolocalization of actin in *Paramecium* cells

Roland Kissmehl*, Ivonne M Sehring, Erika Wagner, and Helmut Plattner

Universität Konstanz
Fachbereich Biologie
Universitätsstraße 10
D-78457 Konstanz, Germany
Tel.: 0049-7531883712
Fax: 0049-7531882245

*) Author for correspondence: helmut.plattner@uni-konstanz.de
Published in: Journal Histochem Cytochem 52:1543-1559

3.1.) Summary
We have selected a conserved immunogenic region from several actin genes of *Paramecium*, recently cloned in our laboratory, to prepare antibodies for Western blots and immunolocalization. According to cell fractionation analysis, most actin is structure bound. Immunofluorescence shows signal enriched in the cell cortex, notably around ciliary basal bodies (identified by anti-centrin antibodies), as well as around the oral cavity, at the cytoproct and in association with vacuoles (phagosomes) up to several µm in size. Subtle strands run throughout the cell body. Postembedding immunogold labeling/EM analysis shows that actin in the cell cortex emanates, together with the infraciliary lattice, from basal bodies to around trichocyst tips. Label was also enriched around vacuoles and vesicles of different size including “discoidal” vesicles that serve the formation of new phagosomes. By all methods used, we show actin in cilia. Although none of the structurally well-defined filament systems in *Paramecium* are exclusively formed by actin, actin does display some ordered, though not very conspicuous, arrays throughout the cell. F-actin may somehow serve vesicle trafficking and as a cytoplasmic scaffold. This is particularly supported by the postembedding/EM labeling analysis we used, which would hardly allow for any large-scale redistribution during preparation.

3.2.) Introduction

Actin is a highly flexible cytoskeletal component that participates in many static and dynamic functions in eukaryotic cells (Pollard et al., 2000). This includes reversible self-assembly of monomeric G-actin to F-actin filaments. Also generally known is that these filaments may be more or less bundled and can serve different functions, such as structural enforcement and restructuring of the cell cortex, rearrangement of cortical components during intracellular signaling, organelle dynamics and transport, etc. The latter includes well-established functions such as phagosome formation and plasma streaming, i.e., cyclosis (Shimmen and Yokota, 2004). However, quite recent results highlight a much broader functional spectrum of F-actin than previously assumed. This applies to early steps of exocytosis, including dense core vesicle docking (Morales et al., 2000; Pendleton and Koffer, 2001; Manneville et al., 2003; Gasman et al., 2004), late steps of endocytosis (Engqvist-Goldstein and Drubin, 2003; Guilherme et al., 2004), exo-endocytosis coupling (Valentijn et al., 1999), endo-phagosome interaction (Kjeken et al., 2004), delivery of endocytosed receptors to lysosomes for degradation (Stoorvogel et al., 2004), vacuole fusion in yeast (Merz and Wickner, 2004), and positioning of the nucleus (Starr and Han, 2003). Some aspects are still poorly understood, particularly, e.g., the role of actin in flagella of algae (Mitchell, 2000; Hayashi et al., 2001; Hirono et al., 2003), whereas its occurrence in cilia has remained a matter of debate. Another line of experiments concerns the potential role of actin in mediating the connection between cortical Ca^{2+}-stores and the plasma membrane (Patterson et al., 1999; Rosado and Sage, 2000; Kunzelmann-Marche et al., 2001; Wang et al., 2002).

Different actin isoforms occurring in many organisms may serve specific functions in the respective cells (Pollard et al., 2000; Wagner et al., 2002). For localization, antibodies (ABs) may be used at the light microscope (LM) and electron microscope (EM) levels, as well as for Western blots. Bicyclic peptide toxins, phalloidin or jasplakinolide, can bind rather specifically to F-actin, thus allowing fluorescence labeling (Wieland and Faulstich, 1978; Bubb et al., 2000). This or the alternative approach, F-actin disruption by toxins of the type cytochalasin B and D or latrunculin A, is also widely used for functional analyses also with ciliates (see below).

In previous times, mainly before molecular biology approaches could be undertaken, biochemical, functional, and immunolocalization studies were tried to probe the potential function of F-actin in ciliates such as *Paramecium* (Tiggemann and Plattner, 1981; Cohen et al., 1984; Fok et al., 1985; Kersken et al., 1986a,b), *Tetrahymena* (Mitchell and Zimmerman, 1985; Hirono et al., 1987b,1989; Hoey and Gavin, 1992), *Pseudomicrothorax* (Hauser et al., 1980), *Histriculus* (Pérez-Romero et al., 1999), *Climacostomum* (Fahrni, 1992), and

Spirostomum (Zackroff and Hufnagel, 1998). However, with ciliates, F-actin–disrupting drugs frequently had to be used in conspicuously high concentrations to abolish, e.g., phagocytosis (Fok et al., 1987; Zackroff and Hufnagel, 1998, 2002). With a variety of protozoa of the phylum Alveolata, actin genes or partial sequences of it have been cloned. This holds in particular for ciliates, such as *Tetrahymena* (Zimmerman et al., 1983; Cupples and Pearlman, 1986; Hirono et al., 1987a) and *Paramecium* (Díaz-Ramos et al., 1998), but also for their pathogenic relatives of the group of Apicomplexans such as *Toxoplasma* (Delbac et al., 2001). Our present analysis also addresses some special subcellular structures in *Paramecium* cells that contain multiple filament systems (Allen, 1971; Cohen et al., 1984, 1987; Cohen and Beisson, 1988; Keryer et al., 1990a, b; Allen et al., 1998; Beisson et al., 2001; Clérot et al., 2001). We focus on regions with dense-core secretory vesicles ("trichocysts"), cortical filament bundles ("infraciliary lattice," cf. Allen 1971, 1988), the narrow space between the plasma membrane and tightly attached cortical Ca^{2+}-stores ("alveolar sacs," see Plattner and Klauke, 2001), in addition to abundant vesicles of the phago-/lysosomal and recycling system (Fok and Allen, 1990; Allen and Fok, 2000). Recent cloning of several actin genes of *Paramecium tetraurelia* in our laboratory opened up a new way to structural localization with this cell, whose regular "design" facilitates such studies. So far, studies on actin in *Paramecium* have not addressed all relevant aspects, and many aspects have remained controversial.

3.3.) Materials and Methods

3.3.1.) Stocks and Cultures

The wild-type strain of *P. tetraurelia* used was stock *7S.* Cells were cultivated in a decoction of dried lettuce monoxenically inoculated with *Enterobacter aerogenes* as a food organism, supplemented with 0.4 $\mu g \cdot ml^{-1}$ ß-sitosterol (Sonneborn, 1970). For subcellular fractionation, we used axenic cultures (Kaneshiro et al., 1979). Cells were grown at 25C to early stationary phase as previously described (Kissmehl et al., 1996).

3.3.2.) Expression of *Paramecium* Actin-specific Peptides in *Escherichia coli*

For heterologous expression of actin-specific peptides we selected the amino acid sequence of actin1-1 (accession number AJ537442). After changing all deviant *Paramecium* glutamine codons (TAA and TAG) into universal glutamine codons (CAA and CAG) by PCR methods, the coding regions of either E57-P243 (N-terminal region) or L251-G366 (C-terminal region) of *Paramecium* actin1-1 were cloned into the XhoI/BamH1 restriction sites of pET 16b expression vector of the pET System from Novagen (Madison, WI) which employs a His_{10} tag for purification of the recombinant peptides.

3.3.3.) Purification of Recombinant Actin1-1 Peptides

Recombinant actin1-1 peptides, actin1-$1_{E57-P243}$ and actin1-$1_{L251-G366}$ were purified by affinity chromatography on Ni^{2+}-nitrilotriacetate agarose under native conditions, as recommended by the manufacturer (Novagen). The recombinant peptides were eluted with a step gradient, 100 to 1000 mM imidazole in 50 mM sodium phosphate (pH 6.0) with 300 mM NaCl added. The fractions collected were analyzed on SDS polyacrylamide gels, and those containing the recombinant peptides were pooled and dialyzed in phosphate-buffered saline (PBS).

3.3.4.) Antibodies Used

ABs against the two recombinant actin peptides, actin1-$1_{E57-P243}$ and actin1-$1_{L251-G366}$, were raised either in rabbits or mice. After several boosts, positive sera were taken at day 60 and purified by two subsequent chromatography steps, a first step on a His-tag peptide column (24-amino acid peptide, to remove His tag-specific ABs), followed by an affinity step on the corresponding actin1-1 peptide. One of these ABs recognizes the N-terminal and the other the C-terminal region of actin1-1, yet results achieved in this study were indistinguishable with either type of ABs. Therefore, no further distinction is made, unless indicated. We used the sequence of *Paramecium* actin 1-1 because it is rather similar for numerous isoforms that we have cloned (R. Kissmehl, J. Mansfeld, E. Wagner, I. Sehring, H. Plattner, unpublished data)

and thus should allow us to establish an overall distribution of actin, notably of F-actin, in *Paramecium*.

Mouse polyclonal ABs against *Paramecium* actin1-1 were selectively used for the colocalization at the LM level, in conjunction with an anti-centrin (*Dictyostelium discoideum*) polyclonal AB produced in rabbits (designation HisDdCentrin2 from R. Gräf, University of Munich) used to identify ciliary basal bodies (Daunderer et al., 2001).

3.3.5.) Cell Fractionation

Cells were deciliated by a Mn^{2+}-shock (for details, see below) and cilia were purified by differential centrifugation (Nelson, 1995). Whole-cell homogenates were prepared in phase buffer (20 mM Tris-maleate, 20 mM NaOH, 20 mM NaCl, 250 mM sucrose, pH 7.0) by ~100 hand strokes in a glass homogenizer equipped with a Teflon pestle. Soluble and particulate fractions were separated by centrifugation at 100,000 x g for 60 min at 4C. Cell surface complexes ("cortices") were prepared according to Lumpert et al. (1990), and trichocysts were isolated by the method of Glas-Albrecht and Plattner (1990). A protease-inhibitor cocktail containing 15 µM pepstatin A, 100 mU/ml aprotinin, 100 µM leupeptin, 0.26 mM TAME, 28 µM E64, and 0.2 mM Pefabloc SC was used throughout.

3.3.6.) Electrophoretic Techniques and Western Blot Analysis

Protein samples were denatured by boiling for 3 min in sample buffer (0.4 M Tris–HCl, 1% SDS, 0.5% DTT, 20% glycerol, pH 8.0) and subjected to electrophoresis on linear gradient (5–20%) SDS polyacrylamide gels using the discontinuous buffer system of Laemmli (1970). Before electrophoresis, samples were alkylated for 30 min at 20C by 2% iodoacetamide. Protein standards were used in accordance with manufacturer directions. Gels were either stained with Coomassie blue R250 or prepared for electrophoretic protein transfer onto nitrocellulose membranes. Protein blotting was performed at 2 mA/cm^2 for 1 hr according to the technique of Kyhse-Andersen (1989) using the semidry blotter from BioRad (Munich, Germany). ABs were diluted 1:1000 in 0.25% (w/v) non-fat dry milk and Tris-buffered saline, pH 7.5, and applied overnight at 4C. AB binding was visualized by a second AB coupled to alkaline phosphatase (Sigma: Taufkirchen, Germany) using 5-bromo-4-chloro-3-indolyl phosphate and Nitro Blue tetrazolium as substrates.

3.3.7.) Immunofluorescence Labeling

3.3.7.1.) Basic Procedure

Cells were washed twice in 5 mM Pipes buffer, pH 7.0, containing 1 mM KCl and 1 mM $CaCl_2$. Cells were fixed in 4% (w/v) freshly depolymerized formaldehyde for 20 min at room temperature. Cells were then permeabilized and fixed in a mixture of 0.5% digitonin and 4% formaldehyde, dissolved in 5 mM Pipes buffer, pH 7.0, for 30 min. Cells were washed twice in PBS, 2 x 10 min in PBS with 50 mM glycine added and 30 min in this solution with 1% bovine serum albumin (BSA) added. The rabbit anti-actin AB was applied in a dilution of 1:50 in PBS (+1% BSA) for 90 min at room temperature. After 4 x 15 min washes in the same solvent, FITC-conjugated anti-rabbit ABs, diluted 1:50, were applied for 90 min, followed by 4 x 15 min washes in PBS. Samples were shaken gently during all incubation and washing steps.

3.3.7.2.) Deciliated Cells

Cells were washed twice in 5 mM Pipes buffer, pH 7.0, each containing 1 mM KCl and $CaCl_2$, at room temperature and suspended in 50 mM $MnCl_2$ solution in 10 mM Tris-HCl, pH 7.2. After 2 min at 4C, cells were removed by centrifugation and resuspended in the same solution. After 10 min of gentle shaking, 90–95% of cells were deciliated. Deciliated cells were removed by centrifugation and washed twice in Pipes buffer before further use.

Deciliated cells were fixed in 8% (w/v) freshly depolymerized formaldehyde with 0.5% digitonin, 1 mM ATP, 10 mM $MgCl_2$, and 10 mM KCl added, for 20 min on ice in Pipes buffer, pH 7.0. After fixation, cells were washed twice in PBS, 2 x 10 min in PBS with 50 mM glycine added and 30 min in this solution with 1% BSA added. The mouse anti-actin AB was applied in a dilution of 1:50 in PBS (+1% BSA) for 90 min at room temperature. After 4 x 15 min washes in the same solvent, FITC-conjugated anti-mouse ABs, diluted 1:50, were applied for 90 min, followed by 4 x 15 min washes in PBS. A second labeling with anti-centrin ABs from rabbits was performed as described above, using Texas Red–conjugated anti-rabbit ABs. Anti-rabbit and anti-mouse fluorescent AB conjugates were from Sigma-Aldrich (St Louis, MO) and Serva (Heidelberg), respectively.

3.3.7.3.) Light Microscopy

Cells were mounted with Mowiol supplemented with n-propylgallate to reduce fading. To analyze fluorescence staining, we used a conventional LM, type Axiovert 100TV (Zeiss; Oberkochen, Germany), or a confocal laser scanning microscope (CLSM) type LSM 510 (Zeiss) equipped with a Plan-Apochromat x63 oil immersion objective (numeric aperture 1.4).

Images acquired with the LSM 510 software were processed with Photoshop software (Adobe Systems, San Jose, CA).

3.3.8.) Fixation and Embedding for Postembedding EM Analysis

Using a quenched-flow apparatus (Knoll et al., 1991), *Paramecium* cells were rapidly injected into 8% formaldehyde plus 0.1% glutaraldehyde dissolved in Pipes buffer, pH 7.2 (0C), with 1 mM KCl and $CaCl_2$ each added, further fixed for 60 min at 4C, washed in PBS (pH 7.4) + 50 mM glycine (2 x 10 min), dehydrated by increasing ethanol concentrations (30%, 50%, 70%, 90%, 96%, 2 x 15 min each, and 2 x 100%, 30 min each), and impregnated with LR Gold resin (London Resin, London, UK) at 0C, with two changes in 2-hr intervals each and then overnight, followed by UV-light polymerization at –35C for 72 hr.

3.3.9.) Immunogold Labeling and EM Analysis

3.3.9.1.) Postembedding Method

Ultrathin sections mounted on formvar-coated Ni grids were pretreated (2 x 10 min) with 20 µl of PBS, then for 10 min with PBS with 50 mM glycine added, and finally immersed in PBS supplemented with 0.5% BSA and 0.5% goat serum (2 x 10 min, room temperature), to eliminate nonspecific gold adsorption. Grids were then incubated with rabbit AB, diluted 1:20 in PBS supplemented with 0.3% BSA-c (BioTrend, Köln, Germany), pH 7.4, 1 hr at room temperature. BSA-c as an acetylated form reduces nonspecific adsorption of gold conjugates due to increased net charge.

Samples were washed in PBS/BSA-c (0.3%) three times, 10 min each, and treated for 1 hr with gold conjugates. We used goat anti-rabbit IgGs coupled to gold of 5 nm (Au_5) provided by Sigma, diluted 1:30.

3.3.9.2.) Preembedding Labeling

Without exception, cells were fixed with 8% formaldehyde + 0.1% glutaraldehyde and simultaneously treated with digitonin (Sigma) and the other additives, as described above for LM analysis of deciliated cells, incubated with primary rabbit ABs against *Paramecium* actin1-1, followed by Au_5-conjugated second ABs, with the aim to make the narrow subplasmalemmal space accessible. After embedding in LR Gold (London Resin), sections were additionally subjected to the postembedding labeling procedure with the same primary and secondary ABs, respectively.

3.3.9.3.) Specificity of Immunogold Labeling and Further Processing

This was verified by the significant reduction of the number of Au_5 particles on sections incubated with ABs that had been preadsorbed with the original antigen.

3.3.9.4.) Further Processing and Quantitative Evaluation

After labeling, sections were rinsed with distilled water, fixed for 5 min with 2% glutaraldehyde, and routinely stained for 3 min with 2% aqueous uranyl acetate (unbuffered, pH ~4.5). EM micrographs were taken at defined magnifications and enlarged to x77,000. Au_5 grains were counted and referred to area size determined by superposition of square lattices with 5, 10.0 and 20.0 mm spacing, respectively, depending on the size of the structure to be analyzed (Plattner and Zingsheim, 1983). The actual area sizes to which the numbers of gold grains were referred were determined from the number of hit points.

3.4.) Results

3.4.1.) Actin-specific ABs, Cell Fractionation, and Western Blot Analysis

Molecular cloning from a pilot sequencing project (Dessen et al., 2001; Sperling et al., 2002) as well as from the ongoing *Paramecium* genome project of the Groupement de Recherche Européen at the Genoscope (Evry, France) revealed that *P. tetraurelia* contains an actin multigene family with at least 30 members, all encoding actin and actin-related proteins with calculated molecular masses ranging between 38 and 45 kD (R. Kissmehl, J. Mansfeld, I. Sehring, E. Wagner, H. Plattner, unpublished data). One of them, actin 1-1 (accession number AJ537442), a member of the actin-1 subfamily with rather conserved immunogenic regions (Fig. 15), was chosen for heterologous expression in *E. coli* (after changing all deviant *Paramecium* glutamine codons into universal glutamine codons) and subsequent production of polyclonal ABs. Various polyclonal ABs were raised against the N-terminal (E57-P243) or C-terminal region (L251-G366, Fig. 15), all readily recognizing the recombinant peptides used for immunization when tested in slot blots and Western blots (data not shown). After affinity purification, the actin-specific ABs were further characterized in ELISA and Western blots. Results obtained were similar, whether ABs were used against the N-terminal or the carboxy-terminal region of actin 1-1, confirming their high specificity against actin or actin-specific peptides (data not shown). The following analyses, including Western blots, and LM and EM analyses, have been performed predominantly with ABs against the C-terminal region of *Paramecium* actin1-1 (Fig. 15).

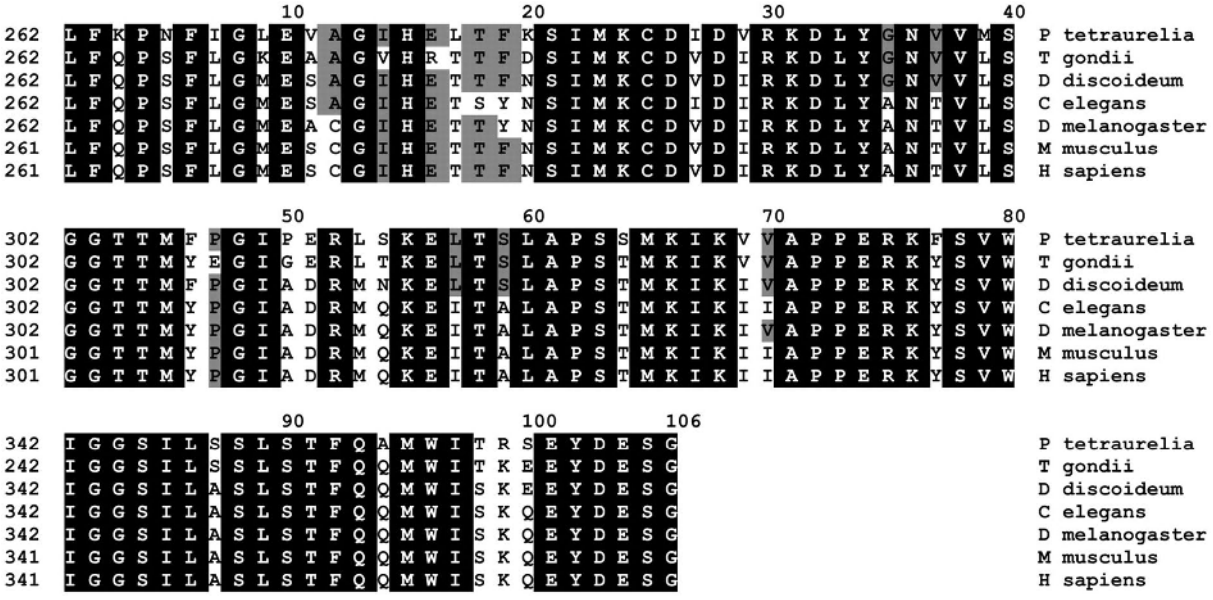

Fig. 15. Multiple alignment of the C-terminal region of *Paramecium* actin1-1. Actin-specific sequences from *Paramecium tetraurelia* (AJ537442), *Toxoplasma gondii* (P53476), *Dictyostelium discoideum* (AA052255), *Caenorhabditis elegans* (X16797), *Drosophila melanogaster* (NP_523625), *Mus musculus* (NP_033739), and *Homo sapiens* (AAH16045) were aligned using the CLUSTALW program. Identical residues are shaded (black), while lesser conserved positions are labeled greyish.

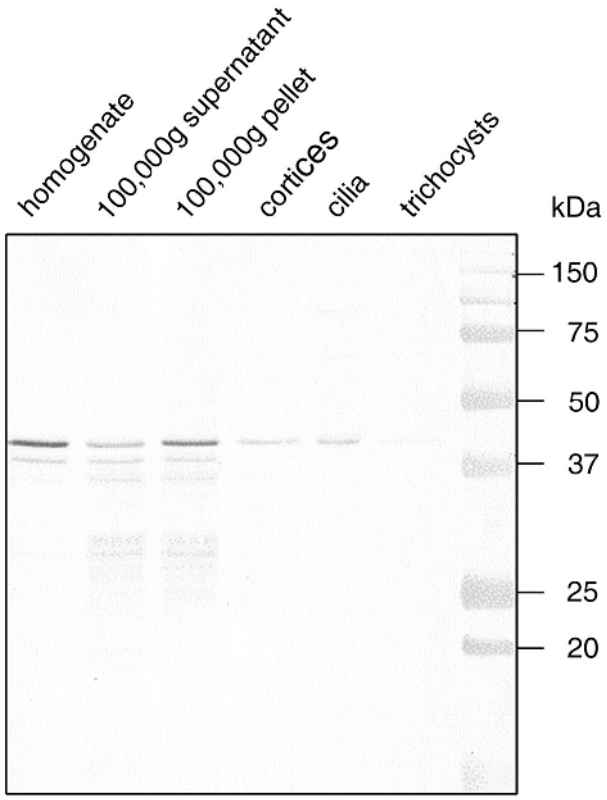

Fig. 16. Western blot using affinity-purified anti-actin (*Paramecium* type 1-1) ABs showing a prominent band of 43 kD in the homogenate and in the fractions indicated, except trichocysts. This band represents preferably structure-bound actin (100,000 x g pellet) and appears also in isolated cortex and ciliary fractions. Note a fainter band of 40 kD in the homogenate and in the 100,000 x g supernatant and pellet, which both contain further weak bands of lower mass (possibly degradation products or cross-reacting actin-related proteins). Right lane: molecular mass markers.

Western blots from homogenates display a strong band of 43 kD and a weak one of 40 kD (Fig. 16). Such bands also occur in the 100,000 x g pellet, while the 43 kD band is much weaker in the 100,000 x g supernatant. The 43 kD band is typical of actin, while the 40 kD band may represent one of the shorter isoforms of the actin or actin-related gene products of *Paramecium* (Kissmehl et al., unpublished data). A 43-kD band also clearly occurs in cilia and in cortices, while it is hardly discernible in the trichocyst fraction. Both the 100,000 x g supernatant and pellet also display some very weak bands of lower size, possibly generated by partial proteolysis during fractionation. None of the bands were visible when Western blots were produced with the corresponding preimmune sera or in controls with the second AB alone (data not shown).

3.4.2) Immunofluorescence Labeling

To account for some variability in the immunofluorescence staining, we present typical extremes of CLSM images from double labeling experiments (Figs. 17A–D), with mouse anti-actin FITC-ABs and rabbit anti-centrin Texas Red-ABs, the latter specific for the centrosome in *Dictyostelium* (Daunderer et al., 2001) and basal bodies in *Paramecium*. This is in contrast to the pattern obtained by the monoclonal AB 20H5 against centrin from *Chlamydomonas* (Sanders and Salisbury, 1994) which in *Paramecium* brilliantly stains not only basal bodies but also the infraciliary lattice (Klotz et al., 1997; Beisson et al,. 2001). Labeling with both anti-actin and anti-centrin ABs in part coincides with ciliary basal bodies of the outer cell surface and along the oral cavity, the outline of the oral cavity, and on the cytoproct. This structure is identified by its “posterovental” position, size, and shape (Allen, 1988). The degree of coincidence (yellow) on basal bodies and in the oral cavity may vary; e.g., it is

higher in Figs. 17A,B than in Figs. 17C,D. The gradient of coincidence in Fig. 17A indicates

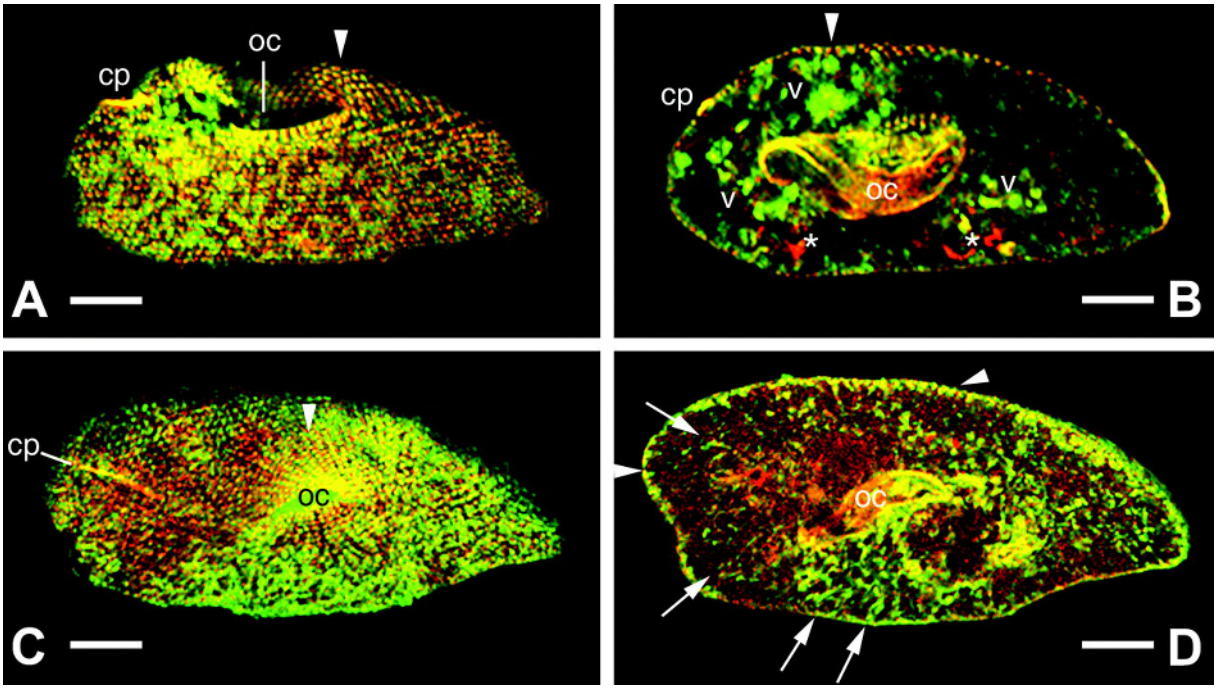

Fig. 17. Colocalization of actin and centrin (yellow) by CLSM using mouse ABs against actin (green) and rabbit ABs against centrin (red). Two deciliated cells (**A,B** vs. **C,D**) showing extreme situations of labeling are presented. (**A,C**) are superficial sections; (**B,D**) are median focal planes. Note colocalization at basal bodies in top-most focal planes (arrowheads), on the cytoproct (cp) and in parts of the oral cavity (oc). Basal bodies located in layers outside the optical section are preferably red (**A**) or green (**C**), thus suggesting a layered arrangement of actin and centrin in these regions of the cell. Note occurrence of actin in the outermost cortex layer particularly in (**D**, arrowheads) as well as of interior actin clusters probably associated with vacuoles (v in **B**) and as filament bundles indicated by arrows (**D**). (**B**) displays centrin staining at two conspicuous sites where the osmoregulatory system is located (asterisks) and actin labeling associated with large vacuoles (v). Bars = 10 µm.

some differential positioning of the respective antigens along the z-axis.

Fig. 17B shows the occurrence of actin around vesicles and vacuoles of various sizes, whereas the position of the red-labeled structures may suggest coincidence with elements of the osmoregulatory system—aspects that have not been followed in any more detail. Fig. 17D documents more clearly a cortical actin layer and actin filaments throughout the cytoplasm, frequently in a radial arrangement, and sometimes with local concentration.

We used conventional LM analysis to analyze immuno-FITC labeling of cilia with anti-actin ABs (Fig. 18), thus taking advantage of a thicker optical section layer. While intracellular details are largely blurred, ciliary basal bodies and cilia on the outer cell surface are clearly labeled. This may also apply to cilia in the oral cavity, although this is not resolved in Fig. 18.

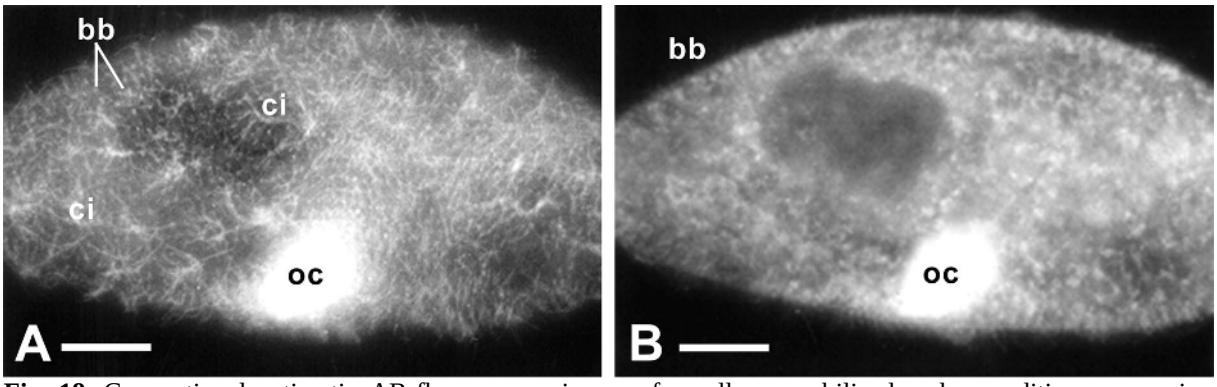

Fig. 18. Conventional anti-actin AB-fluorescence image of a cell permeabilized under conditions preserving cilia. (**A**) superficial, and (**B**) median plane. Note labeling of cilia (ci) in (**A**) and of their basal bodies (bb) in (**A,B**), of specks and strands in (**B**), and of the presumable oral cavity (oc) in (**A,B**). Bars = 10 µm.

3.4.3) Comparative Analysis of CLSM and Immunogold EM Labeling

For most results achieved by CLSM analysis, we find equivalents in the immunogold EM analyses (Figs 19 to 25), as specified below and summarized in Table 1. Off-cell background is low [2.15 gold grains per μm^2 ± 0.85 (SEM)], as it is on irrelevant structures, such as mitochondria, trichocyst contents, and alveolar sacs (2.2, 1.4, and 0.3 gold grains per μm^2, respectively).

After postembedding labeling, gold granules are scattered, yet with specific concentration zones over the cytosolic compartment. This holds for the cell cortex (Figs. 20 to 22) with its ciliary basal bodies, as well as for regions adjacent to the oral cavity, including a zone enriched in ciliary basal bodies (Fig. 24A) and a zone enriched in recycling vesicles (discoidal vesicles) dedicated to phagosome formation (Fig. 24B). It also holds for regions deeper inside the cytoplasm where elements of vesicle trafficking are enriched (Fig. 25). Cilia are also labeled at the EM level (Figs. 19 and 14, Table 2), just as with the other methods used (Figs. 16 and 18). In sum, there is good agreement between LM and EM labeling. Because the cytoproct shows up rarely, we were unable to analyze it at the EM level.

Fig. 23 represents experiments with digitonin-permeabilized cells, showing AB-gold labeling in the narrow subplasmalemmal space between the plasmalemma and the outer side of alveolar sacs, while there is only spurious label occasionally seen after mere section labeling (Figs. 19 and 21). Apart from this aspect, little label only is seen in the cell cortex with permeabilized cells (Fig. 23). While digitonin permeabilisation may be more appropriate than section labeling to show the presence of some actin in the very narrow outermost cytosolic space, particularly when enhanced by additional postembedding labeling (Fig. 23), it may cause a serious overall loss of antigen. The abundance of cortical label after postembedding labeling justifies reliance in this study mainly on the postembedding procedure for further evaluation. Concomitantly, all figures presented with the exception of Fig. 23 were obtained by this method.

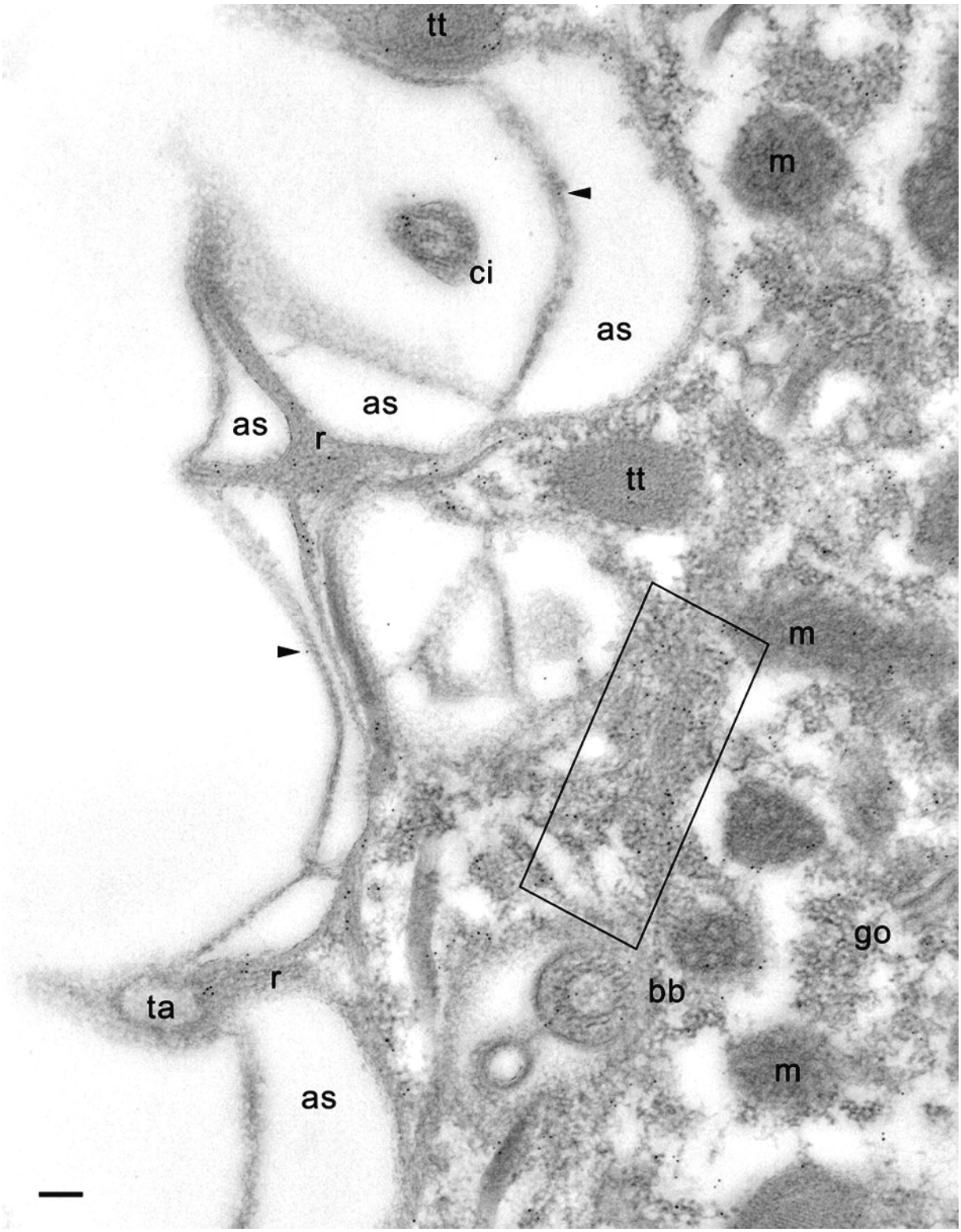

Fig. 19. Postembedding immunogold labeling in the cell cortex. Note almost absence of background outside the cell and within membrane-bound organelles such as alveolar sacs (as), trichocyst tips (tt), mitochondria (m), and a Golgi field (go). This is in contrast to the occurrence of clear, though scattered, labeling of cytoplasmic ridges ® typical of the *Paramecium* cell surface, around a trichocyst tip (top) and close to a trichocyst attachment site (ta), in a cilium (ci), in a ciliary basal body (bb), and along filamentous materials emanating from there (rectangle), probably infraciliary lattice. Note a single gold grains (arrowheads) on the complex formed by the cell membrane and the outer side of an alveolar sac. Bar = 0.1 µm.

3.4.4.) Specification of Results Obtained with Postembedding Labeling

Beyond the general labeling of the cytosolic compartment of the cell cortex (Figs. 19 to 22), we recognize that gold granules are enriched to a variable extent in a variety of structures.

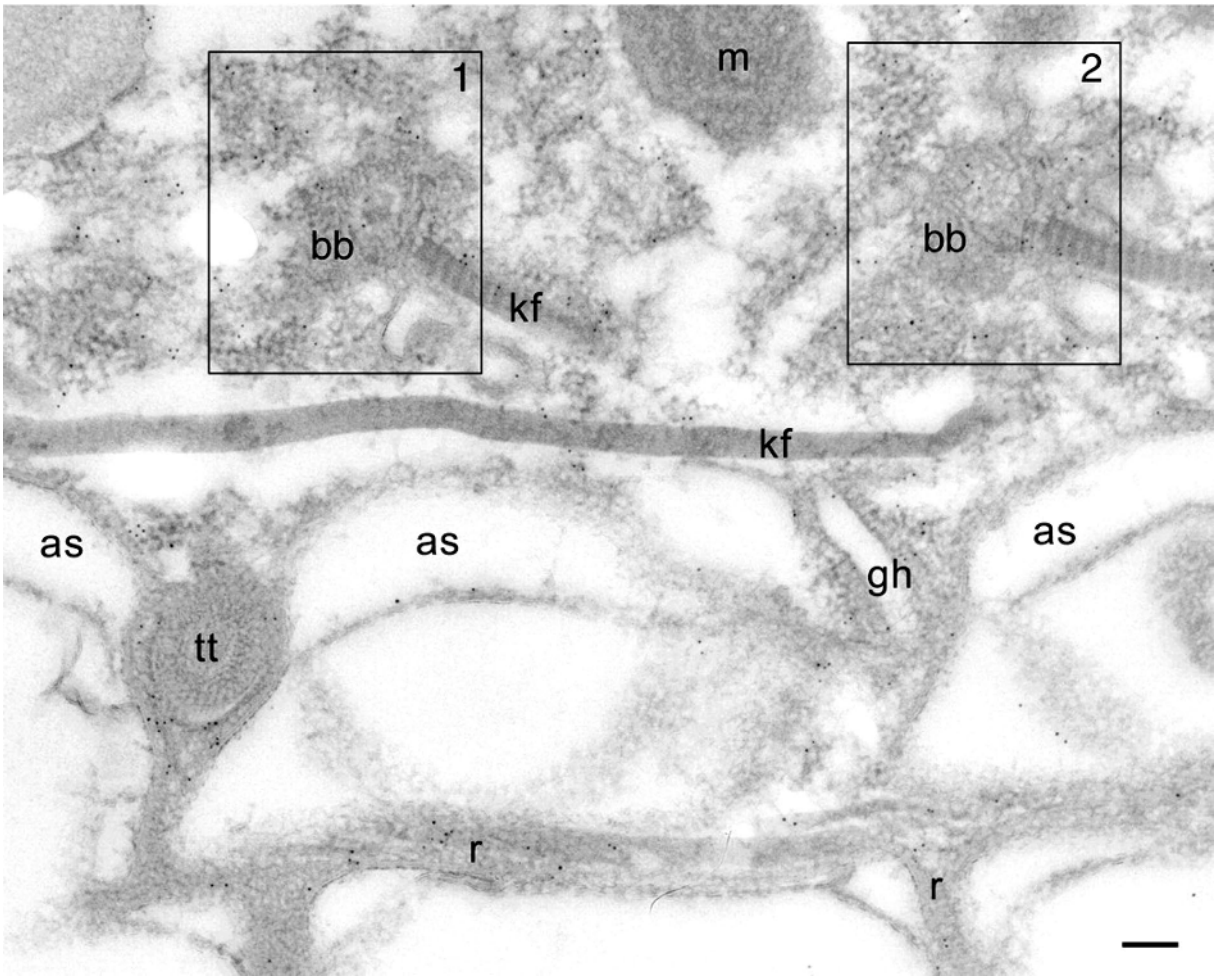

Fig. 20. Similar situation as in Fig 19, but in addition with more distinct label around a trichocyst tip (tt) and a ghost (gh) from a released trichocyst, and much less in diffuse association (frames 1, 2) with two basal bodies (bb) from which typically kinodesmal fibers (kf) originate. Cell surface ridges ® are also labeled. Note almost absence of label outside the cell or inside alveolar sacs (as), the trichocyst tip and ghost, as well as in a mitochondrion (m). Bar = 0.1 µm.

The cytoplasm of cell surface ridges, typical of ciliated protozoa, are labeled (Figs. 19 and 20). This also holds for the cytoplasm surrounding the tips of the elongate trichocyst organelles, as shown in cross-section (Figs. 19 and 20) and in longitudinal section (Fig. 21). The gold label associated with cortical basal bodies is somewhat variable and may in part sit inside this structure, as shown particularly in Fig. 22B, where it shows up below the basal plate (Fig. 22A). Gold label also occurs adjacent to cortical basal bodies, e.g., in the filamentous mass in Fig. 20. This material is associated with the origin of a kinodesmal fiber emanating from a basal body from where the infraciliary lattice also emanates. From there, these filament bundles pass near adjacent trichocyst tips (Fig. 19), as established by Allen (1971) (1988). Although the bulk of the latter filament system is made of centrin (Beisson et

al., 2001), some actin clearly appears to be associated with it. Gold label also surrounds ghosts from discharged trichocysts (Fig. 18).

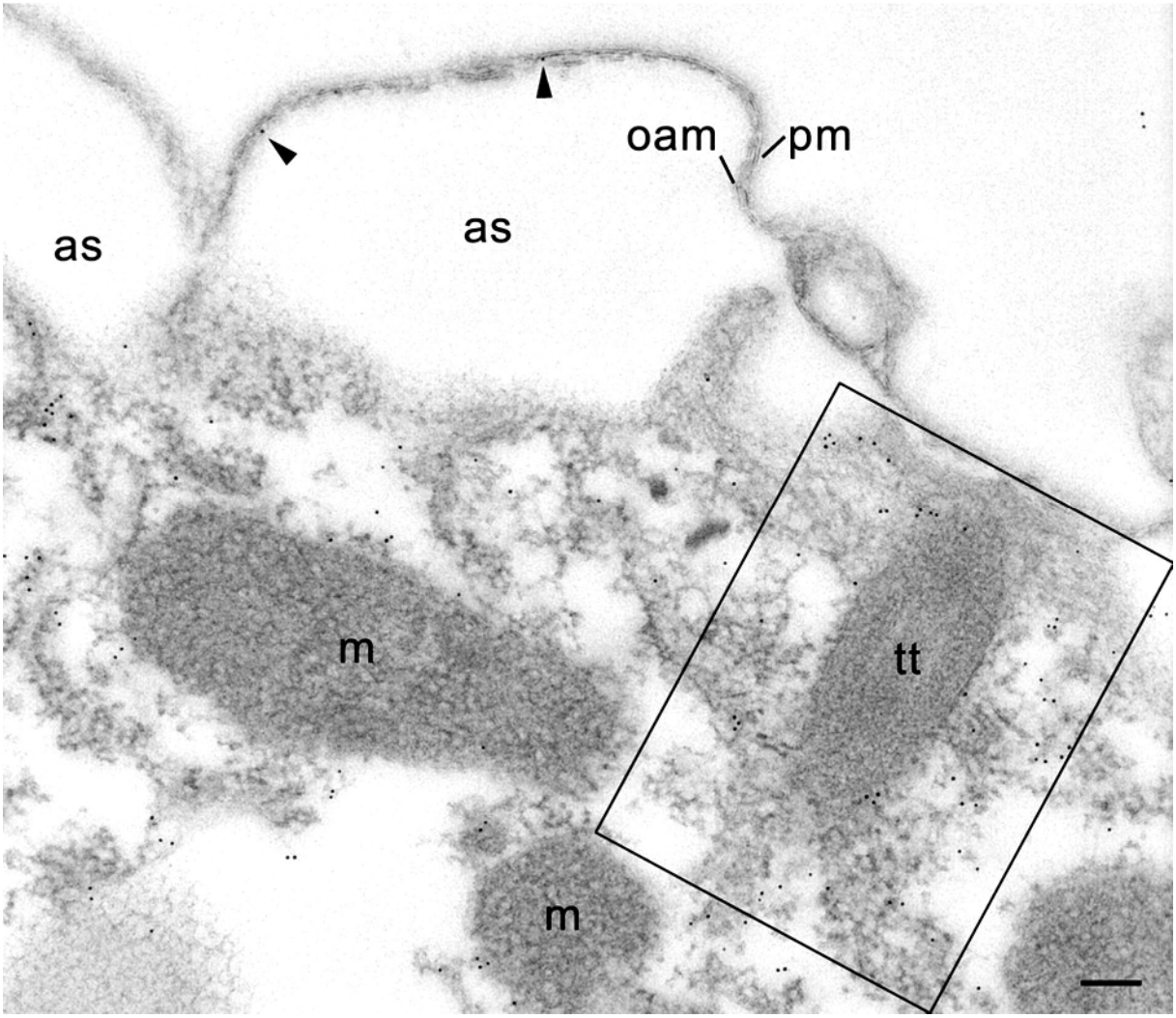

Fig. 21. Similar situation as in 19 and 20, but with more clearly visible label (rectangle) particularly surrounding a longitudinally cut trichocyst tip (tt) and occasional label (arrowheads) in the very narrow subplasmalemmal space between the plasma membrane (pm) and the outer alveolar sacs membrane (oam). Note absence of label from the off-cell region, alveolar sacs (as), and mitochondria (m). Bar = 0.1 µm.

Table 2 summarizes labeling densities on a quantitative level (gold grains per μm^2). These are, in decreasing magnitude, as follows: 301.0 Au/μm^2 for cytoplasmic regions around oral cavity and around food vacuoles, 141.5 for cell surface ridges, 111.9 for immediate surroundings of trichocysts, between 89.5 and 95.6 for infraciliary lattice, ciliary basal bodies, and cilia, followed by cortical cytoplasm (37.8) and the complex formed by the plasma membrane and the outer alveolar sacs membrane (25.9 Au/μm^2). For statistics, see Table 1.

While the abundant filament bundles located in the cytoplasm around the oral cavity are made of materials other than actin (see "Discussion"), the distinct labeling in between such bundles (Fig. 24A) again indicates association with actin. As in the cell cortex, some label may be associated with ciliary basal bodies around the oral cavity. Furthermore, we find intense labeling of cytosolic regions enriched in vesicles accumulated near the cytopharynx (Fig.

24B). Many are oblong and thus represent discoidal vesicles known to serve membrane recycling from the cytoproct, i.e., formation of new phagocytic vacuoles (Fok and Allen, 1988; Allen and Fok, 2000). In these domains of the cell, less labeling is seen immediately below the cell membrane than between the adjacent round and discoidal vesicles.

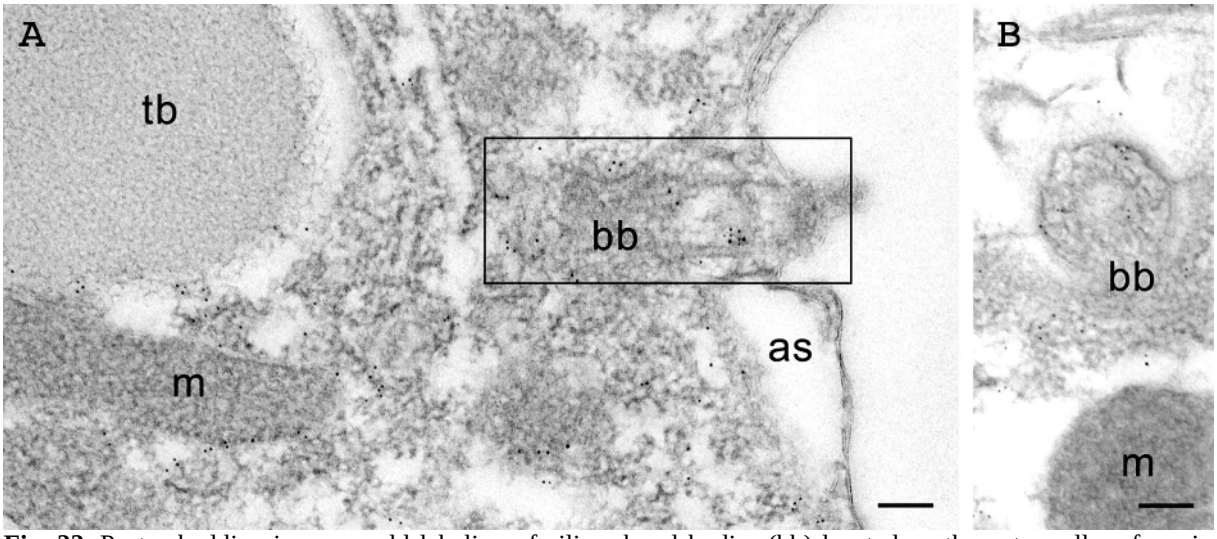

Fig. 22. Postembedding immunogold labeling of ciliary basal bodies (bb) located on the outer cell surface, in longitudinal (**a**) and in cross-section (**b**), with additional label on diffuse materials surrounding the basal body (framed in **a**). Note again absence of label on irrelevant structures, such as alveolar sacs (as), mitochondria (m) and a trichocyst body (tb). Bars = 0.1 µm.

Deeper inside the cell, small vesicles of different diameters are embedded in considerably labeled cytosol, frequently in close association with a large vacuole (Figs. 25A,B). This arrangement suggests their identity either as lysosomes or as acidosomes in typical arrangement with phagosomes. These interpretations are suggested by the work of Allen and Fok (2000); e.g., considering the flat shape of the large vacuole indicating an early biogenetic stage of a food vacuole. Fig. 25B shows association of actin label with parallel microtubular aggregates, the gold label unilaterally concentrated at sites where microtubules enter the section plane. Also in Fig. 25B, a heavily labeled “trail” is in direct extension of the adjacent microtubular bundle. This indicates involvement of actin in phago-lysosomal vesicle trafficking, although after the preparation protocol required for immunogold analysis, distinct filaments are difficult to recognize. However, some of these gold aggregates may be the equivalent of the fluorescent strands visualized by anti-actin ABs in Fig 17.

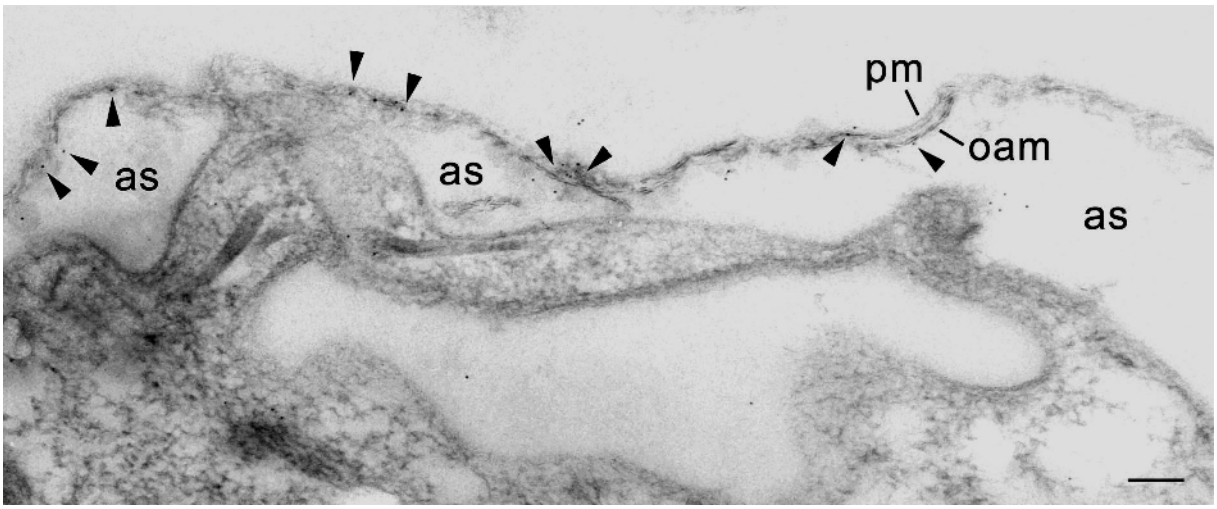

Fig. 23. Combination of pre- and postembedding immunolabeling shows label in the narrow subplasmalemmal space (at/between arrowheads) between the plasma membrane (pm) and the outer alveolar sacs (as) membrane (oam), with little background on irrelevant structures outside the cytosolic compartment. Note deformation of the cell surface membrane complex (pm/oam), with some label attached particularly in regions with a "grazing" section plane, due to the permeabilisation applied. This cell has been digitonized during aldehyde fixation for impregnation with primary AB and IgG-Au_5 and embedded for incubation with the same ABs in sequence. Bar = 0.1 µm.

Table 2. Labeling density (gold grains/μm^2) achieved with anti-actin AB/gold conjugate over different structural components, background [2.15 ± 0.85 (SEM), *n* = 6, determined off cell, or in the lumen of food vacuoles] subtracted.

Structure analyzed	Gold grains/mm2	6SEM	n
Cilia	89.5	±25.5	21
Basal bodies	91.0	±24.9	12
Plasma membrane/outer alveolar membrane complex	25.9	±4.1	14
Cell surface "ridges"	141.5	±56.8	6
Alveolar sacs contents	0.3	±0.3	21
Cortical cytoplasm	37.8	±4.9	5
Infraciliary lattice	95.6	±6.2	3
Surroundings of trichocyst tips	111.9	±27.0	7
Trichocyst contents	1.4	±0.8	8
Mitochondria	2.2	±1.0	11
Small vesicles associated with oral cavity and around food vacuoles	7.0	±7.0	63
Cytoplasmic regions around oral cavity and around food vacuoles	301.0	±7.6	2

SEM = standard error of the mean; *n* = number of structural components analyzed.

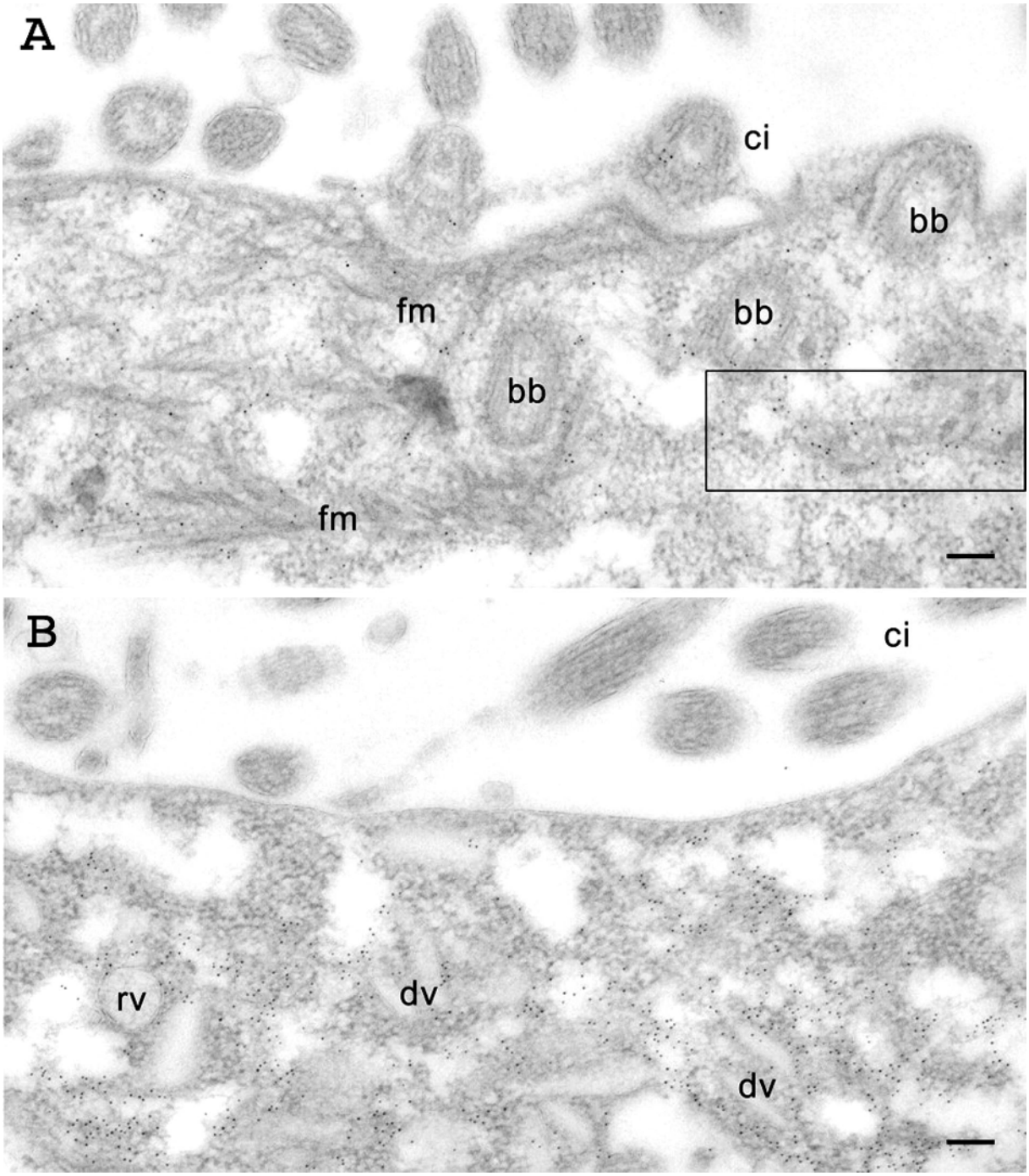

Fig. 24. Label around the oral cavity, in a region enriched in ciliary basal bodies (bb) in (**A**) or in vesicles (**B**). These represent, at least in part, discoidal vesicles (dv) known to recycle membranes for nascent phagosome formation, which may be assisted by round vesicles (rv) as discussed in the text. A particularly densely labeled domain in (**A**) is framed. Some label is located between unlabeled fibrous materials (fm, not actin-type). Also note some label on basal bodies (bb) and within some cilia (ci). In (**B**), the label is scattered between the discoidal vesicles (dv). In (**A**) and (**B**), a ≥1-µm-thick layer below the oral cavity plasma membrane is heavily labeled, starting at a distance from the plasma membrane. Bars = 0.1 µm.

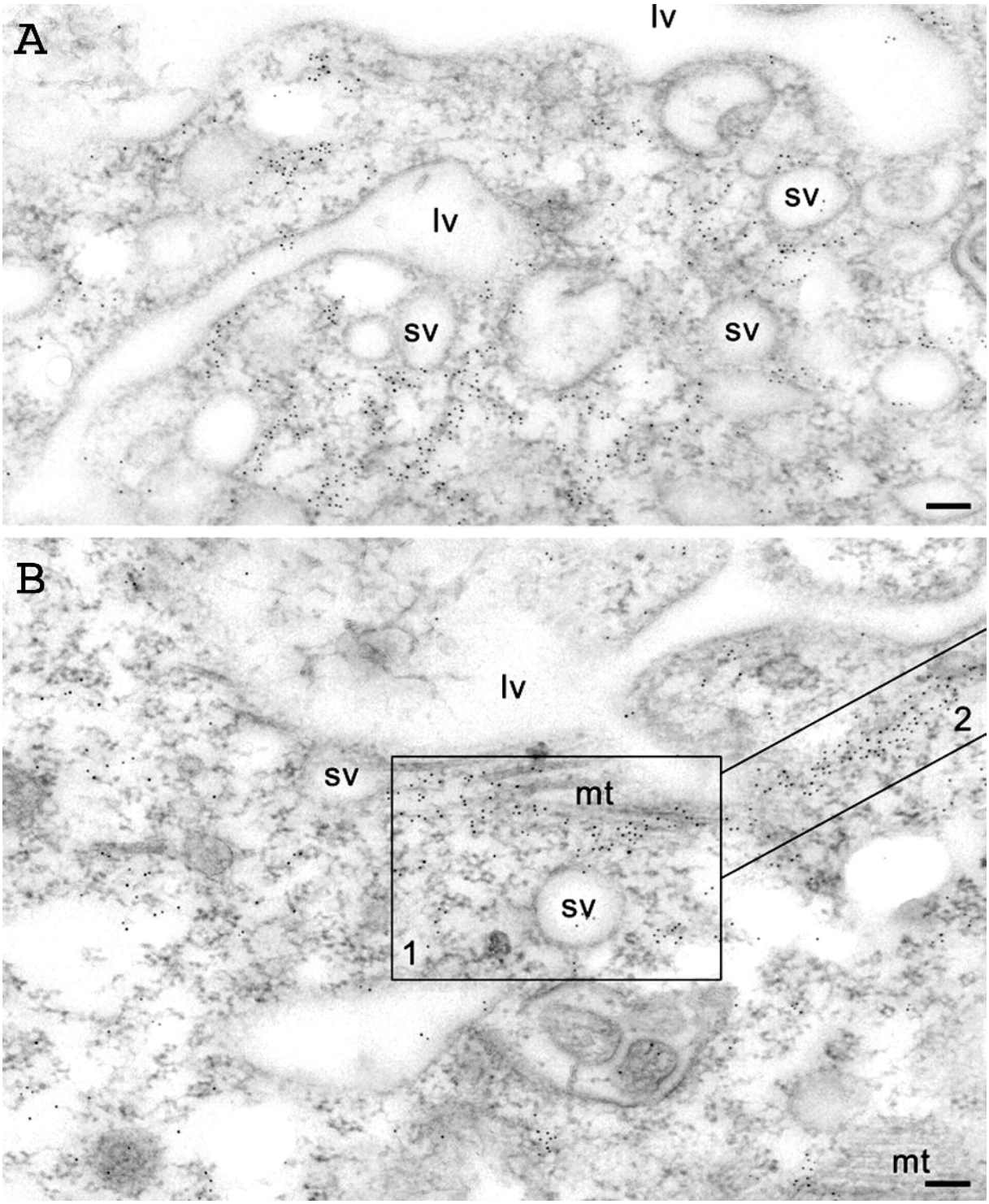

Fig. 25. Label of the cytosolic compartment around small vacuoles (sv), probably acidosomes, approaching a large one (lv), probably a nascent food vacuole (see text). Particularly labeled domains are highlighted (boxes 1, 2). Some of this label is associated with microtubule bundles (mt), e.g., in (**B**), but not in (**A**). In (**B**) a "trail" marked by box 2 is especially strongly labeled, although no distinct filament system can be recognized because of the preparation required. Only occasional gold grains are seen in non-cytosolic compartments, e.g., background in vacuole in (**A**). Bars = 0.1 µm.

3.5) Discussion

3.5.1) Background from Previous Work

Occurrence of most actin in *Paramecium* in structure-bound form contrasts with the abundance of monomeric actin in Apicomplexans (Sibley, 2004), including *Toxoplasma* (Poupel et al., 2000; Wetzel et al., 2003). This makes fluorescence labeling studies with F-actin–specific drugs feasible. In *Paramecium*, phalloidin, heavy meromyosin, and DNaseI have clearly revealed labeling of the cell cortex, particularly of ciliary basal bodies (Tiggemann and Plattner, 1981; Kersken et al., 1986a,b). Phalloidin also has labeled the nascent food vacuole (Kersken et al, 1986a,b). Concomitantly, cytochalasin B has been reported to inhibit formation of phagocytic vacuoles (Allen and Fok, 1983,1985; Fok and Allen, 1988). It also inhibits docking of trichocysts (Beisson and Rossignol, 1975), and it even can detach docked trichocysts from the cell surface (Pape and Plattner, 1990). When phagocytosis has been analyzed with different F-actin–disrupting drugs and analogs, respectively, the requirement of concentrations well above those used with mammalian cells has been confirmed (Beisson and Rossignol, 1975; Pape and Plattner, 1990; Zackroff and Hufnagel, 1998). This is in line with the low sensitivity of F-actin in other ciliates. In total, these data are all compatible with our current results obtained with ABs against the original *Paramecium* antigen.

Previous attempts to localize actin in *Paramecium* have led to controversies. One discrepancy concerned the composition of cortical filament bundles, notably of the infraciliary lattice emanating from ciliary basal bodies. While the bulk of this filament system has been established as centrin (Beisson et al., 2001), this does not necessarily preclude association of centrin filaments with actin, as we can show. Recall that widely different affinity stains for actin, including heavy meromyosin, have resulted in cortical labeling in *Paramecium* (Tiggemann and Plattner, 1981; Kersken et al., 1986a,b), as well as in *Tetrahymena* (Méténier, 1984). Theoretically, previous LM and preembedding-EM localization studies could have faced the problem of soluble antigen relocation and even loss during permeabilisation. This would not easily be possible with the postembedding immuno-EM labeling procedure used now. Another hint to real cortical F-actin localization in *Paramecium* came from the in vivo labeling by injection of fluorescent phalloidin (Kersken et al., 1986a,b), resulting first in cortical labeling and, over longer time periods, in disappearance from the cortex and re-assembly as thick trans-cellular filament bundles of a type not previously seen. Conversely, aberrant phalloidin binding by F-actin formed by some isoforms may preclude labeling (Hirono et al., 1989), while such forms may bind actin-specific ABs.

3.5.2) Additional Functional Aspects Derived from This Study

Cortical F-actin is generally required for cyclosis—an actomyosin-based process (Shimmen and Yokota, 2004). This is a permanent ongoing process also in *Paramecium* (Sikora et al., 1979), where it serves the delivery of trichocysts to the cell cortex (Aufderheide, 1977) and the cycling of phago-lysosomal elements through the cell body (Fok and Allen, 1988,1990; Allen and Fok, 2000). Myosins occur in *Paramecium* (Cohen et al., 1987), just as in other protists (Gavin, 2001).Our present EM analysis verifies that in the *Paramecium* cell cortex, actin is enriched at ciliary basal bodies, as discussed above on the LM level. From there it emanates to the infraciliary lattice and around trichocyst docking sites. The association of actin with ciliary basal bodies has led to the description of the "basal body cage," particularly in *Tetrahymena* (Hoey and Gavin, 1992), where association with myosin has been demonstrated (Garcés et al., 1995). The loose arrangement of gold label within and around basal bodies, as we see it here, suggests that during permeabilisation for LM analysis, F-actin emanating from basal bodies may collapse to a compact arrangement. In sum, a more loosely arranged cortical F-actin in conjunction with myosin may underlie cytoplasmic streaming and possibly trichocyst docking. Concomitantly, inhibition of trichocyst docking by cytochalasin B (Beisson and Rossignol, 1975) would be compatible with both actin-based transport by cyclosis and enrichment of actin around trichocyst tips (this study).

Assembly of F-actin around nascent phagosomes is well established, not only in mammalian cells but also in *Paramecium* cells (Allen and Fok, 1983; Fok and Allen, 1988). In detail, fusion of acidosomes with the nascent food vacuole depends on F-actin (Fok et al., 1987), as does maturation along the phago-lysosomal pathway, where multiple fusion/fission processes occur (Allen and Fok, 1985; Allen et al., 1995). Interestingly, in our study, gold labeling immediately below the cytopharyngeal plasma membrane is less intense than between the closely packed globular and discoidal vesicles slightly below. This can be seen in line with the following reports. In *Dictyostelium*, F-actin prevents clustering of endosomal vacuoles (Drengk et al., 2003). Alternatively, in yeast, actin is required for Ca^{2+}-mediated vacuole interaction leading to fusion (Merz and Wickner, 2004). The final step of this cycle in *Paramecium*, exocytotic release of spent phago-lysosomes, can also be inhibited by cytochalasin B (Allen and Fok, 1985). In agreement with this previous work, the site of phagosome formation, vacuoles of different size, and the cytoproct are clearly labeled with anti-actin ABs in our CLSM and EM pictures. Therefore, the fine filaments described at the cytoproct by Cohen et al. (1984) are, at least to some extent, F-actin. However, centrin also occurs at the cytoproct, according to the CLSM pictures presented in Fig 17.

At the EM level, we see that the cytosolic compartment around large and small vacuoles is frequently heavily labeled (even when filaments are difficult to discern due to faint contrast resulting from preparation for immuno-EM analysis). This holds, e.g., for domains with clearly visible microtubule bundles deep inside the cell and for regions with discoidal vesicles approaching the cytopharynx. The latter are delivered along microtubule rails, using dynein as a motor (Schroeder et al., 1990). Therefore, actin at these sites may serve not as a motor, but rather as a kind of scaffold. In sum, apart from association with non-actin filaments (see below), we see that actin is also associated with the second cytoskeletal element, the microtubules. This agrees with functional data obtained by combined drug application (Fok et al., 1985).

Label also occurs around the oral cavity outside the site of phagosome formation in the cytopharynx. Such filaments are known not to represent actin, either in *Paramecium* (Clérot et al., 2001), or in other ciliates (Viguès et al., 1999). In these regions, F-actin may again serve structuring of these firmly established subcellular domains and/or vesicle trafficking. Interestingly, co-assembly of polymerizing actin with other filament components from *Tetrahymena* can be produced in vitro (Mitchell and Zimmerman, 1985).

Vesicles deeper inside the cytoplasm, often close to a large phagosome, are also surrounded by gold label. All this reflects that actin is present throughout the cell in LM analyses, frequently as strands. Actin may thus participate directly or indirectly in vesicle trafficking, including cyclosis.

Not only ciliary basal bodies, but also the ciliary shaft, are labeled by anti-actin ABs. Labeling of cilia has been reported previously based on peroxidase-based preembedding immunostaining in *Paramecium* (Tiggemann and Plattner, 1981) and in quail oviducts (Sandoz et al., 1982). Because this method is subject to redistribution artifacts (Plattner and Zingsheim, 1983), we considered a re-analysis by Western blots and by the postembedding EM methodology to be necessary. It is known only from flagella of the green alga, *Chlamydomonas* (Mitchell, 2000; Hayashi et al., 2001; Hirono et al., 2003), that actin is mandatory for normal beat activity. This may apply also to cilia of *Tetrahymena*, whose 14S axonemal dynein binds actin (Muto et al., 1994). More details on the role of actin in cilia remain to be elucidated.

Another poorly understood aspect concerns coupling of cortical calcium stores to the cell membrane. With mammalian cells, one of the molecules considered to establish such connections, particularly for store-operated Ca^{2+}-influx, is actin (Patterson et al., 1999; Rosado and Sage, 2000; Kunzelmann-Marche et al,. 2001; Wang et al., 2002). Interestingly, we find gold label that may be associated with the narrow subplasmalemmal space not only using a

variation of the general labeling procedure that facilitates access of ABs (Fig. 23), but also, though to a lesser extent, using postembedding labeling (Figs. 19 and 21). This becomes evident particularly after statistical evaluation (Table 2). Although cytochalasin B application did not change concomitant Ca^{2+} signals (Mohamed et al., 2003), we keep this question open because the different actin isoforms found in *Paramecium* (Kissmehl et al., in preparation) may have different drug sensitivities.

Our present immunogold EM analysis largely depends on the preparation schedule used, whereas we obtained no such clear-cut labeling pattern with other approaches (data not shown). The current approach implied rapid injection (spraying) of cells in 0C aldehyde fixative, containing high formaldehyde and very low glutaraldehyde concentrations, followed by low temperature embedding and UV polymerization at –35C. This can considerably restrict diffusion of macromolecules and, even more, of filamentous aggregates. Therefore, we consider the current approach, elaborated on a (semi-)quantitative basis, more reliable than some previous attempts to localize actin in such cells.

3.6) Acknowledgement

We gratefully acknowledge the kind help of Dr R. Gräf (University of Munich) for a gift of anti-centrin ABs, as well as the help of our group members, of Dr Joachim Hentschel with the quenched-flow preparations, and the skillful technical assistance of Ms Lauretta Schade in the EM documentation. We thank Dr Claudia Stuermer for access to the CLSM and Ms Sylvia Hannbeck von Hanwehr for technical help in the CLSM analysis, as well as Ms Doris Bliestle for electronic image processing. Supported by grants from the Deutsche Forschungsgemeinschaft to HP.

Chapter 4: Manuscript III
The actin multigene family of *Paramecium tetraurelia*

Ivonne Sehring†, Jörg Mansfeld, Christoph Reiner, Erika Wagner, Helmut Plattner and Roland Kissmehl

Universität Konstanz
Fachbereich Biologie
Universitätsstraße 10
D-78457 Konstanz, Germany
Tel.: 0049-7531883712
Fax.: 0049-7531882245

*) Author for correspondence: Ivonne.Sehring@uni-konstanz.de
Submitted in: Eukaryotic Cell, currently under review

4. 1.) Summary

Molecular cloning from a *Paramecium tetraurelia* pilot genome project, the subsequent sequencing of a Megabase chromosome as well as the ongoing genome project revealed that *P. tetraurelia* contains an actin multigene family with at least 30 members encoding actin, actin-related and actin-like proteins. They group into twelve subfamilies; a large subfamily with 10 genes, seven pairs and one trio with >82% amino acid identity, as well as three single genes. The different subfamilies are very distinct from each other. In comparison to actins in other organisms, *P. tetraurelia* actins are highly divergent, with identities topping 80% and falling to 30%. We analyzed their structure on nucleotide level regarding the number and position of introns. On amino acid level, we scanned the sequences for the presence of actin consensus regions, for amino acids of the intermonomer interface in filaments, for residues contributing to ATP binding, and for known binding sites for myosin and actin drugs. Several of those characteristics are lacking in several subfamilies. The divergence of *P. tetraurelia* actins and actin-related proteins within each other as well as with sequences of other organisms is well represented in a phylogenetic tree, where *P. tetraurelia* sequences only partially cluster.

4.2.) Introduction

Actin is described as one of the most abundant and highly conserved proteins in eukaryotic cells. It may be present as monomeric G-actin or as filamentous F-actin and is involved in many vital cellular functions such as organelle transport (Snider et al., 2004), cell motility (reviewed in Pollard and Borisy, 2003), cytokinesis (Otegui et al., 2005), cytoplasmic streaming in plants (Shimmen and Yokota, 2004), in regulating trafficking of membrane proteins like the vacuolar H^+-ATPase (Beaulieu et al., 2005), in exocytosis (Bader et al., 2004) and in different steps during endocytosis (Yarar et al., 2005), phagosome/lysosome fusion (Kjeken et al., 2004; Stockinger et al., 2006) and post-Golgi transport (Cao et al., 2005). Nuclear actin is involved in transcription (reviewed in de Lanerolle et al., 2005). This functional diversification may be accounted for the molecular diversification of actin in the ciliated protozoan, *Paramecium tetraurelia*, where immuno-localization has revealed numerous sites of actin enrichment (Kissmehl et al., 2004).

The number of actin genes in a species can widely vary (Hightower and Meagher, 1986). Multicellular organisms have several isoforms of cytoplasmic actin, which are coexpressed in most cell types and share very similar sequences with each other (Herman, 1993). In addition, a range of actin-like (alp) and actin-related proteins (arp) exist, which are conserved across all eukaryotes (Goodson and Hawse, 2002; Kandasamy et al., 2004; Muller et al., 2005). Arp functions range from specialized effects on conventional G- and F-actin structures to structural activities that are apparently independent of actin. Actins, alps and arps define a large family of homologous proteins, the actin superfamily, which share the same structural architecture, known as the “actin fold”, and an overall sequence similarity to actin (Muller et al., 2005). The actin fold is functionally characterized as an ATPase domain with ATP-binding capacity in the presence of Mg^{2+} or Ca^{2+}. Monomeric actin binds ATP, which is hydrolyzed to ADP after incorporation of the actin monomer into a filament. This hydrolysis is important for the dynamic turnover of actin filaments. Also for several arps, hydrolysis of bound ATP is necessary for their function (Nolen et al., 2004).

A brief look into close relatives of *Paramecium* shows wide variability. Although in most eukaryotes actin is encoded by a multigene family, there are also organisms where only one single actin gene is described so far, e.g. the Apicomplexans *Toxoplasma gondii* and *Cryptosporidium parvum* (Nelson et al., 1991; Kim et al., 1992; Dobrowolski et al., 1997). Genes encoding actin have been cloned also in several other members of the Apicomplexans (Cevallos et al., 2003; Wesseling et al., 1989), which, together with ciliates such as *Paramecium* and *Tetrahymena*, belong to the phylum Alveolata. In *Cryptosporidium*, the actin gene is intronless, and in *Toxoplasma* it has one intron. In *Plasmodium falciparum*,

another Apicomplexan, there are two genes encoding actin (Wesseling et al., 1989). One gene (actin I) is intronless and is expressed throughout the parasite life cycle, while the actin II gene has one intron and is transcribed only in the sexual stages. Several studies on ciliate actin showed that it is different from that of other eukaryotes and therefore described as “unconventional” (reviewed in Villalobo et al., 2001).

In *P. tetraurelia*, a first characterization of actin on the molecular level was achieved when Diáz-Ramos et al. (1998) cloned an actin gene fragment of 1,138 bp, i.e., more than 96% of the coding sequence of a standard actin gene. It was called alpha-actin as it was mostly homologous to that form in other organisms. Sequence data provided by a pilot sequencing project (Dessen et al., 2001; Sperling et al., 2002), the sequencing of a macronucleic one-megabase chromosome (Zagulski et al., 2004) and a current genome project at Genoscope (Evry cedex, France) allowed us to search the *P. tetraurelia* genome for further actin genes. We found 30 genes for actin, arps and alp, to be grouped in 12 widely diverging subfamilies, with varying intron numbers and positions, ATP- and drug-binding sites. This diversification suggests unprecedented specification in localization and function within one cell.

4.3.) Material and Methods

4.3.1.) Stocks and cultures

The wild-type strains of *P. tetraurelia* used were stock strains 7S and d4-2, derived from stock strain 51S (Sonneborn, 1974). Cells were cultivated in a decoction of dried lettuce monoxenically inoculated with *Enterobacter aerogenes* as a food organism, and supplemented with 0.4 $\mu g \cdot ml^{-1}$ ß-sitosterol (Sonneborn, 1970). Bacteria were removed by washing and starving for several hours.

4.3.2.) PCR of genomic DNA and cDNAs

Total wild-type DNA from strain *7S* for PCR was prepared from log-phase cultures as published by Godiska et al. (1987). The open reading frames (ORFs) of individual actin genes were amplified by reverse transcriptase (RT)-PCR using total RNA prepared according to Haynes et al. (1998). RT-PCR was performed in a programmable thermocycler T3 (Biometra, Göttingen, Germany) using 3'-oligo dTT primer and the SuperScript™ III reverse transcriptase (Invitrogen, Karlsruhe, Germany) for first-strand cDNA synthesis. 3'-oligo dTT primer containing the artificial restriction sites EcoRI/NotI was:
5'-AACTGGAAGAATTCGCGGCCGCGGAATTTTTTTTTTTTTT-3'. The subsequent PCR reaction (50 µl) was performed with the Advantage 2 cDNA polymerase mix (Clontech, Palo Alto, California) using actin specific oligonucleotides (Table A1, supplemental material) with or without the artificial restriction sites XhoI, HindIII or StuI added at their 5'-ends. In general, amplifications were performed with one cycle of denaturation (95°C, 1 min), 40-42 cycles of denaturation (95°C, 30 s), annealing (54-58°C, 45 s) and extension (68°C, 3 min), followed by a final extension step at 68°C for 5 min. PCR products were subcloned into the plasmid pCR2.1 by using the TOPO-TA Cloning Kit (Invitrogen) according to the manufacturer's instructions. After transformation into *E. coli* (DH5 cells or TOP10F' cells), positive clones were sequenced as described below.

4.3.3.) Sequencing

Sequencing was done by MWG Biotech (Ebersberg, Germany) custom sequencing service.
DNA sequences were aligned by the CLUSTAL W, integrated in the DNASTAR Lasergene software package (Madison, WI).

4.3.4.) Preparation of non-radioactive and radioactive probes

Oligonucleotide 1 and 2 were also used to generate non-radioactive and radioactive probes by utilizing the PCR DIG Probe Synthesis Kit from Roche Diagnostics (Mannheim, Germany) or

by [γ–^{32}P]dATP incorporation using a Random Primers Labeling System (Gibco-BRL, Cergy-Pontoise, France), according to the supplier's protocol.

4.3.5.) Hybridization cloning

Hybridization cloning from an indexed library of *Paramecium* macronuclear DNA (Keller and Cohen, 2000) was carried out as described previously (Kissmehl et al., 2002).

4.3.6.) Annotation and characterization of further actin genes

In order to identify further actin genes in *Paramecium*, the developing *Paramecium* database (http://www.cgm.cnrs-gif.fr.) was screened by using the nucleotide and amino acid sequence of actins either from other organisms or already identified and annotated *Paramecium* actin genes. Positive hits were further analyzed by performing BLAST searches at the NCBI database (Altschul et al., 1997). Additional classification was performed using ARPAnno (http://bips.u-strasbg.fr/ARPAnno/), an actin-related protein annotation server (Muller et al. 2005). Conserved motif searches were performed with either PROSITE (http://www.expasy.org/prosite; Bairoch et al., 1997), or with BLAST-RPS using pfam entries of the corresponding CDD database (Bateman et al., 2004; Marchler-Bauer et al., 2005). Phylogenetic and molecular evolutionary analyses were performed with either Clustal W and PhyloDraw (version 0.8; Department of Computer Science, Putan National University, Korea [http://pearl.cs.pusan.ac.kr/phylodraw/]), or the Mega version 3 program (Kumar et al., 2004).

4.4.) Results

Molecular cloning from three independently initiated *P. tetraurelia* genome projects, i.e., a pilot sequencing project (Dessen et al., 2001; Sperling et al., 2002), the sequencing of a macronucleic one-megabase chromosome (Zagulski et al., 2004) and the current genome project at Genoscope (Evry cedex, France), revealed that *P. tetraurelia* contains an actin multigene family with 30 members encoding actin, actin-related and actin-like proteins. They can be classified into 12 subfamilies, most of them with several members each.

4.4.1) Actin 1 subfamily

In order to complete the missing ends of the first published actin gene of *P. tetraurelia* (Diáz-Ramos et al., 1998), we took advantage of an indexed genomic library (Keller and Cohen, 2000) by using a ~1 kb probe designed from the sequence of this actin gene (accession number X94954). By performing a two hybridization step, 27 positive spots were detected on type 1 filters, seven of which were also analyzed in detail on type 2 filters. The following clones were then retrieved and sequenced: 47F1, 55B19, 87M3, 96J10, 107D11, 139C10, and 149A2 (internal designations; Keller and Cohen, 2000). One of them, clone 87M3, corresponds to the incomplete actin sequence previously published (Diáz-Ramos et al., 1998). It contains the entire actin sequence including the missing 5'- and 3'-ends, but also 18 nucleotide substitutions (when compared to the sequence published by Diáz-Ramos et al., 1998) predominantly at the ends of the sequence. This actin gene, actin 1-1 (accession number AJ537442), consisting of 1128 bp, encodes a protein of 375 amino acids, with a calculated molecular weight of 41,675 (Table 3). This gene has also been cloned from the cDNA synthesized from the total RNA of vegetative cells. The coding sequence is interrupted by two short introns that display the characteristics of *P. tetraurelia* introns, bordered by 5'-GT and AG-3' and of 21-31 nucleotides in size.

By sequencing the other 6 clones, we found two other isoforms, actin1-2 (accession number AJ537443) and actin 1-3 (accession number AJ537444), which differ from each other by 4 to 8% on the nucleotide level (Table 3). However, on the amino acid level all three actins are identical and they all contain the two introns at the same position. The presence of all three genes in a cDNA library indicates that all three isoforms are expressed. For other actin subfamily 1 members, see below.

Table 3. Molecular characteristics of actins (act), actin-related (arp), and actin-like proteins (alp) in *P. tetraurelia*

			DNA				Protein			
Gene/ subfamily	Accession number	Scaffold number[d]	Length [bp]	*ORF* [bp]	Intron [number]	Identity[a] [%]	Length [aa]	Size [kDa]	Identity[a] [%]	Identity[a, b] [%]
*actin*1										
act1-1[c]	AJ537442	13	1183	1128	2	100	375	41.7	100	100
act1-2[c]	AJ537443	20	1182	1128	2	98.0	375	41.7	100	100
act1-3[c]	AJ537444	32	1184	1128	2	94.8	375	41.7	100	100
act1-4[c]	AJ537445	111	1179	1128	2	78.6	375	41.7	89.9	89.9
act1-5	CR855974	85	1180	1128	2	80.5	375	41.6	91.5	91.5
act1-6[c]	CR548612	1	1128	1128	0	65.8	375	41.2	61.7	61.7
act1-7[c]	CR855973	8	1128	1128	0	71.5	375	41.7	76.9	76.9
act1-8	CR855972	105	1168	1113	2	79.3	370	42.1	70.2	70.2
act1-9[c]	CR855988	41	1158	1131	1	75.2	376	43.3	63.3	63.3
act1-10[c, e]	CR855989	73	1200	1149	1	66.2	103	11.9	10.9	12.2
*actin*2										
act2-1[c]	AJ537446	40	1256	1131	5	100	376	42.4	100	59.6
act 2-2	AJ537447	102	1257	1131	5	89.9	376	42.4	99.5	59.6
*actin*3										
act 3-1[c]	AJ537448	8	1113	1113	0	100	370	42.4	100	44.1
act 3-2[c]	CR548612	1	1113	1113	0	82.7	370	42.1	82.7	44.7
*actin*4										
act 4-1[c]	CR855971	147	1066	1038	1	100	345	38.5	100	28.2
act 4-2	CR856039	128	1062	1038	1	90.8	345	38.5	96.8	28.5
*actin*5 (*arp*1)										
act 5-1[c]	CR855970	156	1282	1131	6	100	376	42.8	100	39.6
act 5-2	CR855969	20	1284	1131	6	93.5	376	42.8	100	39.6
act 5-3	CR855968	13	1284	1131	6	80.3	376	42.9	86.7	39.1
*actin*6										
act 6-1[c]	CR855967	52	1296	1185	4	100	394	44.1	100	30.9
act 6-2	CR855986	60	1294	1185	4	90.5	394	45.0	93.7	31.1
*actin*7 (*arp*4)										
act 7-1[c]	CR855941	115	1217	1164	2	100	387	44.9	100	23.7
act 7-2	CR855965	113	1217	1164	2	89.3	387	44.8	95.4	25.0
*actin*8										
act 8-1[c]	CR548612	1	1100	1056	2	100	351	40.6	100	37.0
*actin*9 (*arp*10)										
act 9-1[c]	CR855964	122	1026	999	1	100	332	38.0	100	17.6
*arp*2										
arp 2-1	CR855976	14	1314	1176	5	100	391	43.8	100	41.2
arp 2-2	CR855992	42	1309	1176	5	90.7	391	43.9	96.2	40.2
*arp*3										
arp 3-1	CR856038	62	1401	1278	5	100	426	48.9	100	36.2
arp 3-2	CR855990	24	1401	1278	5	92.6	426	48.9	98.6	36.2
*alp*1 (*arp*5)										
alp 1-1	CR855977	19	2002	1978	1	100	658	76.9	100	25.0

[a] Sequences were aligned by Clustal W
[b] Numbers are referred to the amino acid sequence of act1-1
[c] Genes are analyzed also on the cDNA level
[d] *Paramecium* genome project, series of cloned pieces of DNA representing overlapping regions of a particular chromosome, that are in the right order
[e] Putative pseudogene

4.4.2.) Actin 2 subfamily

Among the 722 protein encoding genes identified in the course of the pilot sequencing project of the *P. tetraurelia* macronuclear genome we also found a partial sequence with homology to

another mammalian actin. Sequencing of the corresponding clone, clone M07D05u resulted in the identification of the 5'- end of this gene. To obtain the missing 3'- end, we took advantage of the indexed genomic library, which we analyzed in two subsequent hybridization steps by using a specific probe designed from sequence M07D05u. Besides clone M07D05u, another 9 positive spots were detected on type 1 filters, which were analyzed in detail on type 2 filters. The following clones were then retrieved and sequenced: 15M16, 27N16, 27P11, 27P12, 47j22, 74C9, 87H1, 87J8, 93E10, and 134L2. Most of the clones do contain the complete sequence information of this gene, but also of a closely related actin isoform. The two genes were called *actin2-1* (accession number AJ537446) and *actin2-2* (accession number AJ537447). Sequencing from a *Paramecium* cDNA-library revealed the cDNA information of the corresponding genes. The ORFs, which are interrupted by 5 short introns, encode proteins of 376 amino acids with calculated molecular masses of 42.4 kDa (Table 3).

4.4.3.) Other actin subfamilies

During early steps of the *P. tetraurelia* whole genome shotgun sequencing undertaken by Genoscope (http://www.genoscope.cns.fr), and by manual assembly of single reads excluded from the draft assembly we used, we were able to identify further actin coding genes, given a total number of 30 genes encoding actins, arps and alp. Subfamily nomenclature was given in chronological order of their finding.

Interestingly, the megabase chromosome sequencing project (Zagulski et al., 2004) revealed a cluster of three actin genes (scaffold1; accession number CR548612; actin1-6, actin3-2 and actin8-1). On the related sister scaffold (scaffold 8) only two actins were present (actin1-7, accession number CR855973, and actin3-1, accession number AJ537448). The incidence of two closely related isoforms is probably due to recent whole genome duplication in *P. tetraurelia* (J. Cohen and L. Sperling, personal communication; Aury et al., in press).

4.4.4.) Actin sequences

The 30 genes found in *P. tetraurelia* can be divided into twelve subfamilies: seven pairs, one trio, three single genes, and a large subfamily with 10 members, one of those seems to be a pseudogene (Table 3). Within a subfamily, proteins are of equal size. Exceptions are the members of subfamily 1 which vary between 367 and 376 amino acids (aa).

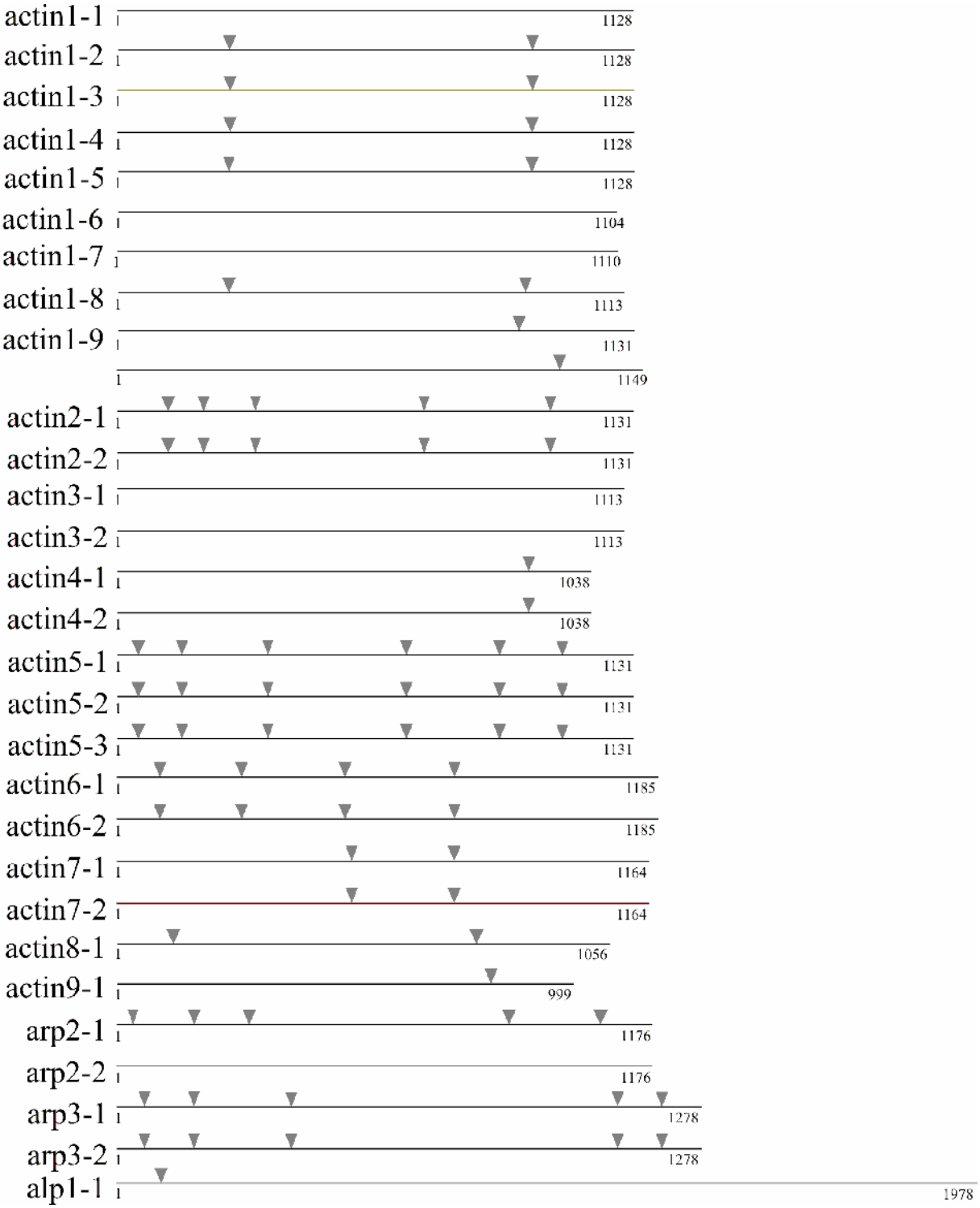

Fig. 26. Position of introns (drawn to scale) in the nucleotide sequence of the different actins and actin-related proteins in *P. tetraurelia*. Within a subfamily, both localization and length of the introns are identical. The position of the introns are as follows (bp): subfamily 1, intron I (241-270), intron II (907-933); subfamily 2, intron I (110-140), intron II (218-243), intron III (332-354), intron IV (731-754), intron V (976-1001); subfamily 4, intron I (900-925); subfamily 5, intron I (45-74), intron II (139-163), intron III (359-381), intron IV (690-716), intron V (922-948), intron VI (1108-1132); subfamily 6, intron I (93-120), intron II (273-303), intron III (530-528), intron IV (799-825); subfamily 7, intron I (514-539), intron 2 (738-766); subfamily 8, intron I (121-141), intron II (780-804); subfamily 9, intron I (818-845); subfamily arp2, intron I (35-57), intron II (169-189), intron III (321-350), intron IV (920-949), intron V (1129-1161); subfamily arp3, intron I (58-82), intron II (168-191), intron III (410-435), intron IV (1170-1196), intron V (1280-1305); subfamily alp1, intron I (84-109).

While several *P. tetraurelia* actin genes encode proteins with the common actin length of 375 aa, there are also smaller (down to 332 aa) and larger proteins (up to 394 aa). Both arp2 and arp3 isoforms, with 391 aa and 426 aa, respectively, are in the range of the usual lengths for those proteins. Additionally one gene encodes a large actin-like protein with 658 aa (Table 3). Amplification with gene-specific primers from *P. tetraurelia* cDNA indicates the expression of selected isoforms and reveals cDNA information about these genes. Comparison of these sequences with the genomic version allows us to determine number, size and position of the introns. The number and positions of introns varies between the different subfamilies, while they are of the same size and position within a subfamily (Fig. 26). An exception is again subfamily 1, where six members possess two introns, while the other four members contain only one, and they are not all at the same position and of the same length. In subfamily 3, the two members do not contain any introns. Subfamily 5, where the ORF is interrupted by six introns, has the highest number of introns (Fig. 26, Table 3). For actin1-10, intron splicing creates a stop mutation and would result in the expression of only a 103 amino acid fragment of the protein. As the presence of spliced act1-10 cDNA was experimentally verified, the existence of such a short peptide is possible. However, this has not been analyzed so far.

Members within a subfamily share more than 80% sequence identity at the nucleotide level (alignment with Clustal W). Exceptions are the members of subfamily 1 whose amino acid composition varies by up to 34%. The different actin subfamilies are highly divergent from each other. Comparing the amino acid sequence of all of them to actin1-1, the isoforms of the actin2 subfamily have the highest identity with less than 60%. All other subfamilies show even less than 50% identity on amino acid level with actin1-1, with the lowest value of 17.6% for actin9. Actin1-1 was chosen as reference sequence as it is, together with the identical (on amino acid level) isoforms actin1-2 and actin1-3, the most conserved actin in comparison to actins from other organisms (Table 4). Nevertheless, even these isoforms share less than 80% identity with actins of selected model organisms. Members of other subfamilies have less than 50% identity between each other, with the most diverse isoform, actin9-1, sharing only 17.6% identity. This wide diversification of *P. tetraurelia* actins is manifested in the differences found in several actin characteristics, as shown below.

Table 4. Identities between *P. tetraurelia* actin paralogs and actins from other organisms on amino acid level

% Identity[a] [aa]	T. thermophila (AAP79896)	*T. gondii* (AAC13766)	*D. discoideum* (P02577)	*S. cerevisiae* (NP_116614)	*C. elegans* (CAA34718)	*D. melanogaster* (AAF57294)	*R. norvegicus* (ATRTC)	*A. thaliana* (AAM65277)	*H. sapiens* (AAH16045)
actin1-1	78.5	73.9	73.9	71.8	72.3	73.4	72.3	73.4	72.6
actin1-2	78.5	73.9	73.9	71.8	72.3	73.4	72.3	73.4	72.6
actin1-3	78.5	73.9	73.9	71.8	72.3	73.4	72.3	73.4	72.6
actin1-4	77.4	70.2	69.9	70.2	69.9	70.2	69.7	69.4	69.9
actin1-5	76.3	70.7	70.5	71.0	69.4	70.2	69.7	69.9	69.9
actin1-6	57.7	54.5	56.1	56.1	56.1	56.1	56.1	56.1	56.4
actin1-7	69.1	66.88	64.4	66.5	66.2	64.4	65.4	64.9	65.7
actin1-8	59.8	58.8	57.1	57.4	56.6	57.1	56.6	56.6	56.6
actin1-9	57.0	53.3	52.3	52.5	51.5	52.5	51.7	51.5	52.0
actin2-1	62.6	61.3	60.5	58.6	60.5	60.5	61.8	60.2	62.1
actin3-1	46.9	44.2	45.0	46.6	45.0	44.7	44.7	44.5	44.7
actin4-1	30.6	29.5	30.3	30.6	30.9	30.6	30.6	30.3	30.6
actin5-1	42.2	40.6	40.3	41.6	40.6	41.1	40.6	40.6	40.6
actin6-1	30.6	29.6	30.1	33.2	30.9	31.1	31.4	30.6	31.4
actin7-1	24.2	22.9	22.7	24.7	23.7	23.5	23.7	23.7	23.7
actin8-1	38.9	35.6	37.5	38.1	38.6	37.8	38.3	36.9	38.1
actin9-1	19.5	20.4	20.4	20.4	20.1	19.5	19.8	19.8	19.5

[a] Sequences were aligned by Clustal W method

4.4.5.) Actin-related proteins (arps)

Because of high sequence identity and similarity between actin and arps sequences, and low sequence identity of *P. tetraurelia* genes to those of other organisms, it is sometimes difficult to unambiguously classify a *P. tetraurelia* sequence from BlastP database searches. Indeed the search of homologs for some isoforms leads to protein hits exhibiting a significant E-value. Among these, conventional actin sequences are dispersed among arp sequences. Therefore, the assignment of some subfamilies could have been exchanged, e.g., actin5 with arp1. Additionally, we used ARPAnno, an actin-related protein annotation server designed by Muller et al. (2005), for classification of our sequences. In general, the results from NCBI Blast search and ARPAnno concur, only in two cases different classifications were obtained (see below). In spite of these variations, to avoid confusion in nomenclature, we do not change the existing names (as deposited in the database).

Several arps are subunits of chromatin remodeling complexes (Olave et al., 2002). The nuclear arps, arp4 and arp6, which are copresent in the SW12-SNF2 complex, are omnipresent in eukaryotic organisms, except for the parasite *Encephalitozoon cuniculi* (Muller et al., 2005). Similarly, in the *P. tetraurelia* genome, we only found orthologs for

arp4 (actin7) but none for arp6. The designation as arp4 is due to blast search hits for arp4 from the NCBI database. In contrast, alignment with ARPAnno gave the best score (score ranging from 0 to 100) for arp2 (29.1), but the score for arp4 is just slightly below (28.8). Arp4 is also member of the chromatin remodeling complex INO80 which also includes arp5 and arp8. Both arp5 and arp8 are generally absent from lower phyla. In the *P. tetraurelia* genome, only an ortholog for arp5 (denominated alp1) exists, none for arp8. In contrast, all cytoplasmic arps are present in the *P. tetraurelia* genome. Both arp2 and arp3 are represented by two isoforms. For the third cytoplasmic arp, arp1, we found three orthologs (actin5-1, actin5-2 and actin5-3). The functionally obligate heterodimeric partners arp7 and arp9, the two arps restricted to fungi so far, are not present. Actin9, the most divergent actin isoform in *P. tetraurelia*, is difficult to classify. While NCBI database blast resulted in hits for both actin and arp10, ARPAnno alignment showed the best, but very low, score (24.8) for both arp2 and orphans (sequences lacking common defining characteristics).

4.4.6.) Phylogenetic distribution

The growing number of sequence data from different organisms available allows us to investigate the phylogenetic distribution of *P. tetraurelia* actins and actin-related proteins. A phylogenetic tree with 71 sequences from 25 other organisms, including 18 sequences from *P. tetraurelia*, was created using PhyloDraw (matrix: neighbor joining). We selected at least one member of each subfamily; for subfamily one, the isoforms actin1-2 and 1-3 were excluded. The diversity of *P. tetraurelia* actins is well presented in the phylogenetic tree (Fig. 27). The first members of subfamily 1 cluster in a single-standing branch (A), while actin1-6 and 1-7 group together with subfamily 3 (B). Subfamilies 4, 8 and 9 group together and are isolated from any other actin or arp (C). A close cluster is formed by actin subfamily 7 and arp subfamily 2 (D). Other subfamilies are scattered throughout the tree, but only alp1-1 is close to an ortholog from other ciliates or Apicomplexans (in this case, *T. thermophila* alp). Only a large branch (E) includes actin from different ciliates, i.e. *P. tetraurelia* subfamily 6, arp subfamily 3 and actin-like protein 1 together with arps from *Tetrahymena* and *Plasmodium*, however with several intermediates. Within this large cluster, *P. tetraurelia* arp3 clusters with arp3 from other organisms (E*). Subfamily 5 is isolated from any other actin or arp.

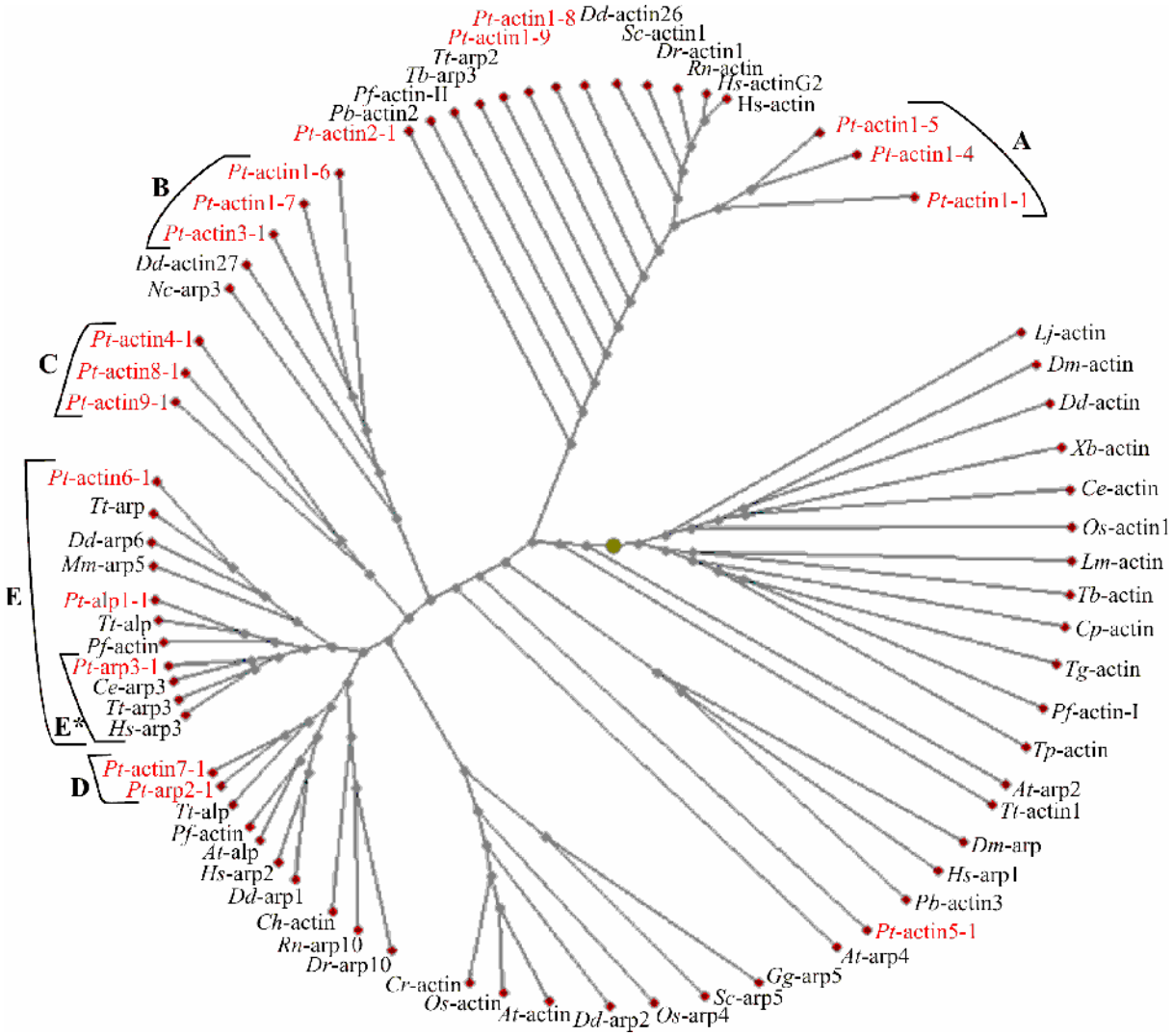

Fig. 27. Phylogenetic tree of actins and arps encompassing (GenBank accession numbers in parentheses) *Arabidopsis thaliana* actin (AAM65277), arp2 (AAC69601), arp4 (AAM53244) and alp (ARP5) (BAB03145); *Caenorhabditis elegans* actin (CAA34718) and arp3 (AAF36012); *Chlamydomonas reinhardtii* actin (BAA09449); *Cryptosporidium hominis* actin (XP_667340); *Cryptosporidium parvum* actin (AAA28295); *Danio rerio* arp1 (NP_998537) and arp10 (AAH45412); *Dictyostelium discoideum* actin (P02577), actin26 (XP_646389), actin27 (XP_636189), arp1 (XP_636500), arp2 (XP_645275) and arp6 (XP_637435); *Drosophila melanogaster* arp (CAA55240), actin, (BAA20058) and actin (AAF57294); *Gallus gallus* arp5 (NP_001008446); *Homo sapiens* actG2(CAG38753), ß-actin (AAH16045), arp1 (AAH06372), arp2 (NP_005713) and arp3 (NP_005712); *Laminaria japonica* actin (ABB80121); *Leishmania major* actin a (CAC22667); *Mus musculus* arp5 (AAH52039); *Neurospora crassa* arp3 (AAC78497); *Oryza sativa* actin1 (XP_475316) and arp4 (XP_479987); *Paramecium tetraurelia* act1-1 (CAD60960), act1-4 (CAD60963), act1-5 (CAH69678), act1-6 (CAH03399), act1-7 (CAH69677), act1-8 (CAH69676), act1-9 (CAH69752), act2-1 (CAD60964), act3-1 (CAD60966), act4-1 (CAH69675), act5-1(arp1-1) (CAH69674), act6-1 (CAH69671), act7-1 (arp4-1) CAH74221), act8-1 (CAH03397), act9-1 (arp10) (CAH69669), alp1-1 (arp5) (CAH69680), arp2-1 (CAH69679) and arp3-1 (CAH74222); *Plasmodium berghei* actin2 (XP_680164) and actin3 (CAC48194); *Plasmodium falciparum* actin (NP_700976), actin I (AAA29465), actin II (AAA29467) and actin(Arp1) (NP_703241); *Rattus norvegicus* ß-actin (ATRTC) and arp10 (AAH87143); *Saccharomyces cerevisiae* act1p (NP_116614) and arp5 (CAA95933); *Tetrahymena thermophila* actin1 (AAP79896), arp (AAN73251), arp2 (AAN73249) arp3 (AAN73250), actin family protein (EAS01136) and actin family protein (EAR99381); *Theileria parva* actin (EAN33188); *Toxoplasma gondii* actin (AAC13766); *Trypanosoma brucei* actin (AAA30151) and arp3 (EAN76600); and *Xenopus borealis* actin (CAA30390).

4.4.7.) Actin consensus pattern

PROSITE has developed three signature patterns which detect most of the sequences known to belong to actin. Two of them (ACTINS_1, [FY]-[LIV]-G-[DE]-E-A-Q-x-[RKQ](2)-G, position 54 to 64, and ACTINS_2, W-[IV]-[STA]-[RK]-x-[DE]-Y-[DNE]-[DE], position 357

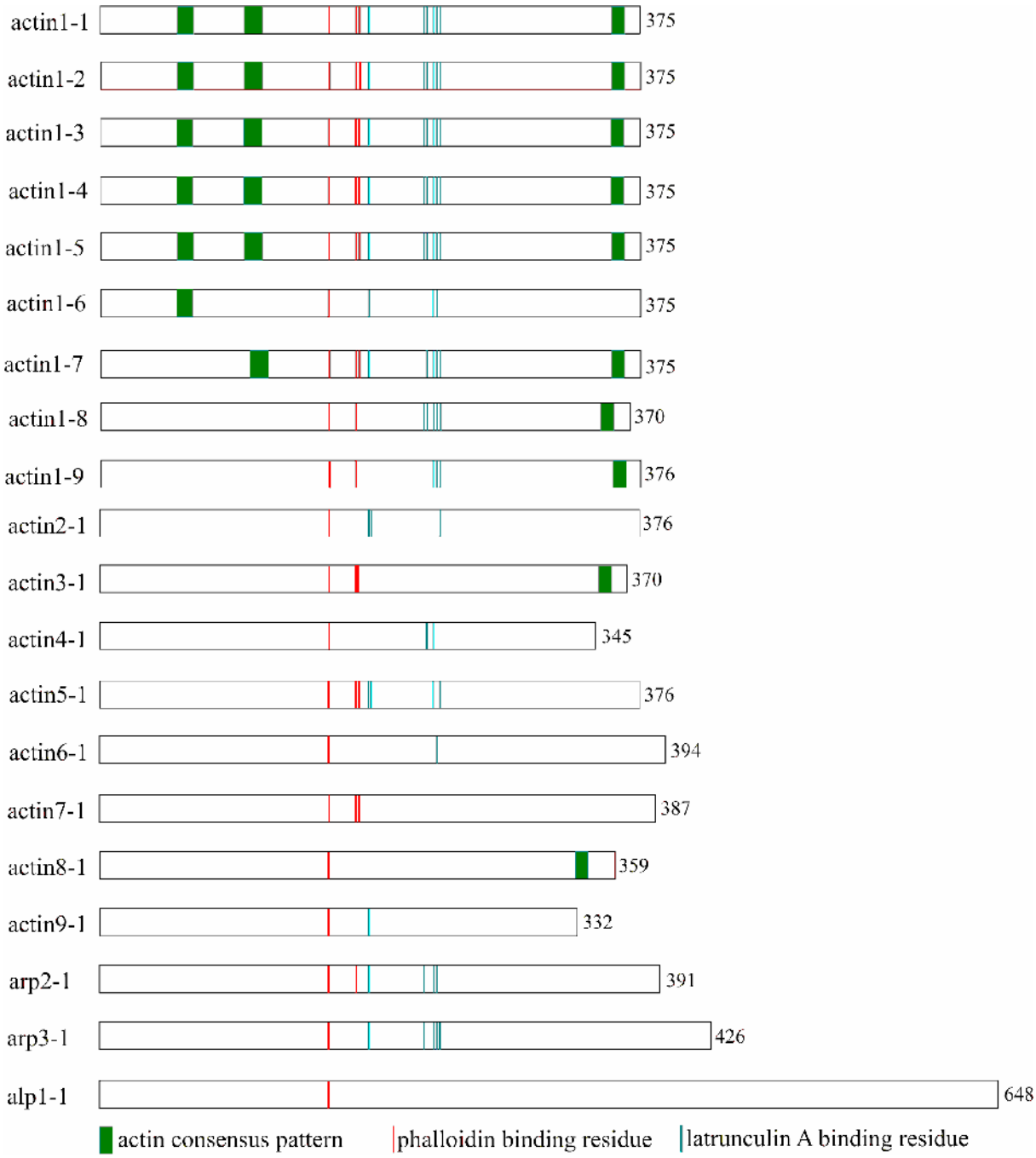

Fig. 28. Characteristic features of *P. tetraurelia* actins, arps and alp, including consensus and drug binding motifs. These are identical within subfamilies wherefore only one isoform of each is shown exemplarily. The actin signatures (green) are based on the three actin consensus pattern according to PROSITE: ACTINS_1, [FY]-[LIV]-G-[DE]-E-A-Q-x-[RKQ](2)-G; ACTINS_2, W-[IV]-[STA]-[RK]-x-[DE]-Y-[DNE]-[DE] and ACTINS_3, [LM]-[LIVM]-T-E-[GAPQ]-x-[LIVMFYWHQ]-N-[STAQ]-x(29-N-[KR]. Not all isoforms contain the typical consensus pattern found in most of the actin genes described in other species. Also the three residues mediating the binding of phalloidin (G158, R177 and D179) are not present in every subfamily (red). The same is true for the residues (blue) relevant for the binding of latrunculin A (D157, R183, D184, R210, D211, K213, E214 and K215).

to 365) are specific for actins, while one signature (ACTINS_3, [LM]-[LIVM]-T-E-[GAPQ]-x-[LIVMFYWHQ]-N-[STAQ]-x(29-N-[KR], position 106 to 118) picks up actins, actin-related proteins and actin-like proteins. We used ScanProsite (http://www.expasy.org/prosite) to search for the actin signatures in *P. tetraurelia* actin sequences. Most of the actin paralogs, namely the actin subfamilies actin2, actin4, actin5, actin6, actin7, actin9, the arps and the alp, do not possess any actin consensus pattern (Fig. 28). Actin signatures are mainly present in the actin1 subfamily, where every isoform has at least one consensus pattern, but only the isoforms actin1-1 to actin1-5 have all three of them. The ACTINS_1 and ACTINS_3 signatures are restricted to the actin1 subfamily. The ACTINS_2 signature is the most common, with an expression in nearly all isoforms of the actin1 subfamily (except for actin1-6), in the actin3 subfamily and in actin8-1.

4.4.8.) Amino acids influencing polymerization

Several specific amino acids were proven to be involved in subunit interaction across the actin filament. An intermolecular coupling of the DNase I binding loop (residues 38-52) and the C terminus (Kim and Reisler, 1996), and of the hydrophobic plug (residues 262-274) and the C terminus (Feng et al., 1997) has been suggested. Examples for intermonomer cross-linking of F-actin are the residue pairs H40/E167, Q41/C374, S265/C374, and Q41/C265 (Hegyi et al., 1992; Kim et al., 2000). We aligned the *P. tetraurelia* actin sequences with a number of actins from other organisms (namely those of Table 2, additionally another *H. sapiens* actin sequence [accession number CAG38753] and a *P. falciparum* sequence [accession number PFL2215w]) and checked for the presence of the above-mentioned residues. Most isoforms do not possess a pair of interacting amino acids (Table 5). Only in subfamily 1 we could find such pairs. This is mainly due to the lack of the residues in the DNase I binding loop, H40 and Q41, respectively, in all other subfamilies. In most subfamilies, the amino acid conservation in the DNase I binding loop is generally weak

Table 3. Amino acids influencing polymerization[a] (Pairs H40/E167, Q41/K113, Q41/S265, Q41/C374, S265/C374)

	H4/E167		***Q41 / K113***		***S265***	***C374***
actin1-1	***H***	***E***	***Q***	***K***	N	***C***
actin1-4	***H***	***E***	K	*K*	N	*C*
actin1-5	***H***	***E***	***Q***	***K***	H	***C***
actin1-6	Q	*E*	N	*K*	K	*C*
actin1-7	Q	*E*	K	*K*	E	*C*
actin1-8	Y	*E*	D	*K*	***S***	***C***
actin1-9	K	*E*	***Q***	E	K	***C***
actin2-1	Q	*E*	P	A	I	*C*
actin3-1	-	*E*	-	*K*	N	*C*
actin4-1	-	D	-	*K*	N	*C*
actin5-1	Y	D	K	Q	E	Q
actin6-1	N	Q	D	*K*	P	T
actin7-1	-	D	-	*K*	P	M
actin8	-	*E*	-	*K*	P	*C*
actin9	-	D	-	E	Y	N
arp2	A	D	D	*K*	W	V
arp3	Q	D	K	P	E	A
alp1	-	D	-	D	*S*	P

(data not shown). The same holds true for the hydrophobic plug. The amino acid S265, which interacts intermolecularly with two residues, is only present in actin1-8.

4.4.9.) ATP binding

Both actin and arps bind ATP. The hydrolysis of ATP to ADP is proposed to induce a conformational change which is required for their biological function (Otterbein et al., 2001; Nolen et al., 2004). The conservation of 17 key reference residues involved in nucleotide binding was analyzed for each isoform (Fig. 29). The isoforms can be clustered in three groups. The first group is composed of actin1-1 till actin1-8, the subfamily actin2, actin5-1, actin5-2, and the arp subfamilies 2 and 3, that all posses >60% conserved residues. The second group, composed of actin1-9, the subfamilies actin3, actin5-3, actin6, and actin8, has 40-60% conserved residues. The third group displays a very low level of conserved residues with less than 30% (subfamilies actin4, actin7 and actin9).

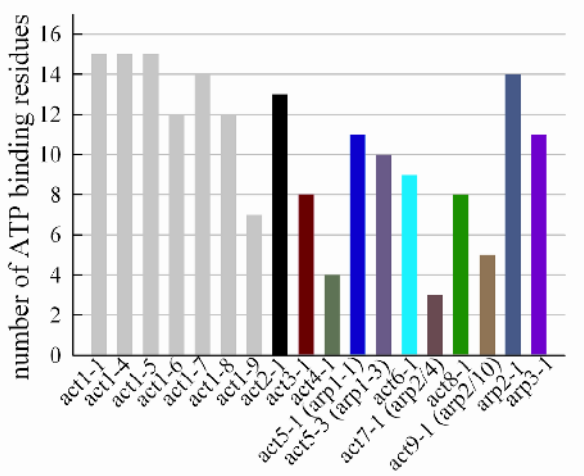

Fig. 29. Conservation pattern of 17 residues (D13, S16, G17, L18, K20, Q139, D156, D159, G160, V161, K215, G304, T305, M307, Y308, and K338) known to participate in ATP binding to actin. For subfamilies in which the conservation pattern is identical for all members, only one is shown.

4.4.10.) Binding residues for myosin II

Actin binds a substantial number of proteins collectively called actin binding proteins. One of the best studied is myosin II. We looked for the expression of myosin II binding residues (Rayment et al., 1993) in *P. tetraurelia* (Fig. 30). The binding site is well conserved in subfamilies 1 (except act1-8), 2 and 4. In several members of subfamily one, all residues are present. Most of the other subfamilies show at least 40% identity, only in some actin/arp subfamilies the conservation is weak.

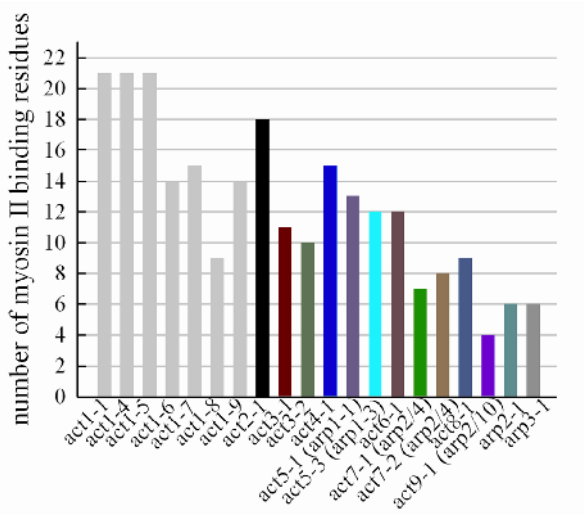

Fig. 30. Conservation pattern of 23 myosin II-binding residues (2, 24, 25, 40, 42, 144-148, and 341-353). For subfamilies in which the conservation pattern is identical for all members, only one is shown.

4.4.11.) Drug binding residues

Not only actin binding proteins, but also several drugs can interact with actin and where they interfere with polymerization and depolymerization. Phalloidin binds to actin filaments and stabilizes them against depolymerization (Wieland and Faulstich, 1978). Using fluorescently labeled phalloidin is a common approach to visualize actin filaments. While microinjection of fluorescent phalloidin in *P. tetraurelia* resulted in distinct labeling pattern, no staining of the cleavage furrow could be achieved (Kersken et al., 1986), despite the fact that actin is unequivocally involved in cell division. Also in the related ciliate, *T. pyriformis*, actin did not bind phalloidin (Hirono et al., 1989). Since mutagenesis studies of actin have been an effective approach to identify binding sites for actin drugs, we had a closer look at phalloidin binding sites. As such, G158, R177 and D179 have been suggested (Drubin et al., 1993; Belmont et al., 1999). Using the multiple sequence alignment of actins, we found that only six actin isoforms possess all three of these amino acids (Table 6, Fig. 28). While G158 is highly conserved and exists in all isoforms, the other two residues are lacking in many subfamilies.

Table 6. Drug binding residues[a]

	phalloidin			latrunculin A[b]								
	G158	***R177***	***D179***	***D157***	***R183/D184***		***R210/D211***		***K21/E214/K215***			
actin1-1	***G***	***R***	***D***	S	*R*	A	***R***	***D***	***K***	***E***	***K***	
actin1-4	***G***	***R***	***D***	S	*R*	A	***R***	***D***	***K***	***E***	***K***	
actin1-5	***G***	***R***	***D***	S	*R*	A	***R***	***D***	***K***	***E***	***K***	
actin1-6	*G*	K	N	S	*R*	L	K	N	*K*	*E*	R	
actin1-7	***G***	***R***	***D***	S	*R*	A	K	*D*	***K***	***E***	***K***	
actin1-8	*G*	*R*	Y	S	S	T	***R***	***D***	***K***	***E***	***K***	
actin1-9	*G*	*R*	C	C	N	A	D	I	***K***	***E***	***K***	
actin2-1	*G*	K	H	S	***R***	***D***	N	A	D	T	*K*	
actin3-1	***G***	***R***	***D***	S	Y	A	S	L	Y	V	A	
actin4-1	*G*	Q	P	I	E	I	P	*D*	*K*	F	I	
actin5-1	***G***	***R***	***D***	V	***R***	***D***	I	I	*K*	Y	*K*	
actin6-1	*G*	F	S	L	A	E	D	K	S	*E*	E	
actin7-1	***G***	***R***	***D***	C	E	Y	S	L	M	Y	G	
actin8	*G*	F	N	S	K	S	L	Q	Q	Q	Q	
actin9	*G*	G	Y	L	*R*	E	C	Y	D	T	Y	
arp2-1	*G*	*R*	N	A	*R*	H	*R*	E	*K*	*E*	A	
arp3-1	*G*	H	P	S	*R*	D	*R*	E	***K***	***E***	***K***	
alp1-1	*G*	R	N	L	L	N	L	Q	Q	E	R	

[a] Analysis was performed using Clustal W. ***Bold and italic***, all interacting residues are present; *italic*, not all residue are present

[b] each combination represents an allele in yeast mutagenesis studies

Latrunculin is another actin binding drug for which mutagenesis studies revealed the binding residues. This drug sequesters actin monomers by making 1:1 complexes (Yarmola et al., 2000). In yeast mutagenesis studies, three mutated alleles (act1-112: K213, E214, K215; act1-113: R210, D211; act1-117: R183, D184) lead to a complete resistance to latrunculin A (Ayscough et al., 1997). Analysis of *P. tetraurelia* actin sequences showed that the residues for latrunculin A binding are mainly present in the actin1 subfamily, but no isoform possesses

all of them (Table 6, Fig. 28). Only sporadic binding residues can be found in the other subfamilies, and none in actin subfamilies 3, 7 and 8. Amino acid D157, which has also been implicated in the binding of latrunculin A (Belmont et al., 1999), is not present in *P. tetraurelia* actins (Table 6).

4.5.) Discussion

In the present work, we describe 30 genes coding for actins, actin-related proteins or actin-like proteins in *P. tetraurelia*, which cluster in 12 subfamilies.

4.5.1.) Identification of arps and alp

The amino acid sequence variation between the different *Paramecium* subfamilies is very high. When compared to actin1-1, which is most identical to conventional actins, most of them show less than 50% identity. In the literature, arps share between 17 and 60% amino acid identity with conventional actins. Due to contradictorily hits with blast searches in the database, some *P. tetraurelia* subfamilies could be assigned to both, actins or arps. Most "double-hits" are confirmed by alignments with ARPAnno. The same holds true for the single alp found in the *Paramecium* database, where NCBI blast search showed also hits with arp5, which is supported by a best ARPAnno score for arp5. Hence, the respective proteins are annotated as actins in the *Paramecium* database, with the indication arp in brackets.

From the eleven arp subfamilies described in the database, six have presumably orthologs in *P. tetraurelia*. The lack of several subfamilies is not unexpected as some of them are restricted to, or absent from different phyla (Muller et al., 2005). All cytoplasmic arps are present in the *Paramecium* genome (named actin5 [arp1], arp2 and arp3). Arp1 (also called centractin), a major component of the dynactin complex, is present in a wide range of organisms, from yeast to humans, but absent from *Arabidopsis*, rice and possibly from other plants (Muller et al., 2005). Yeast has a single arp1 gene, whereas higher eukaryotes have at least two or perhaps three isoforms (Kandasamy et al., 2004). In *P. tetraurelia*, we found three isoforms (actin5-1, 5-2 and 5-3). With a length of 376 amino acids, they match the general length of arp1 in vertebrates, but they are less identical to conventional actins than in general (~40% in comparison to 55-60%, Hollerein and Holzbaur, 1999).

Like arp1, a second actin-related protein is found in the dynactin complex – arp10 (yeast) or arp11 (fly and vertebrates). According to NCBI database blast, actin9 could be an ortholog of arp10. However, ARPAnno alignment resulted in no score for arp10 and an even low score for arp2 and orphans, which makes an accurate classification difficult. The actin-related proteins arp2 and arp3 form the arp2/3 complex, which is a major nucleator of actin polymerization (Pollard and Beltzner, 2002). For both of them two isoforms are present in *P. tetraurelia*, while they are coabsent from Apicomplexans (Gordon and Sibley, 2005). Additionally we found sequences which are presumably orthologs of the nuclear arp4 (actin7) and arp5 (alp1). Admittedly, the classification of actin7 as arp4 according to NCBI blast search might be critical, as ARPAnno gave a slightly better score for arp2. Both, arp4 and

arp5, are thought to be copresent in chromatin remodeling complexes with some other arps. Surprisingly we could not find orthologs of the respective partners (arp6 and arp8) in the database. Arp4 and arp6 are the most conserved arps regarding the distribution among the eukaryotic phyla, while both arp5 and arp8 are absent from several organisms (Muller et al., 2005). It would be interesting to determine if the lack of these arps correlates with a lack of the corresponding complementary subunit, or if their functions are fulfilled by other proteins. However, it its possible that potential genes escaped our data mining approach due to high evolution rates or if they were disrupted by many or unconventional introns.

4.5.2.) Actin isoforms

The high number of actin and arp sequences in *P. tetraurelia* seems to be quite unusual for an unicellular organism. While for several multicellular organisms, an exorbitant number of actin genes was reported (for example, petunia was shown to have over 100 actin genes [Meagher and McLean, 1990), the situation in protists seems to be rather different. Several genome projects (for *Leishmania major, Plasmodium berghei, Plasmodium falciparum, Trypanosoma brucei* and *Tetrahymena thermophila*) revealed only about 10 sequences related to the actin superfamily. However, in *Dictyostelium discoidium*, also over 30 genes for actin and arps were found (Eichinger et al., 2005).

Several possible reasons were discussed why organisms have multiple actin isoforms (Rubenstein, 1990). One argument is that, as actin plays a role in many cellular processes, organisms need a large quantity of actin, and the best way to provide enough actin may be to have multiple genes. In fact, in *P. tetraurelia*, we found three isoforms which are identical one amino acid level (actin1-1, 1-2 and 1-3), and they are all expressed. While their existence could be explained with genome duplications in *P. tetraurelia*, the expression of all three of them might be a tool for gene amplification. A related explanation is that, because some cells need more actin than others, multiple genes provide a mechanism for differential regulation of actin expression. In this case, the amino acid differences would also be less functionally significant, but the regulation of the expression of the genes would be critical. For instance, the two *Drosophila* cytoplasmic actin genes show a differential temporal and spatial expression (Wagner et al., 2002). Finally, amino acid difference may be important, allowing the different isoforms to exert different roles in the same cell. The high degree of divergence observed in *P. tetraurelia* actins might be a hint to the last hypothesis. Mammals synthesize different isoforms of actin in a tissue specific fashion, strongly suggesting that there may be a functional basis for this isoform multiplicity (Vanderkerckhove and Weber, 1978). Plant actins show diversity in their gene sequences, protein isoforms, and tissue distribution. In the

model plant *Arabidopsis*, there are eight actin genes, which can be divided into vegetative and reproductive classes, and are expressed in a tissue-specific manner (Kandasamy et al., 2002). The spectrum of actin proteins may reflect the mixture of actin functions and/or patterns of regulation in plant organs (Meagher and McLean, 1990). But also within a single cell, specialized function could be observed. Within muscle cells, muscle actins may be preferentially utilized for the formation of myofibrils, whereas cytoplasmic actin isoforms may be used exclusively for certain cytoskeletal functions. Several studies in other systems also suggest that different isoforms do have specialized functions (Herman, 1993). This may also be assumed for the numerous isoforms we find in *P. tetraurelia*, considering the multiple localization sites (Kissmehl et al., 2004).

Another interesting point is the possible redundancy of various isoforms. Assuming that the different subfamilies have indeed different functions, could one isoform nevertheless compensate the loss of another? In *Chlamydomonas reinhardtii*, the loss of the conventional actin is compensated by enhanced expression of a highly divergent actin called "novel actin-like protein" (NAP), which is only negligibly expressed in stationary wild type cells (Kato-Minoura et al., 1998). NAP homologues are present in several green algae, order Volvocales (Kato-Minoura et al., 2003).

4.5.3.) Phylogenetic distribution

The diversity of *P. tetraurelia* actins and arps is well represented in the phylogenetic tree (Fig. 27). The tree shows that many *P. tetraurelia* sequences are different from conventional actins, but it also reveals that subfamilies are different from one another. Subfamily 7 clusters together with arp family 2 (D), which is in good agreement with the ARPAnno results defining actin 7 as arp2. Subfamilies 4, 8 and 9 cluster together in an isolated branch (C). As these subfamilies are the most divergent actins within the *P. tetraurelia* actin family, the clustering of these long branches has to be analyzed in more detail. Most subfamilies do hardly cluster with actins from other organisms, even not with those from other ciliates. Apart from the single *T. thermophila* arp sequence in (D), only one large branch where *Paramecium* sequences go together with sequences form other apicomplexans can be observed (E). Alp from *P. tetraurelia* form one branch with *T. thermophila* alp, and another branch can be observed with arp3 sequences from *P. tetraurelia* and several other organisms (E*). This is the single example for a well defined branch with sequences from *P. tetraurelia* and orthologs from other organisms. To verify the resulting tree, a phylogenetic tree with 40 additional sequences was created, as well as an additional program was used (Mega3), which both had the same clusters and isolated branches for *P. tetraurelia* sequences (data not shown). These

findings agree with the diversity within ciliate actins which was recently reported for other ciliates by Kim et al. (2004). Similarly, arps from apicomplexans do not group with any of the known arp clades (Gordon and Sibley, 2005), as we confirm, although they are considered closely related to ciliates.

4.5.4.) Actin consensus pattern

Analyses of the actin sequences known so far allowed PROSITE to develop three actin signatures. In *P. tetraurelia*, only five isoforms (actin1-1 to actin1-5) do possess all three. Most *P. tetraurelia* actins do not contain any of these signatures (Fig. 28). Neither arps nor alp possess the actin consensus pattern which usually serves to detect them. One should keep in mind that these patterns detect most, but not all, actins, arps and alps in the database. There are a number of known false negative hits using these patterns in PROSITE search (http://www.expasy.org/cgi-bin/nicesite.pl?PS00406). The lack of any actin consensus pattern in most of the *P. tetraurelia* isoforms illustrates again the highly divergent character of actins and arps in this organism.

4.5.5.) Amino acids influencing polymerization

The DNase I binding loop, the hydrophobic plug and the C-terminus region are among the structural elements of monomeric actin proposed to form the intermonomer interface in F-actin (Kim et al., 2000). Several amino acids have been shown to be involved in the intermolecular interaction across the actin filament. In *P. tetraurelia* actin subfamilies, many of them are lacking (Table 5). This is especially true of the residues in the DNase I binding loop and the hydrophobic plug, which in general are not well conserved. Among Spirotricha (ciliates), these regions are segments of increased nonconservative sequence variations (Croft et al., 2003). The alteration of the residues H40 and Q41 in the DNase I binding loop may affect filament formation (Schmitz et al., 2005). Both residues are best conserved in subfamily 1, together with the corresponding partners. Concordantly, immuno-localization with antibodies raised against subfamily 1 showed several polymeric structures (Kissmehl et al, 2004). It has to be mentioned that, as the antibodies were designed at a time where not all isoforms had yet been found, it might well be that they also recognize members of subfamily 2 and subfamily 3 (~60% and ~50% identity in the regions selected for antibody production).

Residues that normally mediate binding between adjacent monomers are also largely altered in several apicomplexans, thus providing an explanation for the absence of stable, long filaments in these parasites (Schmitz et al., 2005; Sahoo et al., 2006), apart from sequestration of actin monomers and capping filaments by actin-binding proteins (Poupel et al., 2000). The

absence of residues involved in intermonomer contact does not necessarily mean that these isoforms are not able to polymerize. One should keep in mind that the analysis was based on certain primary structures. It is still possible that, due to the different length of the isoforms, the resulting conformation may allow interaction with the adjacent monomer. Moreover, for several *P. tetraurelia* sequences an explicit classification as actin or arp is not possible. Arp1 is the sole arp able to form a homopolymer filament in vivo in other eukaryotes (Bingham and Schroer, 1999).

4.5.6.) ATP binding

Proceeding from actin1 to actin9, the sequence conservation in *P. tetraurelia* actins relative to actins in other organisms decreases. This raises the important question of nucleotide binding capacity. Binding and hydrolysis of ATP is important for the function of actin and several arps (Otterbein et al., 2001; Nolen et al., 2004). Arp2 was shown to have a higher ATP binding affinity than arp3. This is consistent with the conservation pattern we found in *P. tetraurelia* arp2 and arp3 orthologs (Fig. 29). The lowest residue identity was observed in subfamily 7, which also matches as arp4. Indeed, a recent report suggests that, in yeast, ATP binds weakly to arp4 (Sunada et al., 2005). The identities of binding residues in the different arp subfamilies in *P. tetraurelia* are in accordance with the conservation pattern of the respective arp subfamilies shown in a comparative analysis (Muller et al., 2005). It remains open whether actins/arps with a restricted number of conserved residues are able to bind ATP, though with lower affinity, or whether other residues are involved. Interestingly, ATP binding may not be important for nuclear arps, as several studies have shown that mutation in nucleotide contact residues of several arps did not impair their function (Cairns et al., 1998; Shen *et al*., 2003). Similarly, although arp1 has been shown to bind and hydrolyze ATP (Bingham and Schroer, 1999), the extreme stability of the arp1 filament suggests a lesser role for hydrolysis and depolymerization (Clark and Rose, 2005).

4.5.7.) Binding residues for myosin II

Regarding the variety and diversity of *P. tetraurelia* actin isoforms, the question arises whether differences in actin isoform structure determine which ABPs can bind. The myosin II binding site is very differentially conserved across *P. tetraurelia* subfamilies. Most subfamilies show conservation between 40 to 60%. The possibility of those isoforms to bind myosin II with either lower affinity or via other residues needs to be clarified. The lowest conservation could be observed in orthologs designed as actin/arp and arps, which are not supposed to bind myosin II. Several members of subfamily 1 possess all of the necessary

residues. Immuno-localization studies with antibodies raised against actin subfamily 1 showed cortical actin in *P. tetraurelia* (Kissmehl et al., 2004), both on LM and EM level. Cortical actin interacts with myosin and is essential for cyclosis, an actomyosin-based process (Shimmen and Yokota, 2004).

4.5.8.) Drug binding residues

Surprisingly, for cytochalasins, some of the most common drugs used to influence the dynamics of actin, we could not find any data on putative binding residues. However, for the filament stabilizing drug phalloidin and for the monomer sequestering drug latrunculin A, several studies revealed amino acids involved in their binding. Jasplakinolide, another potent inducer of actin polymerization, binds actin filaments competitively with phalloidin, presumably due to common binding sites (Bubb et al., 1994). The binding residues for phalloidin (Drubin et al., 1993; Belmont et al., 1999) are not well conserved in *P. tetraurelia* actins (Table 6, Fig. 28). May that be an explanation for the failure to label the cleavage furrow in *P. tetraurelia* with fluorescent phalloidin (Kersken et al., 1986)? Indeed, immuno-localization studies with an isoform-specific antibody against actin4, a subfamily lacking the phalloidin binding site, resulted in the labeling of the cleavage furrow (I. M. Sehring, C. Reiner, J. Mansfeld, H. Plattner, and R. Kissmehl, submitted for publication).

A similar situation occurs with the binding residues for latrunculin A. Most of them are lacking in the majority of isoforms, and no isoform possesses all of them (Table 6, Fig. 28). In fact, many studies with *Paramecium* had to apply unusually high drug concentrations. Transferring tools commonly used in other systems to *P. tetraurelia* may be problematic because the drug can not bind to the responsible isoform.

4.5.9.) Conclusion

Analysis of all these different features on nucleotide and amino acid level revealed striking differences in homologs of actin and actin-related proteins in *P. tetraurelia*, both within the organism and in comparison to other organism. This wide diversity may be a hint for different functions and localization of the actin and arp paralogs within a *Paramecium* cell.

4.6.) Acknowledgements

We would like to thank Genoscope (Paris) as well as Drs. Linda Sperling and Jean Cohen (Gif-sur-Yvette) for access to the indexed library and to the server containing the sequencing data. This work has been supported by Deutsche Forschungsgemeinschaft (grants to H.P.)

Chapter 5: Manuscript IV

A Broad Spectrum of Actin Paralogs in *Paramecium tetraurelia* Cells Displays Differential Localization and Function

Ivonne M. Sehring*, Christoph Reiner, Jörg Mansfeld, Helmut Plattner and Roland Kissmehl

Universität Konstanz
Fachbereich Biologie
Universitätsstraße 10
D-78457 Konstanz, Germany
Tel.: 0049-7531883712
Fax.: 0049-7531882245

*) Author for correspondence: Ivonne.Sehring@uni-konstanz.de
Accepted in: Journal Cell Science

5.1.) Summary

To localize the different actin paralogs found in *Paramecium* and to disclose functional implications, we used overexpression as GFP-fusion proteins and AB labeling, as well as gene silencing. Several isoforms are associated with food vacuoles of different stages. GFP-actin either forms a tail at the lee-side of the organelle, or it is vesicle-bound in a homogenous or in a speckled arrangement, thus reflecting an actin-based mosaic of the phagosome surface appropriate for association/dissociation of other vesicles on travel through the cell. Several paralogs occur in cilia. A set of actins are found in the cell cortex where actin outlines the regular surface pattern. Labeling of defined structures of the oral cavity is due to still other actins, while some are distributed in a pattern suggesting association with the numerous Golgi fields. A substantial fraction of actins is associated with cytoskeletal elements that are known to be composed of other proteins. Silencing of the respective actin genes/gene subfamilies entails inhibitory effects on organelles compatible with localization studies. Knock-down of the actin found in the cleavage furrow abolishes cell division, while silencing of some other actin genes alters vitality, cell shape and swimming behavior.

5.2.) Introduction

Actin, a most abundant cytoskeletal protein, is of paramount importance for structuring the cell cortex, amoeboid movement, cyclosis, vesicle trafficking, cell division and for cell contraction etc. In the past few years new aspects have emerged. This includes a contribution to docking of dense-core secretory vesicles (Gasman et al., 2004), endocytosis (Merrifield et al., 2002; Merrifield, 2004; Kirkham and Parton, 2005; Yarar et al., 2005), arrangement of Golgi elements (Lin et al., 2005), formation of Golgi-derived vesicles (Carreno et al., 2004; Cao et al., 2005) and numerous interactions with phagocytic as well as endocytic and lysosomal vesicles of different stages (Damiani and Colombo, 2003; Drengk et al., 2003; Stoorvogel et al., 2004; Yam and Theriot, 2004; Kjeken et al., 2004; Hölttä-Vuori et al., 2005). A universal function of F-actin is the formation of the cleavage furrow in animal cells (Otegui et al., 2005). A plethora of proteins interacting with actin further contributes to the dynamics and specificity of actin interactions (Pollard et al., 2000). Such interactions allow for a broad diversification of the actin cytoskeleton, even though some lower eukaryotes possess only one actin gene (García-Salcedo et al., 2004), while humans have six (Pollard, 2001). The closely related ciliate *T. thermophila* possesses four actin genes (Williams et al., 2006) In addition, a range of actin-like proteins (alp) and actin-related proteins (arp) exist (Goodson and Hawse, 2002; Kandasamy et al., 2004; Muller et al., 2005).

The ciliated protozoan *Paramecium* is a highly organized unicellular organism with an elaborate ultrastructure (Fig. 35). We now can show a widely diversified set of genes encoding paralogs of actin and arp in *Paramecium*. Essentially we found nine subfamilies of actin genes (ten members of subfamily 1, two or three members in the other subfamilies) and two subfamilies of arp (with one or two members each), with identities on the amino acid level ranging between 100 and 63 % (for members of the actin1 subfamily) and 60 to 18% for the other subfamilies, when referred to *Paramecium* actin1 (Table 7; Kissmehl *et al*., in prep.). Indirectly the question as to why this multiplicity has evolved, probably by gene duplications (Ruiz et al., 1998), and maintained during evolution, is addressed in this paper in the context of localization and functional analyses. These reveal differential positioning and functional engagement, in established vesicle trafficking pathways and beyond. Microfilaments of actin may play a role in the transport to the cell cortex and the recognition of the docking sites by trichocysts (Beisson and Rossignol, 1975).

We mainly used overexpression as green fluorescent protein (GFP) fusion proteins, eventually complemented by antibody (AB) localization, and silencing of the respective genes by RNAi. Because of the abundance of many isoforms (Table 7), not all could be analyzed in detail.

In most species actin is sensitive to drugs which stabilize either G-actin (cytochalasin B or D, latrunculin A) or F-actin (phalloidin, jasplakinolide) (Wieland and Faulstich, 1978; Visegrády et al., 2004). However, in lower eukaryotes the situation is rather complex. For instance, Apicomplexan parasites (*Plasmodium*, *Toxoplasma*), close relatives of our non-parasitic ciliates, contain abundant actin mainly in monomeric or short polymeric form (Poupel et al., 2000; Schmitz et al., 2005). Also surprising is the inability of any previous work to visualize in *Paramecium* a cleavage furrow by fluorescent phalloidin (Kersken et al., 1986a) while phagocytosis could easily be inhibited by cytochalasins (Cohen et al., 1984; Allen and Fok, 1985; Fok et al., 1985; Allen et al., 1995).

We now show that the specific localization of different actin paralogs in *Paramecium* is paralleled by functional diversification. Analysis of *Paramecium* cells appears rewarding as they display a most elaborate membrane trafficking system (Fig. 35), with distinct, predictable pathways (Allen and Fok, 1983; 2000; Fok and Allen, 1988; 1990; Plattner and Kissmehl, 2003) in which the different actin isoforms participate, as we now show. In the present work we combined the different techniques to establish a functional and topological overview of actin diversification in a *Paramecium* cell.

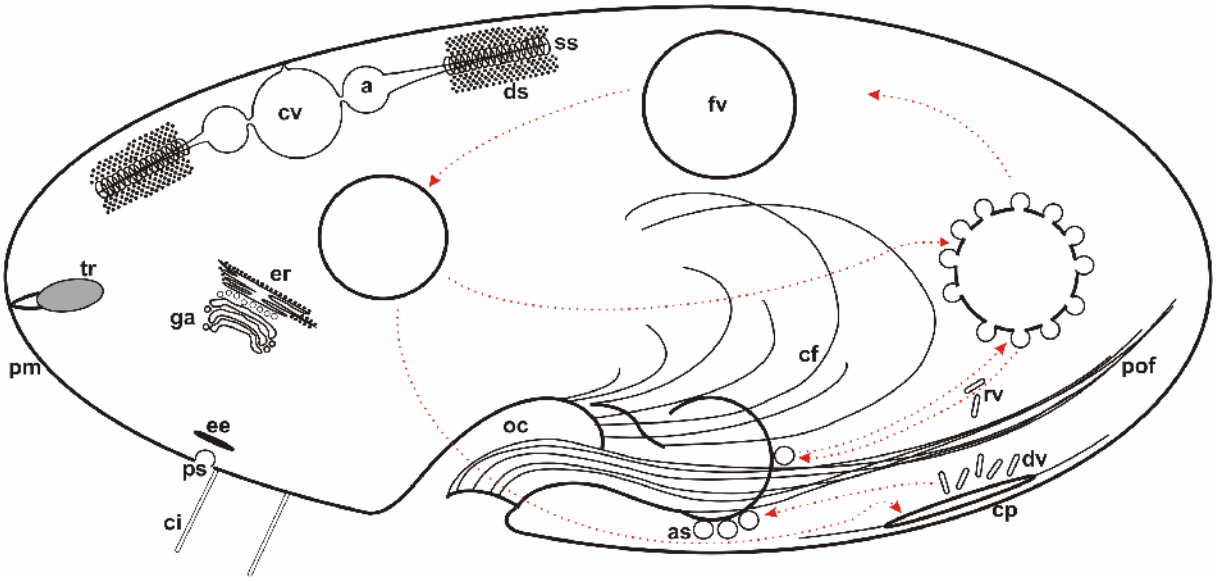

Fig. 35. Schematic *Paramecium* cell. The plasma membrane (pm) is covered with cilia (ci). Along the oral groove, they beat rhythmically to wash food towards the oral cavity (oc). The phagosomal apparatus contains of several elements (as, acidosomes mediating acidification of a food vacuole [fv] after pinching off; cytopharyngal fibers [cf], post oral fibers [pof], cytoproct [cp, site of exocytotic release of spent phagosomes]). Dense-core vesicles (trichocysts, tr), are attached to the plasma membrane. Osmoregulation is executed by two contractile vacuole complexes (a, ampula; cv, contractile vacuole; ds, decorated spongiome; ss, smooth spongiome). The red arrows indicate transport routes during phagosomal processing. Discoidal vesicles (dv) and other recycling vesicles (rv) are responsible for return transport of membranes. The endosomal system, composed of parasomal sacs (ps) and early endosomes (ee), is arrayed in a regular fashion. er, endoplasmatic reticulum; ga, golgi apparatus.

5.3.) Materials and Methods

5.3.1.) Stocks and Cultures

Wildtype *Paramecium* cells derived from stock 51s were used, i.e., d4-2 cells for microinjection of GFP constructs and 7S cells for additional experiments. Cells were cultivated at 25°C in a decoction of dried lettuce inoculated with *Enterobacter aerogenes*, supplemented with 0.4 µg/ml β-sitosterol (Sonneborn, 1970).

5.3.2.) Heterologous Expression and Purification of Paramecium Actin-Specific Peptides

For heterologous expression of peptides of actin4-1 and 5-1, we selected regions of the proteins with less than 25% identity to other subfamilies to obtain subfamily-specific ABs. Within these subfamilies, the identities at these regions were more than 90% on the amino acid level (Kissmehl et al., in prep.), ensuring that each member of one subfamily will be recognized by the ABs. After changing all deviant *Paramecium* glutamine codons (TAA and TAG) into universal Glutamine codons (CAA and CAG) by PCR methods, the coding regions of either M1-A160 (actin 4-1) or H175-L290 (actin 5-1) were cloned into the NcoI/XhoI restriction sites of pRV11a vector which contains a His_6 tag for purification of the recombinant peptides.

Recombinant actin4-1 and actin 5-1 peptides were purified by affinity chromatography on Ni^{2+}-nitrilotriacetate agarose under denaturizing conditions, as recommended by the manufacturer (Novagen, Darmstadt, Germany). The recombinant peptides were eluted with a pH gradient, pH 8 to pH 4.5, containing 8 M urea in 100 mM sodium phosphate buffer. The fractions collected were analyzed on SDS polyacrylamide gels, and those containing the recombinant peptide were pooled and dialyzed in phosphate-buffered saline (PBS).

5.3.3.) Antibodies

ABs against the two recombinant actin peptides act4-1 and act5-1 were raised in rabbits. After several boosts, positive sera were taken at day 60 and affinity purified on a column loaded with the corresponding actin peptide. Finally, both sera were cross-purified against each other.

5.3.4.) Electrophoresis and Western Blots

Protein samples were boiled and subjected to electrophoresis on 10% SDS polyacrylamide gels as previously described (Kissmehl et al., 2004). Gels were stained with Coomassie Blue R250 or prepared for electrophoretic protein transfer onto nitrocellulose membranes. Protein blotting was performed at 1 mA/cm^2 for 1 hour using the semidry blotter from BioRad

(Munich, Germany). ABs were diluted 1:1000 in 0.5% (w/v) non-fat dry milk and Tris-buffered saline, pH 7.5, and applied overnight at 4°C. AB binding was visualized by a second AB coupled to peroxidase using an enhanced chemiluminescence detection (ECL) kit according to the manufacturer (Amersham Biosciences, Freiburg, Germany).

5.3.5.) Immunofluorescence Labeling

Cells were washed twice in 5 mM Pipes buffer, pH 7.0, containing 1 mM KCl and 1 mM $CaCl_2$, fixed in 4% (w/v) formaldehyde for 20 minutes at room temperature (RT) and then permeabilized and fixed in a mixture of 0.5% digitonin and 4% formaldehyde, dissolved in 5 mM Pipes buffer, pH 7.0, for 30 minutes. Cells were washed twice in PBS, 2 x 10 minutes in PBS with 50 mM glycine added and 10 minutes in this solution with 1% bovine serum albumin (BSA) added. The rabbit anti-actin ABs were applied in a dilution of 1:50 in PBS (+1% BSA) for 90 minutes at RT. After 4 x 15 minutes washes in PBS, FITC-conjugated anti-rabbit ABs (Sigma-Aldrich, St Louis, MO), diluted 1:100 in PBS (+ 1% BSA), were applied for 90 minutes, followed by 4 x 15 minutes washes in PBS. Samples were shaken gently during all incubation and washing steps. Cells were mounted on coverslips with Mowiol supplemented with n-propylgallate to reduce fading and analyzed either in conventional fluorescence microscopes, type Axiovert 100TV or type Axiovert 200M, or in a confocal laser scanning microscope, type CLSM 510, equipped with a Plan-Apochromat objective lens (all Carl Zeiss, Jena, Germany). Images acquired with the ProgRes C10plus camera and ProgRes Capture Basic software (Jenoptik, Jena, Germany) were processed with Photoshop software (Adobe Systems, San Jose, CA).

5.3.6.) GFP Constructs

For overexpression of actin, the pPXV-eGFP-vector or pPXV-eGFPmcs-vector (Wassmer et al., 2006) were used (eGFP = enhanced green fluorescent protein, Hauser et al., 2000). All genes were cloned between SpeI and XhoI sites in-frame with the gene encoding GFP, except act8-1 where StuI where used instead of SpeI due to an internal SpeI restriction site. PCR primers used were as follows.

act1-2, 5’aA2, 5’GCTCTAGAGAGGAACAGCATCAGCA3’, 3’aAX, 5’CCGCTCGAGTCAGAAACACTTTCTGTGAACAATGG3’; act1-4, 5’aA4 5’GCTCTAGAGAGGAACAGCATCAGCAGGCCTATGAGTGAAGAACATCCAGC3’, 3’aA4X, 5’CGGCTCGAGTCAGAAGCATTTTCTATGAACC3’; act1-6, 5'SpeI-Act1.6, 5’GCGACTAGTATGTAAGCTTAAT ATCCAGC3’, 3’Xho-Act1.6END, 5’CCGCTCGAGTCAGAAACATTTTCTGTGAAC3’; act1-9, 5’Spe-Act1-9, 5’GG

ACTAGTATGAATGATGAAAAACCAGCAGTCG3', 3'Xho-Act1-9,5'CCGCTCGAGTCAAGTGACTGTCT AACATTTTCTGTG3'; act2-1, 5'bA1, 5'GCTCTAGAGAGGAACAGCATCAGCAGGCCTATGGACGACGTAATCCCAGTTG3', 3'bAX, 5'CCGCTCGAGTCAGAAGCATTTTCTGTGCACATAACC3'; act4-1, 5'Spe-Act4-1,5'GGACTAGTATGAATAGCGATGAAATAATA3', 3'Xho-Act4-1, 5'CCGCTCGAGTCAATTAGGACACTTTCTTTCTA3'; act5-1, 5'SpeI-Act5.1, 5'GCGACTAGTATGGATAATGAC ATATTTGCTAATAACT3', 3´Xho-Act5.1, 5'CCGCTCGAGTCACAATTATTTTTTGATTAAAATG3'; act6-1, 5'SpeI-Act6.1, 5'GCGACTAGTATGGAAAGTGAGTATGACTAAAAAG3', 3´Xho-Act6.1, 5'CCGCTCGA AGTCAAAATGTTCTCTTATGAATAAG3'; act8-1, 5´Stu-Act8.1, 5'GAAGGCCTATGAATAATAATGATTCCAC CTTCTATTA3', 3´Xho-Act8.1, 5'CCGCTCGAGTCAAAAGCACTTTCTTTATACTA3'.

PCR reactions and cloning was carried out according to standard procedures. To avoid possible disturbance of (de-)polymerization and localization, GFP was cloned at the N-terminus of the gene of interest, separated by an 11 amino acid spacer (Doyle and Botstein, 1996; Verkhusha et al., 1999; Wetzel et al., 2003).

5.3.7.) Microinjection of GFP constructs

Plasmid DNA was prepared with a plasmid midi kit (Qiagen, Hilden, Germany) according to the manufacturer's protocol. 50 µg of plasmid DNA was linearized by digestion with 20 units of SfiI overnight at 50°C. The DNA was precipitated with 1/10 (v/v) 3 M sodium acetate pH 5.2, with 2.5 (v/v) ethanol added, and incubated for 60 minutes at –20°C. DNA was pelleted by centrifugation, washed with 70% (v/v) ethanol and dried. The pellet was resuspended in 10 µl Millipore-filtered water and centrifuged for 30 minutes at 4°C. Microinjection of the DNA into the macronucleus was carried out as previously described (Froissard et al., 2002).

5.3.8.) Immuno-Electron Microscopy

Cells derived from clones transformed with GFP-act8-1 were fixed for 1 hour on ice with 8% formaldehyde + 0.1% glutaraldehyde in PBS, pH 7.4, followed by two washes in PBS, pH 7.4 at RT. Cells were dehydrated in an ethanol series followed by embedding in LR-Gold resin (London Resin, London, GB). Ultrathin sections were decorated with affinity-purified, polyclonal anti-GFP antibody (Wassmer et al., 2006), followed by protein A-gold (5 nm) conjugates (pA-Au5nm, Dept. Cell Biol., Univ. Utrecht, Utrecht, NL). These and any further steps for electron microscope (EM) immuno-analysis were essentially as described (Kissmehl et al., 2004).

5.3.9.) Gene Silencing Constructs

The double T7-promotor plasmid pPD129.36 described by Fraser et al. (2000) was used. The following primers were used.

act1-2, 5'aA2Xba1, 5'GCTCTAGAGAGGAACAGCATCAGCA3', 3'aAX, 5'CCGCTCGAGTCAGAAACACTTTCTGTGAACAATGG3'; act1-6, 5´Xba-Act1.6, 5'GCTCTAGAAAATAGGTATAGCGGGAGATGAT3', 3´Xho-Act1.6, 5'CCGCTC GAGCAAAAACAGGTACGCAATGAG3'; act1-9, 5'Xba-Act1-9, 5'GCTCTAGAATGAATGATGAAAAACCAGCAGTCG3', 3'Xho-Act1-9, 5'CCGCTCGAGTCAAGTGACTGTCTAACATTTTCTGTG3'; act2-1, 5'Xba-Act2-1, 5'GCTCTAGAAAGTAGCCTGGTCAAATGG3', 3'Xho-Act2-1, 5'CCGCTCGAGCATATCATCCCAACGAGTG3'; act3-1, 5'Xba-Act3-1, 5'GCT CTAGATACAGGATTCTAAATAAAACAA3', 3'Spe-Act3-1, 5'GGACTAGTCTATTCCATAGCCTCCC3', 5'Stu-Act3-1, 5'GAAGGCCTATGATAGAATCTCATCCTCCTGTTG3', 3'Xba-Act3-1, 5'GCTCTAGATCAA AAACATTTAATGTGAGCAATC3'act3-2, 5'Spe-Act3-2, 5'GGACTAGTTACAAGAATCTTAAACGATTAA3', 3'Xho-Act3-2, 5'CCGCTCGAGCTATCTCTATAGATTCCC3'; act4-1, 5'Xba-Act4-1(518-535), 5'GCTCTAGAAAG CGCCAATCGGAGGAG3', 3'Xho-Act4-1(885-903), 5'CCGCTCGAGTGGTGCCAAAGCAGACAAG3', act5-1, 5'Xba-Act5-1, 5'GCTCTAGATATTGACTGAACCTCCTTATG3', 3'Xho-Act5-1; 5'CCGCTCGAGGTACCTTGCTCTTCTCAAC3'; act6-1, 5´Xba-Act6.1, 5'GCTCTAGACTGCTGTTTTAAATAAGTCTG3', 3´Xho-Act6.1, 5'CCGCTCGAGTCAAAATGTTCTCTTATGAATAAG3'; act7-1, 5'Xba-Act7-1, 5'GCTCTAGAGGCTTAC GAATTACCAGAC3', 3'Xho-Act7-1, 5'CCGCTCGAGAGCTCCCAACCAAGATGC3'; act8-1, 5'Xba-Act8-1, 5'GCTCTAGATTTCCAGTGGAAAAACAACAG3', 3'Xho-Act8-1, 5'CCGCTCGAGACCATCGGGCAAAT CATACA3'; act9-1, 5'Xba-Act9-1, 5'GCTCTAGATTGGCAATGTACTTCCTC3', 3'Xho-Act9-1, 5'CCGCTCGAGT TCCAAAATATGTGTCAGTG3'.

PCR reactions and cloning was carried out according to standard procedures.

5.3.10.) Gene Silencing by Feeding

The RNaseIII-deficient *E. coli* strain HT115 (Timmons et al., 2001) was transformed with the gene silencing plasmids. Overnight cultures in Luria-Broth (LB) medium supplemented with

ampicillin (amp) and tetracycline were diluted with LB/amp medium 1/100 the new cultures were grown to an OD_{600nm} between 0.2 and 0.4. The cultures were induced with 125 µg/ml isopropyl-thio-ß-D-galactopyranoside (IPTG) for 3 hours, centrifuged and the pelleted bacteria resuspended in *Paramecium* culture medium. The OD_{600nm} was adjusted with medium to 0.25 and supplemented with 100 µg/ml ampicillin and 12 µg/ml IPTG.

Single *Paramecium* cells were isolated and grown for about twenty fissions, again isolated and grown for another twenty fissions before each clone was starved to induce autogamy (Berger, 1986). Autogamy was monitored by fluorescence microscopy after staining with Hoechst 33342 (Molecular Probes, Leiden, NL). Autogamous cells were fed, first with normal bacteria and used only 3 days later for RNAi feeding experiments. *Paramecium* cells were washed twice in PIPES buffer and starved for at least 2 hours in PIPES at RT before use in feeding experiments. In single cell experiments, one cell was added to 150 µl feeding solution in a depression well. Cells were cultured at 25°C during the experiment and transferred every 24 hours to a freshly prepared feeding solution. The phenotype was analyzed 96 hours after the start of the feeding experiment.

5.3.11.) Behavioral and Functional Assays

Cells were observed in their wells under a binocular microscope to ascertain their normal swimming behavior. For further tests, cells were transferred in 10 µl drops and observed for 30 seconds after addition of an equal volume of a 2-fold concentrated test solution. Depolarization of the plasma membrane, indicated by ciliary reversal and pronounced backward swimming, was induced by adding 40 mM KCl. Cells that showed any significant backward swimming events were scored as positive responders. Hyperpolarization was induced by adding 20 mM $CaCl_2$, and cells that showed accelerated forward swimming were scored as positive responders. To analyze exocytotic capacity, cells were triggered with 0.2% aminoethyldextran (Plattner et al., 1984) in a buffer consisting of 10 mM Tris/HCl, 0.1 mM $CaCl_2$, pH 7.0. Exocytotic tests were repeated with saturated picric acid, the traditional (lethal) test used in genetic studies.

For evaluation of the phagocytotic capacity, cells were fed with Congo Red-stained yeast, fixed with 4% (w/v) formaldehyde after 3, 5 and 10 minutes and the phagocytotic activity of at least 20 cells was evaluated. The decrease in phagocytotic capacity concerned as well the number of food vacuoles formed as the number of yeast cells per vacuole. While in control cells the amount of yeast displayed a variation of up to 30 yeast cells per vacuole, phagocytotically restricted *Paramecium* cells formed only small vacuoles with less than 10 yeast cells.

5.3.12.) Statistical Evaluation

For statistical evaluation of changes in the division rate and in the phagocytotic capacity in RNAi experiments, One Way Analysis of variance (Anova) was used to determine statistical significance.

5.4.) Results

5.4.1.) Actin Isoforms and their Localization

Based on a *Paramecium* genome data base search (Sehring et al., submitted.), Table 7 summarizes the actin paralogs considered in the present work. Beyond the diversification in numerous subfamilies, with usually only two members each (except subfamily 1) Table 7 also reveals striking similarities between members within the subfamilies 2 to 9.

To investigate the subcellular localization of the different actin isoforms, GFP constructs were made. For the isoforms act1-2, act1-6, act1-9, act2-1, act3-1, act5-1, act6-1 and act8-1, the ORF was cloned into pPXV-eGFP (Hauser et al., 2000), the *Paramecium* overexpression vector (Haynes et al., 1995). The GFP gene was fused to the 5'-end of the actin gene with a spacer interspersed to avoid any possible disturbance of folding and polymerization due to the GFP tag (Doyle and Botstein, 1996; Wetzel et al., 2003). The plasmids (~5µg/µl) were introduced into postautogamous *Paramecium* cells by microinjection into the macronucleus and GFP fluorescence was analyzed in descendants of the injected cells. A summary of the subcellular localization of the actin isoforms investigated is given in Table 8.

Actin subfamily 1. To take into account the wide diversification of the actin1 subfamily (Table 7), the subcellular localization of the isoforms act1-2, act1-4, act1-6 and act1-9 were examined in more detail. GFP-act1-2 formed comet tails at food vacuoles, which propelled them through the cytoplasm (Figs. 36A-C). Alternatively it may be accumulated in patches at the surface of food vacuoles (Figs. 36D-F). Transformation with GFP-act1-4 resulted in diffuse fluorescence throughout the cytoplasm (data not shown), as with GFP-act1-6 (Figs. 36G, H). With GFP-act1-9, pronounced comet tails could be observed, which propelled food vacuoles even in opposite directions through the cytoplasm, with the tail always at the rear side (Figs. 36I-N). Those GFP-act1-9 comet tails could not be observed on every food vacuole, since they were very dynamic structures, which have rapidly polymerized and depolymerized. Furthermore, thin, very dynamic tails were also seen to propel smaller vesicles.

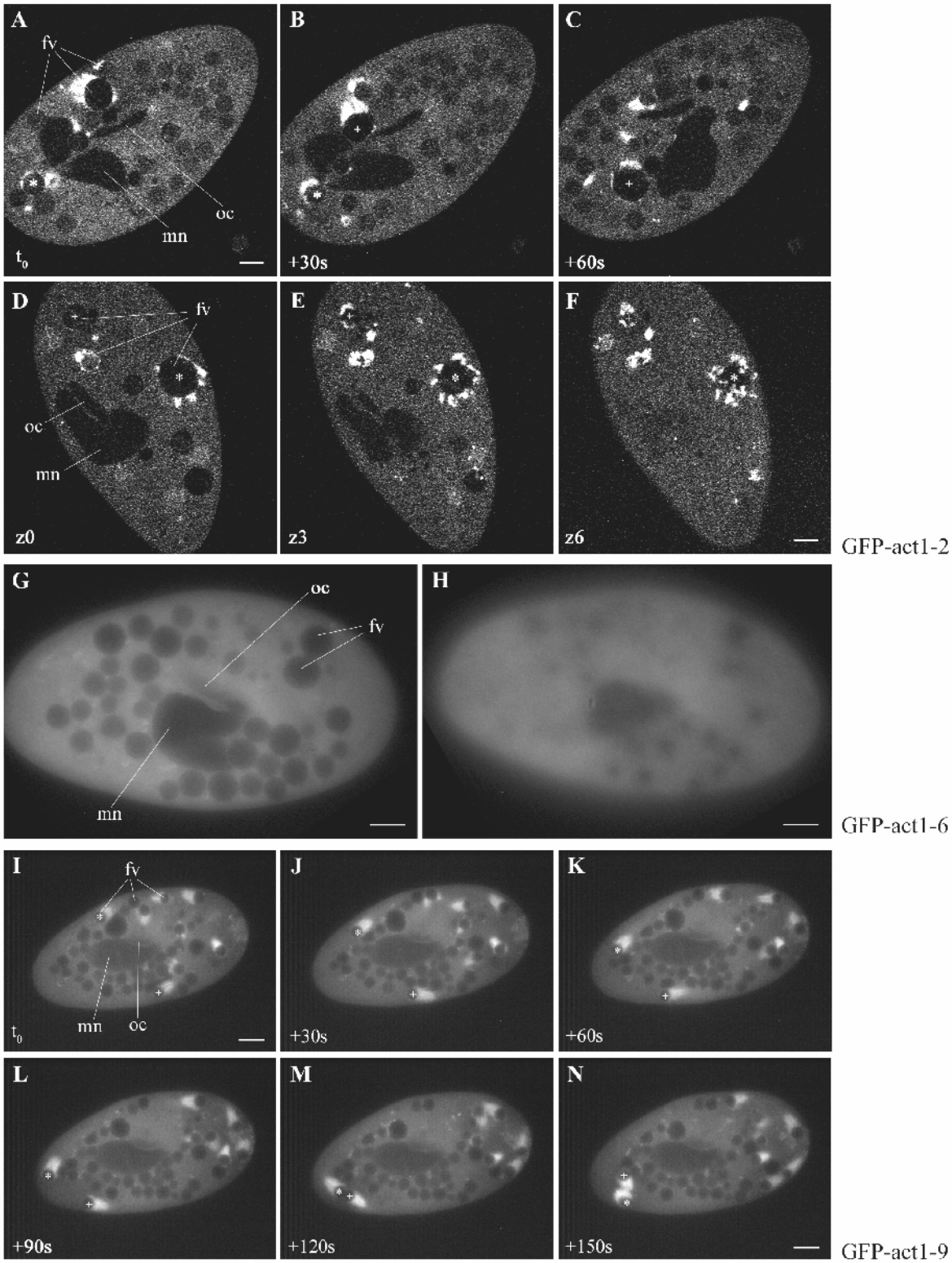

Fig. 36. GFP localization of members of the act1 subfamily. (A-C) A confocal time series of a cell transformed with GFP-act1-2 reveals actin comet tails which propels vacuoles (labeled with * and +) through the cytoplasm. (D-F) Confocal z series of a cell transformed with GFP-act1-2. Note the irregular distribution of patches around the surface of some food vacuoles (fv). (G, H) Transformation with GFP-act1-6 resulted in diffuse cytosolic staining without any specific localization (G, median; H, superficial plane). (I-N) In cells transformed with GFP-act1-9, actin comet tails on food vacuoles occurred. Food vacuoles can move in opposite directions through the cytoplasm (see the movement of the two vacuoles labeled with * and + within 150 seconds). See supplementary material Fig2.mov for the following details related to Fig. 2: Thin, very dynamic tails can propel some food vacuoles and small vesicles through the cytoplasm. From the posterior end of the oral cavity, actin filaments were catapulted into the cytoplasm (Fig2.mov). mn, macronucleus; oc, oral cavity; fv, food vacuoles. Bars = 10 µm.

Actin3-1. Transformation of *Paramecium* cells with GFP-act3-1 resulted in a diffuse staining of the cytoplasm, although a specific labeling also could be observed (data not shown). A GFP signal was found at the surface of food vacuoles, but in this case the vacuoles were almost completely surrounded by a layer of GFP-act3-1 of variable thickness.

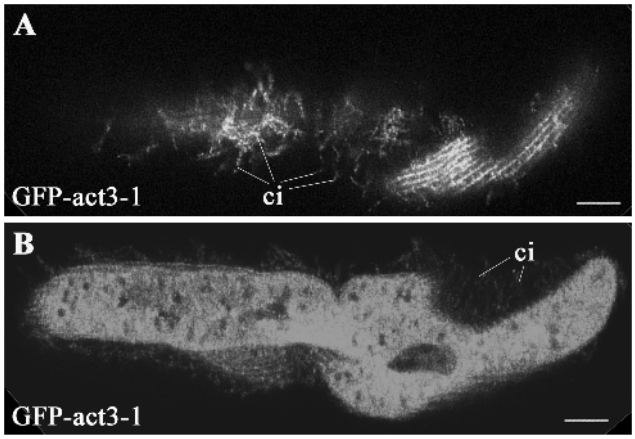

Fig. 37. Application of an anti-GFP AB to cells transformed with GFP-act3-1 constructs. Confocal images from superficial (A) and median (B) focal planes of a dividing cell. Note labeling of cilia (ci) in (A, B), labeling of the cortical "egg-case" relief in (A) and diffuse staining of the cytoplasm in (B). The cleavage furrow is not labeled. Bars = 10 µm.

To enhance the GFP fluorescence, ABs against GFP were applied to transformed cells. In the cell cortex, GFP-act3-1 outlined the ridges of the egg-carton-like cell surface relief typical of *Paramecium* cells, as well as cilia (Fig. 37).

Actin4-1. Examination of the localization of GFP-act4 was not possible, as cells did not divide after microinjection and were too sensitive for observation under the microscope. Therefore, we raised a polyclonal AB against a 160aa peptide of act4-1 to obtain subfamily specific ABs. The region chosen has less than 25% identity to other subfamilies, which makes it unlikely that the ABs will react with any of the other actins or arps. The ABs were affinity-purified not only against the peptide for immunization, but also against peptides used to raise ABs against act1-1 (Kissmehl et al., 2004) and against act5-1, and were tested in Western Blots for their cross-reactivity, which was negative (Fig. 38A). Immunolocalization studies with the ABs against act4 showed labeling of the oral cavity, around nascent food vacuoles (Fig. 38B), in cilia and in the cell cortex (Fig. 38C). In dividing cells, a weak labeling of the micronucleus separation spindles could be observed (data not shown). The most striking labeling was that of the cleavage furrow. Beginning with an early stage of division until fission is completed, act4 was associated with the cleavage furrow (Figs 38D, F). For comparison, act5-1 specific ABs did not label the cleavage furrow (Fig. 38G).

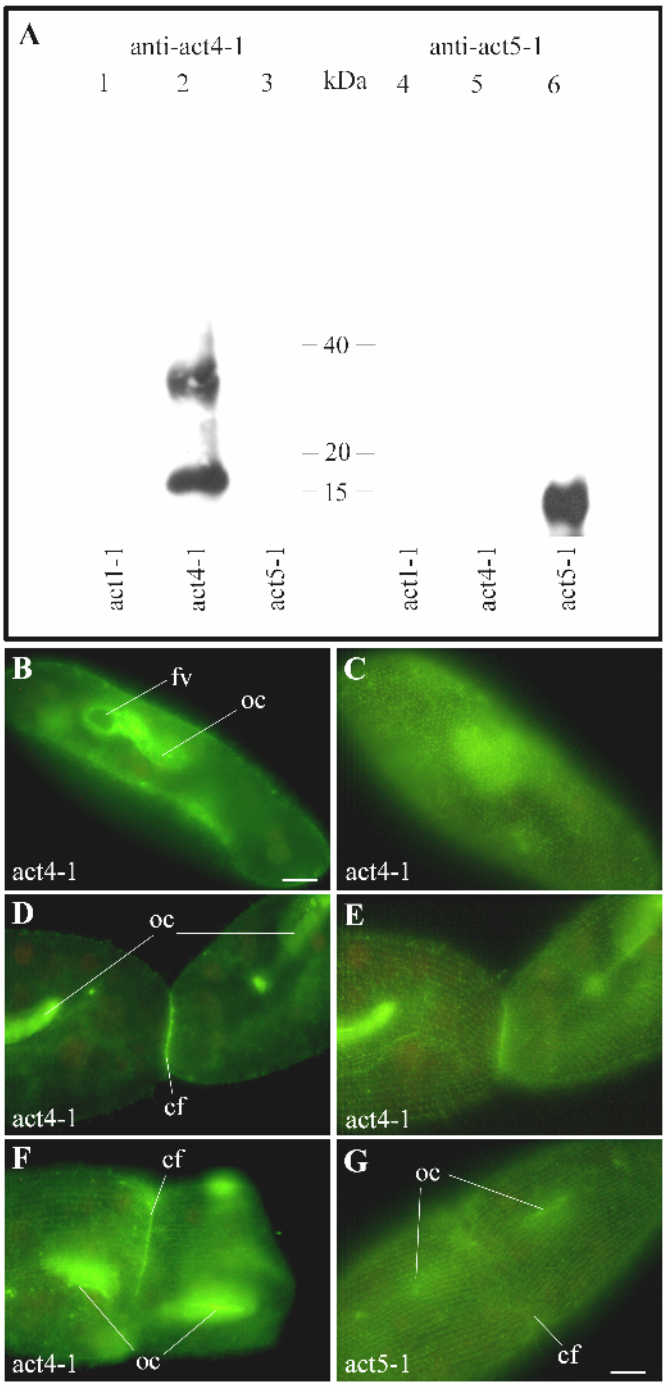

Fig. 38. Immunolocalization of actin using subfamily specific ABs. (A) Western blot analysis of affinity-purified anti-act4-1 AB (lane 1-3) and anti-act5-1 AB (lane 4-6) against the recombinant act1-1 (L_{261}-G_{366}; lane 1, 4), act4-1 (M_1-A_{160}; lanes 2, 5) and act5-1 peptides (H_{175}-L_{290}; lanes 3, 6), respectively. There is no cross-reactivity between the isoforms. The double band in lane 2 is probably due to formation of dimers. (B-E) Localization of act4. (B, C) Superficial and median focus plane showing labeling of the oral cavity (oc), around a nascent food vacuole (fv), of cilia and at the cell cortex. (D, E) Superficial and median plane of a dividing cell. Note labeling of the cleavage furrow (cf) and the old and new oral cavity (oc). (F) Superficial plane of a cell in an earlier stage of division. Again the cleavage furrow is labeled, as well as the old and the new oral cavities. (G) For comparison a cell in the same dividing state as in (F), but labeled with an anti-act5 AB, reveals no labeling of the cleavage furrow. Bars = 10 µm.

Actin5-1. Transformation of *Paramecium* cells with GFP-act5-1 resulted in a discrete labeling around a sub-set of food vacuoles. In contrast to the labeling observed with other GFP-constructs at food vacuoles, GFP-act5-1 formed neither patches nor tails but a fine ring on the surface of the respective food vacuoles. Indeed, there was no consistent covering of the whole food vacuole (arrow head in Fig. 39A), and the label could not be found around all food vacuoles (Figs 39A,B). At the oral cavity, the following structures were labeled. (i) Two half-moon-shaped labeled structures can be assigned to the peniculus (Figure 39B). (ii) Anchored by a wreath-like structure with pointed pattern, probably the quadrulus of the oral

cavity, a dynamic fiber system is emanating into the cytoplasm (arrow in Fig. 39B). (Note that the cell shown in Figure 5A contains numerous autofluorescent crystals). Immunolocalization studies with affinity purified ABs against act5-1 showed similar localization as observed with GFP tagged act5-1, thus excluding possible artifacts due to GFP overexpression or fixation/permeabilisation during preparation for immunolocalization studies.

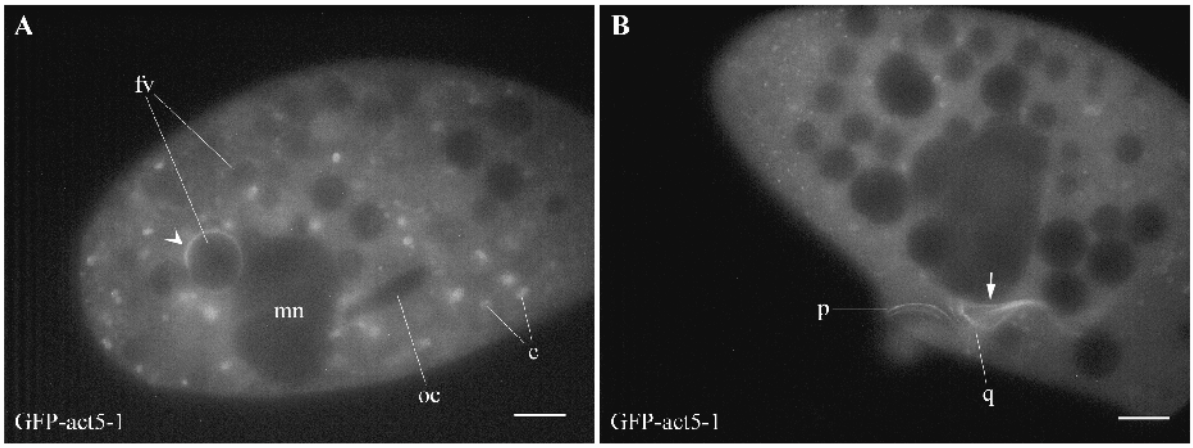

Fig. 39. GFP localization of act5-1. GFP tagged act5-1 occurs predominantly throughout the cytoplasm, although it is also found on individual food vacuoles (fv) (arrowhead, A).The focus plane in (B) reveals a strong signal on different structures of the oral cavity, e.g. the peniculus (p) and the quadrulus (q). A dynamic fiber system emanating from the oral apparatus is indicated by an arrow. mn, macronucleus; oc, oral cavity; c, crystals. Bars = 10 µm.

Actin8-1. The fluorescent signals obtained with GFP-act8-1 were in many cases similar to those obtained with GFP-act5-1. Labeling around single food vacuoles could be observed, but in contrast to the incomplete envelopment with GFP-act5-1, the food vacuoles seem to be entirely covered (Figs 40A,C). The two half-moon-shaped structures at the presumed peniculus and the curved structure of the presumed quadrulus are also labeled, and a dynamic fiber system which originates from the latter could be observed (Figs 40A-C). Careful comparison of cells transformed with GFP-act5-1 with cells transformed with GFP-act8-1 showed that one probably deals with two different fiber systems emanating from the oral cavity. Beyond that, focusing on the surface of transformed cells revealed regular rows of small dots underneath the plasma membrane, arranged in about 2 µm distance to each other (Fig. 40D) which can easily be identified as “parasomal sacs”. They correspond to stationary sites of constitutive exocytosis and coated pit endocytosis (Plattner and Kissmehl, 2003).

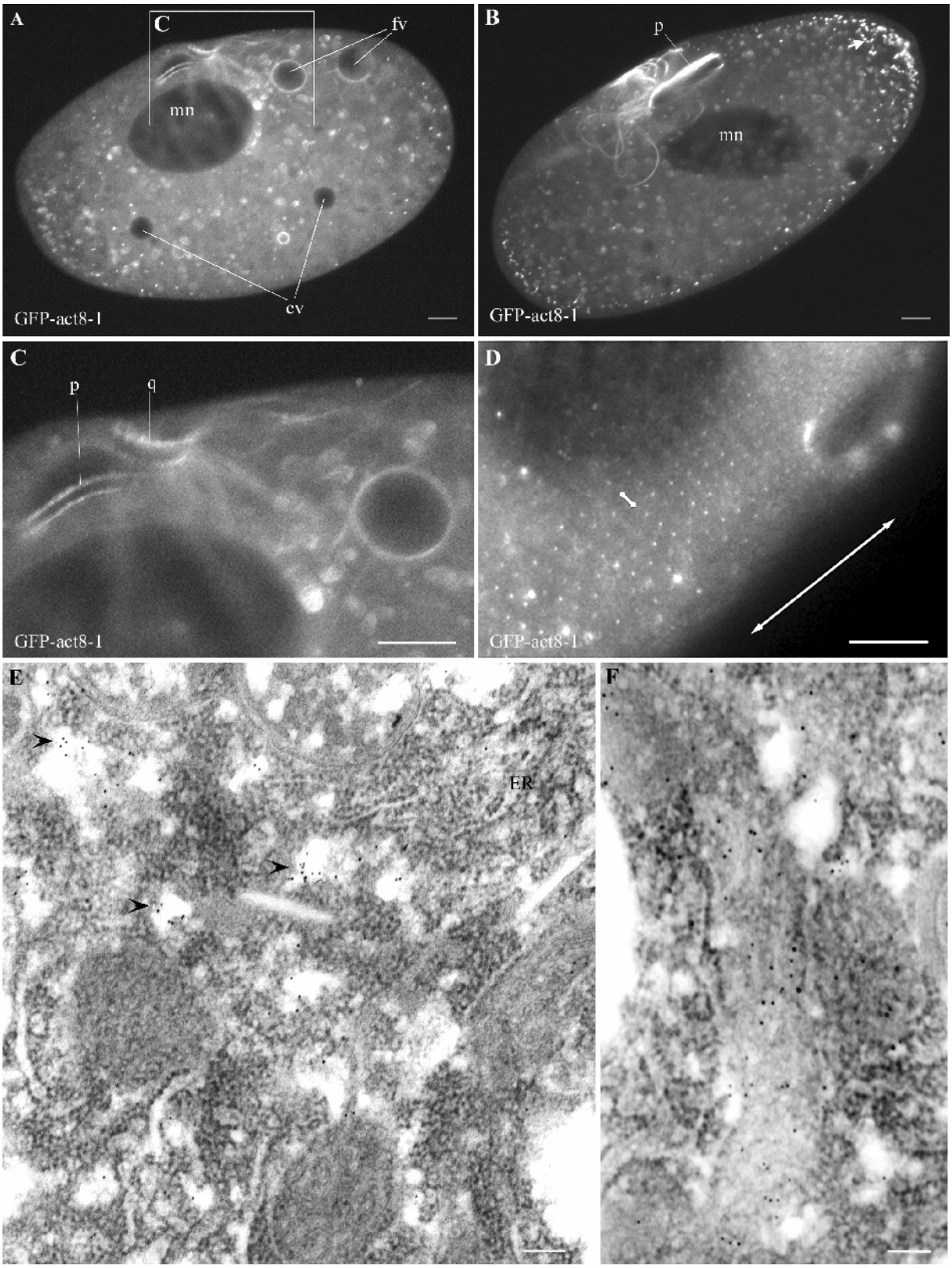

Fig. 40. Transformation of *Paramecium* cells with the GFP-act8-1 construct resulted in a weak cytosolic signal, labeling around some food vacuoles (fv; A, C) and at the presumable peniculus (p) and the quadrulus (q) of the oral cavity (A, B; C, detail). From the latter, a dynamic fiber system originates (B, see also supplemental material Fig6.mov). Close to the surface dotted to elongate structures are labeled (arrows in B) which continue deeper into the cytoplasm and probably represent Golgi fields (see text). The superficial plane in (D) reveals regularly spaced, labeled, very small dots at the plasma membrane (small bar = 2 µm, double arrow = cell axis), i.e., the sites occupied by "parasomal sacs". (E, F) In immuno-gold EM-analyses, using anti-GFP AB/gold, label was enriched at the boundary of the rough ER in association with smooth vesicular, round to elongate membrane-bounded elements (E) or in Golgi fields (F). mn, macronucleus; oc, oral cavity; cv, contractile vacuole. Bars = 10 µm (A-D), 100 nm (E, F).

Furthermore, small point-like to rhod-shaped organelles could be observed (Figure 40B) which, in z-stacks, actually showed some enrichment towards the cell surface (data not shown). Those organelles were smaller than 1.0 µm and did not move with the cyclosis steam. In EM analysis with cells overexpressing GFP-act8, using anti-GFP ABs followed by pA-Au_{5nm}, we frequently found label at the periphery of the rough ER in association with smooth vesicular membrane-bounded elements (Fig. 40, F). These may represent Golgi elements with some deformation, possibly due to the overexpression of actin (García-Salcedo et al., 2004). Fixation used preserves F-actin, its position in filaments and its antigenicity as multiply shown in the literature.

Actin2-1 and actin6-1. GFP localization of act2-1 and act6-1 resulted in a diffuse staining all over the cytoplasm, with no specific highlighted structure. This is similar to the results obtained with GFP-act1-6. However, enhanced with anti-GFP ABs, GFP-act2-1 is found in cilia (data not shown).

The different subcellular localizations achieved by a GFP-tag of specific isoforms or subfamily-specific ABs are summarized in Table 2 and, with the inclusion of previous data, in the final schematic Figure 45.

5.4.2.) RNA Interference by Feeding

For functional analysis of the different actin subfamilies, gene-silencing experiments were performed by using the RNAi approach by feeding. *Paramecium* cells were fed with *E. coli* expressing double-stranded RNA coding for specific actin, which elicits a small interfering RNA mediated silencing process of the target genes. As negative control, the empty feeding vector (pPD) was used for mock silencing. To ascertain the reliability of the RNAi-based feeding procedure, we performed controls with the pPD-nd7 construct (Skouri and Cohen, 1997). Silencing of the nd7 (nondischarge) gene successfully suppressed exocytosis of trichocysts. The effects of gene silencing on various behavioral and physiological aspects were examined. In detail, cell shape, cyclosis, exocytotic capacity, the contraction period of the contractile vacuoles, phagocytotic capacity, the general swimming behavior and the swimming reaction upon depolarization and hyperpolarization have been analyzed. For each actin subfamily, one gene was cloned into the silencing vector. Within the respective subfamilies, the nucleotide identity is high enough to expect co-silencing (Ruiz et al., 1998). An exception is the large actin1 subfamily with 10 members which vary up to 35%, therefore constructs for the specific isoforms act1-2, act1-6 and act1-9 were made. To confirm co-silencing within the subfamilies, and to exclude any functional compensation by the unsilenced paired isoform, we tested a construct where both isoforms of the actin3 subfamily,

act3-1 and act3-2, were cloned in tandem. RNAi with this construct gave identical results compared to those obtained with the isoform act3-1 alone (Table 9). To exclude silencing variation due to the length of the introduced dsRNA or cross-silencing of other subfamilies, constructs of different length were designed for act2-1 and act3-1. Within both subfamilies, all constructs showed the same effects. A summary of the results obtained with the different gene silencing constructs is given in Table 9.

Cell division. Cell fissions per day were calculated to see if silencing of any of the actin subfamilies affects the growth rate of *Paramecium*. In general, a slightly reduced division rate could be observed 24 hour after the start of the feeding experiment, probably due to slower division of cells overcoming autogamy and the change of the bacteria used for feeding. Cell growth was not influenced by most of the silencing constructs (Fig. 41). Only silencing of act4 or act9 resulted in a significant reduction of the division rate. Silencing of act9 led to half of the division rate, while cells silenced in act4 could not divide anymore and subsequently died.

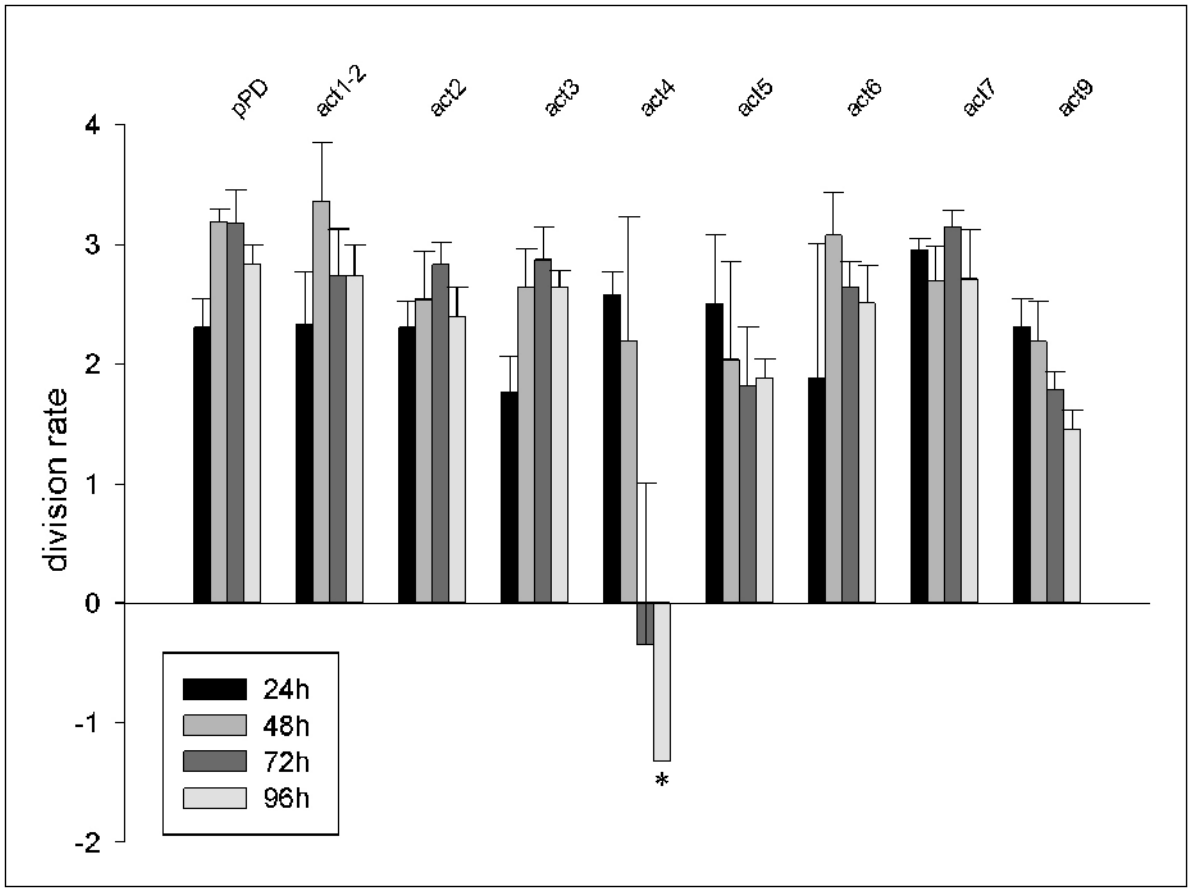

Fig. 41. Comparison of the division rate of cells silenced in different actin subfamilies. Only silencing of act4 and act9 affect the division rate, all other subfamilies show no significant difference when compared with the control (empty pPD vector). While silencing of act9 caused delayed growing, cells silenced in act4 cannot divide anymore and are dying. Error bars = s.e.m., (*) s.e.m. = 0.

Cell shape. We could recognize changes in the general cell shape after silencing of act4, act7 or act9. Act4 silenced cells arrested during division could be observed, named "boomerang" (Fig. 42A). Cells silenced in act7 were generally enlarged with a pointed anterior end, called "dolphin" (Fig. 42B). *Paramecium* cells fed with the act9 silencing construct obtained a triangle cell shape (Fig. 42C).

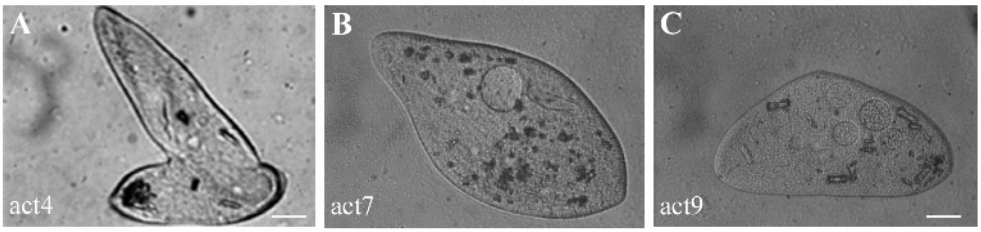

Fig. 42. Morphological changes in cells silenced in act4, act7 or act9. Cells silenced in act4 (A) are not able to divide, thus resulting in a "boomerang" appearance. Cells silenced in act7 become slightly oversized with a pointed anterior end ("dolphin" shape, B). Silencing in act9 results in triangle-shaped cells (C). Bars = 10 µm.

Swimming behavior. The general swimming behavior of *Paramecium* cells was observed. Cells silenced in act2 or act3 showed similar phenotypes. Swimming was impaired as cells were stagnant and accumulated at the bottom of the wells. Cells silenced in act4 showing the boomerang phenotype and cells silenced in act9 with a triangular shape where swimming in narrow circles, probably due to their morphological changes. The swimming reaction upon depolarization or hyperpolarization of the plasma membrane - pronounced backward swimming in the first and accelerated forward swimming in the latter case - was not impaired in any of the silencing assays (Table 9).

Exocytosis of trichocysts. We considered that cytochalasin B treatment abolished trichocyst docking in *Paramecium* (Beisson and Rossignol, 1975) and the occurrence of anti-actin AB labeling around trichocysts docked at the plasmamembrane (Kissmehl et al., 2004). With ongoing cell divisions, every daughter cell has to produce a new arsenal of trichocysts and to transport them to the cell cortex. If any of the actin subfamilies would play an essential role within this process, after 96 hours of feeding (approximately 16 fissions) a reduced number of docked trichocysts would be expected. None of the silencing constructs led to a reduction in exocytosis, except "boomerang" cells (silenced in act4) where the exocytotic capacity was reduced to 10% (Table 9).

Phagocytosis. To analyze the formation and fission of food vacuoles and the possible role of specific actin subfamilies in the process of phagocytosis, *Paramecium* cells were fed with Congo Red-stained yeast to visualize newly formed food vacuoles. Cells silenced in act2, act3, act4, act7 or act9 were found to have a significantly reduced number of phagosomes compared with control cells (Fig. 43). While silencing of act7 reduced the phagocytotic capacity of the cells to ~70%, silencing of both act2 and act3 reduced phagocytosis to 30%. With cells silenced in act4, phagocytosis was reduced to 30% and to 70% with cells silenced in act9, provided cells had retained normal morphology. In contrast, "triangle" cells (act9) had a phagocytotic capacity of only 10%, while in "boomerang" cells (act4) no new food vacuoles were generated at all (Fig. 43, Table 9).

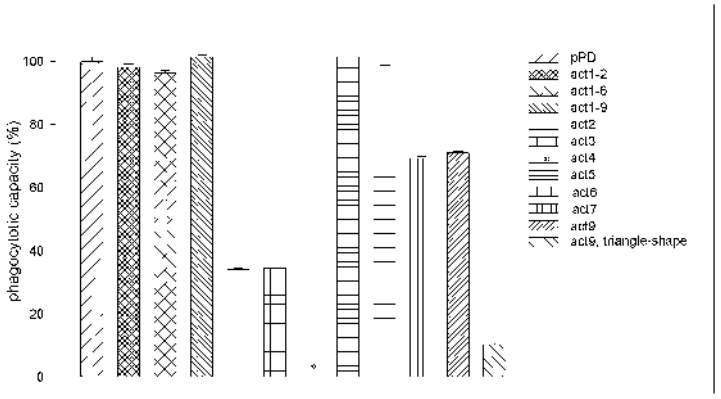

Fig. 43. Comparison of the phagocytotic capacity of cells silenced in different actin subfamilies. While silencing of members of the act1 subfamily, act5 or act6 does not significantly affect phagocytosis ($P<0.05$; control: pPD vector), it is reduced to ~70% in cells silenced in act7 and to ~30% in cells silenced in act2 or act3. With act9, in normally shaped cells phagocytosis is slightly impaired while there is a strong inhibition in triangle shaped cells (~10%). In cells silenced in act4, no phagocytosis could be observed (*). Data were collected in five different experiments from at least 20 cells per group. Error bars = s.e.m.

Contractile vacuole complex and cyclosis. In cells silenced in act9 with a triangle shape, the contractile vacuole complex was severely perturbed. The pumping cycle was increased from a value of 10 to 15 seconds in control cells to more than 100 seconds (Fig. 44). It is noteworthy that no method has demonstrated the occurrence of any actin isoform in the osmoregulatory system. Therefore, any actin silencing effects are probably due to indirect effects outside the system itself. No other subfamily impaired the contractile vacuole complex (Table 9).

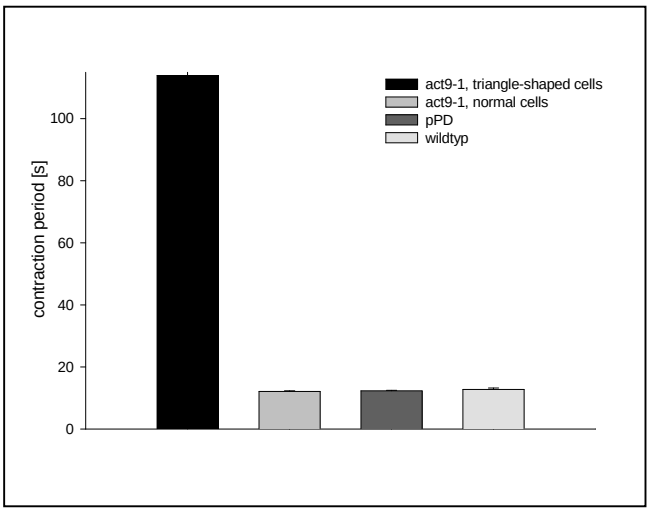

Fig. 44. Silencing of act9 affects the contraction period of the contractile vacuoles in misshapen transformants. While the complex works normal in act9 silenced cells with normal shape, its contraction period is strongly increased in triangle-shaped cells. Feeding with pPD vector does not cause any defect in the cycle of the contractile vacuole complex. Data were collected in three different experiments from at least 10 cells per group. wt: wildtype. Error bars = s.e.m.

In triangular cells achieved by silencing in act9, the velocity of cyclosis was accelerated two to three times when

compared to control cells (Table 9) – an aspect difficult to explain without more detailed studies being performed.

5.4.3.) Salient Features of Results

A variety of actin isoforms are expressed in *Paramecium*, frequently with a specific localization and concomitantly with a specific function. Many of the aspects we describe have remained undetected in previous affinity labeling studies with *Paramecium*. Some of our results are without precedent, also in other cells. The localization of paralogs from different families can overlap. Particularly the interaction of actin isoforms with phagosomes is very complex. Some other isoforms have a unique localization, e.g., in the cleavage furrow, in cilia or in some other prominent cytoskeletal aggregates. It should be stressed, however, that we do not claim that any of the prominent filamentous structures of *Paramecium* would be exclusively or predominantly made up of actin. However, intermingling with actin is a feature known from different cytoskeletal components in other cells (Manneville et al., 2003; Lin et al., 2005).

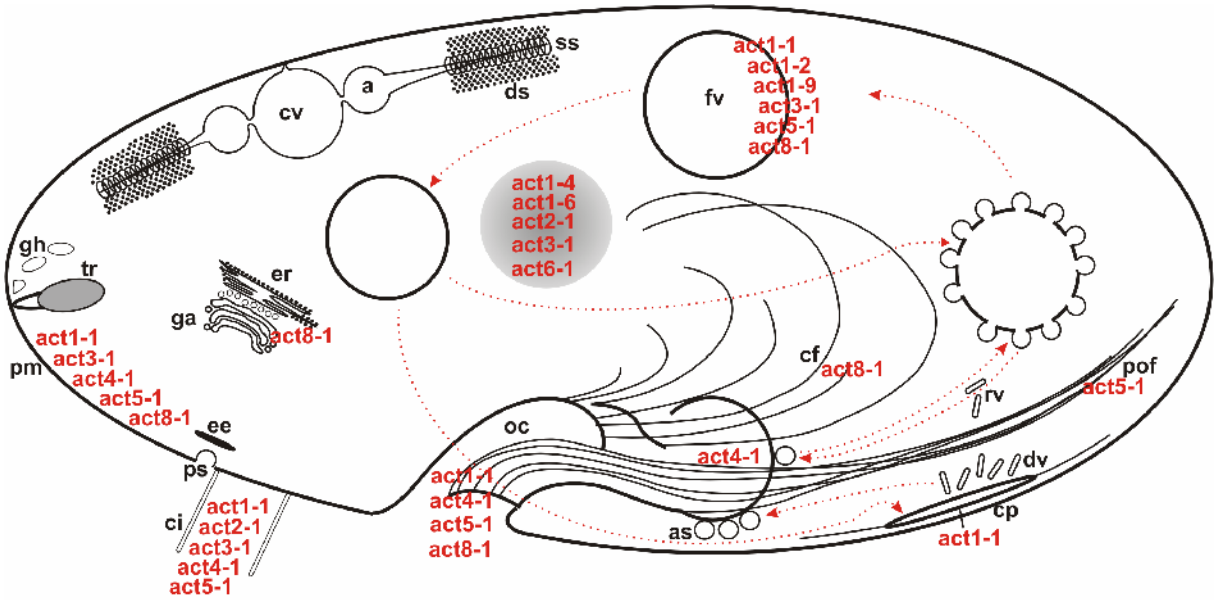

Fig. 45. Schematic distribution of actin isoforms in the *Paramecium* cell, as outlined in Table 1. The trafficking scheme is based on reviews by Fok and Allen (1990), Allen and Fok (2000) and Plattner and Kissmehl (2003). Actin distribution is based mainly on the present data obtained with GFP localization in vivo and with AB labeling, but also takes into account data from previous work (Tiggemann and Plattner, 1981; Kersken *et al*., 1986a, b; Kissmehl *et al*., 2004). The scheme contains elements of the osmoregulatory system (a, ampula; cv, contractile vacuole; ds, decorated spongiome; ss, smooth spongiome), though consistently unlabeled, of the phagosomal apparatus (as, acidosomes mediating acidification of a food vacuole [fv] after pinching off; cf, cytopharyngal fibers; cp, cytoproct [site of exocytotic release of spent phagosomes]), ci, cilia; dv, discoidal vesicles and other recycling vesicles, rv; ee, early endosome; er, endoplasmatic reticulum; ga, golgi apparatus; gh, ghosts (from released trichocysts); oc, oral cavity; pm, plasma membrane; pof, post oral fibers; ps, parasomal sacs; tr, trichocysts.

5.5.) Discussion

5.5.1.) Comparison with Previous Localization Studies

Previously we had localized actin in *Paramecium* by using fluorescently tagged DNase, heavy meromyosin, phalloidin and ABs against actin (Tiggemann and Plattner, 1981; Kersken et al., 1986a, b) and, more specifically, by ABs against actin1-1 (Kissmehl et al., 2004). Altogether this resulted in labeling of cilia, basal bodies, oral cavity, surface of food vacuoles, cytoproct, infraciliary lattice, cell surface ridges, the complex formed by the cortical calcium stores (alveolar sacs) and the cell membrane, surroundings of trichocyst docking sites, between bundled microtubules and $\leq$1.0 µm-sized vesicles.

While these studies anticipated part of our current results, the abundance of actin paralogs (Kissmehl et al., in prep.) found in the context of the *Paramecium* genome project suggested a more complicated pattern. By overexpression as GFP fusion proteins and with subfamily-specific ABs, a variety of new and detailed features for specific isoforms emerged.

5.5.2.) Aspects of Current Localization Studies and their Functional Implications

Cytosolic compartment. The role of actin isoforms with predominantly or exclusively diffuse cytosolic localization (Table 8) is difficult to appreciate. In Apicomplexans the small percentage of F-actin has been attributed to interaction with actin-binding proteins (Delorme et al., 2003). Remarkably, maintenance of cytosolic actin is vital for *Drosophila* although reasons remain unknown (Wagner et al., 2002).

Cilia. Occurrence of actin in cilia has been ascertained already (Tiggemann and Plattner, 1981; Kissmehl et al., 2004). We now show the presence of actin2-1, actin3-1, actin4-1 and actin5-1 in cilia. Actin may serve positioning of the inner dynein arms just as in *Chlamydomonas* flagella (Hayashi et al., 2001, Yanagisawa and Kamiya, 2001).

Swimming behavior is affected by silencing genes for actin2, actin3, actin4 and actin9, all but actin9 certainly occurring in cilia (Table 9). With actin4 and actin9, this could be due to a change in cell shape. Since phagocytosis is reduced, also after silencing of these genes, reduced food/energy supply could compromise cells in their swimming activity. However, there was no effect on the swimming behavior upon de- or hyperpolarization.

Cell cortex structures. GFP-actin3-1 outlines the ridges of the egg case-shaped cell surface. A similar staining pattern is seen with ABs against actin4-1 and actin5-1. It is not possible to attribute this pattern to concise populations of filaments known from the *Paramecium* cortex (Allen, 1971; 1988), e.g., it is rather different from that of the “infraciliary lattice”, a cortical meshwork mainly made up of centrin (Beisson et al., 2001).

Nevertheless, the infraciliary lattice has been shown by post-embedding EM analysis to contain substantial actin (Kissmehl et al., 2004).

GFP-actin8-1 is localized, among others, to parasomal sacs, i.e. coated pits (Allen, 1988). Our identification relies on the small size of labeled dots and their very regular arrangement, both largely excluding any other surface structures. This corresponds to the complex role of actin in endosome formation at the cell membrane, as established for higher eukaryotes (Merrifield et al., 2002; Merrifield, 2004; Kirkham and Parton, 2005; Yarar et al., 2005).

Oral cavity. While actin was known to occur around the oral cavity of *Paramecium* (Cohen et al., 1984; Kersken, 1986b) we now can specify this for actin5 and actin8. They are associated with the peniculus and quadrulus structures, as defined by Allen (1988), but also beyond, and as part of the oral cavity lining (Kissmehl et al., 2004) and the oral filament system. In this context the mobility of these fibers must be emphasized, which could be construed as an auxiliary mechanism to guide the processing food vacuole when leaving the buccal cavity. The identification of actin8-1 as part of the endosomal system, as described above, corresponds to the labeling of the quadrulus and peniculus. These oral elements contain a high number of parasomal sacs, arranged in several rows (Allen et al., 1992).

Phagosomes and cyclosis. Involvement of F-actin in phagosome formation in general (Kjeken et al., 2004) and in *Paramecium* in particular has been repeatedly documented (see above). Beyond that, several functions in the lifespan of a phagosome may require specific actins.

Cyclosis is an established actin-dependent process (Shimmen and Yokota, 2004) also occurring with phagosomes in *Paramecium* (Sikora et al., 1979). In *Tetrahymena*, for directed phagosome transport an unconventional myosin is required (Hosein et al., 2005), but no unilateral actin arrangement has been seen. In contrast, in *Paramecium* we surprisingly see GFP-actin paralogs, (actin1-2 and actin1-9), attached unilaterally to the lee-side, as if pushing phagosomes. This recalls the actin-based propulsion of *Listeria* and related pathogenic bacteria (Tilney and Portnoy, 1989), while this is new for organelles in eukaryotes. Although the actin-tails are short and not seen with immuno-staining using anti-actin1-1 ABs, their occurrence during overexpression may indicate a way of vesicle propulsion during cyclosis.

The surface of some phagosomes displays a speckled appearance of GFP-actin. This can reflect a functional mosaic pattern whereby some vesicles fuse and others pinch off during circulation through the cell (Allen and Fok, 1983; 2000; Fok et al., 1985; Allen et al., 1995). For instance, vacuole fusion in yeast requires F-actin disassembly (Wang et al., 2003).

Fig 42 shows inhibition of phagocytosis by silencing the actin genes of subfamily 2, 3, 4 or 9, particularly when resulting cells are of aberrant morphology (Table 9). Remarkably, actin isoforms investigated are localized to cilia by GFP or AB labeling. Therefore, reduced phagocytosis may be due to effects on engulfing bacteria by reduced ciliary activity and further processing of phagosomes.

Rod-shaped organelles. GFP-actin8-1 also stains rod-shaped, ≤1.0 µm-long organelles scattered throughout the cytoplasm, with some enrichment towards the cell surface (Figure 39B). According to size, form and position, as well as their number these structures may correspond to the numerous Golgi elements found in *Paramecium* (Estève, 1972). In immuno-gold EM-analysis, label was enriched at the boundary of the rough ER (Figs 40E,F), but overexpression may have distorted Golgi stacks, as observed in *Trypanosoma* cells (García-Salcedo et al., 2004), so they could not be identified unequivocally. The labeling resembles that achieved with the GFP fusion protein of the a8 subunit of the V-ATPase in *Paramecium* which was shown to represent the Golgi complex (Wassmer et al., 2006).

Nuclear and cell division. Our observation that the micronuclear cytospindle contains actin4 according to AB labeling is compatible with a role of actin in nuclear positioning (Starr and Han, 2003).

The notorious failure of demonstrating F-actin in the cleavage furrow of *Paramecium* (Kersken et al., 1986a) is apparently due to the absence of phalloidin-binding motifs in actin4 that forms this structure (Sehring et al., submitted). Using specific AB labeling we were successful in visualizing this structure (Figs 38B-F). Concomitantly, silencing of the actin4 genes inhibits cell division (Fig. 41A). Similar results were obtained with the act1 gene of *T. thermophila*, where silencing impaired phagocytosis, motility and cell separation (Williams et al., 2006).

Cell shape and other effects. Some of the *Paramecium* actins may contribute to cell shaping, as seen by changes following silencing of actin7 or actin9 genes (Figs 42B,C). Among them, only silencing of the actin9 gene affected the division rate (Fig. 41).

In addition it greatly reduced the contraction period of the contractile vacuole (Fig. 44). The effects may be very indirect, e.g., due to interaction of actin with transport systems or ion channels (Fukatsu et al., 2004) which then may affect the performance of the contractile vacuole.

Localization of cortical F-actin and its effects can be intriguing. On the EM level, anti-actin1-1 ABs labeled the narrow space between the plasmamembrane and alveolar sacs (Kissmehl et al., 2004). In related Apicomplexans equivalent structures are also connected by short F-actin strands (Jewett and Sibley, 2003). A similar structure/function effect is discussed

for mammalian cells whose cortical Ca^{2+} stores may be positioned by F-actin (Rosado and Sage, 2000; Wang et al., 2002; Roderick and Bootman, 2003; Turvey et al., 2005). Although we could not show in *Paramecium* such effect in response to cytochalasin (Mohamed et al., 2003), this may be due to the involvement of drug-insensitive isoforms. Any disturbance, e.g., by gene silencing, may entail the considerable effects on cell form and performance, as we describe.

5.6.) Acknowledgements

We gratefully acknowledge the availability of genomic library from Dr. J. Cohen (CNRS Gif-sur-Yvette, France) and of an expression library from Dr. J.E. Schultz (University of Tübingen, Germany) and the access to the *Paramecium* genome data base at an early stage of its development (Dr. J. Cohen and Dr. L. Sperling, CNRS, Gif-sur-Yvette, as well as Genoscope, Paris). We thank Dr. C. Stuermer and Dr. E. May for use of their confocal microscopes. Supported by Deutsche Forschungsgemeinschaft.

Chapter 6
Discussion and future perspectives

6.1.) Calcium sources during GTP mediated Ca oscillations in *Paramecium*

In the manuscript "Ca^{2+} oscillations mediated by exogenous GTP in *Paramecium* cells: assessment of possible Ca^{2+} sources" the calcium dynamics upon triggering of *Paramecium* cells with exogenous guanosine trisphosphate (GTP) were investigated using fluorochrome analysis. Triggering of *Paramecium* cells with GTP leads to pronounced back- and forward swimming which is paralleled by oscillating membrane depolarizations, as shown with electrophysiological methods (Clark et al. 1993). The goal of this work was to reveal the changes of the intracellular calcium concentration underlying the membrane depolarization events and to find out the involved sources of calcium and the mechanism of their activation. The cortical calcium stores of *Paramecium*, the alveolar sacs, play a crucial role in important calcium-dependent signal pathways, like the exocytosis of trichocysts. The question arose to what extend those calcium stores participate in the reaction upon GTP stimulation, and which other cellular components are involved. Some aspect in the model of the proposed signal transduction (Figure 6) could be rebutted.

Calcium imaging during triggering with GTP revealed an oscillating pattern of the calcium response. It is similar to the oscillations in membrane depolarization, with the same temporal frequency but with a prominent first peak. To generate the power of the first peak, calcium from the external medium is needed. Our data excludes ciliary voltage-dependent Ca^{2+}-channels as mediators of the Ca^{2+}-influx, because in the *pawnB* strain (lacking ciliary voltage-dependent Ca^{2+}-channels) similar calcium oscillations occurs. As open question remains the nature of the influx channels. It could be both another type of ciliary channel which is yet unknown, or somatic channels localized in domains close to the cilia could be involved. Spill-over of Ca^{2+} from the somatic cytosol into cilia was previously shown (Husser et al., 2004). Our data showed that the first prominent Ca^{2+} peak is important for the induction of the behavioral response. Under experimental conditions where Ca^{2+} oscillations without the first peak where induced, no behavioral response could be observed. These findings indicate the relevance of a Ca^{2+} influx signal. But our data also revealed that external Ca^{2+} is not exclusively responsible for the Ca^{2+} dynamics. For the further peaks, both Ca^{2+} from influx and from store mobilization is involved. The independent processes are superimposed to each other. To further investigate the internal Ca^{2+} source, different experimental conditions were used to exclude specific possible sources, i.e. Ca^{2+} from alveolar sacs. These cortical Ca^{2+} stores do not play a role in GTP-mediated Ca^{2+} signaling, according to our findings. Most

likely the ER, which is known to reach until the ciliary bases where no alveolar sacs occur, is involved as intracellular calcium pool. However, this requires more detailed analysis.

The oscillating pattern of the Ca^{2+} response suggests a quite fast dynamic of calcium release and calcium buffering. A feedback mechanism between Ca^{2+} mobilization and Ca^{2+}-activated and Ca^{2+}-inhibited processes can cause Ca^{2+} oscillations in different cells. Possible components are, e.g., phospholipase C and Ca^{2+}-inhibited Ca^{2+}-release via IP_3 receptors, or the interference of Ca^{2+} pumps and ion exchangers. Also feed-back with intracellular Ca^{2+} binding proteins may play a role. This is another aspect where further investigations can elucidate the molecular machinery involved in the GTP response and subsequently the biological meaning of it. It could clear the question whether the theory of an auto- and/or paracrine effect of GTP via purinergic receptors holds true.

6.2.) Actin in *Paramecium*

Actin is one of the cytoskeletan proteins which are discussed to be involved in the positioning of cortical calcium stores and thus in calcium signaling. The presence of actin in ciliates has been previously reported (Tiggemann at al., 1981; Cohen et al., 1984; Kersken et al., 1986a, b; Cohen and Beisson, 1988), but without many clues as to its function and general organization. For localization studies, phalloidin, heavy meromyosin or the subfragment 1 of myosin as specific probes for polymerized actin were used. In the manuscript "Immunolocalization of actin in *Paramecium* cells" we showed for the first time actin localization with specific antibodies raised against *Paramecium* actin. The polyclonal antibodies were raised against a conserved immunogenic region of several actin genes of the subfamily 1. Immunofluorescence and postembedding immunogold labeling/EM analysis showed label enriched in the cell cortex, around ciliary basal bodies, around the oral cavity, at the cytoproct, in cilia, in association with phagosomes and in the cytoplasm. Actin did display some ordered, though not very conspicuous, arrays throughout the cell. These findings were in coincidence with those of the previous studies mentioned above.

While working with the already identified actins in *Paramecium*, the ongoing *Paramecium* genome project with its growing data base allowed further search for actins and actin related proteins in the *Paramecium* genome. Sequence analysis revealed a large family of actin and actin related proteins. In the manuscript "The actin multigene family of Paramecium tetraurelia" 30 genes encoding actins, actin-related proteins or actin-like proteins were described. The paralogs were grouped into twelve subfamilies, according to their length, the number and position of their introns and the best matches with blast research. Paralogs for

actin-related proteins (arp) could be grouped in two subfamilies, and one actin-like protein (alp) was also found. Due to mixed results obtained with blast research in the database, not all of the identified sequences could be clearly assigned, as they were in part assigned to actin or arp. Alignment with an arp-alignment server confirmed the classification of several actins as arps. Phylogenetic analysis showed the great divergence of *Paramecium* actin/arp sequences; the most conserved actin sequences are less than 80% identical to actin sequences from other organisms. Due to these overall differences, we looked at several actin characteristics in detail. The amino acid sequences was analyzed regarding conserved actin consensus regions, amino acids influencing polymerization, ATP binding sites, and known binding sites for common actin binding protein and drugs. Most isoforms do not possess any of the three actin consensus pattern. With the reservation that analyzes on primary structure does not include possible divergence in conformation due to the different length, our analyzes revealed striking differences in *Paramecium* actin/arp sequences. We could show that the amino acids necessary for the binding of phalloidin, the common drug to label F-actin, are not present in most of the paralogs, e.g. in those occurring in the cleavage furrow. This finding can explain the failure to visualize the cleavage furrow by fluorescent phalloidin in *Paramecium*.

Due to the great number of different actin isoforms, not all of them could be analyzed in detail. In the manuscript “A broad spectrum of actin paralogs in *Paramecium tetraurelia* cells displays differential localization and function”, some of them were investigated. By using GFP constructs we have tagged members of the subfamilies and observed their localization by fluorescence imaging. GFP-localization of the different actin isoforms showed highly specific targeting to different components of the *Paramecium* cell. Using GFP constructs for localization studies has the advantage to visualize the protein in living cells. Especially for a protein with such strong dynamics as actin, with its ongoing polymerization and depolymerization, this could reveal functions of proteins which would not be accessible with other methods. One example is the interesting observations of actin tails on food vacuoles produced by the overexpression of GFP-act1-2 and GFP-actl-9 which seem to be used to push the vacuoles through the cell similar to the pathogenic bacterium *Listeria* during its invasion of a host cell from an adjoining cell.

Nevertheless, additionally for two subfamilies, specific antibodies were raised for immuno-localization studies. Affinity purified polyclonal antibodies against actin4-1 labeled, among other things, the cleavage furrow of dividing cells. Actin4-1 is one of the isoforms lacking the phalloidin-binding motifs. This explains the notorious failure of demonstrating F-actin in the cleavage furrow of *Paramecium.* Immunolocalization studies with affinity

purified antibodies against actin5-1 showed similar localization as observed with GFP tagged actin5-1, excluding possible artifacts due to GFP overexpression or fixation/permeabilisation during preparation for immunolocalization studies.

Another approach used was an RNAi technique to test possible roles of the different actin subfamilies in a variety of behavioral and functional aspects of a *Paramecium* cell. As actin is known to be involved in a broad range of tasks in other organisms, the adequate functions in *Paramecium* were investigated, e.g. motility, phagocytosis, exocytosis, and cell division. Indeed, gene silencing of diverse actin subfamilies lead to different phenotypes. Many of the findings are in coincidence with the localization studies. One example is the silencing of isoforms localized in cilia, which lead to an impairment of the swimming capability. The formation of phagosomes was also disturbed, which could be due to a reduced capability to move food particles into the cytopharynx by beating cilia. Another striking example is the phenotype of cells silenced in actin4, which were unable to divide, in agreement with its localization in the cleavage furrow. Other processes, like the docking of trichocysts, where an involvement of actin could be suspected, were not impaired by any of the investigated subfamilies. In those processes either actin subfamilies not yet investigated could play the major role, or those functions are so crucial that redundant genes step in.

The data presented in this thesis give a first overview about the various localization and function of some members of the large actin family in *Paramecium*. To complete the view of the actin family in *Paramecium*, it would be necessary to investigate all subfamilies by localization and functional studies. For a full understanding of the complexity of actin interactions, a more detailed analysis of the obtained data would be meaningful.

Chapter 7
References

Allen, P. G., Shuster, C. B., Kas, J. Chaponnier, C., Janmey, P. A., and Herman, I. M. (1996). Phalloidin binding and rheological differences among actin isoforms. Biochemistry 35, 14062-14069.

Allen, R. D. (1971). Fine structure of membranous and microfibrillar systems in the cortex of *Paramecium caudatum*. J. Cell Biol. 49, 1-20.

Allen, R. D. (1988). Cytology. *In* H.-D. Görtz (ed.), *Paramecium*, Springer-Verlag, Berlin, Heidelberg, New York, 4-40.

Allen, R. D., Aihara, M. S., and Fok, A. K. (1998). The striated bands of *Paramecium* are immunologically distinct from the centrin-specific infraciliary lattice and cytostomal cord. J. Eukaryot. Microbiol. 45, 202-209.

Allen, R. D., and Fok, A. K. (1983). Phagosome fusion vesicles of *Paramecium*. I. Thin-section morphology. Eur. J. Cell Biol. 29, 150-158.

Allen, R. D., and Fok, A. K. (1985). Modulation of the digestive lysosomal system in *Paramecium caudatum*. III. Morphological effects of cytochalasin B. Eur. J. Cell Biol. 37, 35-43.

Allen, R. D., and Fok, A. K. (2000). Membrane trafficking and processing in *Paramecium*. Int. Rev. Cytol. 198, 277-317.

Allen, R. D., Bala, N. P., Ali, R. F., Nishida, D. M., Aihara, M. S., Ishida, M., and Fok, A. K. (1995). Rapid bulk replacement of acceptor membrane by donor membrane during phagosome to phagoacidosome transformation in *Paramecium*. J. Cell Sci. 108, 1263-1274.

Altschul, S. F., Madden, T. L., Schäffer, A. A., Zhang, J., Zhang, Z., Miller, W., and Lipman, D J. **(**1997). Gapped BLAST and PSI-BLAST: a new generation of protein database search programs. Nucl. Ac. Res. 25, 3389-3402.

Aufderheide, K. J. (1977). Saltatory motility of uninserted trichocysts and mitochondria in *Paramecium tetraurelia.* Science 198, 299-300.

Ayscough, K. R. (2005). Coupling actin dynamics to the endocytic process in *Saccharomyces cerevisiae*. Protoplasma 226, 81-88.

Ayscough, K. R., Stryker, J., Pokala, N., Sanders, M., Crews, P., and Drubin, D. G. (1997). High rates of actin filament turnover in budding yeast and roles for actin in establishment and maintenance of cell polarity revealed using the actin inhibitor latrunculin-A. J. Cell Biol. 137, 399-416.

Bader, M. F., Doussau, F., Chasserot-Golaz, S., Vitale, N., and Gasman, S. (2004). Coupling actin and membrane dynamics during calcium-regulated exocytosis: a role for Rho and ARF GTPases. Biochim. Biophys. Acta. 1742, 37-49.

Bairoch, A., Buche, P., and Hofmann, K. (1997). The PROSITE database, its status in 1997. Nucleic Acids Res. 25, 217-221.

Bakowski, D., Glitsch, M. D., and Parekh, A. B. (2001). An examination of the secretion-like coupling model for the activation of the Ca^{2+} release-activated Ca^{2+} current I(CRAC) in RBL-1 cells. J. Physiol. 532, 55-71.

Barrit, G.J. (1999). Receptor-activated Ca^{2+} inflow in animal cells: a variety of pathways tailored to meet different intracellular Ca^{2+} signalling requirements. Biochem. J. 337, 153–169.

Bateman, A., Coin, L., Durbin, R., Finn, R. D., Hollich, V., Griffiths-Jones, S., Khanna, A., Marshall, M., Moxon, S., Sonnhammer, E. L., Studholme, D. J., Yeats, C., and Eddy, S. R. **(**2004). The Pfam protein families database. Nucl. Ac. Res. 32, D138-D141.

Beaulieu, V., Da Silva, N., Pastor-Soler, N., Brown, C. R., Smith, P. J. S., Brown, D., and Breton S. **(**2005). Modulation of the actin cytoskeleton via gelsolin regulates vacuolar H^+-ATPase recycling. J. Biol. Chem. 280, 8452-8463.

Beisson, J., Clérot, J.-C., Fleury-Aubusson, A., Garreau De Loubresse, N., Ruiz, F., and Klotz, C. (2001). Basal body-associated nucleation center for the centrin-based cortical cytoskeletal network in *Paramecium*. Protist 152, 339-354.

Beisson, J., and Rossignol, M. (1975). Movements and positioning of organelles in *Paramecium aurelia*. In: Nucleocytoplasmic relationships during cell morphogenesis in some unicellular organisms, ed. S. Puiseux-Dao, Amsterdam, New York, London: Elsevier, 291-294.

Belmont, L. D., Orlova, A., Drubin, D. G., and Egelman, E. H. (1999). A change in actin conformation associated with filament instability after Pi release. Proc. Natl. Acad. Sci. USA 96, 29-34.

Berger, J. D. (1986). Autogamy in *Paramecium*: cell cycle stage-specific commitment to meiosis. Exp. Cell Res. 166, 475-485.

Bernatzky, R., and S. D. Tanskley, S. D. (1986a). Genetics of actin-related sequences in tomato. Theor. Appl. Genet. 72, 314-321.

Berridge, G., Cramer, R., Galione, A., and Patel, S.(1994). Metabolism of the novel Ca^{2+}-mobilizing messenger nicotinic acid-adenine dinucleotide phosphate via a 2'-specific Ca^{2+}-dependent phosphatase. Biochem J. 365, 295-301.

Berridge, M. M. (1997). Elementary and global aspects of calcium signalling. J. Physiol. 499, 291-306.

Berridge, M. J., Bootman, M. D., Lipp, P. (1998). Calcium - life and death signal. Nature 395, 645-648.

Berridge, M. J., Bootman, M. D., Roderick, H. L. (2003). Calcium signalling: dynamics, homeostasis and remodelling. Nat. Rev. Mol. Cell Biol. 4, 517-529.

Berridge, M. J., Lipp, P., Bootman, M. D. (2000). The versatility and universality of calcium signalling. Nat. Rev. Cell Mol. Biol. 1, 11-21.

Bingham, J. B., and Schroer, T. A. (19999. Self-regulated polymerization of the actin-related protein Arp1. Curr. Biol. 9, 223-226.

Boyce, A.T., and Schwiebert, E.M. (2003). Extracellular ATP-gated P2X purinergic receptor channels. Curr. Top. Membr. 54, 98-50.

Braunstein, G.M., and Schwiebert, G.M. (2003). Epithelial purinergic receptors and signalling in health and disease. Curr. Top. Membr. 54, 205-241.

Bruzzone, S., Kunerth, S., Zocchi, E., DeFlora, A., and Guse, A. H. (2003). Spatio-temporal propagation of Ca^{2+} signals by cyclic ADP-ribose in 3T3 cells stimulated via purinergic P2Y receptors. J. Cell Biol. 163, 837-845.

Bubb, M. R., Spector, I., Beyer, B. B., and Fosen, K. M. (2000). Effects of jasplakinolide on the kinetics of actin polymerization. An explanation for certain in vivo observations. J. Biol. Chem. 275, 5163-5170.

Burnstock, G. (2003). Introduction: ATP and its metabolites as potent extracellular agents. Curr. Top. Membr. 54, 2-27.

Cairns, B. R., Erdjument-Bromage, H., Tempst, P., Winston, F., and Kornberg, R. D. (1998). Two actin-related proteins are shared functional components of the chromatin-remodeling complexes RSC and SI/SNF. Mol. Cell 2, 639-651.

Cao, H., Weller, S., Orth, J. D., Chen, J., Huang, B., Chen, J. -L., Stamnes, M., and McNiven, M.A. (2005). Actin and Arf1-dependent recruitment of a cortactin-dynamin complex to the Golgi regulates post-Golgi transport. Nature Cell Biol. 7, 483-492.

Carlier, M. F. (1991). Nucleotide hydrolysis in cytoskeletal assembly. Curr Opin Cell Biol. 3, 12-7.

Caron, F. and Meyer, E. (1985). Does *Paramecium primaurelia* use a different genetic code in its macronucleus? Nature 314, 185–188.

Carreno, S., Engqvist-Goldstein, A. E., Zhang, C. X., McDonald, K. L., and Drubin, D. G., (2004). Actin dynamics coupled to clathrin-coated vesicle formation at the trans-Golgi network. J. Cell Biol. 165, 781-788.

Chu, J. W., and Voth, G. (2005). Allostery of actin filaments: molecular dynamics simulations and coarse-grained analysis. Proc. Natl. Acad. Sci. USA 102, 13111-13116.

Cevallos, A. M., Lopez-Villasenor, I., Espinosa, N., Herrera, J., and Hernandez, R. (2003). *Trypanosoma cruzi*: allelic comparisons of the actin genes and analysis of their transcripts. Exp. Parasitol. 103, 27-34.

Clark, K. D., Hennessey, H. M., and Nelson, D. L. (1993). External GTP alters the motility and elicits an oscillating membrane depolarization in Paramecium tetraurelia. Proc. Natl. Acad. Sci. USA 90, 3782-3786.

Clark, K. D., Hennessey, T. M., Nelson, D. L., Preston, R. R. (1997). Extracellular GTP causes membrane-potential oscillations through the parallel activation of Mg^{2+} and Na^{+} currents in Paramecium tetraurelia. J. Membr Biol. 157, 159-67.

Clark, S.W., and Rose, M. D. (2005). Alanine Scanning of Arp1 Delineates a Putative Binding Site for Jnm1/Dynamitin and Nip100/p150^{Glued}. Mol. Biol. Cell. 16, 3999–4012.

Clérot, J. C., Iftode, F., Budin, K., Jeanmaire-Wolf, R., Coffe, G., and Fleury-Aubusson, A. (2001). Fine oral filaments in *Paramecium*: a biochemical and immunological analysis. J. Eukaryot. Microbiol. 48, 234-245.

Cleveland, D. W., Lopata, M. A., MacDonald, R. J., Cowan, N. J., Rutter, W.J., Kirschner, M. W. (1980). Number and evolutionary conservation of alpha- and beta-tubulin and cytoplasmic beta- and gamma-actin genes using specific cloned cDNA probes. Cell 20, 95-105.

Cohen, J., and Beisson, J. (1988). The cytoskeleton. *In* H. D. Görtz (ed.), *Paramecium*, Springer Verlag, Heidelberg, New York, London, Paris, Tokyo, 363-392.

Cohen, J., Garreau De Loubresse, N., and Beisson, J. (1984). Actin microfilaments in *Paramecium*: localization and role in intracellular movements. Cell Motil. 4, 443-468.

Cohen, J., Garreau De Loubresse, N., Klotz, C., Ruiz, F., Bordes, N., Sandoz, D., Bornens, M., et al., (1987). Organization and dynamics of a cortical fibrous network of *Paramecium*: the outer lattice. Cell. Motil. Cytoskel. 7, 315-324.

Cooper, G. M. (2000). The Cell. A molecular approach. 2nd ed., Sunderland,MA: Sinauer Associates

Cooper, J.A. (1987). Effects of cytochalasin and phalloidin on actin. J. Cell. Biol. 105, 1473-1478.

Croft, K. E., Dalby, A. B., Hogan, D. J., Orr, K. E., Hewitt, E. A., Africa, R. J., DuBois, M. L., and Prescott, D. M. (2003). Macronuclear molecules encoding actins in spirotrichs. J. Mol. Evol. 56, 341-350.

Cupples, C. G., and Pearlman, R. E. (1986). Isolation and characterization of the actin gene from *Tetrahymena thermophila.* Proc. Natl. Acad. Sci. USA 83, 5160–5164.

Damiani, M. T., and Colombo, M. I. (2003). Microfilaments and microtubules regulate recycling from phagosomes. Exp. Cell Res. 289, 152-161.

Daunderer, C., Schliwa, M., and Gräf, R. (2001). *Dictyostelium* centrin-related protein (DdCrp), the most divergent member of the centrin family, possesses only two EF hands and dissociates from the centrosome during mitosis. Eur. J. Cell Biol. 80, 621-630.

De Lanerolle, P., Johnson, T., and Hofmann, W. A. (2005). Actin and myosin I in the nucleus. What next? Nature Structural Mol. Biol. 12, 742-746.

Delbac, F., Sänger, A., Neuhaus, E. M., Stratmann, R., Ajioka, J. W., Toursel, C., Herm-Götz, A., et al., (2001). *Toxoplasma gondii* myosins B/C: one gene, two tails, two localizations, and a role in parasite division. J. Cell Biol. 155, 613-623.

DeOndarza, J., Simington, S. B., VanHouten, J. L., and Clark, J. M. (2003). G-protein modulators alter the swimming behavior and calcium influx of *Paramecium tetraurelia*. J. Eukaryot. Microbiol. 50, 349-355.

Delorme, V., Cayla, X., Faure, G., García, A., and Tardieux, I., (2003). Actin dynamics is controlled by a casein kinase II and phosphatase 2C interplay on *Toxoplasma gondii* toxofilin. Mol. Biol. Cell 14, 1900-1912.

Dessen, P., Zagulski, M., Gromadka, R., Plattner, H., Kissmehl, R., Meyer, E., Betermier, M., Schultz, J. E., Linder, J. U., Pearlman, R. E., Kung, C., Forney, J., Satir, B. H., Van Houten, J. L., Keller, A. M., Froissard, M., Sperling, L., and Cohen, J. **(**2001). *Paramecium* genome survey: a pilot project. Trends Genet. 17, 306-308.

Díaz-Ramos, C., Villalobo, E., Pérez-Romero, P., and Torres, A. (1998). *Paramecium tetraurelia* encodes unconventional actin containing short introns. J. Eukaryot. Microbiol. 45, 507-511.

Dobrowolski, J. M., Niesman, I. R., and Sibley, L. D. (1997). Actin in the parasite *Toxoplasma gondii* is encoded by a single copy gene, ACT1 and exists primarily in a globular form. Cell Motil. Cytoskel. 37, 253-262.

Dominguez, R. 2004. Actin-binding proteins - a unifying hypothesis. Trends Biochem. Sci. 29, 572-578.

Dos Remedios, C. G., Chhabra, D., Kekic, M., Dedova, I. V., Tsubakihara, M., Berry, D. A., and Nosworthy, N. J. (2003). Actin binding proteins: regulation of cytoskeletal microfilaments. Physiol. Rev. 83, 433-473.

Doyle, T., and Botstein, D. (1996). Movement of yeast cortical actin cytoskeleton visualized in vivo. Proc. Natl. Acad. Sci. USA 93, 3886-3891.

Drengk, A., Fritsch, J., Schmauch, C., Rühling, H., and Maniak, M. (2003). A coat of filamentous actin prevents clustering of late-endosomal vacuoles in vivo. Curr. Biol. 13, 1814-1819.

Drewes, G., and Faulstich, H. (1991). A reversible conformational transition in muscle actin is caused by nucleotide exchange and uncovers cysteine in position 10. J. Biol. Chem. 266, 5508-13.

Drubin, D. G., Jones, H. D., and Wertman, K. F. **(**1993). Actin structure and function: roles in mitochondrial organization and morphogenesis in budding yeast and identification of the phalloidin-binding site. Mol. Biol. Cell 4, 1277-1294.

Eckert, R. (1972). Bioelectric control of ciliary activity. Science 176, 473-81.

Egelman, E. H., Francis, N., and DeRosier, D. J. (1982). F-actin is a helix with a random variable twist. Nature 298, 131-5.

Eichinger, L., Pachebat, J. A., Glöckner, G., Rajandream, M.-A., Sucgang, R., Berriman, M., Song, J., Olsen, R., Szafranski, K., Xu, Q., Tunggal, B., Kummerfeld, S., Madera, M., Konfortov, B. A., Rivero, F., Bankier, A. T., Lehmann, R., Hamlin, N., Davies, R., Gaudet, P., Fey, P., Pilcher, K., Chen, G., Saunders, D., Sodergren, E., Davis, P. Kerhornou, A., Nie, X., Hall, N., Anjard, C., Hemphill, L., Bason, N., Farbrother, P., Desany, B., Just, E., Morio, T., Rost, R., Churcher, C., Cooper, J., Haydock, S., van Driessche, N., Cronin, A., Goodhead, I., Muzny, D., Mourier, T., Pain, A., Lu, M., Harper, D., Lindsay, R., Hauser, H., James, K., Quiles, M., Madan Babu, M., Saito, T., Buchrieser, C., Wardroper, A., Felder, M., Thangavelu, M., Johnson, D., Knights, A., Loulseged, H., Mungall, K., Oliver, K., Price, C., Quail, M. A., Urushihara, H., Hernandez, J., Rabbinowitsch, E., Steffen, D., Sanders, M., Ma, J., Kohara, Y., Sharp, S., Simmonds, M., Spiegler, S., Tivey, A., Sugano, S., White, B., Walker, D., Woodward, J., Winckler, T., Tanaka, Y., Shaulsky, G., Schleicher, M., Weinstock, G., Rosentha, A., Cox, E. C., Chisholm, R. L., Gibbs, R., Loomis, W. F., Platzer, M., Kay, R. R., Williams, J. Dear, P. H., Noegel, A. A., Barrell B., and Kuspa, A. 2005. The genome of the social amoeba *Dictyostelium discoideum*. Nature 435, 43-57.

Elliott, A. C. (2001). Recent developments in non-excitable cell calcium entry. Cell Calcium 30, 73-93.

Elzinga, M., Collins, J. H., Kuehl, W. M., and Adelstein, R. S. (1973). Complete amino-acid sequence of actin of rabbit skeletal muscle. Proc. Natl. Acad. Sci. USA 70, 2687-2691.

Engqvist-Goldstein, A. E. Y., and Drubin, D. G. (2003). Actin assembly and endocytosis: from yeast to mammals. Annu. Rev. Cell. Dev. Biol. 19, 287-332.

Erxleben, C., and Plattner, H. (1994). Ca^{2+} release from subplasmalemmal stores as a primary event during exocytosis in Paramecium cells. J. Cell Biol. 127, 935-945.

Erxleben, C., Klauke, N., Flötenmeyer, M., Blanchard, M.-P., Braun, C., and Plattner, H. (1997). Microdomain Ca^{2+} activation during exocytosis in *Paramecium* cells. Superposition of local subplasmalemmal calcium store activation by local Ca^{2+} influx. J. Cell Biol. 136, 597-607.

Estève, J. C. (1972). L'appareil de Golgi des ciliés. Ultrastructure, particulièrement chez *Paramecium*. J. Protozool. 19, 609-618.

Evans, J. H., and Sanderson, M. J. (1999). Intracellular calcium oscillations regulate ciliary beat frequency of airway epithelial cells. Cell Calcium 26, 103–110.

Falcke, M. (2003). Buffers and oscillations in intracellular Ca^{2+} dynamics. Biophys. J. 84, 28-41.

Fahrni, J. F. (1992). Actin in the ciliated protozoan *Climacostomum virens*: purification by DNAse I affinity chromatography, electrophoretic characterization, and immunological analysis. Cell Motil. Cytoskel. 22, 62–71.

Fehrenbacher, K.L., Boldogh, I.R., and Pon, L.A. (2003). Taking the A-train: actin-based force generators and organelle targeting. Trends Cell Biol. 13, 472-477.

Feng, L., Kim, E., Lee, W. L., Miller, C. J., Kuang, B., Reisler, E., and Rubenstein, P. A. (1997). Fluorescence probing of yeast actin subdomain 3/4 hydrophobic loop 262-274. Actin-actin and actin-myosin interactions in actin filaments. J. Biol. Chem. 272, 16829-16837.

Flanagan, M. D., and Lin, S. (1980). Cytochalasins block actin filament elongation by binding to high affinity sites associated with F-actin. J. Biol. Chem. 255, 835-838.

Fok, A. K, and Allen, R. D. (1988). The lysosome system. *In* H.-D. Görtz (ed.), *Paramecium*, Springer-Verlag, Berlin, Heidelberg, New York, 301-324.

Fok, A. K., and Allen, R. D. (1990). The phagosome-lysosome membrane system and its regulation in *Paramecium*. Int. Rev. Cytol. 123, 61-94.

Fok, A. K., Leung, S. S. K., Chun, D. P., and Allen, R.D. (1985). Modulation of the digestive lysososmal system in *Paramecium caudatum*. II. Physiological effects of cytochalasin B, colchicine and trifluoperazine. Eur. J. Cell Biol. 37, 27-34.

Fok, A. K., Ueno, M. S., Azada, E. A., and Allen, R. D. (1987). Phagosomal acidification in *Paramecium*: effects on lysosomal fusion. Eur. J. Cell Biol. 43, 412-420.

Forrester, T. (2003). A purine signal for functional hyperemia in skeletal and cardiac muscle. Curr. Top. Membr. 54, 270-305.

Fraser, A. G., Kamath, R. S., Zipperlen, P., Martinez-Campos, M., Sohrmann, M., and Ahringer, J. (2000). Functional genomic analysis of *C. elegans* chromosome I by systematic RNA interference. Nature 408, 325-330.

Froissard, M., Kissmehl, R., Dedieu, J. C., Gulik-Krzywicki, T., Plattner, H., and Cohen, J. (2002). N-ethylmaleimide-sensitive factor is required to organize functional exocytotic microdomains in *Paramecium*. Genetics 161, 643-650.

Fukatsu, K., Bannai, H., Zhang, S., Nakamura, H., Inoue, T., and Mikoshiba, K. (2004). Lateral diffusion of inositol 1,4,5-trisphosphate receptor type 1 is regulated by actin filaments and 4.1N in neuronal dendrites. J. Biol. Chem. 279, 48976-48982.

Garcés, J. A., Hoey, J. G., and Gavin, R. H. (1995). Putative myosin heavy and light chains in *Tetrahymena*: co-localization to the basal body-cage complex and association of the heavy chain with skeletal muscle actin filaments in vitro. J. Cell Sci. 108, 869-881.

García-Salcedo, J. A., Pérez-Morga, D., Gijón, P., Dilbeck, V., Pays, E., and Nolan, D. P. (2004). A differential role for actin during the life cycle of *Trypanosoma brucei*. EMBO J. 23, 780-789.

Gasman, S., Chasserot-Golaz, S., Malacombe, M., Way, M., and Bader, M.-F. (2004). Regulated exocytosis in neuroendocrine cells: a role for subplasmalemmal Cdc42/N-WASP-induced actin filaments. Mol. Biol. Cell 15, 520-531.

Gavin, R. H. (2001). Myosins in protists. Int. Rev. Cytol. 206, 97-134.

Glas-Albrecht, R., and Plattner, H. (1990). High yield isolation procedure for intact secretory organelles (trichocysts) from *Paramecium tetraurelia* strains. Eur. J. Cell Biol. 53,164-172.

Godiska, R., Aufderheide, K. J., Gilley, D., Hendrie, P., Fitzwater, T., Preer, L. B., Polisky, B., and Preer, J. R. (1987). Transformation of *Paramecium* by microinjection of a cloned serotype gene. Proc. Natl. Acad. Sci. USA 84, 7590-7594.

Gomperts, B. D., and Tatham, P. E. R. (1988). GTP-binding proteins in the control of exocytosis. Cold Spring Harbor Symp. Quant. Biol. 53, 983-992.

Goodson, H. V., and Hawse, W. F. (2002). Molecular evolution of the actin family. J. Cell Sci. 115, 2619-2622.

Gordon, J. L., and Sibley, L. D., (2005). Comparative genome analysis reveals a conserved family of actin-like proteins in apicomlexan parasites. BioMed Central Genomics 6, 179-192.

Grimaldi, M., Maratos, M., and Verma, A. (2003). Transient receptor potential channel activation causes a novel form of $[Ca^{2+}]_i$ and is not involved in capacitative Ca^{2+} entry in glial cells. J. Neurosci. 23, 4737-4745.

Guilherme, A., Soriano, N. A., Bose, S., Holik, J., Bose, A., Pomerleau, D. P., Furcinitti, P., et. Al., (2004). EDH2 and the novel EH domain binding protein EHBP1 couple endocytosis to the actin cytoskeleton. J. Biol. Chem 279, 10593-10605.

Halet, G., Marangos, P., FitzHarris, G., and Carroll, J. (2003). Ca^{2+}oscillations at fertilization in mammals. Biochem. Soc. Trans. 31, 907-911.

Hajnóczky, G., and Thomas, A. P. (1997). Minimal requirements for calcium oscillations driven by the IP3 receptor. EMBO J. 16, 3533-3543.

Hardt, M. and Plattner, H. (1999). Quantitative energy-dispersive X-ray microanalysis of calcium dynamics in cell suspensions during stimulation on a subsecond time scale: preparative and analytical aspects as exemplified with *Paramecium* cells. J. Struct. Biol. 128, 187–199.

Hardt, M. and Plattner, H. (2000). Sub-second quenched-flow/X-ray microanalysis shows rapid Ca2+ mobilization from cortical stores paralleled by Ca^{2+}influx during synchronous exocytosis in *Paramecium* cells. Eur. J. Cell Biol. 79, 642-652.

Harper, D. S., and Jahn, C. L. (1989). Differential use of termination codons in ciliated protozoa. Proc. Natl. Acad. Sci. USA 86, 3252-3256.

Hartwig, J. H., and Kwiatkowski, D. J. (1991). Actin-binding proteins. Curr. Opin. Cell. Biol. 3, 87-97.

Haugland, R. P. (ed.), Handbook of Fluorescent Probes and Research Chemicals, 9th ed., Molecular Probes Inc., Eugene, OR, 966.

Hauser, K., Haynes, W. J., Kung, C., Plattner, H., and Kissmehl, R. (2000). Expression of the green fluorescent protein in *Paramecium tetraurelia*. Eur. J. Cell Biol. 79, 144-149.

Hauser, K., Pavlovic, N., Kissmehl, R., and Plattner, H. (1998). Molecular characterization of a sarco(endo)plasmic reticulum Ca2+-ATPase gene from *Paramecium tetraurelia* and

localization of its gene product to sub-plasmalemmal calcium stores. Biochem. J. 334, 31-38.

Hauser, K., Pavlovic, N., Klauke, N., Geissinger, D., and Plattner, H. (2000). Green fluorescent protein-tagged sarco(endo)plasmic reticulum Ca^{2+}-ATPase overexpression in *Paramecium* cells: isoforms, subcellular localization, biogenesis of cortical calcium stores and functional aspects. Mol. Microbiol. 37, 773-787.

Hauser, M., Hausmann, K., and Jockusch, B. M. (1980). Demonstration of tubulin, actin and α-actinin by immunofluorescence in the microtubule-microfilament complex of the cytopharyngeal basket of the ciliate *Pseudomicrothorax dubius.* Exp. Cell. Res. 125, 265-274.

Hayashi, M., Hirono, M., and Kamiya, R. (2001). Recovery of flagellar dynein function in a *Chlamydomonas* actin/dynein-deficient mutant upon introduction of muscle actin by electroporation. Cell Motil. Cytoskel. 49, 146-153.

Haynes, W. J., Ling, K. Y., Saimi, Y., and Kung, C. (1995). Induction of antibiotic resistance in *Paramecium tetraurelia* by the bacterial gene APH-3´-II. J. Euk. Microbiol. 42, 83-91.

Hegyi, G., Michel, H., Shabanowitz, J., Hunt, D. F., Chatterjie, N., Healy-Louie, G., and Elzinga, M. (1992). Gln-41 is intermolecularly cross-linked to Lys-113 in F-actin by N-(4-azidobenzoyl)-putrescine. Protein Sci. 1, 132-144.

Hennessey, T. M. (2005). Responses of the ciliates Tetrahymena and Paramecium to external ATP and GTP. Purinergic Signalling 1: 101-110.

Herman, I. M. (1993) Actin isoforms. Curr. Op. Cell Biol. 5, 48-55.

Hightower, R. C., and Meagher, R. B. (1986). The molecular evolution of actin. Genetics 114, 315-332.

Watanabe, Y. (1987a). *Tetrahymena* actin. Cloning and sequencing of the *Tetrahymena* actin gene and identification of its gene product. J. Mol. Biol. 194, 181-192.

Hirono, M., Nakamura, M., Tsunemoto, M., Yasuda, T., Ohba, H., Numata, O., and Watanabe, Y. (1987b). *Tetrahymena* actin: localization and possible biological roles of actin in *Tetrahymena* cells. J. Biochem. 102, 537-545.

Hirono, M., Kumagai, Y., Numata, O., and Watanabe, Y. (1989). Purification of *Tetrahymena* actin reveals some unusual properties. Proc. Natl. Acad. Sci. USA 86, 75-79.

Hirono, M., Uryu, S., Ohara, A., Kato-Minoura, T., and Kamiya, R. (2003). Expression of conventional and unconventional actins in *Chlamydomonas reinhardtii* upon deflagellation and sexual adhesion. Eukaryot Cell 2, 486-493.

Hoey, J. G., and Gavin, R. H. (1992). Localization of actin in the *Tetrahymena* basal body-cage complex. J. Cell. Sci. 103, 629-641.

Hollerein, E. A., and Holzbaur, E. L. F. (1999). Arp1 (centractin),. *In* T. Kreis and R. Vale (eds.), Guidebook to the Cytoskeletal and Motor Proteins, 2nd ed. A Sambrook and Tooze Publication at Oxford University Press, Oxford, United Kingdom, 42-45

Holmes K. C., Popp, D., Gebhard, W., and Kabsch, W. (1990). Atomic model of the actin filament. Nature 347, 44-49.

,Hölttä-Vuori, M., Alpy, F., Tanhuanpää, K., Jokitalo, E., Mutka, A.-L., and Ikonen, E. (2005). MLN64 is involved in actin-mediated dynamics of late endocytic organelles. Mol. Biol. Cell 16, 3873-3886.

Hosein, R. E., Williams, S. A., and Gavin, R. H. (2005). Directed motility of phagosomes in *Tetrahymena thermophila* requires actin and myo 1p, a novel unconventional myosin. Cell Motil. Cytoskel. 61, 49-60.

Husser, M. R., Hardt, M., Blanchard, M.-P., Hentschel, J., Klauke, N., and Plattner, H. (2004). One-way calcium spill-over during signal transduction in *Paramecium* cells: from the cell cortex into cilia, but not in the reverse direction. Cell Calcium 37, 349–358.

Inesi, G., and Sagara, Y. (1994). Specific inhibitors of intracellular Ca^{2+} transport ATPases, J. Membr. Biol. 141, 1-6.

Itagaki, K., Kannan, K. B., Singh, B. B., and Hauser, C.J. (2004). Cytoskeletal reorganization internalizes multiple transient receptor potential channels and blocks calcium entry into human neutrophils. J. Immunol. 172, 601-607.

Iwamoto, M., and Nakaoka, Y. (2002). External GTP binding and induction of cell division in starved *Tetrahymena thermophila*. Eur. J. Cell Biol. 81, 517-524.

Jeng, R.L., and Welch, M.D. (2001). Cytoskeleton: actin and endocytosis–no longer the weakest link. Curr. Biol. 11, R691-694.

Jennings, H. S. (1976). The behaviour of Infusoria. *In* H.S. Jennings (ed), Behavior of the Lower Organisms, Indiana University Press, London, 1976, 47-54.

Jewett, T. J., and Sibley, L. D. (2003). Aldolase forms a bridge between cell surface adhesins and the actin cytoskeleton in Apicomplexan parasites. Mol. Cell 11, 885-894.

Just, I., Wollenberg, P., Moss, J., and Aktories, K. (1994). Cysteine-specific ADP-ribosylation of actin. Eur. J. Biochem. 221, 1047-1054.

Kabsch, W., Mannherz, H.G-, Suck, D., Pai, E. F., and Holmes, K.C. (1990). Atomic structure of the actin:DNase I complex. Nature 347, 37-44.

Kabsch, W., and Vandekerckhove, J. (1992). Structure and function of actin. Annu. Rev. Biophys. Biomol. Struct. 21, 49-76.

Kandasamy, M. K., Deal, R. B., McKinney, E. C., and Meagher, R. B. (2004). Plant actin-related proteins. Trends Plant Sci. 9, 196-202.

Kandasamy, M. K., McKinney, E. C., and Meagher, R. B. (2002). Functional nonequivalency of actin isovariants in *Arabidopsis*. Mol. Biol. Cell 13, 251-261.

Kaneshiro, E. S., Beischel, L. S., Merkel, S. J., and Rhoads, D. E. (1979). The fatty acid composition of *Paramecium aurelia* cells and cilia: changes with culture age. J. Protozool. 26, 147-158.

Kao, J. P. Y., and Tsien, R. Y. (1988). Ca^{2+} binding kinetics of fura-2 and azo-1 from temperature-jump relaxation measurements. Biophys. J. 53, 635-639.

Kato-Minoura, T., Okumura, M., Hirono, M., and Kamiya, R. **(**2003). A novel family of unconventional actins in volvocalean algae. J. Mol. Evol. 57, 555-561.

Kato-Minoura, T., Uryu, S., Hirono, M., and Kamiya, R. (1998). Highly divergent actin expressed in a *Chlamydomonas* mutant lacking the conventional actin gene. Biochem. Biophys. Res. Commun. 251, 71-76.

Kawano, S., Otsu, K., Shoji, S., Yamagata, K., and Hiraoka, M. (2003). Ca^{2+} oscillations regulated by Na^{+}- Ca^{2+} exchanger and plasma membrane Ca^{2+} pump induce fluctuations of membrane currents and potentials in human mesenchymal stem cells. Cell Calcium 34, 145-156.

Keller, A.-M., and Cohen, J. (2000). An indexed genomic library for *Paramecium* complementation cloning. J. Eukaryot. Microbiol. 47, 1–6.

Kersken, H., Momayezi, M., Braun, C., and Plattner, H. (1986a). Filamentous actin in *Paramecium* cells: functional and ultrastructural changes correlated with phalloidin affinity labeling in vivo. J. Histochem. Cytochem. 34, 455-465.

Kersken, H., Vilmart-Seuwen, J., Momayezi, M., and Plattner, H. (1986b). Filamentous actin in *Paramecium* cells: mapping by phalloidin affinity labeling in vivo and in vitro. J. Histochem. Cytochem. 34, 443-454.

Keryer, G., Adoutte, A., Ng, S. F., Cohen, J., Garreau De Loubresse, N., Rossignol, M., Stelly, N., et al., (1990a). Purification of the surface membrane-cytoskeleton complex (cortex) of *Paramecium* and identification of several of its protein constituents. Eur. J. Protistol. 25, 209-225.

Keryer, G., Iftode, F., and Bornens, M. (1990b). Identification of proteins associated with microtubule-organizing centres and filaments in the oral apparatus of the ciliate *Paramecium tetraurelia.* J. Cell Sci. 97, 553-563.

Kim, E., and Reisler, E. (1996). Intermolecular coupling between loop 38-52 and the C-terminus in actin filaments. Biophys. J. 71, 1914-1919.

Kim, E., Motoki, M., Seguro, K., Muhlrad, A., and Reisler, E. (1995). Conformational changes in subdomain 2 of G-actin: fluorescence probing by dansyl ethylenediamine attached to Gln-41. Biophys. J. 69, 2024-2032.

Kim, E., Wriggers, W., Phillips, M., Kokabi, K., Rubenstein, P. A., and Reisler, E. (2000). Cross-linking constraints on F-actin structure. J. Mol. Biol. 299, 421-429.

Kim, K., Gooze, L., Petersen, C., Gut, J., and Nelson, R. G. (1992). Isolation, sequence and molecular karyotype analysis of the actin gene of *Cryptosporidium parvum*. Mol. Biochem. Parasitol. 50, 105-113.

Kim, K., Messinger, L. A., andNelson, D. L. (1998). Ca^{2+}-dependent protein kinases of *Paramecium*: cloning provides evidence of a multigene family. Eur. J. Biochem. 251, 605-612.

Kim, K., Son, M., Peterson, J. B., and Nelson, D. L. (2002). Ca^{2+}-binding proteins of cilia and infraciliary lattice of *Paramecium tetraurelia*: their phosphorylation by purified endogenous Ca2+-dependent protein kinases. J. Cell Sci. 115, 1973-1984.

Kim, M. Y., Kuruvilla, H. G., and Hennessey, T.M. (1997). Chemosensory adaptation
in *Paramecium* involves changes in both repellent binding and the consequent receptor potentials. Comp. Biochem. Physiol. 118A, 589-597.

Kim, M. Y., Kuruvilla, H. G., Raghu, S., and Hennessey, T. M. (1999). ATP reception and chemosensory adaptation in *Tetrahymena thermophila*. J. Exp. Biol. 202, 407-416.

Kim, O. T., Yura, K., Go, N., and Harumoto, T. (2004). Highly divergent actins from karyorelictean, heterotrich, and litostome ciliates. J. Eukaryot. Microbiol. 51, 227-233.

Kirkham, M., and Parton, R. G. (2005). Clathrin-independent endocytosis: new insights into caveolae and non-caveolar lipid raft carriers. Biochim. Biophys. Acta 1745, 273-286.

Kissmehl, R., Huber, S., Kottwitz, B., Hauser, K., and Plattner, H. (1998). Subplasmalemmal Ca-stores in *Paramecium tetraurelia*. Identification and characterization of a sarco(endo)plasmic reticulum-like Ca2+-ATPase by phosphoenzyme intermediate formation and its inhibition by caffeine. Cell Calcium 24, 193-203.

Kissmehl, R., Sehring, I. M., Wagner, E., and Plattner, H. (2004). Immuno-localization of actin in *Paramecium* cells. J. Histochem. Cytochem. 52, 1543-1559.

Kissmehl, R., Treptau, T., Hofer, H. W., and Plattner, H. (1996). Protein phosphatase and kinase activities possibly involved in exocytosis regulation in *Paramecium tetraurelia.* Biochem. J. 317, 65-76.

Kjeken, R., Egeberg, M., Habermann, A., Kuehnel, M., Peryon, P., Floetenmeyer, M., Walther, P., Jahraus, A., Defacque, H., Kuznetsov, S. A., Griffiths, G., et al., (2004). Fusion between phagosomes, early and late endosomes: a role for actin in fusion between late, but not early endocytic organelles. Mol. Biol. Cell 15, 345-358.

Klauke, N., Blanchard, M.-P., and Plattner, H. (2000). Polyamine triggering of exocytosis in *Paramecium* involves an extracellular Ca^2/(polyvalent cation)-sensing receptor. J. Membr. Biol. 174, 141-156.

Klauke, N., and Plattner, H. (1997). Imaging of Ca^2 transients induced in Paramecium cells by a polyamine secretagogue. J. Cell Sci. 110, 975-983.

Klotz, C., Garreau de Loubresse, N., Ruiz, F., and Beisson, J. (1997). Genetic evidence for a role of centrin-associated proteins in the organization and dynamics of the infraciliary lattice in *Paramecium.* Cell. Motil. Cytoskel. 38, 172-186.

Knoll, G., Braun, C., and Plattner, H. (1991). Quenched flow analysis of exocytosis in *Paramecium* cells: time course, changes in membrane structure, and calcium requirements revealed after rapid mixing and rapid freezing of intact cells. J. Cell Biol. 111, 1295-1304.

Koninck, P. D., and Schulman, H. (1998). Sensitivity of CaM kinase II to the frequency of Ca^2 oscillations. Science 279, 227–229.

Kumar, S., Tamura, K., and Nei, M. (2000). MEGA3: Integrated software for molecular evolutionary genetics analysis and sequence alignment. Brief Bioinform. 5, 150-163.

Kung, C. (1971). Genic mutants with altered system of excitation in Paramecium aurelia. II. Mutagenesis, screening and genetic analysis of the mutants. Genetics 69, 29-45.

Kunzelmann-Marche, C., Freyssinet, J. M., and Martínez, M. C. (2001). Regulation of phosphatidylserine transbilayer redistribution by store-operated Ca^{2+} entry. Role of actin cytoskeleton. J. Biol. Chem. 276, 5134-5139.

Kuruvilla, H. G., Kim, M. Y., and Hennessey, T. M. (1997). Chemosensory adaptation to lysozyme and GTP involves independently regulated receptors in *Tetrahymena thermophila*. J. Eukaryot. Microbiol. 44, 263-268.

Kyhse-Andersen, J. (1989). Multi-chamber apparatus for preparative isoelectric focusing. Electrophoresis 10, 6-10.

Laemmli, U. K. (1970). Cleavage of structural proteins during the assembly of the head of bacteriophage T4. Nature 227, 680-685.

Lang, T., Wacker, I., Wunderlich, I., Rohrbach, A., Giese, G., Soldati, T., and Almers, W. (2000). Role of actin cortex in the subplasmalemmal transport of secretory granules in PC12 cells. Biophys. J. 78, 2863-2877.

Länge, S., Klauke, N., and Plattner, H. (1995). Subplasmalemmal Ca^{2+} stores of probable relevance for exocytosis in *Paramecium*. Alveolar sacs share some but not all characteristics with sarcoplasmic reticulum. Cell Calcium 17, 335-344.

Lansley, A. B., and Sanderson, M. J. (1999). Regulation of airway ciliary activity by Ca^{2+}: simultaneous measurement of beat frequency and intracellular Ca2+. Biophys. J. 77, 629–638.

Lazarowski, E.R. (2003). Molecular and biological properties of P2Y receptors. Curr. Top. Membr. 54, 59-96.

Lefort-Tran, M., Aufderheide, K., Phouphile, M., Rossignol, M., and Beisson, J. (1981). Control of exocytotic processes: cytological and physiological studies of trichocyst mutants in *Paramecium tetraurelia*. J. Cell Biol. 88, 301-311.

Levin, A. E., Travis, S. M., DeVito, L. D., Park, K. A., and Nelson, D. L. (1989). Purification and characterization of a calcium-dependent ATPase from *Paramecium tetraurelia*. J. Biol. Chem. 264, 4544-4551.

Li, W. H., and Graur, D. (1991). Fundamentals of molecular evolution. Sinauer, Sunderland, Mass.

Lin, C.-M., Chen, H.-J., Leung, C. L., Parry, D. A. D., and Liem, R. K. H. (2005). Microtubule actin crosslinking factor 1b: a novel plakin that localizes to the Golgi complex. J. Cell Sci. 118, 3727-3738.

Lorenz, M., Popp, D., and Holmes, K. C. (1993). Refinement of the F-actin model against X-ray fiber diffraction data by the use of a directed mutation algorithm. J. Mol. Biol. 234, 826-836.

Lovett, J. L., Marchesini, N., Moreno, S. N. J., and Sibley, L. D. (2002). *Toxoplasma gondii* microneme secretion involves intracellular Ca2+ release from inositol 1,4,5-trisphosphate (IP3)/ryanodine-sensitive stores. J. Biol. Chem. 277, 25870-25876.

Lumpert, C. J., Kersken, H., and Plattner, H. (1990). Cell surface complexes ('cortices') isolated from *Paramecium tetraurelia* cells as a model system for analysing exocytosis in vitro in conjunction with microinjection studies. Biochem. J. 269, 639-645.

Machemer, H. (1988). Electrophysiology. *In* H.-D. Görtz (ed.), *Paramecium*, Springer-Verlag, Berlin, Heidelberg, New York, 185-215.

Machemer, H, and Ogura, A. (1979). Ionic conductances of membranes in ciliated and deciliated Paramecium. J. Physiol. 296, 49-60.

Machemer, H., and Teunis, P. F. M. (1996).Sensory-motor coupling and motor responses, in: K. Hausmann, P.C. Bradbury (Eds.), Ciliates. Cells and Organisms, Gustav Fischer Verlag, Stuttgart, 379–402.

Maekawa, M., Ishizaki, T., Boku, S., Watanabe, N., Fujita, A., Iwamatsu, A., Obinata, T., Ohashi, K., Mizuno, K., and Narumiya, S. (1999). Signaling from Rho to the actin cytoskeleton through protein kinases ROCK and LIM-kinase. Science 285, 895-898.

Malacombe, M., Chasserot-Golaz, S., Bader, M.-F., and Gasman, S. (2004). Cdc42 and N-WASP regulate actin filament organization during exocytosis in PC12 cells. *In* R. Borges & L. Gandía (eds), Cell Biology of the Chromaffin Cell, Instituto Teófilo Hernando, Spain.

Manneville, J. B., Etienne-Manneville, S., Skehel, P., Carter, T., Ogden, D., and Ferenczi, M. (2003). Interaction of the actin cytoskeleton with microtubules regulates secretory organelle movement near the plasma membrane in human endothelial cells. J. Cell Sci. 116, 3927-3938.

Marchler-Bauer, A.**,** Anderson, J. B., Cherukuri, P. F., DeWeese-Scott, C., Geer, L. Y., Gwadz, M., He, S., Hurwitz, D. I., Jackson, J. D., Ke, Z., Lanczycki, C. J., Liebert, C. A., Liu, C., Lu, F., Marchler, G. H., Mullokandov, M., Shoemaker, B. A., Simonyan, V., Song, J. S., Thiessen, P. A., Yamashita, R. A., Yin, J. J., Zhang, D., and Bryant, S. H. **(**2005). CDD: a conserved domain database for protein classification. Nucleic Acids Res. 33, D192-D196.

McCarron, J. G., Bradley, K. N., MacMillan, D., and Muir, T. C. (2003). Sarcolemma agonist-induced interactions between InsP3 and ryanodine receptors in Ca^{2+} oscillations and waves in smooth muscle. Biochem. Soc. Trans. 31, 920-924.

Mclean, M., Gerats, A. G. M., Baird, W. V. and Meagher, R. B. (1990). Six actin gene subfamilies map to five chromosomes of *Petunia hybrida*. J. Hered. 81, 341-346.

Meagher, R. G., McKinney, E. C., and Kandasamy, M. K. (1999). Isovariant Dynamics Expand and Buffer the Responses of Complex Systems: The Diverse Plant Actin Gene Family. Plant Cell 11, 995-1005.

Meagher, R. B., and McLean, B. G. (1990). Diversity of plant actins. Cell Motil. Cytoskelet. 16, 164-166.

Meagher, R.B., and Williamson, R.E. (1994). The Plant Cytoskeleton. In Arabidopsis, eds E. Meyerowitz and C. Somerville, (Cold Spring Harbor, NY: Cold Spring Harbor Laboratory Press), 1049–1084.

Mehta, D., Ahmmed, G. U., Paria, B. C., Holinstat, M., Voyno-Yasenetskaya, T., Tiruppathi, C., Minshall, R. D., and Malik, A.B. (2003). RhoA interaction with inositol 1,4,5-trisphosphate receptor and transient receptor potential channel-1 regulates Ca^{2+}entry. Role in signaling increased endothelial permeability. J. Biol. Chem. 278, 33492-33500.

Merrifield, C. J. (2004). Seeing is believing: imaging actin dynamics at single sites of endocytosis. Trends Cell Biol. 14, 352-358.

Merrifield, C. J., Feldman, M. E., Wan, L., and Almers, W. (2002). Imaging actin and dynamin recruitment during invagination of single clathrin-coated pits. Nature Cell Biol. 4, 691-698.

Merz, A. J., and Wickner, W. T. (2004). Trans-SNARE interactions elicit Ca^{2+} efflux from the yeast vacuole lumen. J. Cell Biol. 164, 195-206.

Méténier, G. (1984). Actin in *Tetrahymena paravorax*: ultrastructural localization of HMM-binding filaments in glycerinated cells. J. Protozool. 31, 205-215.

Mimikakis, J. L. and Nelson, D. L. (1998). Evidence for two separate purinergic responses in *Paramecium tetraurelia*: XTP inhibits only the oscillatory responses to GTP. J. Membr. Biol. 163, 19-23.

Mimikakis, J. L., Nelson, D. L., and Preston, R. R. (1998). Oscillating response to a purine nucleotide disrupted by mutation in *Paramecium tetraurelia*. Biochem. J. 330, 139-147.

Miyakawa-Naito, A., Uhlén, P., Lal, M., Aizman, O., Mikoshiba, K., Brismar, J., Zelenin, S., and Aperia, A. (2003). Cell signaling microdomain with Na,K-ATPase and inositol 1,4,5-trisphosphate receptor generates calcium oscillations. J. Biol. Chem. 278, 50355-50361.

Miyazaki, S., Shirakawa, H., Nakada, K., and Honda, Y. (1993). Essential role of the inositol 1,4,5,-trisphosphate receptor/ Ca^{2+}release channel in Ca^{2+}waves and Ca^{2+}oscillations at fertilization of mammalian eggs. Dev. Biol. 158, 62-78.

Mitchell, E. J., and Zimmerman, A. M. (1985). Biochemical evidence for the presence of an actin protein in *Tetrahymena pyriformis.* J. Cell Sci. 73, 279-297.

Mitchell, D. R. (2000). *Chlamydomonas* flagella. J. Phycol. 36, 261-273.

Mohamed, I., Klauke, N., Hentschel, J., Cohen, J., and Plattner, H. (2002). Functional and fluorochrome analysis of an exocytotic mutant yields evidence of store-operated Ca^{2+}influx in *Paramecium*. J. Membr. Biol. 187, 1-14.

Mohamed, I., Husser, M., Sehring, I., Hentschel, J., Hentschel, C., and Plattner, H. (2003). Refilling of cortical calcium stores in *Paramecium* cells: in situ analysis in correlation with store-operated calcium influx. Cell Calcium 34, 87-96.

Moniz de Sa, M., and Drouin, G. (1996). Phylogeny and substitution rates of angiosperm actin genes. Mol. Biol. Evol. 13, 1198–1212.

Morales, M., Colicos, M. A., and Goda, Y. (2000). Actin-dependent regulation of neurotransmitter release at central synapses. Neuron 27, 539-550.

Morrissette, N. S., and Sibley, L. D. (2002). Cytoskeleton of Apicomplexan Parasites. Microbiol. Mol. Biol. Rev. 66, 21-38.

Muallem, S., Kwiatkowska, K., Xu, X., and Yin, H. L. (1995). Actin filament disassembly is a sufficient final trigger for exocytosis in nonexcitable cells. J. Cell. Biol. 128, 589-598.

Muhlrad, A., Cheung, P., Phan, B. C., Miller, C., and Reisler, E. (1994). Dynamic properties of actin. Structural changes induced by beryllium fluoride. J. Biol. Chem. 269, 11852-11858.

Muller, J., Oma, Y., Vallar, L., Friederich, E., Poch, O., and Winsor, B. (2005). Sequence and comparative genomic analysis of actin-related proteins. Mol. Biol. Cell 16, 5736-5748.

Muto, E., Edamatsu, M., Hirono, M., and Kamiya, R. (1994). Immunological detection of actin in the 14S ciliary dynein of *Tetrahymena*. FEBS Lett. 343, 173-176.

Drought-induced guard cell signal transduction involves sphingosine-1-phosphate. Nature 410, 596-599.

Naitoh, Y. (1995). Reactivation of extracted *Paramecium* models, Methods Cell. Biol. 47, 211–224.

Naitoh, Y., and Eckert, R. (1969). Ionic mechanisms controlling behavioral responses in *Paramecium* to mechanical stimulation, Science 164, 963–965.

Nelson, D. L. (1995). Preparation of cilia and subciliary fractions from *Paramecium.* Methods Cell Biol. 47, 17-24.

Nelson, R. G., Kim, K., Gooze, L., Petersen, C., and Gut, J. (1991). Identification and isolation of *Cryptosporidium parvum* genes encoding microtubule and microfilament proteins. J. Protozool. 38, 52S–55S.

Nemoto, T., Kojima, T., Oshima, A., Bito, H., and Kasai, H (2004). Stabilization of exocytosis by dynamic F-actin coating of zymogen granules in pancreatic acini. J. Biol. Chem. 279, 37544–37550.

Ng, C. K.-Y., Carr, K., McAinsh, M. R., Powell, B., and Hetherington, A.M. (2001). Drought-induced guard cell signal transduction involves sphingosine-1-phosphate. Nature 410, 596-9.

Noegel, A. A., and Schleicher, M. (1991). Phenotypes of cells with cytoskeletal mutations. Curr. Opin. Cell. Biol. 3, 18-26.

Nolen, B. J., Littlefield, R. S., and Pollard, T. D. (2004). Crystal structures of actin-related protein 2/3 complex with bound ATP or ADP. Proc. Natl. Acad. Sci. USA 101, 15627-15632.

Novick, P., and Botstein, D. (1985). Phenotypic analysis of temperature-sensitive yeast actin mutants. Cell 40, 405-416.

Oda, T., Crane, Z. D., Dicus, C. W,, Sufi, B. A., and Bates, R. B. (2003). Dolastatin 11 connects two long-pitch strands in F-actin to stabilize microfilaments. J. Mol. Biol. 328, 319-324.

Oheim, M., and Stuhmer, W. (2000). Tracking chromaffin granules on their way through the actin cortex. Eur. Biophys. J. 29, 67-89.

Olave, I. A., Reck-Peterson, S. L., and Crabtree, G. R. (2002). Nuclear actin and actin-related proteins in chromatin remodeling. Annu. Rev. Biochem. 71, 755-781.

Orlova, A., and Egelman, E.H. (1992). Structural basis for the destabilization of F-actin by phosphate release following ATP hydrolysis. J. Mol. Biol. 227, 1043-1053.

Otegui, M. S., Verbrugghe, K. J., and Skop, A. R. (2005). Midbodies and phragmoplasts: analogous structures involved in cytokinesis. Trends Cell Biol. 15, 404-413.

Otterbein, L. R., Graceffa, P., and Dominguez, R. (2001). The crystal structure of uncomplexed actin in the ADP state. Science 293, 708-711.

Padmakumar, V. C., Libotte, T., Lu, W., Zaim, H., Abraham, S., Noegel, A. A., Gotzmann, J., Foisner, R., and Karakesisoglou1, I.(2005). The inner nuclear membrane protein Sun1 mediates the anchorage of Nesprin-2 to the nuclear envelope. J. Cell Sci. 118, 3419-3430.

Pape, R., and Plattner, H. (1990). Secretory organelle docking at the cell membrane of *Paramecium* cells: dedocking and synchronized redocking of trichocysts. Exp. Cell Res. 191, 263-272.

Parri, H. R., and Crunelli, V. (2003). The role of Ca^{2+} in the generation of spontaneous astsrocytic Ca2+ oscillations, Neuroscience 120, 979-992.

Patterson, R. L., van Rossum, D. B., and Gill, D. L. (1999). Store-operated Ca^{2+} entry: evidence for a secretion-like coupling model. Cell 98, 487-499.

Pendleton, A., and Koffer, A.(2001). Effects of latrunculin reveal requirements for the actin cytoskeleton during secretion from mast cells. Cell. Motil. Cytoskeleton. 48, 37-51.

Pernberg, J., and Machemer, H. (1995). Fluorometric measurement of the intracellular free Ca2+-concentration in the ciliate *Didinium nasutum* using Fura-2. Cell Calcium 18, 484-494.

Pérez-Romero, P., Villalobo, E., Díaz-Ramos, C., Calvo, P., and Torres, A. (1999). Actin of *Histriculus cavicola*: characteristics of the highly divergent hypotrich ciliate actins. J. Eukaryot. Microbiol. 46, 469-472.

Petersen, O. H., and Wakui, M. (1990). Oscillating intracellular Ca^{2+} signals evoked by activation of receptors lined to inositol lipid hydrolysis: mechanism of generation, J. Membr. Biol. 118, 93–105.

Pines, A., Romanello, M., Cesaratto, L., Damante, G., Moro, L., D'Andrea, P., and Tell, G. (2003). Extracellular ATP stimulates the early growth response protein 1 (Egr-1) via a protein kinase C-dependent pathway in the human osteoblastic HOBIT cell line. Biochem. J. 373, 815-824.

Plattner, H., and Klauke, N. (2001). Calcium in ciliated protozoa: sources, regulation, and calcium regulated cell functions, Int. Rev. Cytol. 201, 115-208.

Plattner, H., and Kissmehl, R. (2003). Molecular aspects of membrane trafficking in *Paramecium*. Int. Rev. Cytol. 232, 185-216.

Plattner, H., and Zingsheim, H. P. (1983). Electron microscopic methods in cellular and molecular biology. Subcell. Biochem. 9, 1-236.

Plattner, H., Braun, C., and Hentschel, J. (1997a). Facilitation of membrane fusion during exocytosis and exocytosis-coupled endocytosis and accerelation of „ghost" detachment in Paramecium by extracellular calcium. J. Membr. Biol. 158, 197-208.

Plattner, H., Habermann, A., Kissmehl, R., Klauke, N., Majoul, I., and Söling, H.-D. (1997). Differential distribution of calcium stores in *Paramecium* cells. Occurrence of a subplasmalemmal store with a calsequestrin-like protein. Eur. J. Cell Biol. 72, 297-306.

Plattner, H., Lumper, c. J., Knoll, G., Kissmehl, R., Höhne, B., Momayezi, M., and Glas-Albrecht, R. (1991). Stimulus-secretion coupling in Paramecium cells. Eur. J. Cell Biol. 55, 3-16.

Plattner, H., Matt, H., Kersken, H., Haacke, B., and Stürzl, R. (1984). Synchronous exocytosis in *Paramecium* cells. I. A novel approach. Exp. Cell Res. 151, 6-13.

Plattner, H., Stürzl, R., and Matt, H. (1985). Synchronous exocytosis in *Paramecium* cells. IV. Polyamino compounds as potent trigger agents for repeatable trigger-redocking cycles, Eur. J. Cell Biol. 36, 32-37.

Plattner, H., Westphal, C., and Tiggemann, R. (1982). Cytoskeleton-secretory vesicle interactions during the docking of secretory vesicles at the cell membrane in Paramecium tetraurelia cells. J. Cell Biol. 92, 368-377.

Pollard, T. D. (2001). Genomics, the cytoskeleton and motility. Nature 409, 842-843.

Pollard, T. D., and Beltzner, C. C. (2002). Structure and function of the Arp2/3 complex. Curr. Op. Struct. Biol. 12, 768-774.

Pollard, T. D., and Borisy, G. G. (2003). Cellular motility driven by assembly and disassembly of actin filaments. Cell. 112, 453-65.

Pollard, T. D., Blanchoin, L., and Mullins, R. D. (2000). Molecular mechanisms controlling actin filament dynamics in nonmuscle cells. Annu. Rev. Biophys. Biomol. Struct. 29, 545-576.

Poupel, O., Boleti, H. Axisa, S., Couture-Tosi, E., and Thardieux, I. (2000). Toxofilin, a novel actin-binding protein from *Toxoplasma gondii*, sequesters actin monomers and caps actin filaments. Mol. Biol. Cell 11, 355-368.

Prajer, M., Fleury, A., and Laurent, M. (1997). Dynamics of calcium ion channel function in *Paramecium* and possible morphogenetic implication. J. Cell Sci. 110, 529-535.

Preston, R. R. (1990). Genetic dissection of Ca^{2+}-dependent ion channel function in *Paramecium.* BioEssays 12, 273–281.

Preston, R. R., Kink, J. A., Hinrichsen, R. D., Saimi, Y., and Kung, C. (1991). Calmodulin mutants and Ca2+-dependent channels in *Paramecium.* Annu. Rev. Physiol. 53, 309-319.

Rayment, I., Holden, H. M., Wittaker, M., Yohn, C. B., Lorenz, M., Holmes, K. C., and Miligan, R. A. (1993). Structure of the actin-myosin complex and its implications for muscle contraction. Science 261, 58-65.

Redondo, P. C., Lajas, A. I., Salido, G. M., Gonzalez, A., Rosado, J. A., Pariente, J. A. (2003). Evidence for secretion-like coupling involving pp60src in the activation and maintenance of store-mediated Ca^{2+}- entry in mouse pancreatic acinar cells. Biochem. J. 370, 255-263.

Reece, K. S., Mcelroy, D., and Wu, R. (1992). Function and evolution of actins. Evol. Biol. 26, 1-34.

Reisler, E. (1993). Actin molecular structure and function. Curr. Opin. Cell. Biol. 5, 41-47.

Roderick, H. L., and Bootman, M. D. (2003). Calcium influx: is Homer the missing link? Curr. Biol. 13, R976-R978.

Rosado, J. A., and Sage, S. O. (2000). The actin cytoskeleton in store-mediated calcium entry. J. Physiol. 526, 221-229.

Rosado, J. A., and Sage, S. O. (2000). Farnesylcysteine analogues inhibit store regulated Ca2+ entry in human platelets : evidence for involvement of small GTP binding proteins and actin cytoskeleton. Biochem. J. 346, 183-192.

Rosado, J. A., Jenner, S., and Sage, S. O. (2000). A role for the actin cytoskeleton in the initiation and maintenance of store-mediated calcium entry in human platelets. Evidence for conformational coupling. J. Biol. Chem. 275, 7527-7533.

Rosado, J. A., Redondo, P. C., Pariente, J. A., and Salido, G. M. (2004). Calcium signalling and tumorigenesis. Cancer Therapy 2, 263-270.

Rosado, J. A., Redondo, P. C., Sage, S. O. Pariente, J. A., and Salido, G. M. (2005). Store-operated Ca^{2+} entry: vesicle fusion or reversible trafficking and de novo conformational coupling? J. Cell Physiol. 205, 262-269.

Rosner, B. N., Bartholomew, J. N., Gaines, C. D., Riddle, M. L., Everett, H. A., Rulapaugh, K. G., Nickeson, L. E., Marshall, M. R., and Kuruvilla, H. G. (2003). Biochemical

evidence for a P2Y-like receptor in *Tetrahymena thermophila*. J. Comp. Physiol. 189A, 781-789.

Rubenstein, P. A. (1990). The functional importance of multiple actin isoforms. BioEssays 12, 309-315.

Ruiz, F., Vayssié, L., Klotz, C., Sperling, L., and Madeddu, L. (1998). Homology-dependent gene silencing in *Paramecium*. Mol. Biol. Cell 9, 931-943.

Sabala, P., Targos, B., Caravelli, A., Czajkowski, R., Lim, D., Gragnaniell, G., Santella, L., and Baranska, J. (2002). Role of the actin cytoskeleton in store-mediated calcium entry in glioma C6 cells. Biochem. Biophys. Res. Commun. 296, 484-491.

Sahoo, N., Beatty, W., Heuser, J., Sept, D., and Sibley, L. D. (2006). Unusual kinetic and structural properties control rapid assembly and turnover of actin in the parasite Toxoplasma gondii. Mol. Biol. Cell 17, 895-906.

Salathe, M., and Bookman, R. J. (1999). Mode of Ca^{2+} action on ciliary beat frequency in single ovine airway epithelial cells. J. Physiol. 520, 851–865.

Salathe, M., and Bookman, R. J. (1999). Calcium and the regulation of mammalian ciliary beating. Protoplasma 206, 234–240.

Sambrock, J., Fritsch, E. F., and Maniatis, T. (1989). Molecular Cloning: A Laboratory Manual. Cold Spring Harbor Laboratory Press. Cold Spring Harbor, NY.

Sanders, M. A., and Salisbury, J. L. (1994). Centrin plays an essential role in microtubule severing during flagellar excision in *Chlamydomonas reinhardtii.* J. Cell Biol. 124, 795-805.

Sandoz, D., Gounon, P., Karsenti, E., Sauron, M. E. (1982). Immunocytochemical localization of tubulin, actin, and myosin in axonemes of ciliated cells from quail oviduct. Proc. Natl. Acad. Sci. USA 79, 3198-3202.

Schafer, D. A. (2003). Actin puts on the squeeze. Nat. Cell Biol 5, 693-694.

Schmitz, S., Grainger, M., Howell, S., Calder, L. J., Gaeb, M., Pinder, J. C., Holder, A. A., and Veigel, C. (2005). Malaria parasite actin filaments are very short. J. Mol. Biol. 349, 113-125.

Schutt, C. E., Myslik, J. C., Rozycki, M. D., Goonesekere, N. C., and Lindberg, U. (1993). The structure of crystalline profilin-beta-actin. Nature 365, 810-816.

Schwiebert, E. M., Zsembery, A., and Geibel, J. P. (2003). Cellular mechanisms and physiology of nucleotide and nucleoside release from cells: current knowledge, novel assays to detect purinergic agonists, and future directions, Curr. Top. Membr. 54, 32-58.

Schroeder, C. C., Fok, A. K., and Allen, R. D. (1990). Vesicle transport along microtubular ribbons and isolation of cytoplasmic dynein from *Paramecium.* J. Cell Biol. 111, 2553-2562.

Selve, N., and Wegner, A. (1986). Rate of treadmilling of actin filaments in vitro. J. Mol. Biol. 187, 627-631.

Shen, X., Ranallo, R., Choi, E., and Wu, C. (2003). Involvement of actin-related proteins in ATP-dependent chromatin remodelling. Mol. Cell 12, 147-155.

Shimmen, T., and Yokota, E. (2004). Cytoplasmic streaming in plants. Curr. Op. Cell Biol. 16, 68-72.

Sibley, L. D. (2004). Intracellular parasite invasion strategies. Science 304, 248-253.

Sikora, J., Wasik, A., and Baranowski, Z. (1979). The estimation of velocity distribution profile of *Paramecium* cytoplasmic streaming. Eur. J. Cell Biol. 19, 184-188.

Simpson, A., Tepikin, A., Quayle, J., and Kamishima T. (2003) (eds.), Biochemical Society Focused Meetings: Calcium Oscillations (Biochem. Soc. Trans. 31), Biochemical Society, London, 3, 907-969.

Skouri, F., and Cohen, J. (1997). Genetic approach to regulated exocytosis using functional complementation in *Paramecium*: identification of the ND7 gene required for membrane fusion. Mol. Biol. Cell 8, 1063-71.

Snider, J., Lin, F., Zahedi, N., Rodionov, V., Yu, C. C., and Gross, S. P. (2004). Intracellular actin-based transport: How far you go depends on how often you switch. Proc. Natl. Acad. Sci. USA 101, 13204-13209.

Solovyova, N., and Verkhratsky, A. (2003). Neuronal endoplasmic reticulum acts as a single functional Ca2+ store shared by ryanodine and inositol-1,4,5-trisphosphate receptors as revealed by intra-ER [Ca2+] recordings in single rat sensory neurones. Eur. J. Physiol. 446, 447-454.

Sonneborn, T. M. (1970). Methods in *Paramecium* research. Methods Cell Physiol. 4, 242-335.

Sonneborn, T. M. (1974). *Paramecium aurelia*. *In* R. C. Kung (ed.), Handbook of Genetics, vol. 2. Plenum Press, New York, N. Y.

Spector, I., Shochet, N. R., Blasberger, D., Kashman, Y. (1989). Latrunculins-novel marine macrolides that disrupt microfilament organization and affect cell growth: I. Comparison with cytochalasin D. Cell. Motil. Cytoskeleton. 13, 127-144.

Sperling, L. P., Dessen, P., Zagulski, M., Pearlman, R. E., Migdalski, A., Gromadka, R., Froissard, M., et al., (2002). Random sequencing of *Paramecium* somatic DNA. Eukaryot. Cell 1, 341-352.

Starr, D. A., and Han, M. (2003). ANCors away: an actin based mechanism of nuclear positioning. J. Cell Sci. 116, 211-216.

Steinmetz, M. O., Stoffler, D., Muller, S. A., Jahn, W., Wolpensinger, B., Goldie, K. N., Engel, A., Faulstich, H., and Aebi, U. (1998). Evaluating atomic models of F-actin with an undecagold-tagged phalloidin derivative. J. Mol. Biol. 276, 1-6.

Stelly, N., Mauge, J. P., Claret, M., and Adoutte, A. (1991). Cortical alveoli of Paramecium: a vast submembranous calcium storage compartment. J. Cell. Biol. 113, 103-112.

Stock, C., Grønlien, H. K., Allen, R. D., and Naitoh, Y. (2002). Osmoregulation in *Paramecium*: in situ ion gradients permit water to cascade through the cytosol to the contractile vacuole. J. Cell Sci. 115, 2339-2348.

Stockinger, W., Zhang, S. C., Trivedi, V., Jarzylo, L. A., Shieh, E. C., Lane, W. S., Casoreno, A. B., and Nohturfft, A. (2006). Differential requirements for actin polymerization, calmodulin, and Ca^{2+} define distinct stages of lysosome/phagosome targeting. Mol. Biol. Cell 17, 1697-1710.

Stoorvogel, W., Kerstens, S., Fritzsche, I., Den Hartigh, J. C., Oud, R., Van Der Heyden M. A. G., Voortman, J., and Van Bergen En Henegouwen, P. M. P. (2004). Sorting of ligand-activated epidermal growth factor receptor to lysosomes requires its actin-binding domain. J. Biol. Chem. 279, 11562-11569.

Sunada, R., Görzer, I., Oma, Y., Yosida, T., Suka, N., Wintersberger, U., and Harata, M. (2005). The nuclear actin-related protein Act3p/Arp4p is involved in the dynamics of chromatin-modulating complexes. Yeast 22, 753-768.

Tamm, S. (1994). Ca^{2+}channels and signalling in cilia and flagella. Trends Cell Biol. 4, 305-310.

Tanimura, A., Tojyo, Y., And Turner, R. J. (2000). Evidence that type I, II, and III inositol 1,4,5-trisphosphate receptors can occur as integral plasma membrane proteins. J. Biol. Chem. 275, 27488-27493.

Thomas et al. 1996

Tiggemann, R., and Plattner, H. (1981). Localization of actin in the cortex of *Paramecium tetraurelia* cells by immuno- and affinity-fluorescence microscopy. Eur. J. Cell Biol. 24, 184-190.

Tilney, L. G., and Portnoy, D. A. (1989). Actin filaments and the growth, movement, and spread of the intracellular bacterial parasite, *Listeria monocytognes*. J. Cell Biol. 109, 1597-1608.

Tomida, T., Hirose, K., Takizawa, A., Shibasaki, F., and Iino, M. (2003). NFAT functions as a working memory of Ca^{2+} signals in decoding Ca^{2+} oscillation. EMBO J. 22, 3825-3832.

Timmons, L., Court, D. L., and Fire, A. (2001). Ingestion of bacterially expressed dsRNAs can produce specific and potent genetic interference in *Caenorhabditis elegans*. Gene 263, 103-112.

Tirion, M. M., ben-Avraham, D., Lorenz, M., and Holmes, K. C. (1995). Normal modes as refinement parameters for the F-actin model. Biophys. J. 68, 5-12.

Torre, V., Ashmore, J. F., Lamb, T. D., Menini, A. (1995). Transduction and adaptation in sensory receptor cells. J. Neurosci. 15, 7757-7768.

Trelles-Sticken, E., Adelfalk, C., Loidl, J., and Scherthan, H. (2005). Meiotic telomere clustering requires actin for its formation and cohesin for its resolution. J. Cell. Biol. 170, 213-223.

Tsien, R.W., and Tsien, R.Y. (1990). Calcium channels, stores, and oscillations. Annu. Rev. Cell. Biol. 6, 715-760.

Turvey, M. R., Fogarty, K. E., and Thorn, P. (2005). Inositol (1,4,5)-trisphosphate receptor links to filamentous actin are important for generating local Ca^{2+} signals in pancreatic acinar cells. J. Cell Sci. 118, 971-980.

Valentijn, K., Valentijn, J. A., and Jamieson, J. D. (1999). Role of actin in regulated exocytosis and compensatory membrane retrieval: insights from an old acquaintance. Biochem. Biophys. Res. Commun. 266, 652-661.

Valentijn, J.A., Valentijn, K., Pastore, L.M., and Jamieson, J.D. (2000). Actin coating of secretory granules during regulated exocytosis correlates with the release of rab3D. Proc. Natl. Acad. Sci. USA 97, 1091–1095.

Vandekerckhove, J. (1990). Actin-binding proteins. Curr. Opin. Cell. Biol. 2, 41-50.

Vandekerckhove, J., and Weber, K. (1978). At least six different actins are expressed in a higher mammal: an analysis based on the amino acid sequence of the amino-terminal tryptic peptide. J. Mol. Biol. 126, 783-802.

VanHouten, J. (1978). Two mechanisms of chemotaxis in Paramecium. J. comp. Physiol. 127, 167-174.

Venkatachalam, K., van Rossum, D. B., Patterson, R. L., Ma, H. T., and Gill, D. L. (2002). The cellular and molecular basis of store-operated calcium entry. Nature cell Biol. 4, E263-E272.

Verkhusha, V. V., Tsukita, S., and Oda, S. (1999). Actin dynamics in lamellipodia of migrating border cells in the *Drosophila* ovary revealed by a GFP-actin fusion protein. FEBS Lett. 445, 395-401.

Verkhratsky, A., and Toescu, E. C. (eds.), Integrative Aspects of Calcium Signalling, Plenum Press, New York, London, 1998, p. 408.

Vickerman, K., and Cox, F. E.G. (1967). The protozoa. *In* Introductory studies in biology, London: John Murray

Viguès, B., Blanchard, M. P., and Bouchard P. (1999). Centrin-like filaments in the cytopharyngeal apparatus of the ciliates *Nassula* and *Furgasonia*: evidence for a relationship with microtubular structures. Cell Motil. Cytoskel. 43, 72-81.

Villalobo, E., Perez-Romero, P., Sanchez-Silva, R., and Torres, A. (2001). Unusual characteristics of ciliate actins. Int. Microbiol. 4, 167-174.

Visegrády, B., Lörinczy, D., Hild, G., Somogyi, B., and Nyitrai, M. (2004). The effect of phalloidin and jasplakinolide on the flexibility and thermal stability of actin filaments. FEBS Lett. 565, 163-166.

Wagner, C. R., Mahowald, A. P., and Miller, K. G. (2002). One of the two cytoplasmic actin isoforms in *Drosophila* is essential. Proc. Natl. Acad. Sci. USA 99, 8037-8042.

Wang, L., Merz, A. J., Collins, K. M., and Wickner, W. (2003). Hierarchy of protein assembly at the vertex ring domain for yeast vacuole docking and fusion. J. Cell Biol. 160, 365-374.

Wang, Y. J., Gregory, R. B., and Barritt, G. J. (2002). Maintenance of the filamentous actin cytoskeleton is necessary for the activation of store-operated Ca^{2+} channels, but not other types of plasma-membrane Ca^{2+} channels, in rat hepatocytes. Biochem. J. 363, 117-126.

Wassenberg, J. J., Clark, K. D., and Nelson, D. L. (1997). Effect of SERCA pump inhibitors on chemoresponses in Paramecium. J. Eukaryot. Microbiol. 44, 574-581.

Wassmer, T., Kissmehl, R., Cohen, J. and Plattner, H. (2006). Seventeen a-subunit isoforms of *Paramecium* V-ATPase provide high specialization in localization and function. Mol. Biol. Cell 17, 917-930.

Weber, K., and Kabsch, W. (1994). Intron positions in actin genes seem unrelated to the secondary structure of the protein. EMBO J. 13, 1280-1286.

Weber, K., Lazarides, E., Goldman, R. D., Vogel, A., and Pollack, R. (1975). Localization and distribution of actin fibers in normal transformed and revertant cells. Cold Spring Harb. Symp. Quant. Biol. 39, 363-369.

Wesseling, J. G., Snijders, P. J., van Someren, P., Jansen, J., Smits, M. A., and Schoenmakers, J. G. (1989). Stage-specific expression and genomic organization of the actin genes of the malaria parasite *Plasmodium falciparum*. Mol. Biochem. Parasitol. 35, 167-176.

Wetzel, D. M., Hakansson, S., Hu, K., Roos, D., and Sibley, L. D. (2003). Actin filament polymerization regulates gliding motility by apicomplexan parasites. Mol. Biol. Cell 14, 396–406.

Wieland, T., and Faulstich, H. (1978). Amatoxins, phallotoxins, phallolysin, and antamanide: the biologically active components of poisonous *Amanita* mushrooms. Crit. Rev. Biochem. 5, 185-260.

Wood, C. R. and Hennessey, T. M. (2003). PPNDS is an agonist, not an antagonist, for the ATP receptor in *Paramecium*. J. Exp. Biol. 206, 627-636.

Xie, Q., Zhang, Y., Zhai, C., Bonanno, J. A. (2002). Calcium influx factor from cytochrome P-450 metabolism and secretion-like coupling mechanisms for capacitative calcium entry in corneal endothelial cells. J. Biol. Chem. 277, 16559-66.

Yam, P. T., and Theriot, J. A. (2004). Repeated cycles of rapid actin assembly and disassembly on epithelial cell phagosomes. Mol. Biol. Cell 15, 5647-5658.

Yanagisawa, H.-A., and Kamiya, R. (2001). Association between actin and light chains in *Chamydomonas* flagellar inner-arm dyneins. Biochem. Biophys. Res. Commun. 288, 443-447.

Yarar, D. (2003). Cortical patches on the move. Cell 115, 373-375.

Yarar, D., Waterman-Storer, C. M., and Schmid, S. L. (2005). A dynamic actin cytoskeleton functions at multiple stages of clathrin-mediated endocytosis. Mol. Biol. Cell 16, 964-975.

Yarmola, E. G., Somasundaram, T., Boring, T. A., Spector, I., Bubb, M.R. (2000). Actin-latrunculin structure and function. Differential modulation of actin-binding protein function by latrunculin A. J. Biol. Chem. 275, 28120-28127.

Young, K. W., Nash, M. S., Challiss, R. A. J., and Nahorski, S. R. (2003). Role of Ca^{2+} feedback on single cell inositol 1,4,5-trisphosphate oscillations mediated by G-protein-coupled receptors. J. Biol. Chem. 278, 20753-20760.

Zagulski, M., Nowak, J. K., Le Mouel, A., Nowacki, M., Migdalski, A., Gromadka, R., Noel, B., Blanc, I., Dessen, P., Wincker, P., Keller, A. M., Cohen, J., Meyer, E., and Sperling, L.

(2004). High coding density of the largest *Paramecium tetraurelia* somatic chromosome. Curr. Biol. **1**4, 1397-1404.

Zackroff, R. V., Hufnagel, L. A. (1998). Relative potencies of different cytochalasins for the inhibition of phagocytosis in ciliates. J. Eukaryot.Microbiol. 45, 397-403.

Zackroff, R. V., Hufnagel, L. A. (2002). Induction of anti-actin drug resistance in *Tetrahymena.* J. Eukaryot. Microbiol. 49, 475-477.

Zhang, L., and Sanderson, M. J. (2003). Oscillations in ciliary beat frequency and

intracellular calcium concentration in rabbit tracheal epithelial cells induced by ATP. J. Physiol. 546, 733–749.

Zimmerman, A. M., Zimmerman, S., Thomas, J., Ginzburg, I. (1983). Control of tubulin and actin gene expression in *Tetrahymena pyriformis* during the cell cycle. FEBS Lett. 164, 318-322.

Chapter 8
Supplemental material

TABLE A1: Oligonucleotides used to study gene expression (cDNA)

DNA	Oligonucleotide	Sequence
Synthesis of cDNA		
cDNA	3'-EcoRI/NotI-dTT	5'-AACTGGAAGAATTCGCGGCCGCGGAATTTTTTTTTTTT-3'
Primers used to clone actins from the actin 1 subfamily		
act1-1	5'-Act1-1	5'-CCGGTATTGCAGGAGATGATG-3'
act1-1	3'-Act1-1	5'-ACCGCTTTCGTCGTATTCG-3'
Pairs of actin specific (5') and unspecific (3') primers		
act1-1	5'-XhoI-Act1-1	5'-CCGCTCGAGATGTCTGAAGAACACCCAGCAG-3'
	3'-EcoRI/NotI	5'-AACTGGAAGAATTCGCGGCCGCGG-3'
act1-2	5'-StuI-Act1-2	5'-CCGAGGCCTATGTCTGAAGAACACCCAGCAGTTG-3'
	3'-EcoRI/NotI	5'-AACTGGAAGAATTCGCGGCCGCGG-3'
act1-3	5'-StuI-Act1-3	5'-CCGAGGCCTATGTCTGAAGAACACCCAGCAGTCG-3'
	3'-EcoRI/NotI	5'-AACTGGAAGAATTCGCGGCCGCGG-3'
act1-4	5'-HindIII-Act1-4	5'-GGGGTTTTAAGCTTAAAGTATCC-3'
	3'-EcoRI/NotI	5'-AACTGGAAGAATTCGCGGCCGCGG-3'
Pairs of actin specific (5' and 3') primers		
act1-6	5'-StuI-Act1-6	5'-AAAAGGCCTATGTAAGCTTAATATCCAGC-3'
	3'-XhoI-Act1-6	5'-CCGCTCGAGTCAGAAACATTTTCTGTGAAC-3'
act1-7	5'-StuI-Act1-7	5'-GAAGGCCTATGTCAGATTAATTACCAGCAGTTATAAT-3'
	3'-XhoI-Act1-7	5'-CCGCTCGAGCAATGAGTAACTCCATCTCCTGAATCG-3'
act1-9	5'-StuI-Act1-9	5'-GAAGGCCTATGAATGATGAAAAACCAGCAGTCG-3'
	3'-XhoI-Act1-9	5'-CCGCTCGAGTCAAGTGACTGTCTAACATTTTCTGTG-3'
act2-1	5'bAStu	5'-AAGGCCTATGGACGACGTAATCCCAGTTGTG
	3'bAX	5'-CCGCTCGAGTCAGAAGCATTTTCTGTGCACATAACC
act3-1	5'A3	5'-GTAATTGAAAATGCTTCTTGC
	3'A3X	5'-CCGCTCGAGTCAGAAACATTTAATATGTGC
act3-2	5'Stu-Act3-2	5'-GAAGGCCTATGATAGAATCTCATCCTCCTGTTG
	3'Xba-Act3-2	5'-GCTCTAGATCAAAAACATTTAATGTGAGCAATC
act4-1	5'Stu-Act4-1	5'-GAAGGCCTATGAATGATGAAAAACCAGCAG
	3'Xho-Act4-1	5'-CCGCTCGAGTCAAGTGACTGTCTAAGATTTTC
act5-1	5'Stu-Act5-1	5'-AGGCCTATGGATAATGACATATTTGCTAATAACTCG
	3'Xho-Act5-1	5'-CCGCTCGAGTCACAATTATTTTTTGATTAAAATG
acti6-1	5'Spe-Act6-1	5'-GCGACTAGTATGGAAAGTGAGTATGACTAAAAAG
	3'Xho-Act6-1	5'-CCGCTCGAGTCAAAATGTTCTCTTATGAATAAG
act7-1	5'Stu-Act7-1	5'-GAAGGCCTATGTTCATACCATACAAAAAAAATAAAGGG
	3'Xho-Act7-1	5'-CCGCTCGAGTCAATAAAACATTTTTTTTTCTATTAG
act8-1	5'Stu-Act8-1	5'-GAAGGCCTATGAATAATAATGATTCACCTTCTATTA
	3'Xho-Act8-1	5'-CCGCTCGAGTCAAAAGCACTTTCTTTATACTA
act9-1	5'Stu-Act9-1	5'-GAAGGCCTATGAGTCTAGACAAATAATCAAGG
	3'Spe-Act9-1	5'-GGACTAGTTCACGGTTTAATAGAAATAAAA

Chapter 9
Summary

Summary

This thesis works on two themes. In the first part of the work, calcium dynamics upon triggering of *Paramecium* cells with GTP were performed using fluorochrome analysis. The results are presented in Sehring et al. (2004). *Paramecium* reacts upon GTP response with periodic back- and forward swimming. A reversion of the cilia stroke is achieved by high levels of calcium in cilia. On electrophysiology level, this behavioural response is accompanied with depolarisations of the membrane potential. In this work, different components which were proposed to be involved in the intracellular signaling (according to the model of Wessenberg et al. 1997; Figure 6) were investigated. We showed that calcium from the external medium as well as from intracellular stores is involved in signal transduction. In contrast to the model, neither the voltage-dependent ciliary calcium channels nor the cortical calcium stores, the alveolar sacs, participate in the reaction. The identity of the influx channels is still unknown. As intracellular store the ER could take part. Both needs further investigations.

As could be shown, the alveolarsacs are not involved in the reaction upon triggering with GTP. But as cortical calcium stores, they play a major role in exocytosis. An open question is their positioning and structural connection to the plasma membrane. A potential candidate is actin, as it was shown to be involved in calcium signaling in other systems. Thus, in the second part of this thesis, actin in *Paramecium* was investigated. At the beginning, a polyclonal antibody against actin1-1 was available which was used for immunohistological studies. The data obtained were published in Kissmehl et al. (2004). With the ongoing genome project, all genes coding for actin, actin-related proteins or actin-like proteins in *Paramecium* could be identified. A characterization of the paralogs on nucleotide and amino acid level is presented in the manuscript Kissmehl et al. (2006). Some of the genes were analyzed in detail, especially their localization using green-fluorescent proteins and/or specific antibodies, and their functional significance using RNAi (RNA interference). The obtained data revealed a specific targeting for some of the paralogs with a consistent differentiation function. The results are presented in the manuscript Sehring et al. (2006).

Zusammenfassung

In dieser Doktorarbeit wurden zwei Themenkomplexe bearbeitet. Im ersten Teil der Arbeit wurde die Calciumdynamik während der Erregung von Parameciumzellen durch GTP mittels Fluorochromanalyse untersucht. Die Ergebnisse wurden in der Arbeit Sehring et al. (2004) veröffentlicht. Zugabe von GTP in das Medium führt zu periodischen Vor- und Rückwärtsschwimmen der Zellen. Eine Umkehrung des Cilienschlags wird durch einen Anstieg der Calciumkonzentration in den Cilien ausgelöst. Elektrophysiologisch ließen sich währenddessen Depolarisationen des Membranpotentials mit gleicher Periodizität aufnehmen. In dieser Arbeit wurde durch verschiedene Versuchsansätze überprüft, inwieweit die nach dem Modell von Wessenberg et al. (1997) beteiligten Komponenten (siehe Figur 6) tatsächlich bei der Weiterleitung des extrazellulären Signals eine Rolle spielen. Es konnte gezeigt werden, das sowohl Calcium aus dem Medium als auch aus intrazellulären Speichern an der Signalvermittlung beteiligt ist. Allerdings sind, im Gegensatz zum vorgeschlagenem Modell, weder die spannungsabhängigen Calciumkanäle in den Cilien noch die kortikalen Calciumspeicher, die Alveolarsäcke, in die Reaktion eingebunden. Über welche Calciumkanäle der Einfluss in die Zelle vonstatten geht ist noch ungeklärt. Als intrazellulärer Speicher könnte das ER beteiligt sein. Beides bedarf weiterer Analysen.

Die Alveolarsäcke sind, wie gezeigt werden konnte, nicht an der Calciumreaktion auf GTP beteiligt. Als kortikale Calciumspeicher spielen sie jedoch während der Exocytose eine wichtige Rolle. Eine nach wie vor offene Frage ist dabei die Positionierung und strukturelle Verbindung der Alveolarsäcke an der Zellmembran. Ein möglicher Kandidat hierfür ist Aktin, dessen Beteiligung bei Calciumreaktionen in anderen Systemen nachgewiesen werden konnte. Im zweiten Teil der Arbeit wurde daher Aktin in *Paramecium* untersucht. Zu Beginn der Doktorarbeit stand ein polyklonaler Antikörper gegen Aktin 1-1 zur Verfügung, der für immunhistologische Studien verwendet wurde. Die Ergebnisse wurden in der Arbeit Kissmehl et al. (2004) veröffentlicht. Mit dem fortschreitendem *Paramecium* Genomprojekt während dieser Doktorarbeit konnten alle Gene, die Aktin, actin-related proteins oder actin-like proteins in *Paramecium* codieren, identifiziert werden. Eine Analyse der unterschiedlichen Paraloge auf Nucleotid- und Aminosäurenebene wird im Manuskript Kissmehl et al. (2006) gezeigt. Mehrere Gene wurden im Detail analysiert, speziell in Bezug auf Lokalisierung unter Verwendung des „Green-fluorescent-proteins“ und/oder spezifischer Antikörper, und auf ihre funktionelle Bedeutung mit RNAi (RNA interference). Es konnte gezeigt werden, dass die einzelnen Subfamilien zum Teil unterschiedlich in der Zelle lokalisiert sind, und dass diese

Lokalisierung mit differenzierten Funktionen der Paraloge übereinstimmt. Die Ergebnisse werden in dem Manuskript Sehring et al. (2006) dargestellt.

Acknowledgements

Bedanken möchte ich mich bei Prof. Plattner fürd die Betreuung dieser Doktorarbeit und die vielen Diskussionsmöglichkeiten. Ebenfalls bedanken möchte ich mich bei Prof. Werner Hofer für die freundliche Bereitschaft, diese Arbeit zu begutachten.

Mein Dank gilt allen aktuellen und ehemaligen Mitgliedern der Arbeitsgruppe:
Anja Helbig, Jochen Hentschel, Ruth Hohenberger-Bregger, Nicole Kasielke, Anne Keller, Roland Kissmehl, Sylvia Kolassa, Eva-Maria Ladenburger, Lauretta Nejedli, Christina Schilde, Oluscha Traub, Christoph Reiner, Kathrin Nühse, Carsten Danzer, Tilman Treptau, Ihab Mohamed, Thomas Waßmer, und Martina Reiss für die vielfältige Unterstützung.

Und natürlich geht mein Dank an meine Familie und meine Freunde, die immer für mich da waren.

Eigenabgrenzung

A.) Manuskript I:
"Ca^{2+} oscillations mediated byx exogenous GTP in *Paramecium* cells: assessment of possible Ca^{2+} sources"
von Ivonne M. Sehring und Helmut Plattner

1.) Die Experimente wurden von H. Plattner geplant.

2.) Alle Experimente wurden von I. M. Sehring ausgeführt.

3.) Das Manuskript wurde von H. Plattner verfasst mit der Unterstützung von I. M. Sehring, kontrollgelesen und verbessert wurde das Manuskript von H. Plattner und I. M. Sehring.

B.) Manuskript II:
"Immunolocalization of actin in *Paramecium* Cells"
von Roland Kissmehl, Ivonne M. Sehring, Erika Wagner, und Helmut Plattner

1.) Die Experimente wurden von R. Kissmehl und I. Sehring geplant.

2.) Immunlokalisierungen wurden von I. M. Sehring ausgeführt.

3.) Das Manuskript wurde von H. Plattner und R. Kissmeh verfasst.

C.) Manuskript III:
"The actin multigene family of *Paramecium tetraurelia*"
von Ivonne M. Sehring, Jörg Mansfeld, Christoph Reiner, Erika Wagner, Helmut Plattner and Roland Kissmehl

1.) Die Experimente wurden von I. M. Sehring und R. Kissmehl geplant

2.) Alle Analysen wurden von I. M. Sehring ausgeführt, außer:
- Analyse der *Paramecium*-Datenbank erfolgte durch R. Kissmehl
- Hybridization cloning und Verifizierung von act1-1, act1-2, act1-3, act2-1 und act3-1 erfolgte durch J. Mansfeld und E. Wagner.
- Verifizierung von act1-6, act6-1 und act8-1 erfolgte durch C. Reiner.

3.) Das Manuskript wurde von I. M. Sehring verfasst, Kontrollen und Verbesserung von H. Plattner und R. Kissmehl

D.) Manuskript IV:
"A Broad Spectrum of Actin Paralogs in *Paramecium tetraurelia* Cells Displays Differential Localization and Function"
Ivonne M. Sehring, Christoph Reiner, Jörg Mansfeld, Helmut Plattner and Roland Kissmehl

1.) Die Experimente wurden von R. Kissmehl, I. M. Sehring und J. Mansfeld geplant.

2.) Eliminierung aller internen Stop-Codons, rekombinante Expression und Reinigung von act4-1 wurde von I. M. Sehring durchgeführt, ebenso die Aufreinigung der anti-act5 Antikörper, sämtliche Western Blot Analysen und Immunlokalisierungen. Alle

Silencing-Konstrukte und Silencing-Experimente wurden von I. M. Sehring erstellt bzw. durchgeführt. GFP-Konstrukte für act1-9 und act4-1 wurden von I. M. Sehring erstellt und die EM-Einbettung durchgeführt.

3.) Das Manuskript wurde von H. Plattner und I. M. Sehring erstellt, Kontrollen und Verbesserung von C. Reiner und R. Kissmehl